5-2014

CAR-MODIFIED T CELLS CAPABLE OF DISTINGUISHING NORMAL CELLS FROM MALIGNANT CELLS

Hillary G. Caruso

CAR-MODIFIED T CELLS CAPABLE OF DISTINGUISHING MALIGNANT CELLS FROM NORMAL CELLS

by

Hillary Gibbons Caruso, B.S.

APPROVED:

_____
Laurence Cooper, M.D., Ph.D., Supervisory Professor

_____
Oliver Bögler, Ph.D.

_____
Bradley McIntyre, Ph.D.

_____
Jeffrey Molldrem, M.D.

_____
Kimberly Schluns, Ph.D.

APPROVED:

_____
Dean, The University of Texas
Graduate School of Biomedical Sciences at Houston

CAR-MODIFIED T CELLS CAPABLE OF DISTINGUISHING MALIGNANT CELLS FROM NORMAL CELLS

A

DISSERTATION

Presented to the Faculty of
The University of Texas
Health Science Center at Houston
and
The University of Texas
MD Anderson Cancer Center
Graduate School of Biomedical Sciences
in Partial Fulfillment

of the Requirements

for the Degree of

DOCTOR OF PHILOSOPHY

by

Hillary Gibbons Caruso
Houston, Texas

May 2014

DEDICATION

To my best friend, my husband, Andrew

For teaching me that

“Laughter is timeless,

Imagination has no age,

And dreams are forever.”

- *Walt Disney*

ACKNOWLEDGMENTS

The road journeyed to complete my doctorate work and dissertation could not have been traveled without the support from those around me. There are many I am eternally grateful to for their unending encouragement.

First, my profound appreciation goes to my mentor, Dr. Laurence Cooper. He has been the most enthusiastic, understanding, and supportive mentor one could ask for, and I am glad that I was able to undertake my work in his laboratory. His passion is contagious and necessary for successful pursuit of scientific research, and I am grateful to have studied under his mentorship. Additionally, my sincerest thanks go to Dr. Dean Lee for his input and guidance through my graduate career. Through advice with experimental design to guidance with writing manuscripts, his advice has been invaluable. I would also like to thank all members of my advisory committee, Drs. Oliver Bögler, Brad McIntyre, Jeffrey Molldrem, and Kimberly Schluns, for their insightful input and guidance through this journey.

Next, I would like to thank everyone in the Cooper Lab, past and present members included, for the congenial work atmosphere and supportive collaborations through the years. I thank Harjeet Singh for taking on the role of training me in day-to-day lab practices and being my "go-to" guru for input on experimental design and interpretation through the years. I'd also like to thank Sourindra Maiti, Simon Olivares, and Sonny Ang for assistance in designing vectors and molecular biology techniques, David Rushworth and Bipulendu Jena for manufacture and construction of CAR-L, Ling Zhang for sharing her *in vitro* transcription protocol, and Drew Deniger for assistance with lentiviral transduction. I owe many thanks to Tiejuan Mi, Kirsten Switzer, Lenka Hurton, and Amer Najjar for assistance and valuable company during many long days in the mouse facility. I would also like to thank Lenka Hurton, Denise Crossland, Drew Deniger, and Radhika Thokala for the brainstorming sessions, suggestions, advice and collegial atmosphere within our own little office for the past five years. Working alongside you, learning from you, and sharing our experiences over the past several years have been among some of the most distinguishing joys of this process, and I'm glad to have had you along for the ride. Finally, many, many thanks to Helen Huls, the glue that holds everything together in the Cooper Lab. Between your responsibilities in clinical translation of all of our work and day-to-day guidance and structure to keep our lab afloat, we would be lost without everything you do for us.

Many funding agencies have supported the work completed in this dissertation. I would like to thank the American Legion Auxiliary for their hard work fundraising for cancer research and their support of this project. I would also like to thank the Cancer Answers and the Sylvan Rodriguez Foundations, who have offered their support through the Andrew Sowell Wade Huggins fellowship. In addition, I offer thanks to the friends and family of R.W. Butcher, who have supported my work through the R.W. Butcher fellowship. And finally, much of this work was supported by the Center for Clinical and Translational Sciences at the University of Texas at Houston Health Science Center, funded through the National Center for Advancing Translational Science of the National Institutes of Health under award number TL1TR000369.

I have been fortunate enough to have educators and mentors along the road that encouraged me from a young age to succeed in all I do. First, my sincerest thanks to Jim Dixon. As a young student interested in music, Mr. Dixon had more faith in me than I did in myself. Through his teaching and support, he taught me not only to play the flute, but to have passion and dedication for music, and to work as hard as I could to achieve my goals. Applying the dedication instilled in me at that young age has fueled my progress through graduate school, and I am grateful for all his support. I would not be where I am today without the influence of two wonderful high school teachers, Ms. Janice Pyles and Ms. Hope Stevens. Ms. Pyles saw my enthusiasm for science as a student in her Pre-AP Chemistry class and encouraged me to take not only AP Chemistry II, but AP Biology II. My love for chemistry was immediate, but I only discovered a love for biology through this course, and I wouldn't be where I am today without her guidance. Ms. Stevens encouraged me to take AP Biology II as a guided independent-study during her off-period, as I was the only enrollee. In usual circumstances, the class would have been canceled, but because I was allowed to study in this manner, I discovered a profound and deep appreciation for biology on the cellular and molecular level, which has lead me to this point in my career.

Finally, I have been blessed beyond words with a caring and endlessly supportive family. My parents have been the best role models a child could ask for. They have shown what dedication and hard work can achieve, paramount among those achievements being true happiness and contentment with life. I owe the person I am today, and everything I have accomplished thus far, to their love and support, for they are constantly behind me, my own perpetual cheering section. My brother, Ryan, was among the first people to push me to do my best. His encouragement to achieve pushed my academic endeavors in high

school, which has flowed right through each stage of my education. My entire family has been a network of love and support, which grows from the center of our family, my grandparents. To Maw Maw and Paw Paw, and to Grandma and Grandpa McBrayer, thank you for all you have done for us. I am lucky to have an entire network of in-laws that treat me as family, including my mother-in-law, Diana, father-in-law, Vincent, and brother-in-laws, Vin and Patrick. Thank you for taking me into your family as one of your own; I am lucky to be a member of the Caruso clan. I am also fortunate to have three sister-in-laws that I treasure as my own sisters. Stacey, Melissa, and Lenka, I am so happy to have you not only as family, but as friends.

Last, but not certainly not least, my eternal love and gratitude to my own family, my husband, Andrew, and my daughter, Olivia. Andrew, you are the glue that holds our family together. Your constant love and hard work to take care of us, even before yourself, is a perfect example of what a marriage should be. You make me work harder to be a better person every day, and I am beyond blessed to have you as a husband. Olivia, you are the happiness in my every day. You are such a bright, quirky, and cheerful little girl, and I can't wait to see who you will become. Your smile has given me hope and carried me through more than one hard day, and I am lucky to be your mother.

CAR-MODIFIED T CELLS CAPABLE OF DISTINGUISHING MALIGNANT CELLS FROM NORMAL CELLS

Hillary Gibbons Caruso, B.S.

Advisory Professor: Laurence Cooper, M.D., Ph.D.

T cells can be redirected to target tumor-associated antigen (TAA) by genetic modification to express a chimeric antigen receptor (CAR), which fuses the specificity derived from an antibody to T-cell activation domains to result in lysis of TAA-expressing cells. Due to the potential for on-target, off-tissue toxicity, CAR^+ T-cell therapy is currently limited to unique or lineage-restricted TAAs. Glioblastoma, a grade IV brain malignancy, overexpresses epidermal growth factor receptor (EGFR) in 40-50% of patients. EGFR also has widespread normal tissue expression. To target EGFR on glioblastoma while reducing the potential for normal tissue toxicity, EGFR-specific CAR generated from cetuximab, Cetux-CAR, was transiently expressed in T cells by RNA-modification. RNA-modified CAR^+ T cells demonstrated similar cytotoxicity against $EGFR^+$ cells, including normal renal cells, as DNA-modified CAR^+ T cells. However, RNA-modified T cells lost CAR expression over time, concomitant with loss of functional specificity to EGFR. Transient expression of CAR limits potential for off-tissue toxicity at the expense of anti-tumor activity, and does not protect normal tissue from immediate toxicity. Recognizing that EGFR is overexpressed at a higher density on glioblastoma relative to normal tissue, we generated an EGFR-specific CAR from nimotuzumab, an EGFR-specific antibody with reduced binding to low density EGFR. While Cetux-CAR^+ T cells produced cytokine and mediated lysis independent of EGFR density, function of Nimo-CAR^+ T cells directly correlated with the EGFR density of targets, with reduced activity in response to low density EGFR, but equivalent activity in response to high density EGFR relative to Cetux-CAR^+ T cells. Cetux-CAR^+ T cells and Nimo-CAR^+ T cells demonstrated equivalent control of intracranial glioma xenograft with intermediate EGFR density, but only Cetux-CAR^+ T cells controlled xenografts with low EGFR density. In sum, transient expression of CAR has the potential to reduce long-term toxicity to normal tissue, but at the expense of anti-tumor activity. Rational design of CAR based on an antibody with reduced binding to low density EGFR generated EGFR-specific CAR able to tune T-cell function to antigen density resulting in discrimination of high EGFR density on malignant cells from low EGFR density on normal tissue.

TABLE OF CONTENTS

LIST OF FIGURES

LIST OF TABLES

LIST OF ABBREVIATIONS

2D: two-dimensional

3D: three-dimensional

aAPC: artificial antigen presenting cell

ABC: antibody binding capacity

ADCC: Antibody-dependent cell-mediated cytotoxicity

AICD: activation induced cell death

ALL: acute lymphoblastic leukemia

APC: antigen presenting cell

ATP: adenosine triphosphate

BBB: blood-brain barrier

BLI: bioluminescent imaging

CAIX: carbonic anhydrase IX

CAR: chimeric antigen receptor

CAR-L: chimeric antigen receptor ligand

CDK4: cyclin dependent kinase 4

CEA: carcinoembryonic antigen

CID: chemical inducer of dimerization

CLL: chronic lymphocytic leukemia

CNS: central nervous system

cSMAC: central supramolecular activation cluster

DAG: diacylglycerol

dSMAC: distal supramolecular activation cluster

E:T: effector to target ratio

EGF: epidermal growth factor

EGFR: epidermal growth factor receptor

EGFRvIII: epidermal growth factor receptor variant III

Erk1/2: extracellular regulated kinase ½

E-PAP*: E.coli* poly(A) polymerase

FBS: fetal bovine serum

ffLuc: firefly luciferase

GADS: Grb2-related adaptor downstream of signaling

GFP: green fluorescent protein

Grb2: growth factor receptor-bound protein 2

HER2: human epidermal growth factor receptor 2

HRCE: human renal cortical epithelial cells

HSV-TK: herpes simplex derived thymidine kinase

ICAM-1: intracellular adhesion molecule-1

iCasp9: inducible caspase 9

ICOS: inducible costimulator

IDH: isocitrate dehydrogenase

IFN-γ: interferon-γ

IgG: immunoglobulin class G

IL-2: interleukin-2

IL-6: interleukin-6

IL-10: interleuking-10

IL13Rα2: interleukin 13 receptor α2

IL-21: interleukin-21

ITAMs: immunoreceptor tyrosine-based activation motifs

Itk: inducible T cell kinase

IP3: inositol triphosphosphate

IR/DR: inverted repeat/direct repeat

JNK: c-Jun n-terminal kinase

K_d: dissociation constant

K_{off}: rate of dissociation

k_{on}: rate of association

LAT: linker of activated T cells

LMO-2: LIM-only protein 2

mAb: monoclonal antibody

MAPK: mitogen activated protein kinase

MDSC: myeloid derived suppressor cell

MFI: mean fluorescence intensity

MGMT: O-6-methylguanine-DNA-methyltransferase

MHC: major histocompatibility complex

NFAT: nuclear factor of activated T cells

NFκB: nuclear factor κ-light-chain-enhancer of activated B cells

OKT3: anti-CD3 antibody

PBMC: peripheral blood mononuclear cell

pepMHC: peptide in the context of MHC

PD1: programmed death receptor 1

PDGFR: platelet derived growth factor receptor

PD-L1: programmed death receptor ligand 1

PGE2: prostaglandin E2

PI: propidium iodide

PI3K: phosphoinositol-3-kinase

PIP_2: phosphatidylinositol 4,5-biphosphate

PKCθ: protein kinase Cθ

PLCγ1: phospholipase Cγ1

pSMAC: peripheral supramolecular activation cluster

PTEN: phosphatase and tensin homolog

Rb: retinoblastoma protein

RTK: receptor tyrosine kinase

scFv: single chain variable fragment

SCID: severe combined immunodeficiency

SLP-76: lymphocyte cytosolic protein 2

SMAC: supramolecular activation clusters

STAT: signal transducer and activator of transcription

$t_{1/2}$: half-life

T_{reg}: regulatory T cell

TCR: T cell receptor

TGFα : transforming growth factorα

TGFβ: transforming growth factor β

TIL: tumor infiltrating lymphocytes

TNF-α: tumor necrosis factor-α

UTR: untranslated region

VDJ: Variable, diversity, joining

VEGF: vascular endothelial growth factor

VEGFR2: vascular endothelial growth factor receptor 2

ZFN: zinc finger nucleases

CHAPTER 1

Introduction

1.1 T cells

T cells are a lymphocyte of the adaptive immune system characterized by sensitive and highly specific response to foreign antigen (1). CD8 T cells, or cytotoxic T cells, are capable of initiating target cells lysis upon recognition of foreign antigen, whereas CD4 T cells, or helper T cells, support immune responses, primarily through secretion of cytokines. Both CD8 T cells and CD4 T cells recognize peptide in the context of presentation by major histocompatibility complex (MHC) through the αβ T cell receptor (TCR). CD8 and CD4 function as co-receptors, binding to MHC class I and MHC class II, respectively, to facilitate T cell recognition of foreign peptide.

1.1.1 Structure and function of T-cell receptor in T-cell activation

Each TCR is a heterodimer composed of disulfide-linked α and β chains, which are composed of two immunoglobulin-like domains each, a variable and constant domain, anchored into the cell membrane via a transmembrane region and short cytoplasmic tail with no intrinsic signaling capacity. The variable domain is formed from recombination of variable (V), diversity (D), and joining (J) gene segments in β chain, and V and J segments in the α chain in a process known as VDJ recombination. The large magnitude of permutations that can result from VDJ-rearrangement generates a remarkable range of T-cell specificities for peptide presented in MHC (pepMHC). The TCR is expressed on the T-cell surface in association with three CD3 signaling dimers (δε, γε, and ζζ) through polar interactions among the transmembrane domains, such that δε and γε associate with each other on one side of the αβ TCR and ζζ is on the other (2). Because the ζ chain has a small extracellular domain, one face of the αβ TCR open for dimerization, which has been proposed as a mechanism for TCR signal transduction (3, 4). Each CD3 subunit contains immunoreceptor tyrosine-based activation motifs (ITAMs), which become phosphorylated following TCR recognition of pepMHC by Src kinase family member Lck to initiate a signaling cascade (1). ZAP-70 is recruited to phosphorylated ITAMs and phosphorylates two adaptor proteins, lymphocyte cytosolic protein 2 (SLP-76) and linker of activated T cells (LAT), a palmitoylated transmembrane protein with a long cytoplasmic domain containing many phosphorylation sites which recruits many proteins to form a signalosome (5).

Proteins recruited to the signalosome include: SLP-76, growth factor receptor-bound protein 2 (Grb2), Grb2-related adaptor downstream of signaling (GADS), phospholipase C γ1 (PLCγ-1), inducible T cell kinase (Itk), Nck, and Vav1. Nck and Vav1 are adaptor molecules the regulate actin cytoskeleton reorganization. PLCγ-1 is phosphorylated by Itk and hydrolyzes phosphatidylinositol 4,5-biphosphate (PIP_2) into two second messengers, diacylglycerol (DAG) and inositol triphosphate (IP_3). DAG activates signaling through protein kinase C-θ (PKCθ) to ultimately activate transcription factor nuclear factor κ-light-chain-enhancer of activated B cells (NFκB), and mitogen activated protein kinase (MAPK) pathways extracellular regulated kinase 1/2 (Erk1/2), p38, and c-Jun n-terminal kinases (JNK). IP_3 triggers release of Ca^{2+} from the endoplasmic reticulum to ultimately activate the transcription factor nuclear factor of activated T cells (NFAT).

T-cell activation and signaling is tightly integrated with cytoskeleton organization (6-8). The actinomyosin cytoskeleton is important before and during T-cell activation by influencing T-cell motility while scanning for antigen prior to TCR triggering, providing scaffolding to assemble signalosome during TCR triggering, and translocating TCR signaling clusters prior to termination of signaling. Evidence of the necessity for cytoskeletal mediation of T-cell signaling comes from the potent inhibitory activity of actin depolymerization agents latrunculin A and cytochalasin D on T-cell activation (9, 10). Recently, actin remodeling has been shown to be a requirement for initiation of T-cell signaling (11). Actin restricts lateral diffusion of molecules in the cell membrane, and has been shown to sequester signaling intermediates, but the exact contribution the actin cytoskeleton makes to T-cell signaling has yet to be completely elucidated (12, 13).

1.1.2 Impact of T-cell receptor affinity on T-cell function

The binding kinetics of an individual TCR molecule to pepMHC can be described by an association rate, or on-rate of binding (k_{on}) and dissociation rate, or off-rate of binding (k_{off}) (14). A relationship between these two biochemical parameters is used to derive a dissociation constant (K_d) to describe the overall affinity TCR/pepMHC interaction, such that:

$$K_d = \frac{k_{off}}{k_{on}}$$

A half-life ($t_{1/2}$) for the interaction of TCR with pepMHC can be derived from the k_{off} by the equation:

$$t_{1/2} = \frac{\ln 2}{k_{off}}$$

Typically, these binding parameters are derived from surface plasmon resonance (SPR) assays, in which immobilized pepMHC interact with free TCR in solution, and K_d is equal to the concentration of unbound TCR when the concentration of unbound pepMHC equals the concentration of bound pepMHC. Wild type TCR affinities producing productive T-cell responses are often described as low affinity, particularly relative to kinetics described for antibody interaction with antigen, and are characterized by slow on-rates and intermediate off-rates of binding with pepMHC (14).

Altering binding affinity of pepMHC ligands for TCR has demonstrated the distinct impact of low affinity interactions on T-cell signaling, including reduced phosphorylation of CD3ζ, calcium release, granule polarization, downregulation of TCR, and activation of MAPK pathways (15-21). However, the parameter of TCR binding primarily correlating with T-cell function has been a matter of extensive debate (14). Evidence supports both K_d and k_{off} as determinants of T-cell function (15, 16, 22-25). The kinetic proofreading model of T cell triggering suggested that dissociation rates must be sufficiently long for signaling and T-cell activation to take place. This has been contradicted by findings that TCRs with short half-lives can produce functional responses and that T-cell activation can take place in a matter of seconds following TCR interaction with pepMHC (25, 26). Additionally, it has been observed that excessively long half-lives of interactions can result in impaired T-cell function (27, 28). When combined with the observation that multiple TCR can be internalized following interaction with a single pepMHC complex (29), it has been hypothesized in such prolonged interactions, serial triggering of multiple TCR by a single pepMHC complex is impaired, resulting in impaired T-cell activation. This addendum to kinetic proofreading model, termed the optimal dwell time model, purports a window of dissociation rates in which functional TCR/pepMHC binding can occur (27). The requirement of serial triggering for TCR triggering has also been called into question, as it has been observed that T cells require interaction with as little as 3 pepMHC to induce target lysis (30). Additionally, engineered TCRs with very long half-lives, up to 425 minutes, are capable of producing functional T-cell responses (31, 32). It seems that serial triggering for T-cell activation may be a requirement when pepMHC is limiting, such that increasing pepMHC density can dispense the requirement for serial triggering (33). Subsequent studies have evaluated the contribution of association rate of binding to T-cell activity. In transgenic TCR systems

evaluating peptides with altered affinity, T-cell activity was found to correlate with association rate and not dissociation rate of binding (16, 24, 25). The high degree of correlation between K_d and k_{off} values and the small range of k_{on} values in many datasets complicates determining the roles of individual biochemical parameters on T-cell function. By analyzing datasets of TCR and pepMHC binding pairs that minimized the correlation between K_d and k_{off} and included a wider dynamic range of k_{on} values, Aleksic, et.al. proposed a model such that T-cell confinement, derived from the mathematical relationship of k_{on}, k_{off} and diffusion of TCR and pepMHC in their respective membranes, accounts for the duration of TCR/pepMHC interaction and resulting T-cell function (34). Interestingly, this model can reduce to simpler models. When k_{on} is fast relative to diffusion rate, confinement time is proportional to K_d, however, when k_{on} is slow relative to diffusion rate, confinement is governed solely by the k_{off} because the TCR/pepMHC will diffuse without multiple binding events. Thus, previously contradictory studies can be resolved within one model of TCR triggering (26, 34).

Discrepancies between previous studies can also be accounted for by methodological differences. Read-outs of T-cell function vary from study to study, and include proliferation, phosphorylation of signaling molecules, cytokine production, and lytic capacity. It has been demonstrated that TCRs elicit effector responses in an TCR clone-specific and antigen-dose dependent hierarchy, such that some responses are more easily triggered at low antigen doses than others (17). Thus, differences in TCR clone employed in the study and functional read-outs complicate inter-study comparisons. It has been described that T-cell activation is achieved by a cumulative signal, which can be reached at different time points for different ligands, such that low affinity ligands induce functional T-cell responses, including calcium release, upregulation of activation marker CD69, and proliferation, kinetically delayed relative to higher affinity ligands (16, 35, 36). Therefore, difference in assay time points may also contribute to differences in findings.

Recently, studies have acknowledged an inherent limitation in measuring TCR binding kinetics in three-dimensional (3D) assays. In 3D kinetic assays, one binding partner is immobilized, while the other is free in solution. This does not mimic conditions of physiological T-cell activation, in which both binding partners are constrained to two-dimensional (2D) movement within their respective cell membranes, which ensures proper orientation of molecules and limits intercellular volume to increase the likelihood of TCR/pepMHC binding (37, 38). Accordingly, Huang et. al. developed two 2D mechanical

assays to measure TCR binding kinetic to pepMHC (37). Association and dissociation rates measured in 2D were accelerated and characterized by broader ranges relative to 3D measurements. All 2D kinetic parameters, K_d, k_{off} and k_{on}, correlated with T-cell function. In contrast to 3D assays, in which durable interaction through slow k_{off} resulted in enhanced T-cell function, faster 2D k_{off} correlated with superior T-cell function. Interestingly, disrupting cytoskeletal involvement in T-cell signaling by actin depolymerization results in 2D kinetic measurements similar to 3D measurements, indicating cytoskeletal involvement in destabilizing TCR/pepMHC interaction (38). Similarly, measurement of binding in a 2D cell-free system described dissociation rates equivalent to those obtained from 3D assays (39). Thus, an integrated process involving dynamic cellular processes and cytoskeletal rearrangement during T cell interaction with antigen presenting cells influences the rates of association and dissociation between TCR and pepMHC.

1.1.3 TCR clustering during T-cell activation

While monomeric affinity describes the kinetic association and dissociation of individual TCR/pepMHC interactions, avidity describes the contribution of multiple TCR/pepMHC binding pairs to stabilizing interactions and enhancing T-cell activation. Prior to TCR ligation with pepMHC, TCRs are present in oligomeric structures termed “nanoclusters”, facilitated by cholesterol and sphingomyelin in the cell membrane (40-43). These static preformed TCR aggregates are hypothesized to contain 2-20 TCR αβ pairs, and increase sensitivity to low antigen doses by enhancing avidity of interaction (40, 43). In fact, the size of the nanocluster has been shown to be directly related to antigen sensitivity (42). Additional clustering of TCR following engagement by multivalent pepMHC complexes is a requirement for complete T-cell activation (4, 44). Formations of microclusters, containing 30-300 TCR, initiate T-cell signaling, and precede establishment of a mature immunological synapse (45-48). The size and number of TCR microclusters increases with ligand density or agonist strength (49). Agonist- and actin-dependent, TCR microclusters co-localize with activated Lck, ZAP-70, and LAT, and provide a scaffold for signal amplification (9, 49). Thus, the formation of nanocluster of TCRs prior to antigen interaction enhances sensitivity to antigen through increased avidity, and formation of microclusters after antigen interaction amplify signal and contribute to overall T-cell functional response.

1.1.4 Immunological synapse formation during T-cell activation

An immunological synapse describes the stable interaction between a T cell and antigen presenting cell (APC), characterized by highly orchestrated molecular organization and cytoskeletal rearrangement within the T cell. The synapse is organized in a bullseye configuration with three distinct concentric rings of molecules, termed supramolecular activation clusters (SMAC). The central SMAC (cSMAC) is traditionally characterized by high density of TCR, while the peripheral SMAC (pSMAC) contains adhesion molecules, such as intercellular adhesion molecule-1 (ICAM-1). The distal SMAC (dSMAC) typically contains molecules with long extracellular domains, such as CD45. The synapse is not required for transient T cell activation, as initiation of signaling and directed cytotoxicity can occur before the establishment of a stable immune synapse (30, 46, 50). However, the immunological synapse forms stable interactions between T cells and APCs on the order of hours and promotes continuous signaling to reach full effector function (51). The cSMAC enhances signaling by localizing TCR, pepMHC, and intracellular signaling molecules, such as Lck in a small, defined region, facilitating rapid molecular associations. The cSMAC is a site of both increased TCR triggering and TCR degradation and functions to amplify weak signals while tempering strong signals by enhancing downregulation of TCR (52-54). In the case of weak agonists, zeta chain is only partially phosphorylated and triggers minimal downregulation of TCR (17, 53, 55). However, in the case of a strong agonist, intense signaling and phosphorylation enhances TCR degradation, tempering T-cell signaling and activation. Thus, the balance between enhanced signaling and TCR degradation that occurs in the cSMAC facilitates further distinction of T cell activation and function induced strength of TCR/pepMHC interaction.

1.1.5 Contribution of pepMHC density to T-cell activation

In vivo, a correlation has been found between high antigen density, stability of interaction between T cells and pepMHC on dendritic cells, and cytolytic function, indicating the role of antigen density in contributing to overall avidity of T-cell interaction with pepMHC and influence on T-cell activation (56, 57). Low affinity of pepMHC can be compensated by increasing pepMHC density to increase the number of TCRs triggered (17, 59, 60). Triggering an equivalent number of TCR with high affinity, low density pepMHC and low affinity, high density pepMHC can elicit similar levels of T-cell proliferation (29, 61). However, pepMHC affinity and density can have distinct influences on T-cell activation.

Gottschalk, et.al. described that while increasing antigen density can compensate for low affinity to induce T cell proliferation, defects in interleukin-2 (IL-2) production could not be compensated by increased antigen (60). Microarray analysis revealed two distinct groups of genes: those regulated by cumulative TCR signal and thus able to be compensated by increasing density of low affinity antigen and those regulated by affinity of TCR/pepMHC interaction and not able to be compensated by increasing antigen density. Disparate ability of quantity of antigen to compensate for affinity of interaction in the induction of certain gene subsets indicates that increasing the avidity of interaction may not be able to overcome the influence of weak monomeric affinity of TCR/pepMHC interactions to achieve T-cell functional responses equivalent to more stable interactions (57). Therefore, affinity of monomeric TCR and avidity influenced by antigen density can have distinct influences on T-cell signaling, activation, and function.

1.1.6 Impact of TCR affinity and pepMHC density *in vivo*

Enhancing TCR affinity results in increased antigen sensitivity and functional avidity *in vitro* and *in vivo*, up to a certain threshold (23, 62). However, superior function of high affinity T cells *in vitro* does not necessarily correlate to better *in vivo* function. In a vaccination model, high affinity ligand, beyond a certain ceiling, demonstrated attenuated T-cell responses *in vivo*, characterized by reduced *in vivo* expansion, accumulation, and diminished cytokine production upon restimulation (63). Likewise, in a model of microbial infection, low affinity ligands for TCR demonstrate T-cell activation, but curtailed expansion and shorter duration in lymphoid organs (64). *In vivo* tumor models also demonstrate that CD8 T cells with high affinity TCRs lose cytotoxic function after tumor infiltration, and are deleted in the tumor and peripheral lymphoid tissues (65-67). Thus, it is likely a window of intermediate affinity exists in which T cells demonstrate optimal *in vivo* responses, including expansion, cytotoxic function, and memory formation. However, due to the complex nature of pepMHC presentation, TCR interaction with pepMHC, and the role of antigen density influencing T cell avidity, it is unlikely that any single biochemical parameter universally determines optimal T cell function.

T cells with high-affinity TCRs have demonstrated loss of specificity and cross-reactivity to self-peptides (68, 69). In a clinical study with a high-affinity, engineered TCR directed to MAGE-A3 for treatment of melanoma and myeloma, 2/2 patients died of cardiogenic shock days after T-cell infusions with autopsies revealing severe myocardial damage and T-cell

infiltration (70). Subsequent studies identified that MAGE-A3 TCR was cross-reactive with titin, which is expressed on the striated muscle tissue of the heart, resulting in T-cell activation and elimination of cardiomyocytes *in vitro*, demonstrating loss of specificity attributed to affinity maturation of TCR (71). One hypothesis for the development of such cross-reactivity is that enhancing affinity for MHC reduces peptide sensitivity, and therefore, enhancing affinity in portions of TCR that interact only with peptide may prevent development of cross-reactivity to self-peptide (72).

1.2 T-cell immunotherapy for cancer

The theory of cancer immunoediting suggests that when the immune system is capable of recognizing cancer cells, tumor growth is inhibited (73). Tumors are thought to develop through evasion of immune detection through two primary mechanisms: central and peripheral tolerance (74, 75). Central tolerance is obtained during T-cell development by deletion of T cells with self-reactive TCRs, necessary to protect the host from autoimmune responses. Tumors often overexpress self-antigens, but self-tolerized T cells are unable to mount functional response to these antigens. Peripheral tolerance is often exploited by tumors and describes the blunting of immune responses due to cultivation of an immunosuppressive microenvironment (76-78).

Cancer immunotherapy approaches aim to reactivate the immune system to recognize tumors as foreign and mediate their destruction. Though many cell types can be employed to achieve anti-tumor effects, T cells provide unique antigen-specificity, ability to extravasate and home to chemo-attractants, and potential to establish immunological memory and mediate tumor regression upon relapse. Vaccination can be employed to activate T cells within cancer patients in response to antigenic peptide unique to tumor, but requires a pre-existing population of T cells with TCR responsive to introduced peptide and activation must overcome mechanisms of immune suppression (79). To overcome some of these limitations, patient's autologous T cells can be manipulated *ex vivo*, outside the influence of an immunosuppressive tumor, and re-infused for tumor immunotherapy (74). Some of the earliest successes in adoptive T-cell therapy isolated tumor-infiltrating lymphocytes (TIL) from tumors for selection for reactivity to tumor antigen and *ex vivo* expansion to restore effector function prior to re-infusion into patients with melanoma (80-82). Importantly, these early seminal studies delimited the requirement for persistent T-cell responses for effective anti-tumor responses (83, 84). However, this strategy still requires the presence of

endogenous TCR with specificity for unique tumor antigen. To overcome this limitation, T cells can be genetically modified to redirect their specificity through two primary mechanisms: introduction of genetically engineered αβ TCR or artificial, engineered TCR commonly referred to as chimeric antigen receptor (CAR) (74).

1.2.1 Chimeric antigen receptors: Overview

A CAR is formed from the single chain variable fragment (scFv) of a monoclonal antibody (mAb) with desired specificity fused by a flexible linker to an extracellular hinge region, often a member of the immunoglobulin class G (IgG), followed by a transmembrane and intracellular signaling domain (**Figure 1**) (85). A major advantage of CAR-based genetic modification over engineered αβ TCRs is that CAR is capable of recognizing antigen independent of MHC presentation and therefore overcomes limitations of allelic diversity of MHC for broad application to wider subset of patients and overcomes MHC downregulation on tumors as an immune escape mechanism (86, 87).

1.2.2 Genetic modification of primary T cells

Two primary strategies exist for permanent integration of CAR into host T cell DNA: viral transduction and non-viral plasmid integration. Initial CAR clinical trials utilized γ-retrovirus transduction to express CAR, which show an integration preference for transcriptional start sites (88, 89). Although no evidence of genotoxicity has been observed in trials with γ-retrovirally transduced T-cells, gene therapy for X-linked severe combined immunodeficiency (SCID) patients demonstrated the potential for insertional mutagenesis and genotoxicity (90, 91). Integration of γ-retrovirus into gene encoding LIM-only protein-2 (LMO-2), associated with lymphocyte proliferation and leukemia, resulted in aberrant overexpression of LMO-2 transcript resulting in development of monoclonal lymphocytosis (91). Self-inactivating lentiviruses have proven to be a good vehicle for gene therapy because they can deliver a large DNA cargo load, efficiently transduce T cells, and demonstrate reduced susceptibility to promoter silencing relative to retroviruses (74, 89). While lentiviruses do not show preference for integration at transcriptional start sites as seen with γ-retroviruses, they do show a predilection for transcriptionally active units, shown by higher integration frequency into gene-coding segments of DNA (89). However, lentiviral vectors are expensive to produce; therefore a low cost alternative to speed translation to clinical testing is desirable. Sleeping Beauty (SB) is a non-viral gene transfer system in which the genetic cargo load is expressed as a transposon between two inverted repeats

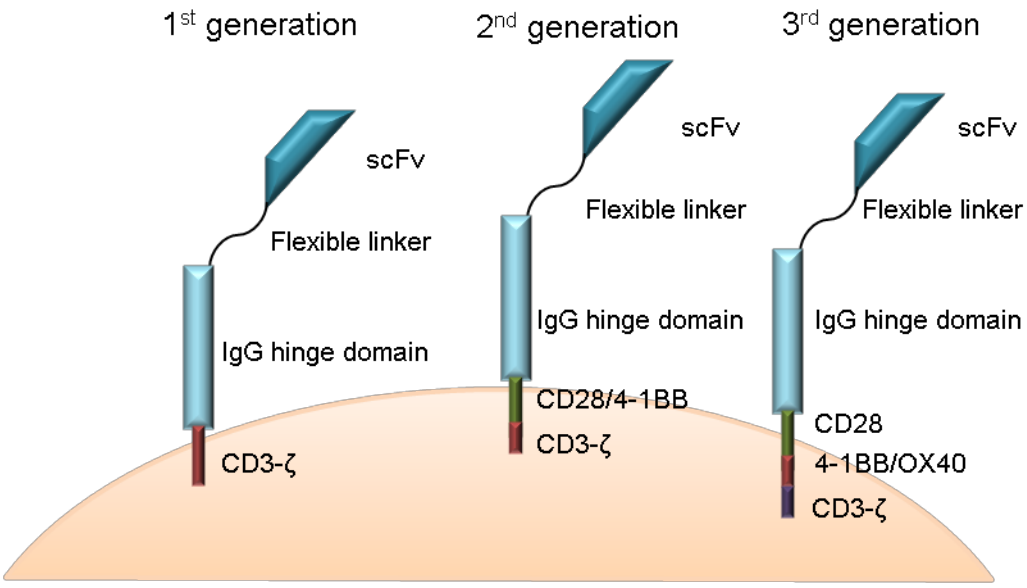

Figure 1. Schematic representation of CARs. First generation CARs fuse the specificity of the scFv domain from a monoclonal antibody to a flexible linker and IgG hinge domain attached to CD3-ζ transmembrane and cytosolic signaling domains. Second generation CARs include an additional costimulatory domain upstream of CD3-ζ, such as CD28 or 4-1BB, which contains transmembrane region and cytosolic signaling domains. Third generation CARs include two costimulatory domains upstream of CD3-ζ, often CD28 and 4-1BB or OX40.

containing direct repeated sequences (IR/DR) and is co-expressed with a transposase enzyme, SB11, which can cut and paste the genetic cargo into the host cell genome at sites of TA dinucleotide repeats (92-94). SB gene-transfer system is advantageous because it (i) does not show integration bias for transcriptionally active sites, (ii) has reduced capacity of remobilization due to fish-derivation of SB transposition elements, and (iii) is low-cost relative to lentiviral vectors (89, 92). Transfer of transposon containing CAR and SB11 transposase is achieved via electroporation of resting peripheral blood mononuclear cells (PBMCs). CAR transfer via the SB system results in stable CAR integration and expression (93, 94). Subsequent culture of T cells on artificial antigen presenting cells (aAPC) expressing antigen can cull out CAR-expressing T cells over time by selective propagation of CAR-expressing T cells. aAPC can be genetically modified to express costimulatory molecules, providing additional opportunities to support T-cell expansion and reprogram function during *ex vivo* culture (95-97).

1.2.3 Structure and function of CAR

Originally, T-cell activation via CAR was achieved through inclusion of intracellular CD3-ζ, termed a first generation CAR (85). T cells expressing first generation CARs demonstrated modest anti-tumor activity, presumably due to limited *in vivo* expansion and persistence (98-100). Second generation CARs were engineered to include a costimulatory signaling endodomain and have been shown to enhance CAR-mediated T-cell function. The most commonly described second generation CAR includes signaling through CD28, which resulted in increased proliferation, upregulation of anti-apoptotic genes, production of interferon-γ (IFN-γ) and IL-2, *in vivo* persistence and anti-tumor efficacy (101, 102, 104). Moreover, inclusion of CD28 signaling is also associated with increased resistance to immunosuppressive regulatory T cells (103). Interestingly, enhanced function of CAR containing CD28 endodomain over CAR signaling through CD3-ζ only was only apparent when target cells had no expression of CD86, the natural ligand for CD28 (105). Inclusion of other costimulatory domains has been investigated, including CD137 (4-1BB), CD134 (OX-40), CD244, CD27, and inducible costimulator (ICOS) (106-110). CARs containing 4-1BB endodomains result in improved *in vivo* persistence, anti-tumor activity, and tumor infiltration relative to first generation or CD28-containing second generation CARs, and have been associated with recent reports of clinical success targeting CD19 on B-cell malignancies (106, 111, 112). Third generation CARs have also been evaluated, in which a third endodomain is included to further augment T cell function. The most studied

combinations are CD28-41BB-CD3ζ and CD28-OX40-CD3ζ. Whether either of these configurations exhibit functional advantage over second generation CARs is unclear. While one study showed increased anti-tumor activity of a CAR containing CD28-41BB-CD3ζ signaling domains, another found no appreciable difference relative to 41BB-CD3ζ CAR alone (106, 113). A study comparing CAR signaling through CD28-OX40-CD3ζ and CD28-41BB-CD3ζ found that inclusion of OX40 increased sensitivity to low density antigen and increased lytic potential of T cells, but 41BB did not (114, 115). The optimal combination of CAR endodomains is undetermined and the subject of ongoing clinical investigation.

The distance of the epitope recognized by CAR scFv from the cell membrane can impact antigen sensitivity. It has been reported that targeting epitopes distal from the cell surface impaired lytic function in response to all levels of antigen expression, caused by both impaired T-cell degranulation and impaired targeting of granules due to delivery distance from the membrane (115-117). James, et.al. demonstrated this phenomenon was independent of affinity of CAR interaction with antigen by truncating the CD22 receptor such that a previously distal epitope was made membrane-proximal and showing the ability of CD22-specific CAR T cells to target cells expressing truncated CD22 was restored. The hinge region also influences T-cell interaction with target cells by impacting the length and flexibility of the CAR. Optimal hinge region length seems to vary from CAR to CAR, with reports of hinge regions enhancing and reducing function in the context of different specificities (118, 119). Recently, ROR1-specific CARs were shown to have superior anti-tumor activity with hinge regions of intermediate length (119). Because the distance between T cell and target cells during CAR interaction with antigen is determined both by epitope distance from membrane and length of hinge, and the impact of one on T-cell function is not without the influence of the other (118). Therefore, in the absence of specific rules that govern hinge length and epitope location, empirical evaluation of combinations of scFvs and hinge regions should be used to determine optimal CAR design.

1.2.4 CAR affinity and avidity in T-cell activation

The impact of affinity of scFv used in CAR design has not been evaluated in depth. Endogenous TCRs are described to have wild type affinities much lower than the monoclonal antibodies used to redirect CAR specificity, however, CD8 co-receptor binding to pepMHC can enhance avidity up to 10^6 over wild type affinity (31, 66). Because CAR binds surface antigen independent of MHC presentation, CAR interaction with antigen is

unlikely to benefit from increased avidity through co-receptor binding. Thus, the difference in overall avidity between wild type TCRs and CAR is unknown, but may not be as extensive as previously thought.

Design of multiple CARs specific for human epidermal growth factor receptor 2 (HER2) based on a library of affinity matured scFvs described a minimum threshold of CAR affinity that needed to be met to induce T-cell activity against HER2-expressing targets, but above which T-cell activity was not improved (120). The scFvs from which CAR were derived differed primarily in k_{off} with little variation in k_{on} values, and thus higher affinity was due to prolonged association with antigen, not change in rates of association with antigen. Importantly, affinity of HER2-specific CARs above the minimum affinity threshold did not correlate with increased antigen sensitivity or function. Recently, CARs specific for ROR1 for the treatment of murine model of mantle cell lymphoma with varying affinity of scFv were evaluated to determine the impact of affinity on CAR-mediated T-cell function. In this study, the scFv with increased affinity was achieved by both increasing k_{on} and decreasing k_{off}. Higher affinity ROR-1-specific CAR was associated with increased T-cell function, measured by increased cytokine production, proliferation, and *in vivo* anti-tumor efficacy, analogous to observations with affinity-matured TCRs (119).

The role of affinity in CAR design is impacted by factors that influence avidity, such as CAR expression density and antigen expression density (**Figure 2**). A minimum CAR density required for T-cell activation has been defined, below which CAR-mediated T-cell activation is abrogated. Above a maximum CAR density, however, T cells undergo increased apoptotic death following interaction with antigen (121). However, within this window, CAR density does not appear to impact T-cell activation (122). In conditions where both CAR expression and antigen expression are low, CAR-mediated T-cell activation is impaired (123). This phenomenon appears to be dependent on affinity, such that high affinity CAR^+ T cells have impaired function when CAR and antigen expression is low, but low affinity CAR^+ T cells do not (124).

In sum, these data suggest maximal CAR-dependent T-cell activation is determined by overall binding avidity, contributed to by affinity, density of CAR expression, and density of antigen expression (119). Further studies are required to elucidate the role of CAR affinity, and the individual roles for on- and off-rate binding in CAR^+ T cell function.

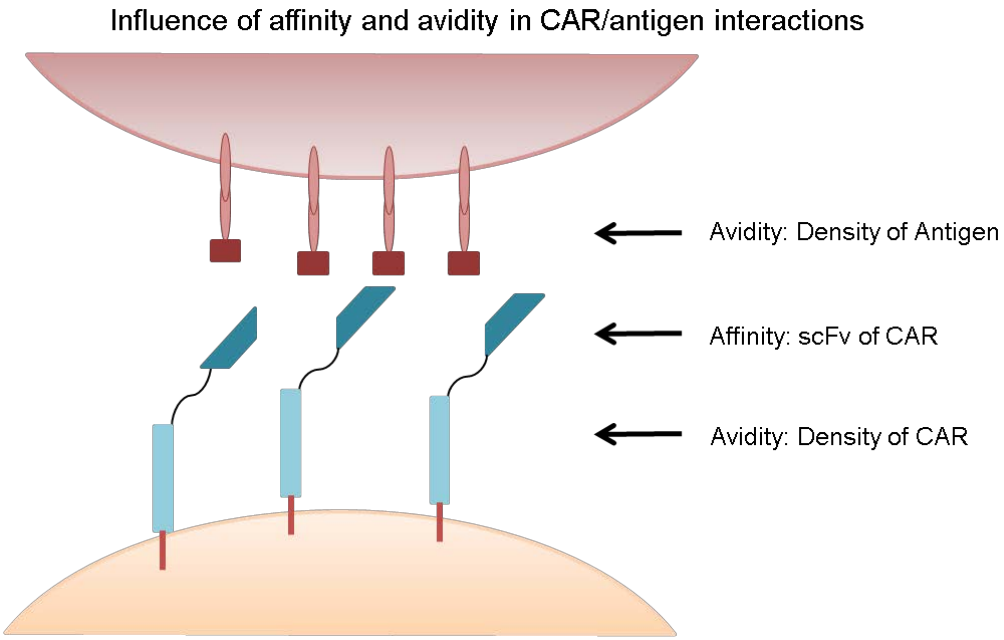

Figure 2. Influence of affinity and avidity in CAR/antigen interactions. CAR-dependent activation of T cells can be influenced by affinity of the scFv of CAR, density of antigen on target cell surface and density of CAR on T-cell surface, of which the latter two affect avidity of interactions. Cumulative CAR-dependent T-cell activation is determined by a combination of all three variables.

1.2.5 Mechanisms of CAR-mediated T cell activation

Mechanisms used by CAR to elicit functional T-cell responses and basic structural interactions of CAR with T-cell signaling molecules are not well understood. In CAR harboring CD3ζ transmembrane domain, CAR can signal through homodimerization or heterodimerization through association with endogenous TCR complex (125, 126). Mutation of highly polar amino acids associated with endogenous CD3ζ was associated with impaired dimerization of CAR and interaction with endogenous CD3ζ and TCR, both of which reduced T-cell activation. However, in studies with a second-generation CAR expressing CD28 transmembrane and cytosolic domains, eliminating endogenous TCR expression by targeting with zinc finger nucleases (ZFN), and therefore precluding expression of CD3ζ from the T-cell surface, showed no reduction in CAR-mediated T-cell function (127). Second generation CARs are capable of dimerization through mutation of proline to serine at amino acid position 241 in the IgG4 scaffold region to create a predisposition for interchain disulfide bond formation and dimerization (128). Analysis of CAR in reducing and non-reducing western blots revealed bands of predicted monomeric size (69 kDa) and oligomeric size (190 kDa), respectively, indicating the CAR undergoes some degree of static clustering in T-cell membrane. In sum, these data suggest that CAR can signal independent of the endogenous TCR complex; however this interaction is crucial for activation of CAR^+ T cells in the absence of second generation transmembrane and endodomain. In the presence of second generation endodomain, association with endogenous CD3-ζ may be dispensable for T-cell activation. Both CAR configurations support some degree of dimerization/oligomerization on the surface of the T cells, but whether or not the CAR forms aggregates after initiation of signaling is currently unknown.

While serial triggering appears to be an important mechanism mediating wild-type TCR sensitivity to low levels of antigen expression, recent studies have suggested CARs do not signal by serial triggering. Mathematically modeling CAR triggering based on Verhulst equation for population growth suggested that CAR triggering can be described akin to endogenous TCR triggering in a special condition in which serial triggering is abrogated (122). This may partially explain reduced sensitivity of CAR relative to wild type TCRs, such that CARs require higher CAR expression and higher antigen density to induce functional T-cell responses. Descriptions of downregulation and serial triggering of CAR have currently been described for first generation CARs, and the impact of costimulation through second generation CAR recognition of antigen in these processes has not been determined.

1.2.6 CARs in the clinic: hematological malignancies

Early phase clinical trials evaluating efficacy of CARs are numerous, with upwards of 20 phase I/II trials targeting CD19 antigen for B-cell malignancies alone in a number of different CAR configurations (85, 129). The most commonly studied configurations contain CD28-CD3ζ or 41BB-CD3ζ endodomains. Early clinical trial reports include evidence of anti-tumor efficacy, long-term B-cell aplasia, and acute toxicity related to elevated serum inflammatory cytokine (**Table 1**) (101, 112, 130-134, 136-138). Early clinical trials with first generation CD19-specific CARs revealed minimal anti-tumor efficacy due to failed T-cell persistence (130). A trial comparing CD19-specific second generation CAR containing CD28-CD3ζ signaling domains and first generation CAR containing CD3ζ signaling domain by infusing both populations simultaneously into patients demonstrated improved persistence of second generation CAR over first generation CAR (101). Lymphoablative preconditioning prior to CAR^+ T-cell transfer appears to improve objective clinical responses. Infusion of CD19 CAR T cells with CD28-CD3ζ endodomain demonstrated no clinical response in the absence of a preconditioning regimen, but stable disease and lymph node mass reduction was achieved in patients when CAR^+ T cells were administered following cyclophosphamide preconditioning (133, 136, 137). Notably, clinical trials at University of Pennsylvania for adult patients with relapsed chronic lymphocytic leukemia (CLL) and pediatric patients with relapsed acute lymphoblastic leukemia (ALL) have demonstrated remarkable efficacy with 2 of 3 and 1 of 2 patients achieving complete responses, respectively (111, 112, 138). Anti-tumor efficacy was associated with *in vivo* expansion of T cells, transient toxicity related to elevated serum cytokine, long-term persistence of CAR^+ T cells and persistent B-cell aplasia. One patient with pediatric ALL treated with CD19-redirected CAR T cell demonstrated transient response and relapse of $CD19^{neg}$ tumor, indicating tumor escape can occur via outgrowth of antigen negative tumor cells (111). Recent reports from trials at Memorial Sloan Kettering also demonstrate remarkable efficacy, achieving complete remission in 14 of 16 patients, again concomitant with toxicity associated with elevated serum cytokine (131, 132). Optimal preconditioning regimen, CAR configuration, and dosing schedule are still components of on-going clinical investigation, but CD19-specific CAR^+ T cells demonstrate significant promise for treatment of B-cell lineage malignancies.

Institution	Tumor classification	Signaling domains	Preconditioning	Normal B cell aplasia	Tumor regression	Cytokine-associated toxicity	Number of patients
Baylor College of Medicine	Non-Hodgkins Lymphoma	CD28CD3ζ or CD3ζ	None	No	No	No	6
City of Hope	Diffuse large cell /Follicular lymphoma	CD3ζ	None or fludarabine	No	No	No	4
Memorial Sloan Kettering	CLL	CD28CD3ζ	None or Cyclophosphamide	No	Yes	Yes	9
Memorial Sloan Kettering	ALL	CD28CD3ζ	Cyclophosphamide	No	Yes	Yes	16
National Cancer Institute	Follicular Lymphoma/ CLL	CD28CD3ζ	Cyclophosphamide and fludarabine	Yes	Yes	Yes	8
University of Pennsylvania	CLL	41BBCD3ζ	Variable	Yes	Yes	Yes	3
University of Pennsylvania	ALL	41BBCD3ζ	Variable	Yes	Yes	Yes	2

Table 1. Results of clinical trials with CD19-specific CAR$^+$ T cells. Summary of published results from clinical trials targeting B-lineage malignancies with CD19-specific CAR$^+$ T cells, highlighting differences in CAR configuration, preconditioning regimen and specific outcomes, such as observed tumor regression, B-cell aplasia apparent greater than 3 months following T-cell treatment, and induction of cytokine-associated toxicity.

1.2.7 CARs in the clinic: solid malignancies

Beyond targeting hematological malignancies, CARs have been developed for treatment of solid tumors. Initial clinical trials targeting carbonic anhydrase IX (CAIX) and α-folate receptor for treatment of renal cell carcinoma and ovarian cancer, respectively, demonstrated no clinical response and limited persistence of CAR-modified T cells (139, 140). Clinical trial of a CAR redirected to GD2 for treatment of neuroblastoma demonstrated regression or necrosis in half of treated patients and complete response persisting longer than 6 weeks in 3 of 11 patients (141, 142). Two clinical trials have revealed the potential for detrimental on-target, off-tissue toxicity. Targeting renal cell carcinoma with CAR redirected to CAIX showed activity against normal tissue CAIX expression, resulting in damage to bile ducts and reversible cholangitis (140). Infusion of HER2-redirected CAR T cells for treatment of colorectal cancer resulted in respiratory distress and death in one patient following massive T-cell infiltration to the lungs, attributed to normal tissue expression of HER2 in pulmonary tissue (143). Additional trials have been initiated with CARs targeting various antigens, such as carcinoembryonic antigen (CEA) for colorectal cancer, epidermal growth factor receptor variant III (EGFRvIII) and interleukin-13 receptor α2 (IL13Rα2) for glioblastoma, mesothelin for mesothelioma, and vascular endothelial growth factor receptor 2 (VEGFR-2) to target angiogenic processes, due to promising preclinical data (144-153).

Early trials have highlighted some difficulties in extending CAR T-cell therapy, which has shown success in treatment of hematological malignancies. T cells must extravasate and home to sites of solid tumors to exert therapeutic efficacy. Engineering T cells with chemokine co-receptors can induce T-cell homing to chemokine produced by tumors. Engineering T cells with CXCR2 to redirect to CXCL1 and CXCL8 secretion by melanoma results in enhanced tumor infiltration and anti-tumor activity (154). Likewise, expressing CCR2 in mesothelin- and GD2-specific CAR^+ T cells for treatment of mesothelioma and neuroblastoma, respectively, or expressing CCR4 in CD30-specific CAR T cells for Hodgkin lymphoma demonstrate enhanced tumor infiltration and anti-tumor activity when compared to CAR-modified T cells without engineered homing molecules (155-157).

1.2.8 Safety and toxicity of genetically modified T cells

Initial clinical trials with genetically engineered T cells have demonstrated the potential for toxicity. Currently, there are four primary mechanisms of toxicity of genetically engineered T cells: (i) on-target, off-tissue, (ii) off-target, (iii) cytokine-induced, and (iv)

anaphylactic response due to immune response to foreign CAR moieties (**Figure 3**). On-target, off-tissue toxicity refers to toxicity against normal cells expressing tumor antigen, e.g. bile duct destruction after treatment with CAIX-specific CAR and activity against pulmonary tissue after treatment with HER2-specific CAR (140, 143). Off-target toxicity refers to cross-reactivity with unintended antigen resulting in T-cell activation and destruction of normal tissue. While this has not been documented with CAR T-cell treatment, off-target toxicity has been noted in T-cell trials with high affinity αβ TCRs specific for MAGE-A3 cross-reacting with titin, a protein expressed in striated muscle, resulting in cardiovascular arrest and death in two patients (70, 71). Cytokine-induced toxicity is associated with *in vivo* T-cell expansion and tumor destruction, resulting in release of high levels of inflammatory cytokines, such as IFN-γ, tumor necrosis factor-α (TNF-α), and interleukin-6 (IL-6), causing high fevers and hypotension (111, 112, 131, 132, 158). This has been noted in clinical trials with CD19-specific CAR T cells for B-cell malignancies and is directly correlated with tumor burden at the time of treatment. Corticosteroid treatment can curb inflammatory responses to treat these toxicities, however, there is concern that treating with steroids will also impair anti-tumor efficacy of CAR T-cell therapy (158). Treatment using IL-6 antagonist tocilizumab can rapidly reverse cytokine-induced toxicity, and may not negatively impact T-cell activity (111). Mouse models of syngeneic B-cell lymphomas from patients treated with CD19-specific CAR T cells containing CD28-CD3ζ endodomain configuration did not show any acute toxicity due to cytokine release, potentially due to altered metabolic profile of mice (159). Finally, recent trials with multiple infusions of CAR with scFv derived from murine sequences has resulted in anaphylaxis and cardiac arrest in one patient, most likely due to intermittent dosing schedule and development of IgE antibodies in response to murine scFv of CAR (160).

Strategies to limit toxicity are paramount for continued development of CAR^+ T-cell therapies for clinical application. Introduction of suicide genes has been employed to result in T-cell death following treatment with a chemical inducer to specifically ablate T cells in the event of observed toxicity. Initially, T cells were modified with herpes simplex derived thymidine kinase (HSV-TK) to result in ablation of T cells upon treatment with ganciclovir. However, HSV-TK proved to be highly immunogenic, eliciting anti-transgene immune responses that negatively affected T-cell persistence (161, 162). A novel inducible caspase 9 (iCasp9) has been developed in which a chemical inducer of dimerization (CID), AP1903, can be introduced into patient to induce iCasp9 dimerization and activation to initiate T-cell

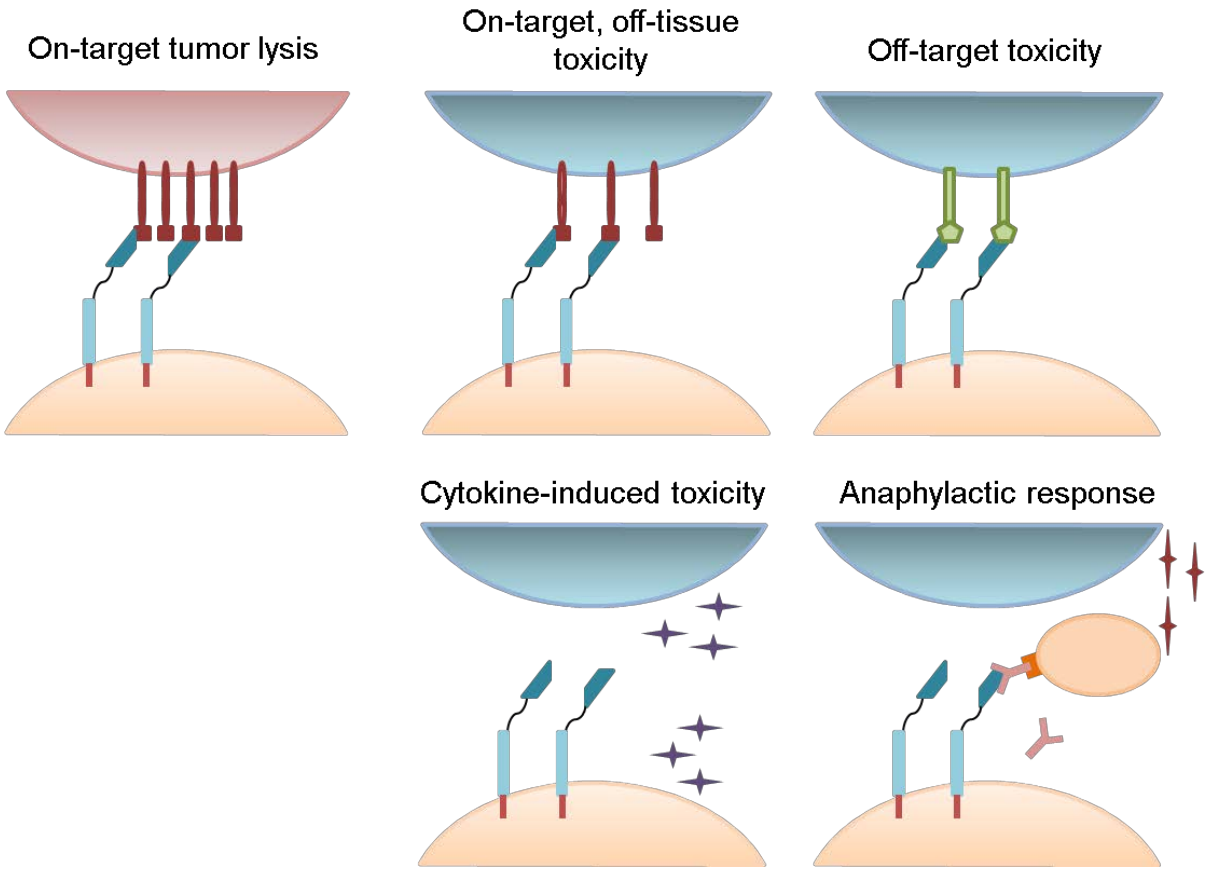

Figure 3. Potential mechanisms of toxicity of CAR$^+$ T cells. Depiction of four potential mechanisms of toxicity of CAR$^+$ T-cell treatments. On-target, off-tissue toxicity (top, left) describes CAR$^+$ T-cell recognition of antigen expressed on normal tissue. Off-target toxicity (top, right), describes the potential for non-specific CAR$^+$ T-cell recognition of normal tissue. While this has not been observed in CAR$^+$ T cells, loss of specificity has been described with T cells modified to express engineered TCRs. Cytokine-induced toxicity (bottom, left) describes toxicity mediated by CAR$^+$ T-cell activation and release of inflammatory cytokines, as described in clinical trials with CD19-specific CAR$^+$ T cells. Anaphylactic response (bottom, right) describes development of an IgE immune response to foreign CAR moieties that activates mast cell degranulation. This response was proposed to be the cause of anaphylaxis in one patient treated with an intermittent dosing schedule of mesothelin-specific CAR$^+$ T cells.

apoptosis. This strategy is appealing as it has proven highly effective in elimination of iCasp9 T cells, resulting in >90% T cell elimination within 30 minutes of CID administration and reversal of T-cell related toxicity and the inducing agent is otherwise biologically inert, enhancing safety (163, 164).

An alternative strategy to limit CAR^+ T-cell persistence is to introduce CAR as RNA species. CD19-specific CAR, mesothelin-specific CAR, and HER2-specific CAR have been transiently expressed by RNA transfer in human primary T cells (152, 165-169). CAR transgene is placed under control of T7 promoter, and RNA is transcribed *in vitro* from linearized DNA template by incubation with T7 polymerase, then subsequently transferred to activated T cells by electroporation. Prior T-cell activation is crucial for efficient RNA transfer as is typically achieved via activation with anti-CD3 and CD28 antibodies coated on microbeads in the presence of IL-2 (165, 169). RNA-modification is generally more efficient and less-toxic than DNA-modification, primarily attributed to smaller size of transcripts. RNA transcripts have been optimized to increase stability (152). Three primary determinants of stability of *in vitro* transcribed RNA are (i) presence of 3' untranslated region (UTR), (ii) long poly tail, which can be included in DNA template and in vitro transcribed or added after transcription by *E. coli* poly(A) polymerase (E-PAP), and (iii) use of RNA cap analog to ensure incorporation in proper orientation, thereby increasing the number of "readable" transcripts. Expression of CAR from introduced mRNA is directly correlated to amount of RNA transferred, therefore, this system allows for efficient, high expression of transcript (165, 167). Thus, both quality and quantity of RNA transcript affects the levels and duration of CAR expression. Increased expression of CAR prolonged the duration of CAR expression and specific lysis, but did not increase lytic ability at any given time point. On average, CAR expression remains detectable 5-7 days from RNA transfer.

While this strategy limits potential for deleterious long-term on-target, off-tissue toxicity, it also limits anti-tumor potential of T cells. Although multiple infusions can reduce tumor burden and prolong survival, tumors recur after cessation of treatment. Therefore anti-tumor efficacy can be inferior to treatment with lentivirally-introduced CAR (152, 167). Investigations of dosing and preconditioning have identified that lymphodepletion immediately before infusion and weighted split-dosing, with one larger, front-loaded dose followed by smaller maintenance doses result in superior anti-tumor activity of RNA-modified CAR^+ T cells (168).

1.3 Glioblastoma multiforme

Glioblastoma multiforme is a classified as a grade IV central nervous system (CNS) tumor of astrocytic origin. Despite aggressive investigation of new therapeutic approaches, patients diagnosed with glioblastoma still face dismal prognosis, with median survival from diagnosis around 12 months with current standard of care, which includes surgical resection of tumor and treatment with chemotherapeutic alkylating agent temozolomide and whole-brain radiotherapy (170). Glioblastoma is characterized as a diffuse and heterogenous tumor, both hallmarks giving rise to difficulties in successful treatment (171). While glioblastoma can involve any neuroatomical structure, it is most common in cerebral hemispheres. Total microscopic resection cannot be achieved due to diffuse nature, and remnant cells are often the source of disease recurrence. Glioblastoma arises from two distinct routes: primary, in which glioblastoma is diagnosed *de novo*, or secondary, in which glioblastoma progresses from initial diagnosis of a lower grade glioma (172, 173). Primary glioblastoma typically arises in older patients, and is associated with epidermal growth factore receptor (EGFR) gene amplification, phosphatase and tensin homolog (PTEN) mutation, absence of isocitrate dehydrogenase (IDH) mutations and accounts for 95% of diagnosed glioblastomas. In contrast, secondary glioblastoma is more commonly diagnosed in younger patients, and is associated with lack of EGFR amplification, p53 mutations, IDH mutations and accounts for ~5% of diagnosed glioblastomas. Age is an important prognostic indicator of survival with older patients having significant worse survival outcomes than younger patients (174, 175).

1.3.1 Heterogeneity of glioblastoma

Gene expression profiling categorizes glioblastomas into several subtypes. Initially, Phillips, et. al. described 3 subtypes characterized by distinct genetic signatures: proneural, proliferative, and mesenchymal. More recently, the Cancer Genome Atlas defined four subtypes: classical, proneural, mesenchymal and neural. The mesenchymal and proneural subtypes match previous descriptions of primary and secondary glioblastomas, respectively. Mesenchymal subtypes show mesenchymal differentiation and occur in older patients, associated with abnormal EGFR amplification and PTEN loss, while proneural show neuronal differentiation, occur in younger patients and are associated with better outcomes.

The molecular heterogeneity of glioblastoma is incredibly complex and varies widely from patient to patient. Commonly described genomic alterations in glioblastoma include:

Loss of heterozygosity of chromosome 10q, loss/mutation of PTEN, O-6-methylguanine-DNA-methyltransferase (MGMT) promoter methylation, mutations of p53, IDH1 and IDH2 mutations, loss of p16/INK4A, and EGFR gene amplification and overexpression (171, 173, 176-178). Loss of heterozygosity of chromosome 10q is frequently described in primary and secondary glioblastoma patients, although more commonly in older patients, and is associated with poor survival (173, 174, 179). PTEN deletion is due to loss of heterozygosity at chromosome 10q and occurs in 50-70% of primary glioblastoma and 54-63% of secondary glioblastoma patients (173, 178). PTEN inhibits signaling through phosphoinositol-3-kinase (PI3K)/Akt pathway by inhibiting Akt phosphorylation. Thus, loss of PTEN results in dysregulated signaling through PI3K/Akt and is associated with poor prognosis (180). MGMT is a DNA repair protein that can remove alkyl groups for the O6 position of guanine, a common mechanism of cell toxicity of chemotherapeutic agents like temozolomide (178, 181). Epigenetic silencing MGMT by promoter methylation results in defective DNA repair, and is associated with favorable prognosis of glioblastoma patients. TP53 encodes a well described tumor suppressor protein that is commonly mutated in glioblastoma. TP53 mutations occur in about 30% of primary glioblastomas and 50% of secondary glioblastomas. So far, TP53 mutation status has not been associated with prognosis (173, 182). IDH is an enzyme of the citric acid cycle, which is involved in metabolic cell processes, including oxidative stress and respiration and lipid synthesis. Mutation of IDH1 or IDH2 occurs in ~10% of glioblastomas, more frequently in younger patients, and confers a prognostic advantage (176). P16/INK4A binds cyclin-dependent kinase 4 (CDK4) and inhibits its formation of complex with cyclin D1, which inhibits phosphorylation of retinoblastoma protein (Rb), a tumor suppressor protein responses for inhibiting cell proliferation. Loss of p16/INK4A occurs in 20-57% of glioblastoma patients. There is a significant association between loss of p16/INK4A and EGFR amplification (173, 175, 178, 183).

1.3.2 EGFR amplification and overexpression in glioblastoma

One of the most common gene-amplified and overexpressed oncogene in glioblastoma is EGFR, present in 40-50% of patients (176, 181). The epidermal growth factor receptor family contains four tyrosine kinase receptors, including EGFR/ErbB, Her2/ErbB2, ErbB3, and ErbB4. The first family member, EGFR, is expressed on many normal tissues and commonly overexpressed and/or mutated in many cancers, including head and neck, lung, esophagus, stomach, colon, kidney, bladder, breast, uterus, cervix,

ovarian, prostate, and brain (184, 185). EGFR is composed of an extracellular region with four domains with distinct function (domains I, II, III, and IV), a transmembrane region, a tyrosine kinase domain and a C-terminal domain. Ligands that bind EGFR include epidermal growth factor (EGF), transforming growth factor α (TGF-α), and amphiregulin. Ligands bind the extracellular domains I and III, which frees the dimerization arm of domain II from its interaction with domain IV to interact with another molecule of EGFR to form a homodimer or another family member (HER2, ErbB3, or ErbB4) to form a heterodimer. A conformational change associated with dimer formation activates the tyrosine kinase domain, which binds adenosine triphosphate (ATP) and autophosphorylates multiple tyrosine residues in the C-terminal domain of EGFR (186, 187). The primary signaling pathways activated by EGFR include MAPK, PI3K/Akt, PLC, signal transducer and activator of transcription (STAT), and SRC/FAK (185, 188).

Overexpression of EGFR leads to dysregulation of signaling pathways, and results in enhanced cell survival, proliferation, migration, invasion, and support of angiogenesis to contribute to tumor growth and metastatic spread (184, 189). In 30-50% of patients with EGFR amplification, a mutant form of EGFR, EGFRvIII is overexpressed (190). EGFRvIII has deletion of exons 2-7, resulting in truncated extracellular domain, which is weakly, but constitutively active (191). Weak signaling through EGFRvIII results in inefficient internalization and degradation, causing sustained signaling (192). Overexpression of EGFRvIII causes proliferation of cells and can induce transformation (193-195). Prognostic implications of EGFR overexpression have been contradictory. Several reports describe no impact of EGFR amplification on survival when analyzing the whole population of glioblastoma patients (196-199). By stratifying into groups based on age, EGFR may be linked to poor prognosis in younger patients, less than 60 years old (197, 198, 200). Further division based on p53 mutation status identified EGFR as a significant indicator of poor prognosis only in younger patients with no p53 mutations (198). A recent study analyzing the impact of EGFR expression on newly diagnosed patients with uniform diagnosis of glioblastoma identified EGFR amplification as a poor indicator of survival, and described EGFRvIII overexpression correlating with worse survival within EGFR amplified tumors (190). In contrast, EGFR has been reported as a predictor of prolonged survival, particularly in patients over 60 years old with glioblastoma (180, 183). EGFR gene amplification has also be associated with improved prognosis when present concomitant with homozygous p16/INK4A deletion, and worse prognosis when present concomitant with chromosome 7

polysomy (200). Thus, impact of EGFR on survival in patients with glioblastoma is influenced by age and complex relationships with other molecular characteristics of the tumor.

1.3.3 Targeting EGFR in glioblastoma: tyrosine kinase inhibitors

Because EGFR is overexpressed in glioblastoma and does not have expression reported in normal CNS tissue, it has been the target of many novel therapeutic strategies for glioblastoma treatment (189, 201). Small molecule tyrosine kinase inhibitors, such as erlotinib and gefitinib, compete for the ATP-binding site in the tyrosine kinase domain of EGFR to inhibit phosphorylation and downstream signal propagation (189). Studies with head and neck and colorectal cancer cell lines showed induction of cell cycle arrest and apoptosis when treated with erlotinib (202). *In vitro* inhibition of glioblastoma cell lines with erlotinib demonstrated inhibition of anchorage-independent cell proliferation and inhibition of molecular effectors of cell invasion, such as serine proteases and metallaproteases (203, 204). Phase III clinical trials for non-small cell lung carcinoma, erlotinib demonstrated significant improvement in median survival (205). However, trials in patients with newly diagnosed or recurrent glioblatoma have demonstrated limited or no therapeutic benefit of erlotinib treatment (206, 207). *In vitro* study of gefitinib demonstrated inhibition of growth in a variety of EGFR-expressing cell lines, such as breast, colon and ovarian, and evidence of induction of cell cycle arrest and apoptosis (208-210). However, in clinical trials with newly diagnosed or recurrent glioblastoma, patients given gefitinib given concomitant with or following radiation therapy did not demonstrate improvement in survival (211, 212). Analysis of tumor tissue from glioblastoma patients following gefitinib treatment showed efficient dephosphorylation of EGFR, but not significant inhibition of downstream signaling pathways, demonstrating the role of compensatory signaling pathways and altered signaling regulation in drug resistance (213). Irreversible tyrosine kinase inhibitors, which form covalent bonds to tyrosine kinase domain of EGFR to permanently inhibit function, enhance EGFR inhibition and are in preclinical development (185, 189).

1.3.4 Targeting EGFR in glioblastoma: Monoclonal antibodies

Monoclonal antibodies specific for EGFR can also be used to inhibit EGFR signaling, such as cetuximab, which binds the extracellular domain III of EGFR to prevent ligand binding and extracellular dimerization, thus inhibiting EGFR signaling (214). Treatment of murine intracranial and subcutaneous glioma xenografts with cetuximab has demonstrated

decreased tumor cell proliferation and improved overall survival (215, 216). In a phase II clinical trial of cetuximab as a monotherapy in recurrent gliomas, minimal anti-tumor activity was reported and was found to be independent of EGFR amplification status (217). However, patients with EGFR-amplified glioblastoma that did not express EGFRvIII demonstrated improved progression-free survival relative to those expressing EGFRvIII (218). Similar to finding with tyrosine kinase inhibitors, cetuximab inhibits EGFR phosphorylation, but does not sufficiently inhibit downstream pathways, reaffirming the role of compensatory signaling and pathway regulation as mechanisms of therapy resistance (219). Activation of other ErbB family members, such as HER2 or ErbB3, can overcome cetuximab inhibition of EGFR, therefore, targeting multiple EGFR family members may be a strategy for enhanced therapeutic efficacy (220). While largely ineffective as a monotherapy, cetuximab has been shown to enhance radiosensitivity when combined with radiotherapy *in vitro* and *in vivo* (215, 221). Clinical evaluation of cetuximab in combination with temozolomide and radiation is underway (222).

Nimotuzumab is an EGFR-specific monoclonal antibody which binds to an epitope in domain III of EGFR that highly overlaps with that of cetuximab, and inhibits ligand binding and EGFR activation (223, 224). Similar to cetuximab, nimotuzumab sensitizes cells to radiation (225). Treatment with nimotuzumab as a monotherapy administered following standard treatment in newly diagnosed glioblastoma patients demonstrated no significant improvement in overall survival, but may benefit a subset of patients with EGFR amplified tumors with non-methylated MGMT promoters (226). When combined with radiation therapy, nimotuzumab demonstrated significant survival benefit for patients with high grade gliomas (grade III anaplastic astrocytomas and grade IV glioblastomas) and excellent tolerability (227).

While cetuximab and nimotuzumab bind an overlapping epitope on EGFR and have similar mechanisms of action, there are notable differences between the two antibodies (**Table 2**). Clinical trials with nimotuzumab have noted no incidence of EGFR-related toxicity, in contrast to trials with cetuximab in which grade III and IV acneiform rash is common (228-230). Further investigation into differences between cetuximab and nimotuzumab have identified a role of the intermediate affinity of nimotuzumab, with a K_d value ~1 log higher than cetuximab and 59-fold slower rate of association, in reduction of normal tissue toxicity (231). Nimotuzumab has demonstrated a requirement for bivalent binding to recognize EGFR resulting in reduced binding when EGFR is expressed at low levels, such as the

	Cetuximab	Nimotuzumab
K_d (mol/L)	$1.8x10^{-9}$	$2.1x10^{-8}$
k_{on} $([s*mol/L]^{-1}$	$3.1x10^{6}$	$5.2x10^{4}$
k_{off} (1/s)	$5.8x10^{-3}$	$1.1x10^{-3}$
$t_{1/2}$	120 s	630 s
Isotype	IgG1	IgG1
Mechanism	Inhibits proliferation, induces apoptosis, ADCC, complement	Inhibits proliferation, induces apoptosis, ADCC, complement, inhibits angiogenesis
Toxicity	Common grade 3-4 skin rash	No observed skin rash

Table 2. Differences and similarities between cetuximab and nimotuzumab. Nimotuzumab has a 1-log higher dissociation constant than cetuximab, characterized by 59-fold decreased rate of association and 5.3-fold decreased rate of dissociation, resulting in a 5.3-fold longer half-life of interaction with EGFR than cetuximab. Both antibodies are class IgG1, and therefore can mediate antibody-dependent cell cytotoxicity (ADCC) and complement activation. Both antibodies function by inhibiting cell proliferation and inducing apoptosis, but only nimotuzumab inhibits angiogenesis. While patients treated with cetuximab commonly develop a grade 3-4 skin rash, patients treated with nimotuzumab do not.

levels expressed in normal tissue, but efficient binding of high density. In contrast, cetuximab binds EGFR when expressed as a monovalent fragment or bivalent antibody, and does not show any ability to distinguish low EGFR density from high EGFR density, offering at least a partial explanation for the reduced normal tissue toxicity observed in patients treated with nimotuzumab. While nimotuzumab demonstrates reduced normal tissue binding, the intermediate affinity of nimotuzumab does not result in reduced activity relative to cetuximab against *in vivo* A431 xenografts, which express high levels of EGFR (231). Consequently, because cetuximab has a higher binding affinity than nimotuzumab, lower doses of cetuximab are required for EGFR inhibition, and at the same dose, cetuximab more markedly inhibits downstream EGFR signaling (224, 225, 232). Direct *in vivo* comparison of treatment of A431 xenografts shows that while nimotuzumab inhibited cell proliferation and reduced blood vessel formation, presumably by inhibiting vascular endothelial growth factor (VEGF) production, cetuximab does not, indicating some difference in mechanism of action (225). Despite these differences, both cetuximab and nimotuzumab are IgG1 isotype antibodies, and thus can mediate NK-cell cytolysis and activation of complement.

1.3.5 Targeting EGFR in glioblastoma: EGFRvIII peptide vaccine

Vaccination strategies have also been developed to activate the immune system to target glioblastoma. The most advanced of these strategies involves vaccination with a peptide or peptide-pulsed dendritic cells to activate T cells specific for a peptide of the fusion region of mutated EGFRvIII existing within the patient's natural TCR repertoire. A phase II clinical trial in newly diagnosed glioblastoma patients revealed treatment with peptide-based EGFRvIII vaccine significantly increased time to progression and overall survival (233). Similarly, a phase II trial in which newly diagnosed glioblastoma patients were treated with autologous, mature dendritic cells pulsed with the same peptide increased median survival of glioblastoma patients with only grade II side effects noted, demonstrating the immune system can be harnessed within the CNS to mediate anti-tumor effects without severe toxicity (234). However, despite prolonged time to progression in treated patients relative to control cohort, tumors eventually recurred and 82% were negative for EGFRvIII, demonstrating immunological escape as a mechanism of resistance (235). Vaccination approaches for glioblastoma treatment are promising; however, they face several limitations. Successful priming of a T-cell response in a patient requires a pre-requisite T-cell population with specificity for antigenic peptide. In addition, because the self-reactive T cells are tolerized during development, vaccination requires use of tumor-specific neoantigens.

Finally, vaccinations activate the immune system within the patient, often in the presence of immunosuppressive factors that may blunt the T-cell response to the vaccine.

1.3.6 Mechanisms of resistance to therapy of glioblastoma

The molecular heterogeneity of glioblastoma endows the ability to escape monotherapy targeted to inhibit EGFR activation, such as TK inhibitors and monoclonal antibodies, through activation of compensatory signaling through other receptor tyrosine kinases (RTK), most commonly hepatocyte growth factor receptor (MET) and platelet-derived growth factor receptor α and β (PDGFR α and β) (219, 236-238). Expression of EGFR and PDGFRα in distinct subpopulations of glioblastoma cells demonstrates a mosaic-like pattern of intratumoral heterogeneity and inhibition of both required to completely abrogate PI3K signaling (236, 237). Likewise, expression of MET has been shown to compensate EGFR inhibition in glioblastoma cell lines and inhibiting c-Met and EGFR restored sensitivity to treatment (239). Another potential explanation for reduced activity of TKIs and monoclonal antibodies in glioblastoma relates to their relatively large size and difficulty crossing the blood-brain barrier (BBB). While the BBB is compromised at the site of the tumor, intact BBB surrounding normal tissue with infiltrating glioblastoma is more difficult to access by such therapies, reducing overall anti-tumor efficacy. There is mounting evidence that a population of glioma-initiating stem cells play an important role in resistance to chemotherapy and radiotherapy, due altered DNA checkpoint activation and enhanced capacity for DNA repair (240, 241).

1.3.7 Immunosuppressive mechanisms of glioblastoma

Glioblastomas also exploit multiple immunosuppressive mechanisms to avoid recognition by the immune system (242, 244-247). Secretion of immunosuppressive factors transforming growth factor-β (TGF-β), interleukin-10 (IL-10), prostaglandin E2 (PGE2), and galectin-3 by glioma and glioma-initiating cells have been associated with inhibited T-cell proliferation, cytokine production and T-cell apoptosis (247, 248). Glioma cells also express cell surface receptors that inhibit T cell function, such as programmed death receptor ligand 1 (PD-L1) and Fas ligand (Fas-L) (249, 250). PD-L1 expression has been associated with induction of T-cell apoptosis, anergy, and T cells with T regulatory (T_{reg}) phenotype and cell contact dependent and independent suppressive function. Increased presence of T_{regs} has been observed in glioblastoma patients, both in tumors and peripheral blood, relative to normal donor peripheral blood (251). Myeloid-derived suppressor cells (MDSC) have also

been described to be present at a higher frequency in glioblastoma patients and suppress T-cell functions by secretion of immunosuppressive cytokines, expression of PD-L1, and induction of activated T-cell apoptosis (252).

1.3.8 CARs for glioblastoma

To avoid activation of tumor-specific T cells within immunosuppressed glioblastoma patients, and to avoid the requirement of a population of pre-existing T cells with desired specificity, CAR-modified T cells for adoptive transfer have been developed for glioblastoma with specificity for IL13Rα2, HER2, EGFRvIII and EphA2. An IL13 zetakine to is a CAR-based strategy in which and IL13 mutein with specific binding to IL13Rα2, present on 50-60% of glioblastomas, is fused to CD3ζ (253, 254). IL13 zetakine T cells display proliferation through zetakine stimulation, cytokine production, *in vitro* lysis of tumor targets and mediate regression of glioblatoma cell lines in an *in vivo* xenograft model (150, 254, 255). Importantly, IL13Rα2 zetakine T cells have demonstrated the ability to lyse glioma stem-like cells, indicating susceptibility of this chemotherapy and radiotherapy resistant population to T cell-mediated cytotoxicity (149). Early reports from a phase I trial with first generation IL13Rα2 CAR T cells injected intratumorally have shown good tolerability and some clinical benefit (256). However, studies with a second generation IL13Rα2 zetakine have demonstrated activity against normal tissue expressing IL13Rα1 (148). The potential for normal tissue toxicity may restrict IL13Rα2 CAR T cells from systemic administration. Second generation CAR specific for HER2, reported to be expressed in as many as 80% glioblastoma patients, has shown HER-2 specific cytokine production and tumor cell lysis, as well as cytotoxicity against $CD133^+$ glioma stem cells and regression of autologous patient gliobastoma xenografts (257, 258). A phase I clinical trial for treatment of glioblastoma patients with a HER2-specific CAR T cells is currently underway, however, HER2 is expressed on normal tissue, and there is potential for deleterious normal tissue toxicity (143). Likewise, targeting EGFRvIII on glioblatoma via an EGFRvIII-specific third generation CAR has exhibited specific T cell responses to EGFRvIII, but not wild type EGFR, expressing cells, including cytokine production and cytotoxicity of glioma cell lines as well as glioma stem cell lines, and *in vivo* anti-tumor activity against glioblastoma xenografts (145-147). Third generation EGFRvIII-specific CAR T cells are currently in clinical trial in combination with a chemotherapeutic lymphodepletion prior to T cell transfer (256). EGFRvIII is an ideal target for CAR-based T cell therapy as it is a true neo-antigen with no normal tissue expression, however, vaccine trials targeting EGFRvIII have demonstrated

immunologic escape of EGFRvIII negative glioma cells (235). Similarly, preclinical studies with HER2-specific CAR have also shown ability for immunological escape by outgrowth of $HER2^{neg}$ glioma cells. Because of the significant inter- and intra-tumoral heterogeneity of glioblastomas, it is very likely that targeting of two or more antigens will be required to completely eliminate tumor. Simultaneous targeting of two glioma antigens via introduction of two CAR constructs enhances anti-tumor efficacy and minimizes antigen escape mechanisms, demonstrating the potential for combinatorial antigen targeting within CAR-based therapies to mediate more complete anti-tumor responses (259).

Specific Aims

EGFR is an attractive target for glioblastoma therapy, however, expression on normal tissue and risk of on-target, off-tissue toxicity does not make it an ideal target traditional CAR-based T-cell immunotherapy approaches. The overarching goal of this dissertation is to develop an EGFR-targeted, CAR-based T cell therapy that minimizes the potential on-target, off-tissue deleterious toxicity without hampering anti-tumor activity.

Specific Aim 1: To reduce the potential for deleterious on-target, off-tissue toxicity, the goal of this specific aim is to transiently express EGFR-specific CAR derived from cetuximab, Cetux-CAR, by RNA transfer to human primary T cells and evaluate specific function relative to T cells stably expressing Cetux-CAR by DNA modification. In order to transfer RNA into human primary T cells on a scale feasible for clinical adaptation, we explored activating T cells with aAPC to facilitate numeric expansion prior to RNA transfer and optimized a protocol to transfer RNA into numerically expanded, activated T cells. DNA-modified and RNA-modified T cells were compared for (i) phenotype by flow cytometry, (ii) production of IFN-γ and TNF-α in response to $EGFR^{+}$ target cells by intracellular cytokine staining, (iii) specific lysis of $EGFR^{+}$ target cells by chromium release assay, and (iv) stability of CAR expression by flow cytometry. The *hypothesis* of this specific aim is that RNA-modification of T cells to express EGFR-specific CAR derived from cetuximab, Cetux-CAR, will result in (i) transient expression of Cetux-CAR, (ii) redirected specificity of RNA-modified T cells to EGFR similar to DNA-modified T cells, and (iii) loss of CAR expression which will coincide with loss of specific T-cell function in response to EGFR-expressing targets.

Specific Aim 2: Because the loss of CAR expression in RNA-modified T cells also abrogates anti-tumor activity, the goal of this specific aim is to generate a CAR with the capacity to distinguish between malignant and normal tissue by altering the scFv of CAR.

Recognizing that EGFR on glioblastoma is expressed at a higher density than EGFR on normal tissue, we developed a CAR based on the scFv on nimotuzumab, a monoclonal antibody that demonstrates reduced capacity to bind to low EGFR density on normal tissue while maintaining binding to high EGFR density on malignant tissue, Nimo-CAR. Cetux-CAR$^+$ T cells and Nimo-CAR$^+$ T cells were compared for T-cell phenotype by flow cytometry. CAR$^+$ T-cell function was compared by (ii) phosphorylation of signaling molecules Erk1/2 and p38 by phosflow cytometry, (iii) production of IFN-γ and TNF-α by intracellular cytokine staining, and (iv) specific cytotoxicity in response to EGFR$^+$ target cells with expressing EGFR at varying densities. The *hypothesis* of this specific aim is that Nimo-CAR$^+$ T cells will exhibit similar levels of T-cell activation, cytokine production, and specific lysis of targets at Cetux-CAR$^+$ T cells in response to target cells with high EGFR density, but reduced activation, cytokine production and specific lysis in response to target cells with low EGFR density.

Specific Aim 3: The goal of this specific aim is to determine anti-tumor activity of Cetux-CAR$^+$ T cells and Nimo-CAR$^+$ T cells *in vivo* against intracranial glioma xenografts with intermediate or low EGFR density. Mice bearing glioma xenografts were treated by intratumoral injection of CAR$^+$ T cells. Anti-tumor activity of Cetux-CAR$^+$ and Nimo-CAR$^+$ T cells was determined by (i) comparing relative tumor burden as determined by serial bioluminescent imaging of tumor to mice receiving no treatment and (ii) comparing overall survival of mice compared to mice receiving no treatment. The *hypothesis* of this specific aim is that Cetux-CAR$^+$ and Nimo-CAR+ T cells will demonstrate equivalent anti-tumor activity and control of xenografts with intermediate EGFR density, but only Cetux-CAR$^+$ T cells and not Nimo-CAR$^+$ T cells will demonstrate anti-tumor activity and control of xenografts with low EGFR density.

CHAPTER 2

Transient expression of EGFR-specific CAR by RNA-modification

2.1 Introduction

T cells can be genetically modified to express a CAR to redirect specificity for tumor-associated antigen (TAA) and adoptively transferred to patients for the purpose of tumor immunotherapy (94, 260). In recent clinical successes reported from CD19-specific CAR^+ T-cell therapy trials, complete response in 2 patients was observed with concomitant *in vivo* expansion of T cells and measurable IFN-γ response (111, 112). Patients experienced persistent B-cell aplasia, indicating the ability of infused CAR^+ T cells to persist *in vivo* and target normal tissue expressing CD19 antigen. While such toxicities are considered tolerable in the setting of CD19-redirected activity due to restriction of antigen expression to cell of B-cell lineage, antigens restricted or absent from normal tissue are rare. Serious adverse events in trials with CAIX-specific CAR, resulting in significant liver toxicity, and HER2-specific CAR, resulting in one patient death, demonstrate intolerable toxicities that can occur when targeting tumor antigen also expressed on normal tissue (140, 143).

Glioblastoma is the most common and aggressive primary brain and central nervous system malignancy (261). With conventional therapy, including surgical resection, radiation and chemotherapy with alkylating agents, overall median survival is approximately 1 year from diagnosis (170). EGFR is aberrantly overexpressed in more than 60% of adult primary glioblastoma and contributes to gliomagenesis by promoting cell division and invasion, promoting angiogenesis and inhibiting apoptosis (182, 262). However, current methods to target EGFR in glioblastoma, including tyrosine kinase inhibitors or monoclonal antibody therapy, have been largely negative due to the molecular complexity and heterogeneity of glioblastoma, drug resistance mechanisms, and poor penetration of blood brain barrier (171, 173, 177, 263). Targeting EGFR can cause toxicity, primarily observed in skin, gastrointestinal system, and kidney, due to its wide distribution of normal tissue expression (201).

Introducing an EGFR-specific CAR to T cells as RNA species has the potential transiently express CAR to reduce normal tissue toxicity by limiting CAR expression. Previous studies have demonstrated efficient transfer of CAR and TCR transgenes into human primary T cells following *ex vivo* stimulation (165, 167, 169, 264, 265). Expression of

CAR as RNA species has been shown to transiently redirect T-cell specificity to the desired antigen and mediate tumor regression by multiple injections in preclinical models of mesothelioma and leukemia and two patients with mesothelioma in a recently published case study (152, 168, 266). T-cell activation has been shown to be a prerequisite for successful introduction of RNA species (169). In addition, numeric expansion of T cells prior to introduction of RNA species is necessary to achieve clinically relevant T-cell numbers. T-cell activation for RNA transfer has been most commonly achieved by stimulation with anti-CD3 and anti-CD28 antibodies covalently linked to paramagnetic beads, however, while anti-CD3 and anti-CD28 beads mediate robust expansion of $CD4^+$ T cells, they do not efficiently expand $CD8^+$ T cells (97, 267). Development of a cell-based artificial antigen presenting cell platform derived from the erythroid leukemia cell line K562 for *ex vivo* T-cell expansion has several advantages over bead based approaches (95, 97). First, K562 do not express HLA-A, HLA-B, or HLA-DR, and therefore limit allogeneic-mediated T-cell expansion, but do express ICAM-1 and LFA-3 to mediate stable, stimulatory interactions with T cells. Additionally, K562 can be stably, genetically modified to express desired costimulatory molecules to support T-cell expansion (95). Stable expression of CD64, the high affinity Fc receptor, allows monoclonal antibodies to be "loaded" on the surface of K562 via Fc binding to CD64 to provide additional stimulatory properties (268). Studies evaluating K562 loaded with anti-CD3 (OKT3) and co-expressing co-stimulatory molecules CD86 and 41BB-L have demonstrated robust numeric expansion of $CD8^+$ T cells with improved production of IFN-γ and perforin (269).

We sought to transiently express an EGFR-specific CAR by RNA transfer to limit CAR expression and limit the potential for on-target, off-tissue toxicity. To achieve clinically relevant T-cell numbers, we evaluated RNA transfer to human primary T cells that had undergone numeric expansion by stimulation with OKT3-loaded K562 and compared their function to EGFR-specific CAR^+ T cells modified by stable DNA integration. We hypothesized that (i) stimulation of T cells with OKT3-loaded K562 could mediate numeric expansion of $CD8^+$ T cells favorable for RNA transfer, (ii) EGFR-specific CAR^+ T cells modified through RNA transfer would have equivalent lytic function as EGFR-specific CAR^+ T cells modified by stable DNA integration, and (iii) EGFR-specific CAR^+ T cells modified by RNA transfer would have transient redirected specificity for EGFR.

2.2 Results

2.2.1 Numeric expansion of T cells by artificial antigen presenting cells loaded with anti-CD3

Antigen-dependent stimulation through stable CAR expression achieved by DNA integration can be used to numerically expand CAR^+ T cells to clinically feasible numbers. The transient nature of CAR expression via RNA transfer requires numeric expansion of T cells to clinically feasible numbers to be achieved prior to RNA transfer of CAR. To determine the ability of aAPC to numerically expand T cells independent of antigen, we loaded anti-CD3 (OKT3) onto K562 via stable expression of the high affinity Fc receptor CD64 (**Figure 4A**). K562 also expressed CD86, 41BB-L, and a membrane bound IL-15 for additional T-cell costimulation. To determine the impact of aAPC density in co-culture to stimulate T cell expansion, peripheral blood mononuclear cells (PBMC) derived from healthy human donors were co-cultured with γ-irradiated aAPC at low density, 10 T cells to 1 aAPC (10:1), or high density, 1 T cell to 2 aAPC (1:2), in the presence of IL-2. T cells were restimulated with aAPC after 9 days. Following two cycles of aAPC addition, T cells numerically expanded when stimulated 10:1 and 1:2 with aAPC, however T cells with higher density of aAPC (1:2) achieved statistically superior numerical expansion (10:1 = 1083 ± 420 fold expansion, 1:2 = 1891 ± 376 fold expansion, mean ± S.D., n=6) ($p<0.0001$) (**Figure 4B**).

T cells expanded with lower density of aAPC contained a higher proportion of $CD8^+$ T cells than T cells expanded with higher density aAPC (10:1 = 53.9 ± 11.6% CD8, 1:2 = 28.1 ± 16.2% CD8, mean ± S.D., n=6) ($p<0.001$) (**Figure 5A**). $CD8^+$ T cells demonstrated similar fold expansion when stimulated with either ratio of aAPC, however, $CD4^+$ T cells demonstrated inferior fold expansion when stimulated with fewer aAPC (10:1 = 369 ± 227 $CD4^+$ fold expansion, 1:2 = 1267 ± 447 $CD4^+$ fold expansion, mean ± S.D., n=6) ($p<0.0001$) (**Figure 5B**). To determine if reduced fold expansion was due to increased $CD4^+$ T-cell death in cultures with fewer aAPC, $CD4^+$ and $CD8^+$ T cells were stained with annexin V and propidium iodide (PI) and analyzed by flow cytometry to determine cell viability. There was no difference in the proportion of viable cells in $CD4^+$ or $CD8^+$ T cells when stimulated with low or high density aAPC (**Figure 5C**). To determine if reduced fold expansion of $CD4^+$ T cells was due to decreased rate of proliferation, we stained T cells 9 days following stimulation with aAPC for intracellular Ki-67 expression and analyzed by flow cytometry. $CD8^+$ T cells demonstrated similar proliferation when stimulated with either low or high

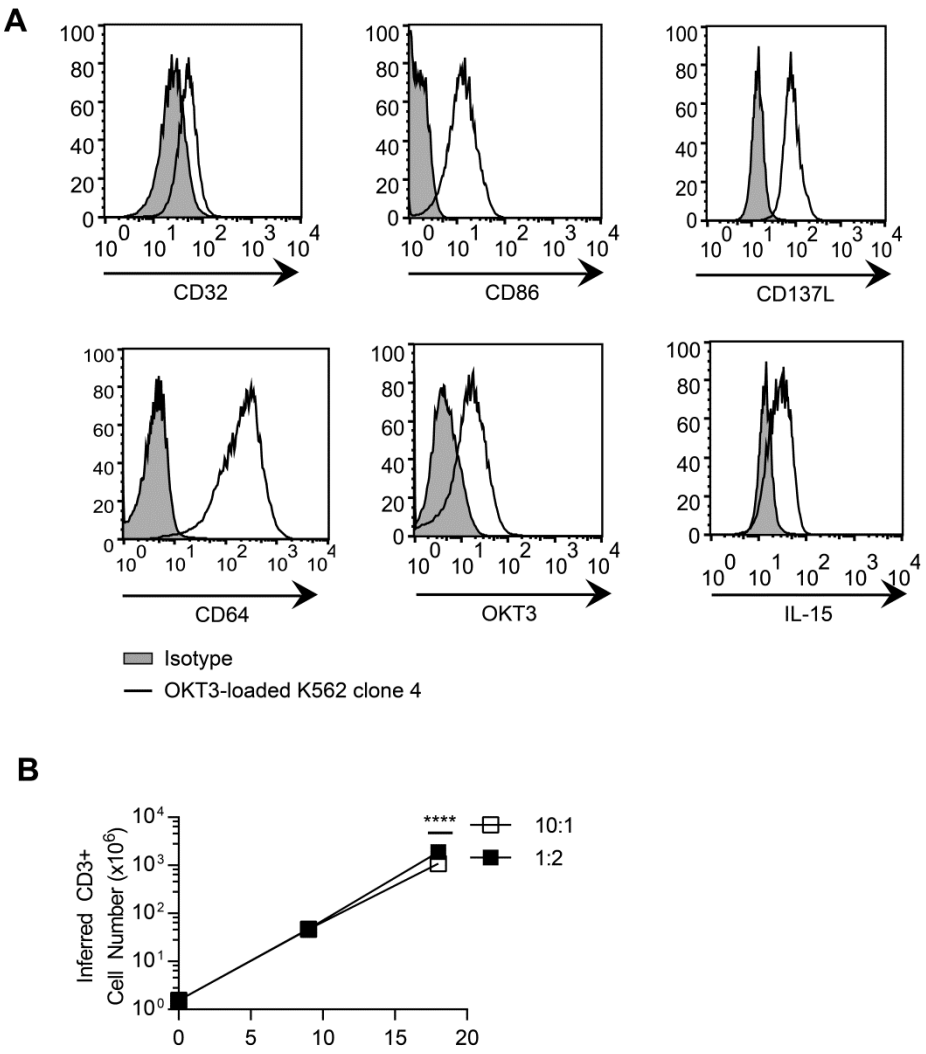

Figure 4. Numeric expansion of human primary T cells with artificial antigen presenting cells loaded with anti-CD3. (A) Phenotype of K562 clone 4 loaded to express anti-CD3 (OKT3) and irradiated to 100 gray measured by flow cytometry. (B) Numeric expansion of $CD3^+$ T cells following stimulation with low density of OKT3-loaded K562 (10 T cells to 1 aAPC) or high density of OKT3-loaded K562 (1 T cell to 2 aAPC). Inferred cell count calculated by multiplying fold expansion following a stimulation cycle to the total number of T cells prior to stimulation cycle. Data represented as mean ± SD, n=6, **** $p<0.0001$, two-way ANOVA (Tukey's post-test).

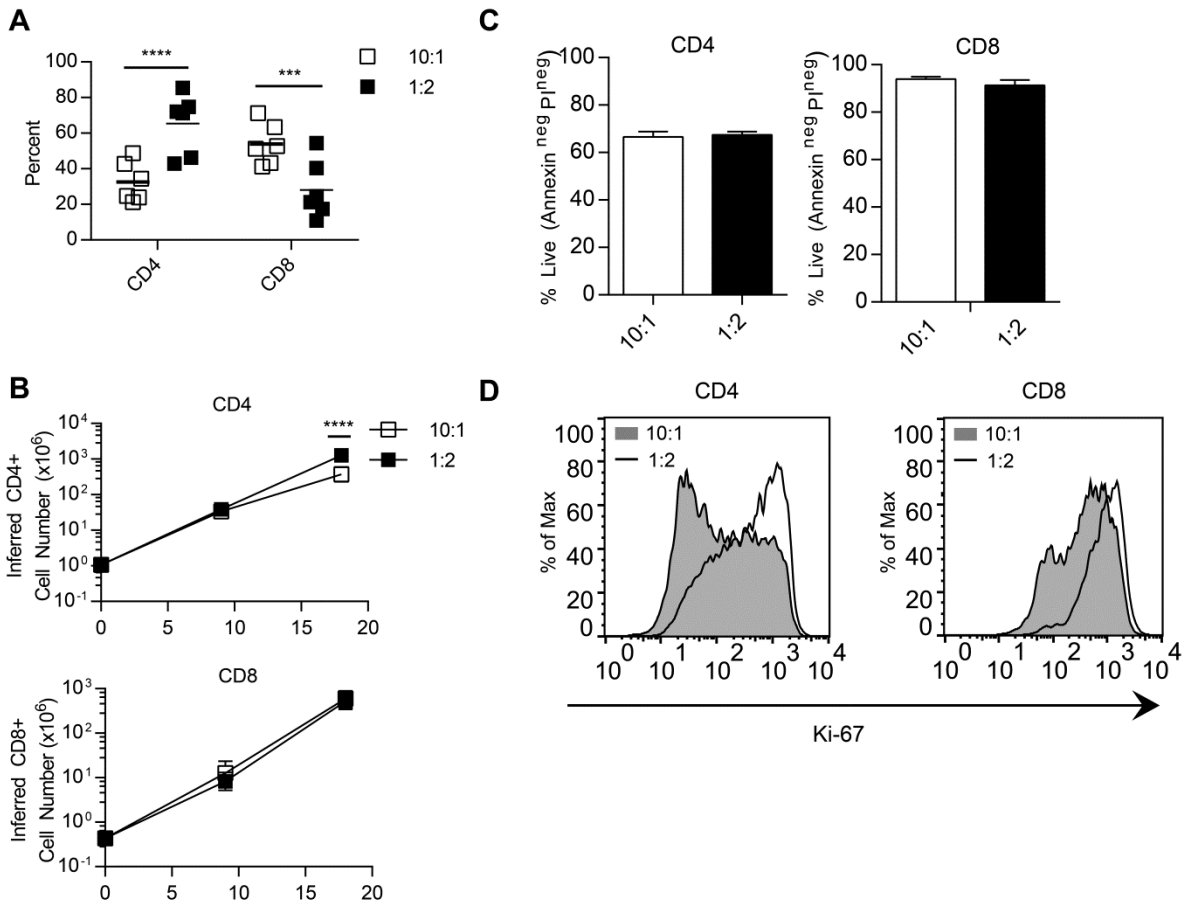

Figure 5. T cells expanded on low density aAPC contain higher ratio of CD8$^+$ T cells. (A) T cells expanded with low density aAPC (10 T cells to 1 aAPC) contain significantly more CD8$^+$ T cells and less CD4$^+$ T cells than T cells expanded with high density aAPC (1 T cell to 2 aAPC) as measured by flow cytometry following two stimulation cycles. Data represented as mean, n=6, *** p<0.001, **** p<0.0001, two-way ANOVA (Tukey's post-test). (B) Differences in CD4/CD8 ratio in T cells expanded with low density aAPC and high density aAPC is due to reduced fold expansion of CD4$^+$ T cells when expanded with low density aAPC. Data represented as mean ± SD, n=6, **** p<0.0001, two-way ANOVA (Tukey's post-test). (C) Differences in CD4/CD8 ratio in T cells expanded with low density aAPC and high density aAPC is not due to differences in cell viability. Viability of cells was determined by flow cytometry for Annexin V and PI staining following two stimulation cycles where Annexin V^{neg} PI^{neg} cells are considered live cells. Data represented as mean ± SD, n=3. (D) CD4$^+$ T cells have less proliferation when stimulation was low density aAPC than high density aAPC. Ki-67 was measured by intracellular flow cytometry as a marker for cellular proliferation following two stimulation cycles. Data shown as representative histogram of three independent donors.

density of aAPC, however $CD4^+$ T cells demonstrated reduced proliferation when stimulated with low density aAPC (**Figure 5D**). These data indicate that stimulating T cells with low density of aAPC results in less total T-cell expansion than T cells stimulated with high density of aAPC, characterized by increased proportion of $CD8^+$ T cells due to reduced proliferation of $CD4^+$ T cells.

2.2.2 T cells expanded with lower density aAPC demonstrate a more memory-like phenotype than T cells expanded with higher density aAPC

To determine if expansion with low density or high density aAPC impacted T-cell phenotype, we analyzed expression of a panel of mRNA transcripts (**Appendix A**) by multiplex digital profiling using nCounter analysis (Nanostring Technologies, Seattle, WA). Significant differential gene expression was determined by a $p<0.01$ and fold change greater than 1.5 in sorted $CD4^+$ or $CD8^+$ T cells expanded with low density (10:1 T cell:aAPC) or high density (1:2 T cell:aAPC) aAPC. $CD4^+$ and $CD8^+$ T cells expanded with high density aAPC demonstrated increased expression of genes associated with T-cell activation, such as CD38 and granzyme A in $CD4^+$ T cells and CD38 and NCAM-1 in $CD8^+$ T cells (**Figure 6**). In contrast, $CD4^+$ and $CD8^+$ T cells expanded with low density aAPC showed increased expression of genes associated with central memory or naïve T cells, including Wnt signaling pathway transcription factors Lef1 and Tcf7, CCR7, CD28, and IL7Rα (270, 271).

To further evaluate differential phenotype of T cells expanded with low or high density aAPC, we analyzed T cells for phenotypic markers by flow cytometry and evaluated subsets by coexpression of CCR7 and CD45RA where $CCR7^+CD45RA^+$ indicates naïve phenotype, $CCR7^+CD45RA^{neg}$ indicates central memory phenotype, $CCR7^{neg}CD45RA^{neg}$ indicates effector memory, and $CCR7^{neg}CD45RA^+$ indicates a $CD45RA^+$ effector memory phenotype (272). $CD4^+$ T cells expanded with low density aAPC contained less T cells with effector memory phenotype (10:1 = 61.9 ± 9.1%, 1:2 = 92.1 ± 3.9%, mean ± S.D., n=3) ($p<0.05$), but more T cells with a central memory phenotype (10:1 = 36.5 ± 9.4%, 1:2 = 13.6 ± 2.4%, mean ± S.D., n=3) ($p<0.05$) T cells (**Figure 7A**). Similarly, $CD8^+$ T cells expanded with low density aAPC contained significantly fewer T cells with effector memory phenotype (10:1 = 66.1 ±12.5%, 1:2 = 89.1 ± 1.7%, mean ± S.D., n=3) ($p<0.05$), but more central memory phenotype (10:1 = 32.3 ± 11.7%, 1:2 = 6.5 ± 2.8%, mean ± S.D., n=3) ($p<0.05$). When stimulated with low density aAPC, fewer $CD4^+$ T cells produce granzyme B ($p<0.001$) and fewer $CD8^+$ T cells produce granzyme B ($p<0.05$) and perforin ($p<0.001$) (**Figure 7B**).

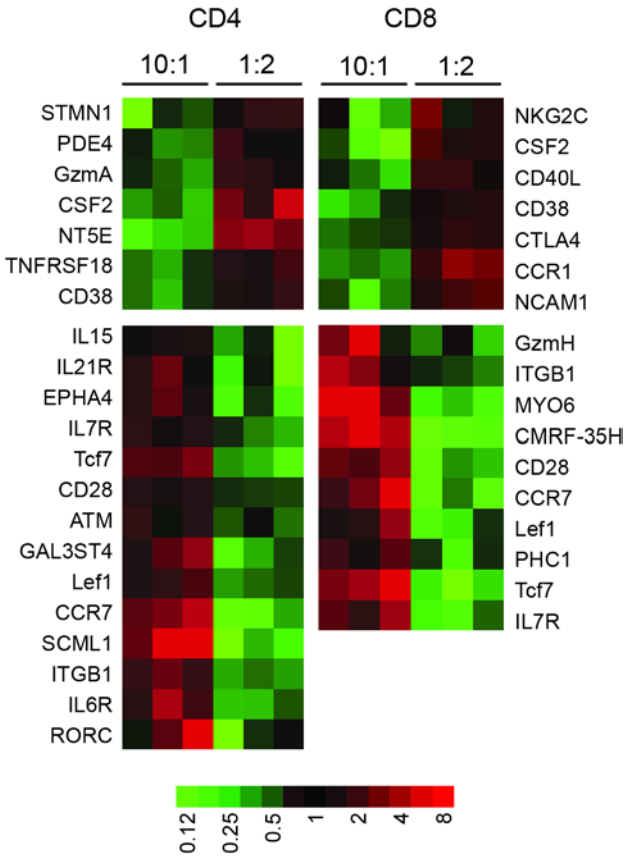

Figure 6. Differential gene expression in T cells stimulated with low or high density aAPC. Differential gene expression between $CD4^+$ and $CD8^+$ T cells stimulated with low or high density aAPC measured by multiplexed digital profiling of mRNA species following two cycles of stimulation. Significant up- or down-regulated transcripts was determined by greater than 1.5 fold difference in transcript level in 2/3 donors and $p<0.01$. Data represented by heat-map of fold difference, n=3.

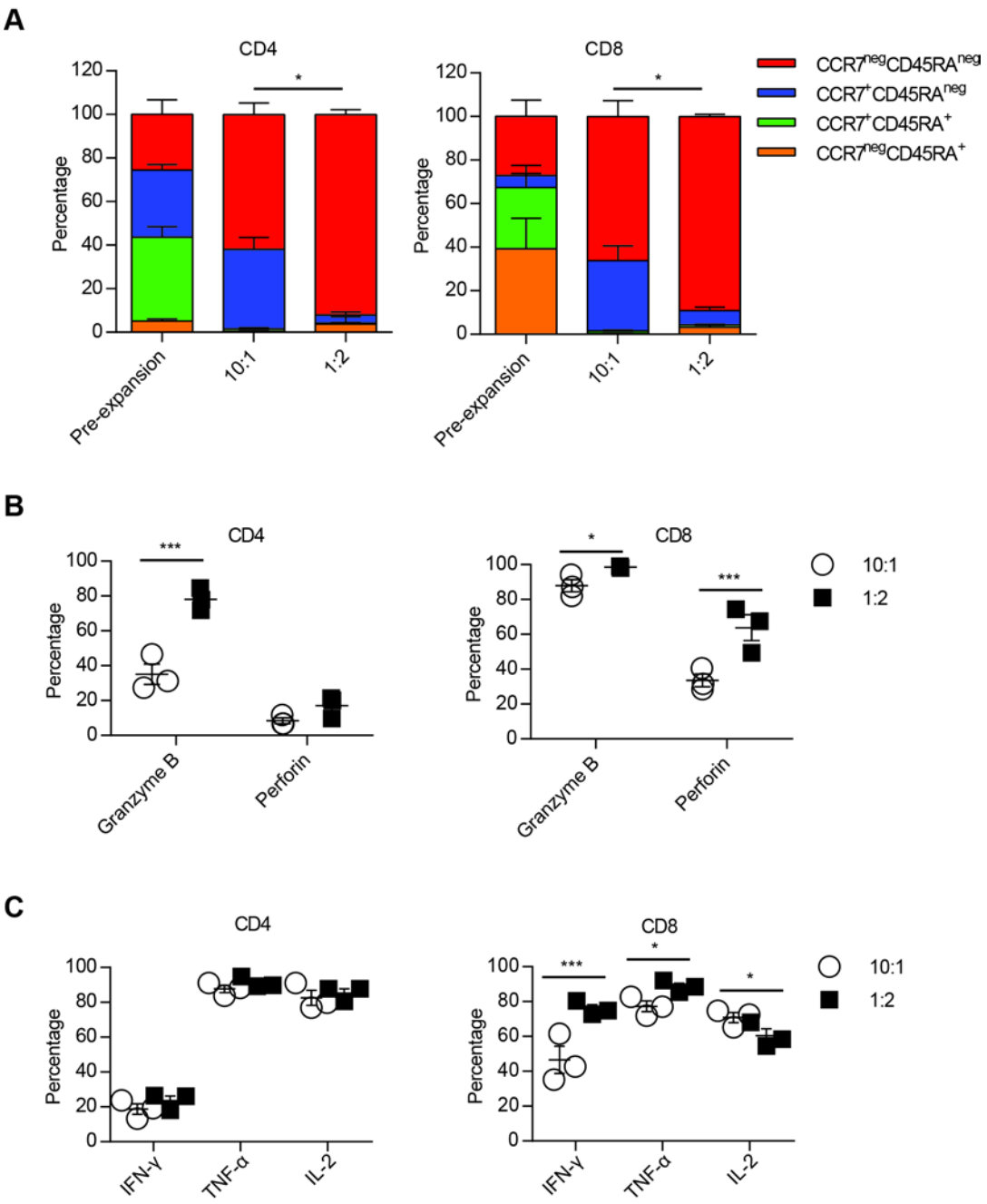

Figure 7. T cells expanded with low density aAPC have more central-memory phenotype T cells. (A) Memory marker analysis of T cells expanded with low density or high density aAPC was measured by flow cytometry for CCR7 and CD45RA following two cycles of stimulation. Cell populations in gated $CD4^+$ and $CD8^+$ T cell populations were defined as follows: effector memory = $CCR7^{neg}CD45RA^{neg}$, central memory = $CCR7^+CD45RA^{neg}$, naïve = $CCR7^+CD45RA^+$, effector memory RA = $CCR7^{neg}CD45RA^+$. Data represented as mean ± SD, n=3,* $p<0.05$, two-way ANOVA (Tukey's post-test). (B) Intracellular staining for granzyme and perforin in T cells following two stimulation cycles was measured by flow cytometry in $CD4^+$ and $CD8^+$ gated T-cell populations. Data represented as mean ± SD, n=3, *$p<0.05$, *** $p<0.001$, two-way ANOVA (Tukey's post-test). (C) Cytokine production following stimulation with PMA/Ionomycin was measured by intracellular cytokine staining in T cells following two cycles of stimulations by flow cytometry in $CD4^+$ and $CD8^+$ gated T cell populations. Data represented as mean ± SD, n=3, *$p<0.05$, *** $p<0.001$, two-way ANOVA (Tukey's post-test).

When stimulated with PMA/Ionomycin, $CD4^+$ T cells expanded with low and high density aAPC demonstrated equivalent production of IFN-γ, TNF-α, and IL-2, but $CD8^+$ T cells stimulated with low density aAPC demonstrated significantly less production of IFN-γ ($p<0.001$) and TNF-α ($p<0.05$), and more production of IL-2 ($p<0.05$) (**Figure 7C**). Collectively, these data suggest that T cells expanded with lower density of aAPC contain an increased proportion of T cells with central memory phenotype, reduced production of effector molecules granzyme B and perforin, and reduced production of effector cytokines IFN-γ and TNF-α compared to T cells expanded with higher density of aAPC.

2.2.3 Numeric expansion of T cells results in minimal change in TCRαβ diversity

We profiled TCRα and TCRβ diversity prior to and following expansion with low and high density aAPC by multiplex digital profiling using nCounter analysis (Nanostring Technologies, Seattle, WA) and calculated the relative abundance of each TCRα and TCRβ chain as a percentage of total T-cell population (**Appendix B**). Following *ex vivo* expansion with low and high density aAPC, $CD4^+$ and $CD8^+$ T cells expressed diverse TCRα and TCRβ alleles, indicating that the resulting population maintained oligoclonal TCRα and TCRβ repertoire (**Figure 8 and Figure 9**). High throughput sequencing of CDR3 regions using the ImmunoSEQ platform (Adaptive TCR Technologies, Seattle, WA) in the TCRβ chain in T cells prior to and following expansion with low and high density of aAPC was performed to determine if *ex vivo* expansion resulted in change in clonal composition of T cells. Relative counts of individual CDR3 sequence prior to and following expansion were plotted and fitted with a linear regression. If the number of CDR3 sequences prior to and following expansion were identical, the slope of the linear regression would be expected to be 1.0. In T cells expanded with low density aAPC, the slope of the linear regression was 0.75 ± 0.001, while in T cells expanded with high density aAPC the slope of the linear regression was 0.29 ± 0.003 (**Figure 10**). This indicates that T-cell populations expanded with low density aAPC maintain more CDR3 sequences from the input T-cell population than T cells expanded with high density aAPC. In sum, *ex vivo* expansion of T cells results in oligoclonal T-cell population when expanded with low and high density aAPC, but T cells expanded with low density aAPC may demonstrate less clonal loss following expansion.

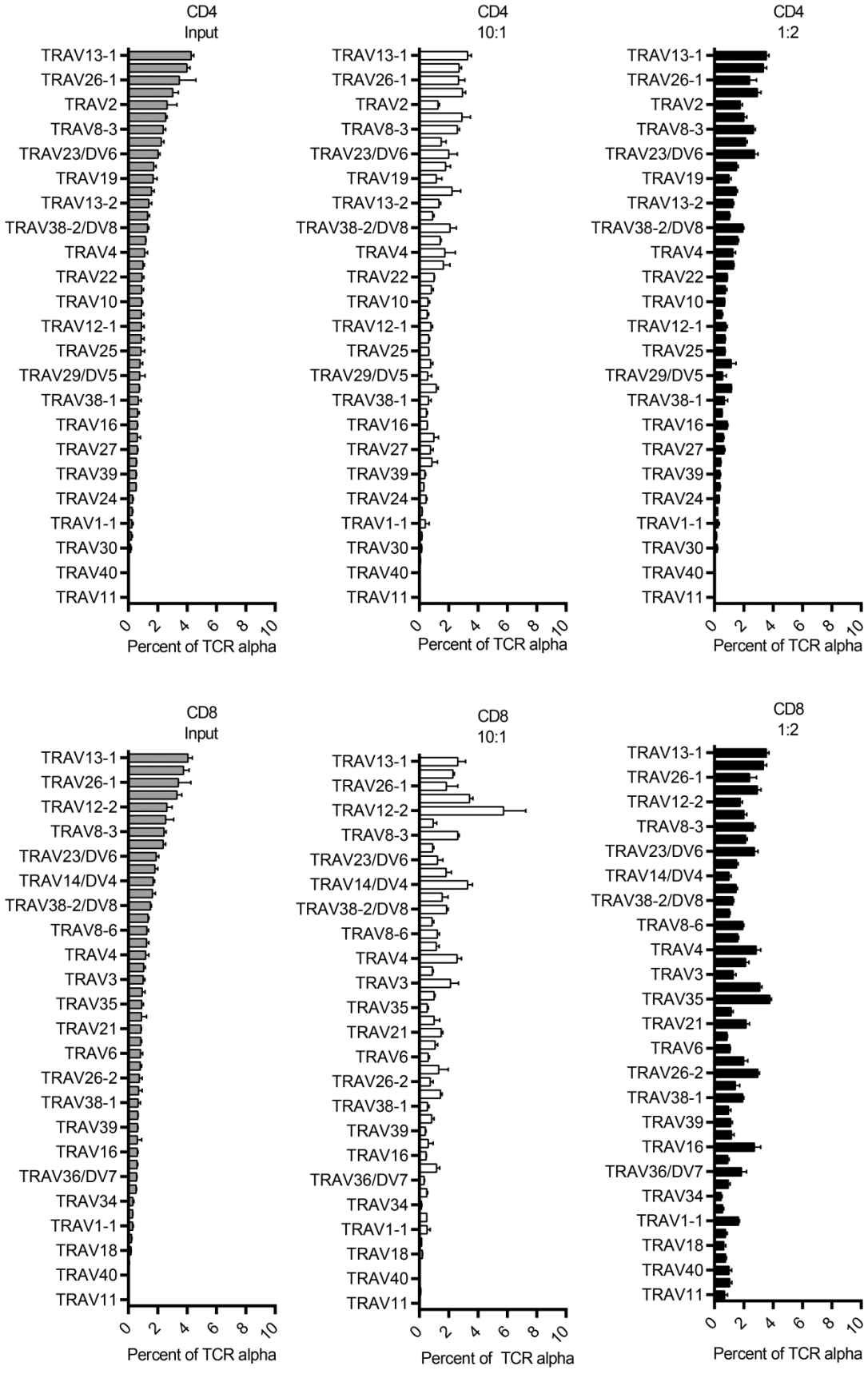

Figure 8. Diversity of TCR Vα after numeric expansion of T cells on aAPC. Diversity of TCR Vα in T cells expanded with low or high density aAPC was measured by digital multiplexed profiling of mRNA species and relative abundance of each TCR Vα was calculated as percent of total TCR Vα transcripts. Data represented as mean ± SD, n=3.

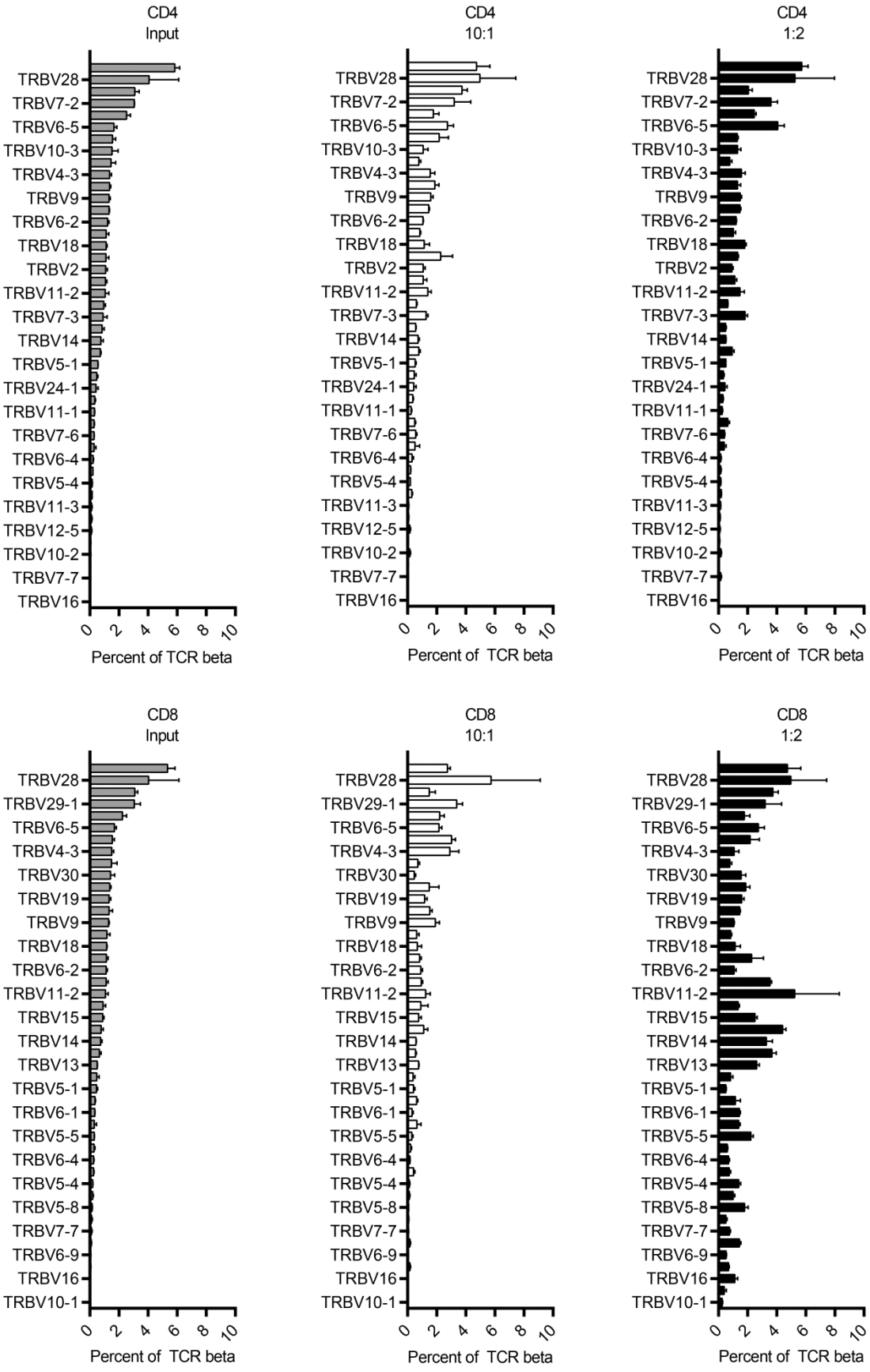

Figure 9. Diversity of TCR Vβ after numeric expansion of T cells on aAPC. Diversity of TCR Vβ in T cells expanded with low or high density aAPC was measured in sorted $CD4^+$ and $CD8^+$ T cells by digital multiplexed profiling of mRNA species and relative abundance of each TCR Vα was calculated as percent of total TCR Vα transcripts. Data represented as mean ± SD, n=3

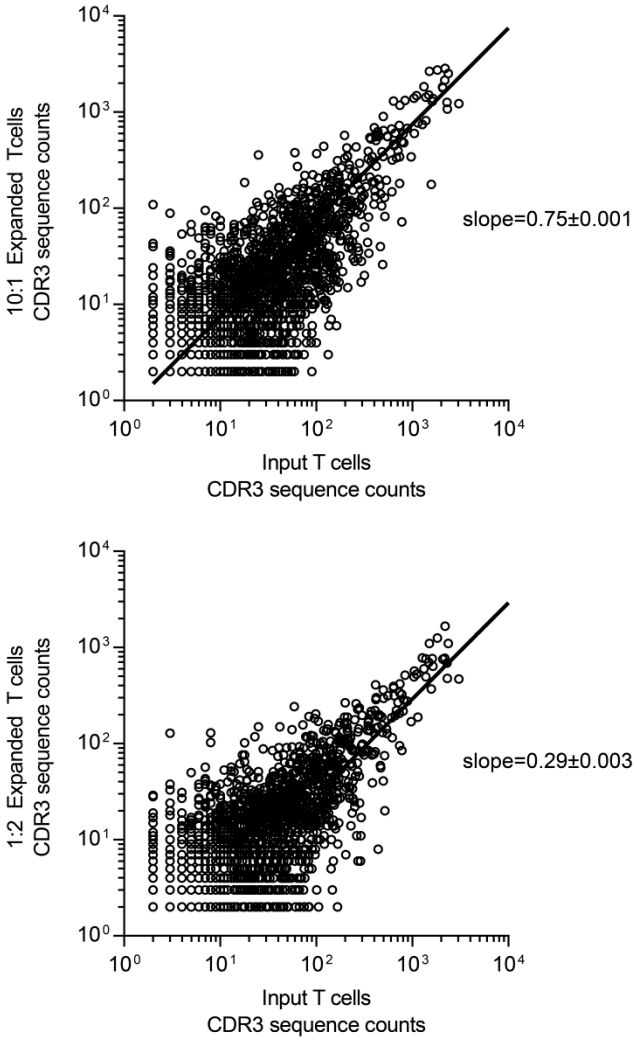

Figure 10. Diversity of CDR3 sequences in T cells after numeric expansion on aAPC. CDR3 sequences of TCR Vβ chain were determined by high-throughput sequences on ImmunoSEQ platform. Numbers of each unique sequence before numeric expansion were plotted against the numbers of the same sequence after numeric expansion with low density (10 T cells to 1 aAPC) or high density (1 T cell to 2 aAPC) aAPC. Data were fit with a linear regression and slope was determined. Data representative of two individual donors.

2.2.4 Optimization of RNA transfer to T cells numerically expanded with aAPC

To determine the ability of T cells stimulated with low and high density aAPC to accept RNA by electro-transfer, we electro-transferred *in vitro* transcribed RNA encoding green fluorescent protein (GFP) using the Amaxa Nucleofector 4D transfection system (Lonza, Cologne, Germany) using a variety of electroporation programs, including program EO-115, the manufacturer's recommended program for stimulated T cells, 4 days following stimulation with aAPC. Plotting the mean fluorescent intensity (MFI) of GFP versus the viability of T cells determined by PI staining revealed an inverse correlation between GFP expression and T-cell viability following RNA transfer. Compared to T cells stimulated with low density aAPC, T cells stimulated with high density aAPC demonstrated both reduced expression of GFP by RNA transfer and reduced viability in response to every electroporation program evaluated (**Figure 11A**). As a result, T cells stimulated with low density aAPC (10 T cells to 1 aAPC) were used for further experimentation. Because T-cell numeric expansion prior to RNA transfer is desirable to achieve clinically relevant T-cell numbers for infusion, we evaluated the capacity of T cells undergoing multiple rounds of stimulation by recursive addition of aAPC every 9 days to accept RNA transcripts by electro-transfer. In each successive round of stimulation, expression of GFP following RNA electro-transfer decreased (**Figure 11B**, left panel). However, following two rounds of stimulation, T cells demonstrated improved viability after electro-transfer compared to T cells undergoing a one or three rounds of stimulation (**Figure 11B**, right panel). Therefore, a protocol of two rounds of stimulation with 10 T cells to 1 aAPC was selected for further optimization of RNA transcript transfer. Because RNA is less toxic to cells and transferred more readily into many cell types than DNA (165), we reasoned RNA transfer efficiency could be improved without compromising T-cell viability by altering the strength of the manufacturer recommended electroporation program for stimulated T cells, EO-115. By plotting the percentage of cells expressing GFP versus viability determined by PI staining, we identified a program that resulted in ~100% GFP expression 24 hours following electroporation and similar T-cell viability as T cells that were not electroporated, program DQ-115 (**Figure 11C**). T-cell phenotype was assessed following electroporation with the optimized protocol and no changes in T-cell phenotype were detected following electroporation (**Figure 11D**). Thus, we developed a platform for RNA transfer to T cells that following numeric expansion via co-culture with aAPC that resulted in high expression of RNA transcript without compromising T-cell viability.

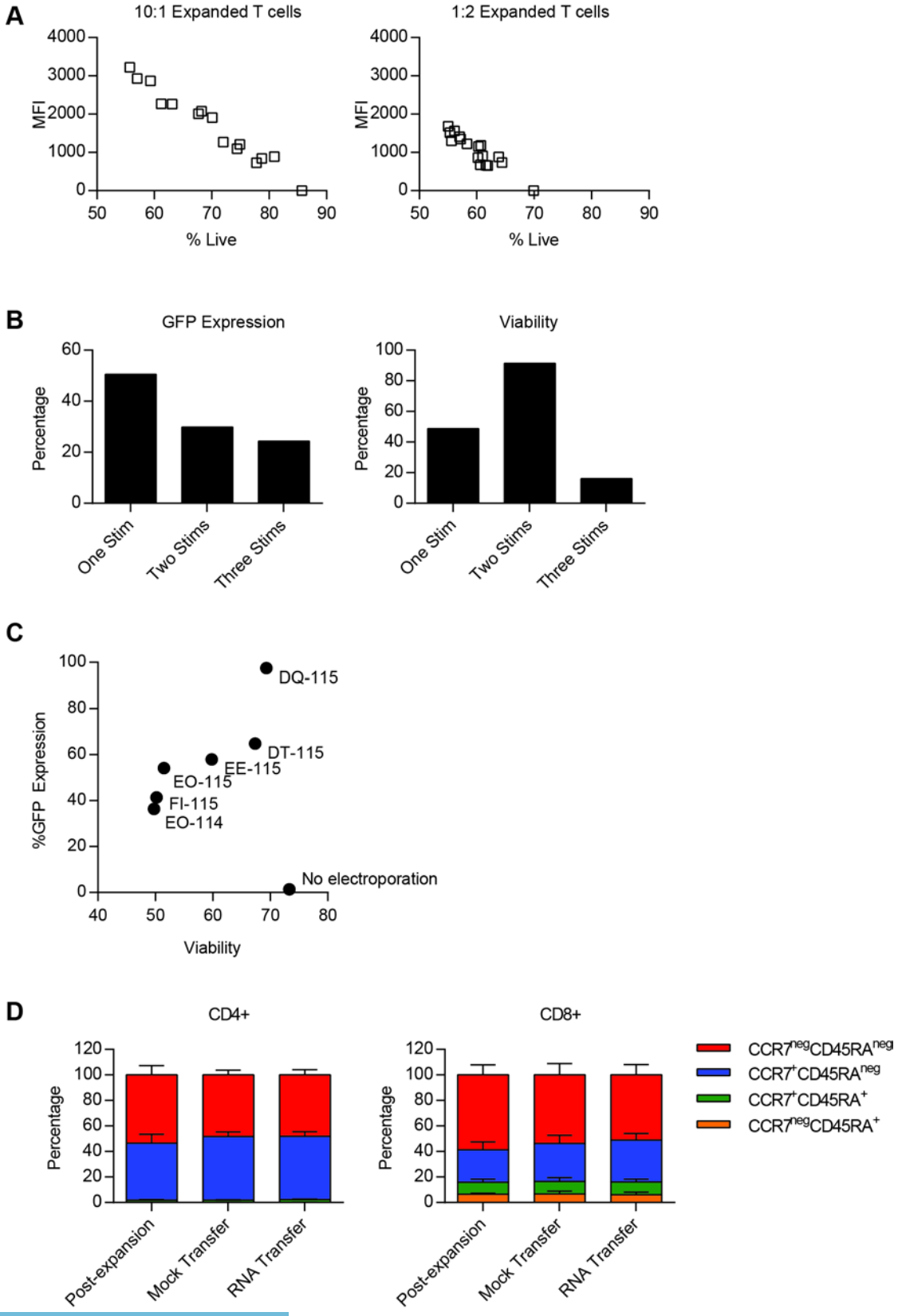

Figure 11. Optimization of RNA transfer to T cells numerically expanded with aAPC. (A) Expression of GFP RNA and viability of T cells electroporated with various programs. Median fluorescence intensity of GFP was determined by flow cytometry. Viability was determined by PI stain and flow cytometry. Data representative of two individual donors. (B) Expression of GFP RNA and viability in T cells expanded with aAPC at low density (10 T cells to 1 aAPC) following one, two or three cycles of stimulation. Percentage of T cells expressing GFP was determined by flow cytometry. Viability was determined by PI stain and flow cytometry. Data representative of two individual donors. (C) Expression of GFP RNA and viability of T cells stimulated at an aAPC density of 10 T cells to 1 aAPC for two stimulation cycles after electroporation with various programs. Percentage of T cells expressing GFP was determined by flow cytometry. Viability was determined by PI stain and flow cytometry. Data representative of two individual donors. (D) Expression of memory markers CCR7 and CD45RA measured by flow cytometry in $CD4^+$ and $CD8^+$ gated T cells following two cycles of stimulation with aAPC at a density of 10 T cells to 1 aAPC, mock electroporated with no RNA, and electroporated with RNA. Data represented as mean ± SD, n=3.

2.2.5 CAR expression and phenotype T cells modified by DNA or RNA transfer

To compare expression of CAR and function of CAR^+ T cells manufactured by RNA and DNA modification, we developed an EGFR-specific CAR from the scFv of cetuximab, a clinically available anti-EGFR monoclonal antibody. The scFv of cetuximab was fused to an IgG4 hinge region, CD28 transmembrane and cytoplasmic domains, and CD3-ζ cytoplasmic domain to form a second generation CAR, termed Cetux-CAR, and expressed in a Sleeping Beauty transposon for permanent DNA integration as well as under a T7 promoter in the pGEM/A64 vector for in vitro transcription of RNA transcripts. For stable DNA integration, Cetux-CAR expressed in SB transposon was electroporated into human primary T cells with the SB11 transposase, a cut-and-paste enzyme, which excises the CAR from the transposon and inserts into the host T-cell genome at inverted TA repeats. Recursive stimulation with γ-irradiated $EGFR^+$ K562 aAPC results in selective expansion of CAR-expressing T cells over time, and T cells were evaluated for CAR expression following 28 days consisting of 5 cycles of recursive aAPC addition, every 7 days (**Figure 12A**). RNA-modification of T cells was achieved by electro-transferring *in vitro* transcribed Cetux-CAR into T cells stimulated twice with OKT3-loaded K562 aAPC, four days following the second stimulation (**Figure 12B**). CAR expression was evaluated 24 hours following electro-transfer. Expression of Cetux-CAR by RNA-modification and DNA-modification in $CD4^+$ and $CD8^+$ as determined by flow cytometry for the IgG4 hinge region of CAR was not statistically different ($p>0.05$), however, RNA-modification resulted in greater variation in expression intensity (**Figure 13A**). Of Cetux-CAR-expressing T cells, the proportion of $CD4^+$ and $CD8^+$ T cells was not statistically different between T cells modified with RNA or DNA, however, there was greater variability in the proportion of $CD4^+$ and $CD8^+$ T cells present in DNA-modified than RNA-modified CAR^+ T cells (**Figure 13B**).

To compare the phenotype of T-cell populations modified by RNA or DNA transfer, we measured phenotypic markers by flow cytometry. $CD4^+$ RNA-modified CAR^+ T cells had more T cells with central memory phenotype ($CCR7^+CD45RA^{neg}$) than $CD4^+$ DNA-modified CAR^+ T cells (DNA-modified = 6.6 ± 1.9%, RNA-modified = 49.6 ± 3.0%, mean ± S.D., n=3) ($p<0.0001$), but fewer T cells with effector memory phenotype ($CCR7^{neg}CD45RA^{neg}$) (DNA-modified = 89.8 ± 2.6%, RNA- modified=48.1 ± 3.3%, mean ± S.D., n=3) ($p<0.0001$) (**Figure 13C**). Similarly, $CD8^+$ RNA-modified CAR^+ T cells had significantly more T cells with central memory phenotype than $CD8^+$ DNA-modified CAR^+ T cells (DNA-modified = 10.4 ± 4.9%, RNA-modified = 32.8 ± 4.2%, mean ± S.D., n=3) ($p<0.001$), but fewer T cells with effector

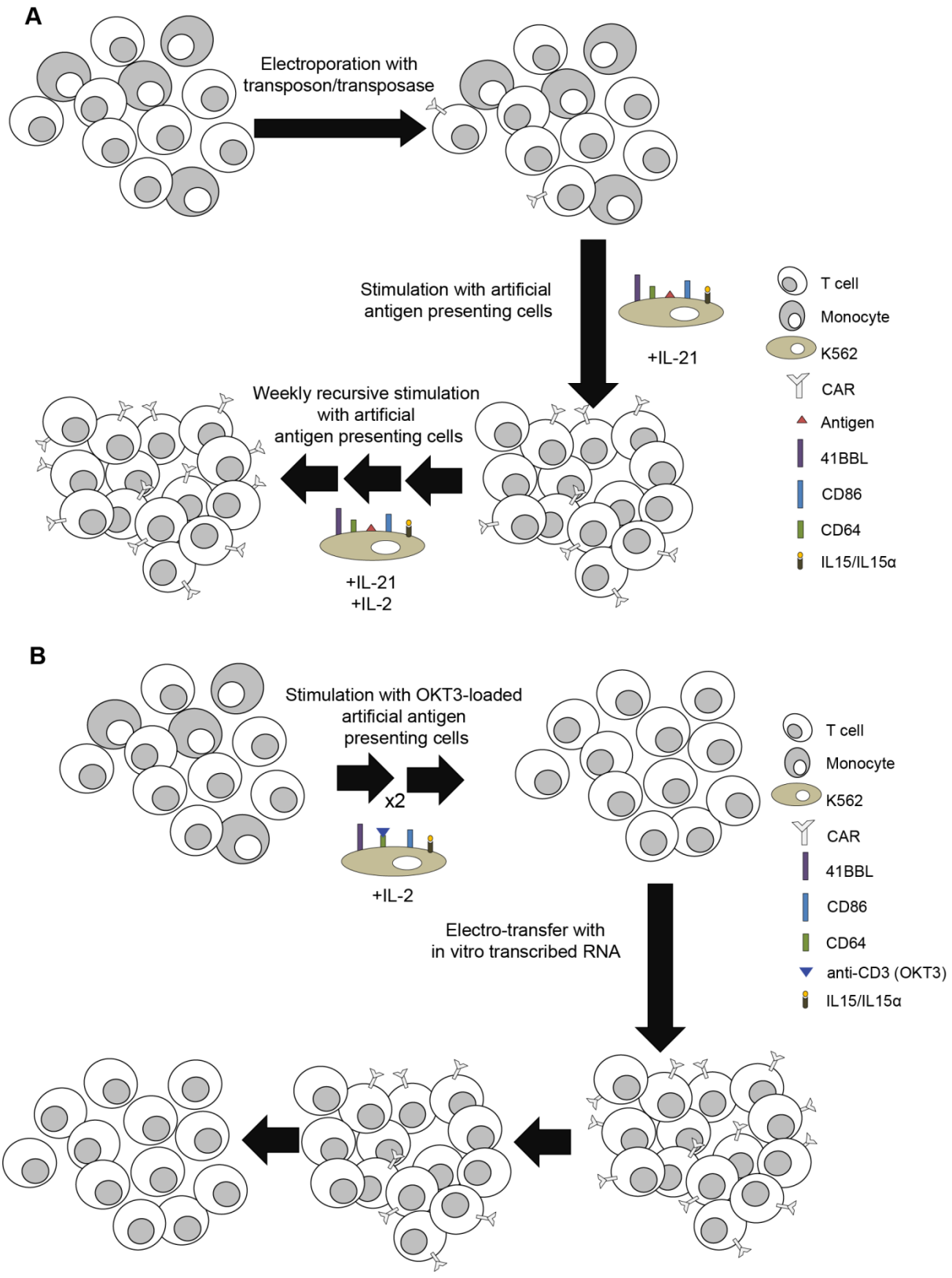

Figure 12. Schematic of CAR expression by DNA and RNA modification. (A) DNA modification of T cells by electroporation with SB transposon/transposase. Normal donor PBMCs were electroporated with SB transposon containing CAR and SB11 transposase to result in stable CAR expression in a fraction of T cells. Stimulation with γ-irradiated antigen expressing aAPC in the presence of IL-21 (30 ng/mL) and IL-2 (50 U/mL) culled out CAR^+ T cells over time, resulting in >85% CAR^+ T cells following 5 stimulation cycles and T cells were evaluated for CAR-mediated function. (B) Modification of T cells by RNA electro-transfer. Normal donor PBMCs were stimulated with γ-irradiated anti-CD3 (OKT3) loaded K562 clone 4 aAPC. Three to five days following second stimulation, T cells were electroporated with RNA to result in >95% CAR^+ T cells 24 hours after RNA electro-transfer, and evaluated for CAR-mediated function.

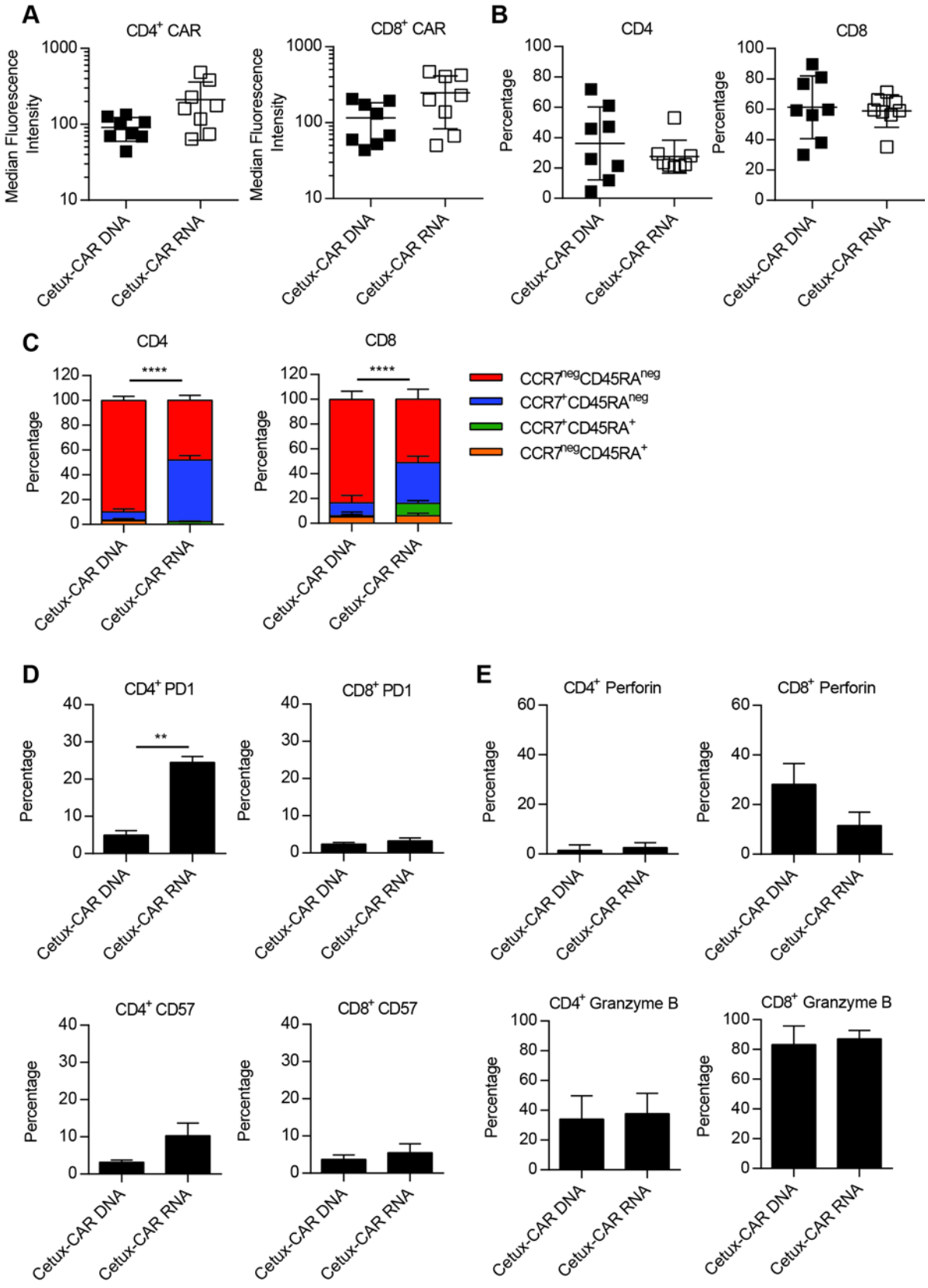

Figure 13. Phenotype of Cetux-CAR$^+$ T cells modified by DNA and RNA. (A) Median fluorescence intensity of CAR expression in RNA-modified and DNA-modified T cells was determined by flow cytometry for IgG region of CAR in CD4$^+$ and CD8$^+$ gated T-cell populations. Data represented as mean ± SD, n=8. (B) Proportion of CD4$^+$ and CD8$^+$ T-cell populations in RNA- and DNA-modified T cells determined by flow cytometry for CD4 and CD8 in CAR$^+$ gated T cells. Data represented as mean ± SD, n=8. (C) Expression of memory markers CCR7 and CD45RA determined by flow cytometry in CD4$^+$ and CD8$^+$ gated T-cell populations. Memory populations were defined as follows: effector memory = CCR7^{neg}CD45RA^{neg}, central memory = CCR7$^+$CD45RA^{neg}, naïve = CCR7$^+$CD45RA$^+$, effector memory RA = CCR7^{neg}CD45RA$^+$. Data represented as mean ± SD, n=3, **** p<0.0001, two-way ANOVA (Tukey's post-test). (D) Expression of inhibitory receptor PD-1 and marker of replicative senescence CD57 as determined in CD4$^+$ and CD8$^+$ gated T-cell populations by flow cytometry. Data represented as mean ± SD, n=3, ** p<0.01, two-way ANOVA (Tukey's post-test). (E) Expression of granzyme B and perforin determined by intracellular cytokine staining in CD4$^+$ and CD8$^+$ gated T-cell populations by flow cytometry. Data represented as mean ± SD, n=3.

memory phenotype (DNA-modified = 83.5 ± 5.4%, RNA-modified = 51.1 ± 6.6%, mean ± S.D., n=3) ($p>0.0001$). $CD4^+$ Cetux-CAR^+ T cells modified by RNA also demonstrated significantly higher expression of the inhibitory receptor programmed death receptor 1 (PD-1) than $CD4^+$ Cetux-CAR^+ T cells, ($p<0.01$), but similar, low expression of CD57, a marker of T-cell senescence (**Figure 13D**). $CD8^+$ Cetux-CAR^+ T cells expressed low levels of PD-1 and CD57 and there was no appreciable difference RNA-modified and DNA-modified CAR^+ T cells. Finally, expression of the cytotoxic molecules perforin and granzyme B, was similar in $CD4^+$ and $CD8^+$ T cells modified by DNA or RNA transfer of Cetux-CAR (**Figure 13E**). In sum, RNA-modification and DNA-modification of CAR^+ T cells resulted in similar expression levels of CAR, though RNA transfer resulted in increased variability of the intensity of CAR expression. RNA-modified T cells expressed more central memory phenotype $CD4^+$ and $CD8^+$ T cells, less effector memory phenotype $CD4^+$ and $CD8^+$ T cells, and had higher expression of inhibitory receptor PD-1 on $CD4^+$ CAR^+ T cells than DNA-modified T cells.

2.2.6 DNA-modified CAR^+ T cells produce more cytokine and display slightly more cytotoxicity than RNA-modified CAR^+ T cells

Cytokine production of RNA-modified or DNA-modified CAR+ T cells was evaluated in response to a mouse T cell lymphoma cell line EL4 modified to express truncated EGFR, $tEGFR^+$ EL4, or irrelevant antigen, CD19, and $EGFR^+$ cell lines, including human glioblastoma cell lines U87, T98G, LN18 and human epidermoid carcinoma cell line A431. Fewer $CD8^+$ CAR^+ T cells modified by RNA transfer produced IFN-γ in response to all EGFR-expressing cell lines (**Figure 14A**, left panel). Because fewer RNA-modified T cells produced IFN-γ in response to antigen-independent stimulation with PMA/Ionomycin, it is not likely that reduced IFN-γ production is due to reduced sensitivity of CAR to antigen, but rather reduced capacity of T cells expressing CAR by RNA-modification to produce cytokine. It was noted that DNA-modified CAR^+ T cells also demonstrated higher background production of IFN-γ in the absence of T-cell stimulation. Similarly, fewer RNA-modified $CD8^+$ CAR^+ T cells produced TNF-α in response to EGFR-specific stimulation from T98G, LN18, A431 and antigen-independent stimulation from PMA/Ionomycin than DNA-modified $CD8^+$ CAR^+ T cells (**Figure 14A**, right panel).

Because RNA-modified CAR^+ T cells demonstrated reduced capacity to produce cytokine relative to DNA-modified CAR^+ T cells, cytotoxicity of RNA-modified and DNA-modified T cells was compared to determine the cytotoxic potential of RNA-modified CAR^+ T

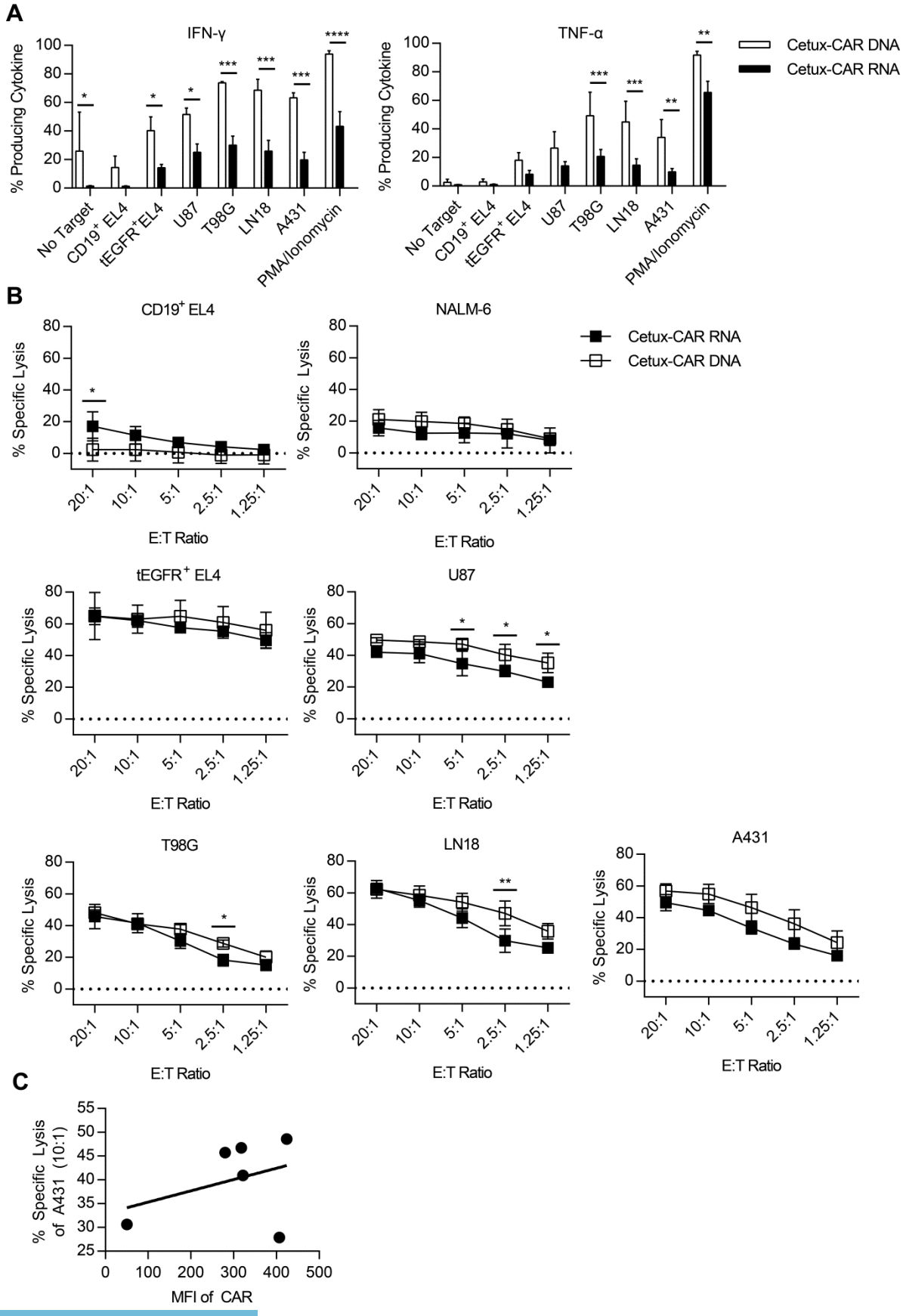

Figure 14. DNA-modified CAR$^+$ T cells produce more cytokine and display slightly more cytotoxicity than RNA-modified CAR$^+$ T cells. (A) Cytokine production of DNA-modified (following 5 stimulation cycles) and RNA-modified CAR$^+$ T cells (24 hours post RNA transfer) was measured by intracellular staining and flow cytometry following 4 hr incubation with targets or PMA/Ionomycin in CD8$^+$ gated T cells. Data represented as mean ± SD, n=3, * p<0.05, ** p<0.01, *** p<0.001, **** p<0.0001, two-way ANOVA (Tukey's post-test). (B) Specific cytotoxicity of DNA-modified (following 5 stimulation cycles) and RNA-modiifed CAR$^+$ T cells (24 hours post RNA transfer) was determined by standard 4-hour chromium release assay. Data represented as mean ± SD, n=3, *p<0.05, two-way ANOVA (Tukey's post-test). (C) Specific cytotoxicity of A431 by RNA-modified CAR$^+$ T cells at 10:1 effector:target ratio plotted against median fluorescence intensity of CAR. Linear regression was fit to the data, yielding a slope of slope=0.0237±0.030, not significantly different from a slope of 0, p=0.4798.

cells relative to DNA-modified CAR$^+$ T cells. In response to CD19$^+$ EL4 cells, RNA-modified and DNA-modified CAR$^+$ T cells had low levels of background killing, although at high effector to target ratio (E:T = 20:1), RNA-modified CAR$^+$ T cells demonstrated significantly more background lysis than DNA-modified CAR$^+$ T cells ($p<0.05$) (**Figure 14B**). Similarly, RNA-modified and DNA-modified CAR$^+$ T cells demonstrated low and equivalent levels of background lysis against B-cell lymphoma cell line, NALM-6. In response to tEGFR$^+$ EL4 and A431, there was no appreciable difference in cytotoxicity mediated by RNA-modified or DNA-modified CAR$^+$ T cells. In response to the three glioma cell lines U87, T98G, and LN18, DNA-modified CAR$^+$ T cells demonstrated slightly increased cytotoxicity over RNA-modified CAR$^+$ T cells only detected at low E:T ratios. Because RNA-modified T cells have more variability in CAR expression than DNA-modified T cells from donor to donor, we evaluated the impact of CAR expression, as determined by median fluorescence intensity of CAR expression, on specific lysis of A431. Median fluorescence intensity of CAR expression was plotted versus specific lysis of A431, and a linear regression of the relationship yielded a slope not significantly different than zero, and therefore, showed no significant trend detected between CAR expression and specific lysis (slope = 0.0237 ± 0.030, $p=0.4798$) (**Figure 14C**). In sum, these findings suggest that DNA-modified CAR$^+$ T cells have significantly increased production of effector cytokines IFN-γ and TNF-α relative to RNA-modified CAR$^+$ T cells, may demonstrate slightly more cytotoxicity when present at low E:T ratios, and that the variability of CAR expression in RNA-modified CAR+ T cells does not significantly impact specific lysis of targets.

2.2.7 Transient expression of Cetux-CAR by RNA modification of T cells

To determine the stability of CAR expression by RNA transfer, T cells were modified to express CAR by RNA transfer, and CAR expression was measured over time by flow cytometry. Following RNA transfer, expression of Cetux-CAR on T cells decreased over time, and 96 hours following electro-transfer, CAR was expressed at low levels (**Figure 15A**). Because RNA transcripts are divided between daughter cells during T-cell proliferation, stimulation of T-cell proliferation should accelerate the loss of CAR expressed by RNA-modification. To determine the effect of cytokine stimulation on CAR expression level, exogenous IL-2 and IL-21 were added to RNA-modified CAR$^+$ T cell culture 24 hours after RNA transfer and CAR expression was monitored by flow cytometry. Stimulation of CAR$^+$ T cells with IL-1 and IL-21 accelerated the loss of CAR expression (**Figure 15B**). Following 72 hours, CAR expression was low on RNA-modified T cells, and 96 hours after

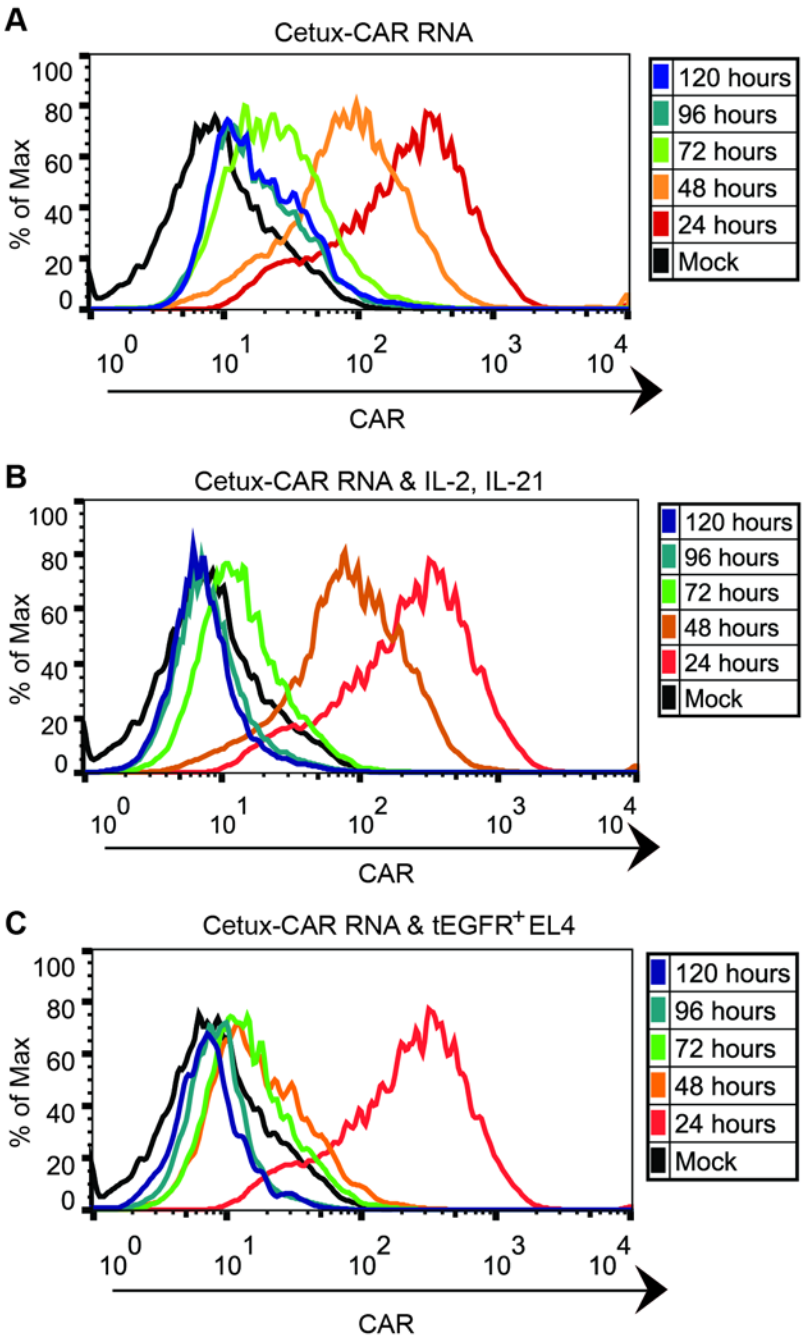

Figure 15. Transient expression of Cetux-CAR by RNA-modification of T cells. (A) Expression of CAR measured daily by flow cytometry for IgG portion of CAR with no cytokines or stimulus added to T cells. Data representative of three independent donors. (B) Expression of CAR measured daily by flow cytometry for IgG portion of CAR following addition of IL-2 (50 U/mL) and IL-21 (30 ng/mL) 24 hours after RNA transfer. Data representative of three independent donors. (A) Expression of CAR measured daily by flow cytometry for IgG portion of CAR after addition of tEGFR$^+$ EL4 cells 24 hours after RNA transfer. Data representative of three independent donors.

transfer, T cells no longer expressed CAR at a detectable level. Stimulation of RNA-modified CAR^+ T cells with $tEGFR^+$ EL4 24 hours after RNA transfer accelerated the loss of CAR expression even further (**Figure 15C**). While CAR was detected at high level in RNA-modified CAR^+ T cells prior to addition of $tEGFR^+$ EL4, 24 hours after $tEGFR^+$ EL4 addition (48 hours following RNA transfer), CAR expression was low. Collectively, these data indicate the CAR expression by RNA transfer is transient, detectable at low levels up to 120 hours after RNA transfer, however, stimulation of T cells through cytokine or recognition of antigen accelerated the loss of CAR expression.

2.2.8 Transient expression of Cetux-CAR by RNA modification reduces cytokine production and cytotoxicity to EGFR-expressing cells.

Activity of T cells modified to express Cetux-CAR by RNA transfer was measured 24 and 120 hours after RNA transfer to determine the effect of loss of CAR expression on activity of T cells in response to EGFR-expressing cells. While RNA-modified T cells demonstrated equivalent production of IFN-γ by PMA/Ionomycin stimulation when assessed at 24 hours and 120 hours after RNA transfer, production of IFN-γ in response to $tEGFR^+$ EL4 by T cells was abrogated 120 hours after RNA transfer (24 hrs = 14.2 ± 2.5%, 120 hrs = 1.1 ± 0.03%, mean ± S.D., n=3) (p=0.012) (**Figure 16A**). In contrast, DNA-modified CAR^+ T cells demonstrated equivalent production of IFN-γ in response to $tEGFR^+$ EL4 at both time points assessed (24 hrs = 40.3 ± 9.6%, 120 hrs = 48.6 ± 10.0%, mean ± S.D., n=3) (p=0.490). Similarly, specific cytotoxicity was measured against epidermoid carcinoma cell line A431 and human normal renal cortical epithelial cells (HRCE), a primary kidney cell line which expresses EGFR. RNA-modified and DNA-modified CAR^+ T cells demonstrated equivalent specific lysis of A431, and similar cytotoxicity against HRCE, statistically equivalent at higher effector to target ratios (20:1 and 10:1, $p>0.05$) (**Figure 16B**). Similar to observations with other cell lines, DNA-modified CAR^+ T cells mediated slightly higher specific lysis of HRCE than RNA-modified CAR^+ T cells at lower E:T ratios (5:1, $p<0.05$; 2.5:1, $p<0.01$, 1.25:1, $p<0.05$). However, 120 hours after RNA transfer, when CAR expression of RNA-modified T cells is abrogated, DNA-modified T cells mediated significantly higher specific lysis in response to A431 and HRCE at every E:T ratio evaluated (A431, all E:T ratios, $p<0.0001$; HRCE, all E:T ratios, $p<0.0001$). While DNA-modified T cells demonstrated no change in specific lysis of HRCE at each time point (10:1 E:T ratio, 24 hrs = 45.5 ± 8.0%, 120 hrs = 51.6 ± 7.8%, $p>0.05$, n=3), RNA-modified T cells significantly reduced specific lysis of HRCE 120 hours after RNA transfer (10:1 E:T ratio, 24 hrs = 39.5

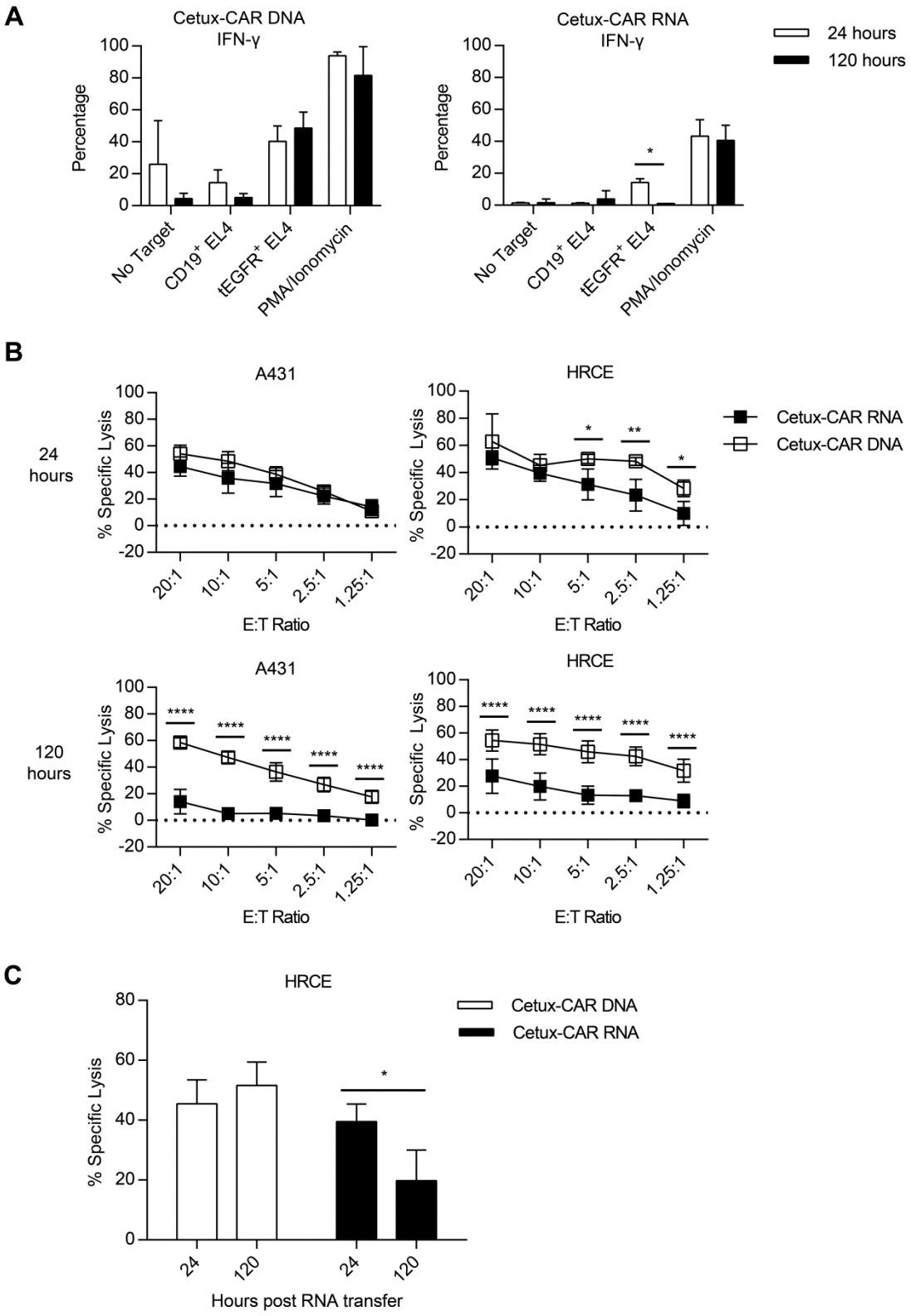

Figure 16. Transient expression of Cetux-CAR by RNA modification reduces cytokine production and cytotoxicity to EGFR-expressing cells. (A) Production of IFN-γ measured by intracellular staining and flow cytometry in DNA-modified and RNA-modified $CD8^+$ T cells 24 hours and 120 hours after RNA transfer after 4 hour incubation with target cells or PMA/Ionomycin. Data represented as mean ± SD, n=3, * $p<0.05$, two-way ANOVA (Tukey's post-test). (B) Specific cytotoxicity of DNA-modified and RNA-modified T cells measured by standard chromium release assay 24 hours and 120 hours after RNA transfer. Data represented as mean ± SD, n=3, * $p<0.05$, ** $p<0.01$, **** $p<0.0001$, two-way ANOVA (Tukey's post-test). (C) Change in specific cytotoxicity of DNA-modified and RNA-modified T cells from 24 hours post RNA transfer to 120 hours post RNA transfer measured by standard chromium release assay at an effector to target ratio of 10:1. Data represented as mean ± SD, n=3, * $p<0.05$, two-way ANOVA (Tukey's post-test).

± 5.9%, 120 hrs = 19.8 ± 10.2%, mean ± S.D., n=3) (**Figure 16C**). These data indicate that activity of RNA-modified T cells in response to EGFR-expressing targets is reduced by loss of CAR expression.

2.3 Discussion

Transient expression of CAR by RNA transfer has been proposed to reduce the potential for long-term, on-target, off-tissue toxicity of CAR T cell therapy directed against antigens with normal tissue expression. Numeric expansion of T cells prior to RNA transfer is appealing to obtain clinically relevant T cell numbers needed for patient infusion. We explored numeric expansion of T cells independent of antigen-specificity by co-culturing on aAPC loaded with anti-CD3 antibody, OKT3. Altering the ratio of aAPC to T cells in culture altered the phenotype of the resultant T cell population. T cells expanded with low density of aAPC (10 T cells to 1 aAPC) were associated with increased proportion of $CD8^+$ T cells, increased presence of central memory phenotype T cells, reduced production of IFN-γ and TNF-α, but increased production of IL-2, and potentially less clonal loss of TCR diversity following expansion relative to T cells expanded with high density aAPC. T cells expanded with low density aAPC were more amenable to RNA electro-transfer, demonstrating higher expression of RNA transcripts and improved T-cell viability following electro-transfer than T cells expanded with high density aAPC.

A potential benefit of use of aAPC for T-cell expansion is the ability to form stable interactions with T cells by virtue of expression of adhesion molecules LFA-3 and ICAM-1 (95, 97). Additionally, aAPC can be modified with relative ease to express desired arrays of costimulatory molecules. Thus, aAPC for numeric T-cell expansion provides a platform to evaluate various combinations of costimulatory molecules for T-cell expansion to achieve determine and achieve an optimal T-cell phenotype for adoptive T-cell therapy. In addition to modification of aAPC, we have described the impact of the density of aAPC in T cell culture on the phenotype of resulting T-cell populations. While $CD8^+$ T cells, or cytotoxic T cells, are often thought of as the ideal T-cell population for anti-tumor immunotherapy, evidence suggests that $CD8^+$ T cells require $CD4^+$ T-cell help *in vivo* to achieve optimal anti-tumor response and memory formation (273-275). However, the ideal ratio of $CD4^+$ to $CD8^+$ T cells is unknown (276). By altering density of aAPC in expansion cultures to skew CD4/CD8 ratio in T cells for adoptive immunotherapy, whether they be TIL isolated from patients or gene-modified T cells, these questions may be addressed in clinical trials.

Finally, reducing density of aAPC in culture resulted in more T cells with a central memory phenotype ($CCR7^{+}CD45RA^{neg}$) than T cells expanded with higher density of aAPC. While the benefit of enhanced persistence of central memory phenotype T cells may not extend to RNA-modified T cells, which are only transiently redirected for tumor antigen, persistence of T cells has been shown to improve the anti-tumor efficacy of T-cell therapy (104, 277-279). Therefore, future studies will examine the ability of *ex vivo* expansion with low density aAPC to reprogram stably genetically modified T cells or TIL to a central memory phenotype for enhanced persistence.

Expression of CAR by RNA-modification in *ex vivo* expanded T cells was found to be more variable than expression of CAR by non-viral DNA-modification and donor-dependent. Expression of CAR at different densities did not impact the ability of the T cells to specifically lyse targets, although it is reasonable to expect that below a certain threshold, low CAR expression would have a negative impact on specific lysis of targets, as previously reported (123). Others have described tunable expression of CAR by RNA modification of T cells, such that the dose of RNA determines the level of transgene expression (165-167). RNA modification of T cells in the present study was conducted using the same quantity of RNA, therefore, alteration of RNA dose does not account for variability of CAR expression. Instead, it is likely that variability between donors accounts for differences in CAR expression intensity following electro-transfer. Our novel protocol for T-cell expansion prior to RNA transfer may play a role in altering the sensitivity of T cells from certain donors to RNA uptake, and increasing the RNA quantity in electro-transfers may increase expression of CAR in these donors. High expression of CAR by transferring relatively high quantities of RNA can result in prolonged CAR expression and CAR-mediated activity over an extended period of time (167). Prolonged CAR expression from RNA transfer may be beneficial for anti-tumor activity, particularly since stimulation of T cells seems to accelerate the loss of CAR expression. However, prolonging the expression of CAR may also increase T-cell activity in response to normal tissue antigen. Thus, optimization of CAR expression to determine the optimal duration of expression to maximize anti-tumor activity while reducing normal tissue toxicity warrants further investigation.

RNA-modification of T cells did not alter the proportion of effector memory and central memory T cells found in *ex vivo* expanded T cells prior to electro-transfer of RNA, similar to previous reports (280). Only T cells expanded at relatively low aAPC density, 10 T cells to 1 aAPC, were capable of efficient RNA transcript uptake without significant toxicity,

even with various electroporation conditions evaluated. This population of T cells also demonstrated a substantial proportion of T cells with a central memory phenotype ($CCR7^{+}CD45RA^{neg}$) that had reduced production of IFN-γ and TNF-α, and cytotoxic effector molecules granzyme B and perforin. As a result, RNA-modified T cells contained significantly more central memory phenotype T cells than DNA-modified T cells, demonstrated reduced production of IFN-γ and TNF-α in response to EGFR-expressing cells and slightly less specific lysis at low E:T ratios. Thus, the precursor T-cell population for RNA-modification has a strong influence on CAR-mediated T-cell function following RNA transfer and the reduced cytokine production and slightly less specific lysis of RNA-modified T cells may translate to reduced anti-tumor efficacy in an *in vivo* model where cytotoxic potential of T cells is short-lived and the enhanced persistence of a central memory T-cell population may not be beneficial. RNA-modification of T cells expanded at 1 T cell to 2 aAPC, which demonstrated a more significant proportion of effector memory phenotype T cells, similar to DNA-modified CAR+ T cells, and consequently the capacity for higher production of IFN-γ and TNF-α is desirable. Future work evaluating the addition of cytokines prior to RNA transfer to improve viability and additional electroporation programs may identify a protocol to efficiently transfer RNA into these T cells.

Importantly, Cetux-CAR introduced to T cells through RNA transfer was transiently expressed, and loss of expression was accelerated by stimulus to T cells, including addition of cytokines IL-2 and IL-21 and antigenic-stimulus through addition of EGFR-expressing cell lines. Concomitant with loss of CAR expression, RNA-modified T cells demonstrated reduced cytotoxicity against EGFR-expressing cell lines, including tumor cells and normal renal cells. One concern for the use of RNA-modified T cells is that their inherently reduced capacity to target tumor over time will result in reduced anti-tumor efficacy relative to stably-modified T cells. Multiple injections of T cells modified to express a mesothelin-specific CAR by RNA transfer for the treatment of murine model of mesothelioma demonstrated that biweekly, intratumoral injections controlled tumor growth, but following cessation of treatment, tumors relapsed (152). Treatment of an *in vivo* disseminated leukemia murine model has shown that while RNA-modified CAR^{+} T cells specific for CD19 have anti-tumor activity after a single injection, tumors often relapse after a time period consistent with CAR degradation (167). In contrast, a single intratumoral injection of T cells stably expressing mesothelin-specific CAR mediated superior anti-tumor activity and was capable of curing most mice. Optimization of dosing of RNA-modified T cells demonstrated that a combination

of cyclophosphamide to eliminate residual CAR^{neg} T cells before subsequent infusions and a weighted, split-dosing regimen was more effective in controlling disease burden, and was similar in anti-tumor efficacy to stably modified T cells (168). Thus, it appears that optimizing a dosing regimen can improve the anti-tumor activity of RNA-modified T cells.

A clinical trial of RNA-modified T cells expressing mesothelin-specific CAR for treatment of patients with mesothelin-expressing tumors, such as mesothelioma, is currently underway. Early reports have demonstrated tolerability of multiple injections mesothelin-specific CAR^+ T cells in most patients, despite normal tissue expression of mesothelin at low levels of mesothelial surfaces of peritoneal, pleural and pericardial spaces (266). In addition, anti-tumor activity has been demonstrated by radiographic measurement of tumor remission and measurement of serum biomarkers. One serious adverse event has been reported from this trial directly related to CAR^+ T cell treatment in which a patient experienced anaphylactic shock and cardiac arrest within minutes of receiving a T-cell infusion, attributed to development of an IgE antibody response to murine moieties of the CAR (160). Therefore, the trial was revised dose multiple infusions over a span of no more than 21 days with individual infusions no more than 10 days apart in order to complete treatment within a time frame shorter than that required for isotype switching of antibody responses from IgG to IgE to occur. While anaphylactic response to CAR^+ T cells might best be avoided by single infusion of stably modified T cells to avoid multiple dosing strategies, even stably modified T cells are often given over multiple infusions due to limited *in vivo* persistence.

An additional limitation of RNA-modified Cetux-CAR^+ T cells lies in their capacity to recognize EGFR on normal human renal cells prior to appreciable degradation of CAR. While transient expression of CAR by RNA modification reduces potential of Cetux-CAR^+ T cells to recognize normal tissue EGFR in the long-run, it does not protect normal tissue expressing EGFR from the potential of immediate toxicity mediated by CAR^+ T cells. Since CAR loss is accelerated following interaction with EGFR and normal tissue in the CNS are not reported to express EGFR, intratumoral delivery of Cetux-CAR^+ T cells to ensure encounter with tumor prior to normal tissue expressing EGFR may reduce the potential for on-target, off-tissue normal tissue toxicity. However, for many other EGFR-expressing tumor types, there is not such a distinct separation between location of tumor and normal tissue expressing EGFR. To expand CAR^+ T cell therapy to other EGFR-expressing malignancies

that may reside in close proximity to EGFR-expressing normal cell, additional mechanisms to reduce the potential for normal tissue recognition are needed.

In sum, numeric expansion of T cells prior to RNA transfer can be achieved through co-culture with OKT3-loaded K562 aAPC. While CAR^+ T cells modified through RNA transfer may exhibit reduced cytokine production and reduced cytotoxicity relative to DNA-modified CAR^+ T cells, the expression of CAR is transient and following loss of CAR expression, activity of T cells in response to EGFR-expressing targets is greatly reduced. However, transient expression of Cetux-CAR by RNA modification is limited by the potential for reduced anti-tumor activity due to transient nature of CAR expression and by the capability of Cetux-CAR^+ T cells to exert specific cytotoxicity on normal tissue expressing EGFR prior to appreciable degradation of CAR. Thus, investigation of additional mechanisms to reduce toxicity of stably modified CAR^+ T cells is ongoing.

CHAPTER 3

CAR$^+$ T cells can distinguish malignant cells from normal cells based on EGFR density

3.1 Introduction

In Chapter 2, we acknowledged that Cetux-CAR$^+$ T cells can recognize normal tissue antigen, which could result in on-target, off-tissue toxicity and investigated expression of CAR as RNA species as a method to control on-target, off-tissue toxicity through transient expression of CAR. While CAR expression was transient and reduced potential for cytotoxicity against normal tissue EGFR after degradation of CAR, it did not address the potential for immediate T-cell effector function upon recognition of normal tissue EGFR before considerable degradation of CAR. Additionally, by limiting CAR expression, T cells are rendered non-responsive to EGFR-expressing tumor following CAR degradation, and the potential for lasting anti-tumor activity is compromised by this approach. Therefore, we continued to investigate mechanisms to control CAR activity in the presence of normal tissue to limit deleterious on-target, off-tissue toxicity without compromising anti-tumor activity.

Endogenous T-cell activation is dependent on both affinity of the TCR and density of peptide presented via MHC (17, 59-61). T cells are activated by a cumulative signal through the TCR that surpasses a certain threshold required for elicitation of effector functions (16, 17, 59). For high affinity TCRs, relatively low antigen density is sufficient to trigger T-cell responses; however, low affinity TCRs required higher antigen density to achieve similar effector T cell responses (60). Many tumors overexpress TAA at higher densities than their normal tissue expression (281-283). Amplification and overexpression of EGFR in glioma highlight this relationship as EGFR is overexpressed in glioma relative to normal tissue, and overexpression correlates with tumor grade, such that grade IV glioblastoma expresses the highest density of EGFR (180, 182, 199). Therefore, we sought to determine if EGFR-specific CAR-modified T cells could target distinguish malignant cells from normal cells based on EGFR density by reducing the binding affinity of the CAR.

The portion of Cetux-CAR that endows antigenic specificity is derived from the scFv portion of the monoclonal antibody cetuximab, which is characterized by a high affinity (K_d=1.9x10^{-9}) (223). Therefore, we generated a CAR from the monoclonal antibody

nimotuzumab, which shares a highly overlapping epitope with cetuximab and a 10-fold higher dissociation constant (K_d=2.1x10^{-8}), characterized by a 59-fold reduced rate of association (223, 231, 284, 285). The reduced association rate and subsequent reduction in overall affinity imposes a requirement for bivalent recognition of EGFR by nimotuzumab which only occurs when EGFR is expressed at high density. We hypothesized that a CAR derived from nimotuzumab would enable T cells to distinguish malignant tissue from normal tissue based on density of EGFR expression.

3.2 Results

3.2.1 Cetux-CAR$^+$ and Nimo-CAR$^+$ T cells are phenotypically similar

A second generation CAR derived from nimotuzumab, designated Nimo-CAR, was generated in a *Sleeping Beauty* transposon by fusing the scFv of nimotuzumab with an IgG4 hinge region, CD28 transmembrane domain and CD28 and CD3ζ intracellular domains, an identical configuration to Cetux-CAR. Cetux-CAR and Nimo-CAR were expressed in primary human T cells by electroporation of each transposon with SB11 transposase into peripheral blood mononuclear cells (PBMC). T cells with stable integration of Cetux-CAR or Nimo-CAR were selectively propagated by weekly recursive stimulation with γ-irradiated tEGFR$^+$ K562 artificial antigen presenting cells (aAPC) (**Figure 17A**). Both CARs mediated ~1000-fold expansion of CAR$^+$ T cells over 28 days of co-culture with aAPC, yielding T cells which almost all expressed CAR (Cetux-CAR = 90.8 ± 6.2%, Nimo-CAR = 90.6 ± 6.1%; mean ± SD, n=7) (**Figure 17B and 17C**). Proportion of Cetux-CAR and Nimo-CAR$^+$ T cells expressing CAR was statistically similar following 28 days of numeric expansion (p=0.92, student's two-tailed t-test). Density of CAR expression, represented by median fluorescence intensity, was measured by flow cytometry and was statistically similar between Cetux-CAR$^+$ and Nimo-CAR$^+$ T-cell populations (Cetux-CAR = 118.5 ±2 5.0 A.U., Nimo-CAR = 112.6 ± 21.2 A.U.; mean ± SD, n=7) (p=0.74) (**Figure 17D**).

In order to determine the impact of CAR scFv on T-cell function, we first established that electroporation and propagation of Cetux-CAR$^+$ and Nimo-CAR$^+$ T cells resulted in phenotypically similar T-cell populations. Each donor yielded variable ratios of CD4$^+$ and CD8$^+$ T cells (**Table 1**), however, there was no statistical difference in the CD4/CD8 ratio between Cetux-CAR$^+$ and Nimo-CAR$^+$ T cells (p=0.44, student's two-tailed t-test) (**Figure 18A**). Expression of differentiation markers CD45RO, CD45RA, CD28, CD27, CCR7 and CD62L were not statistically significant (p>0.05), and indicate a heterogeneous T-cell

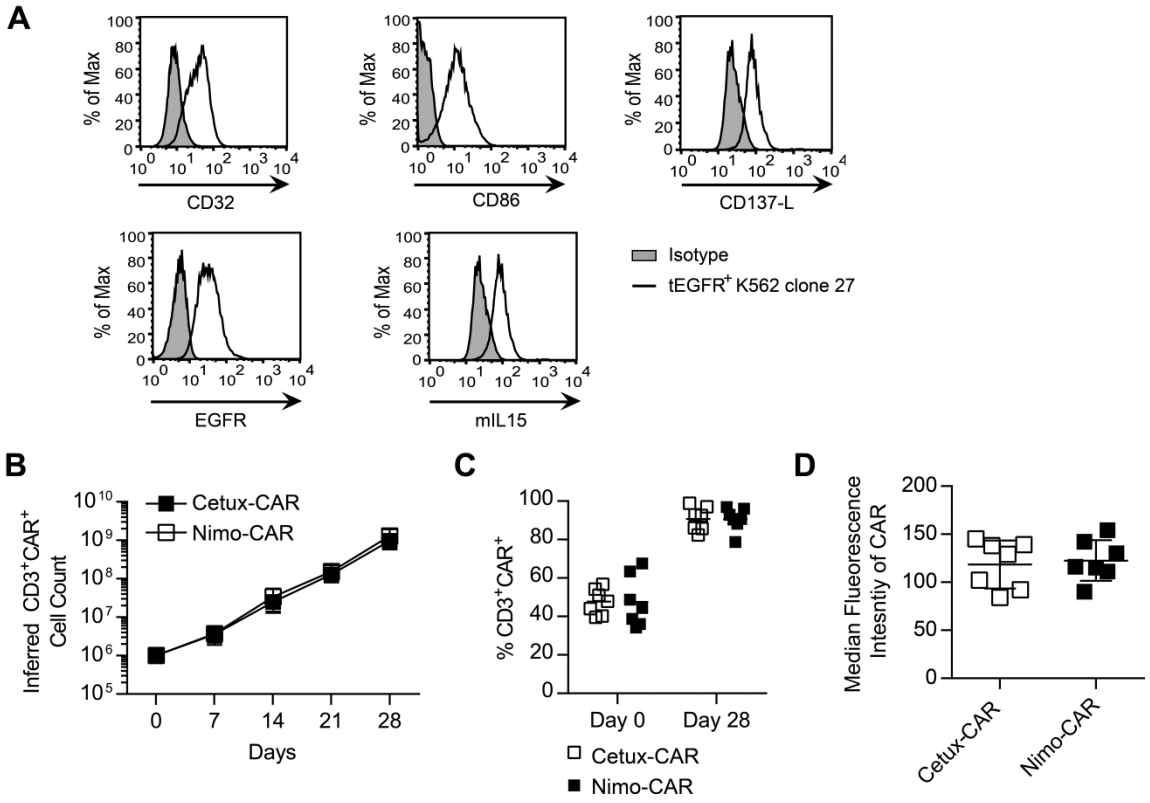

Figure 17. Numeric expansion of Cetux-CAR$^+$ and Nimo-CAR$^+$ T cells. (A) Phenotype of γ-irradiated tEGFR$^+$ K562 clone 27 determined by flow cytometry. (B) Numeric expansion of Cetux-CAR$^+$ and Nimo-CAR$^+$ T cells. Prior to each stimulation cycle, percentage of CD3$^+$CAR$^+$ T cells was determined by flow cytometry. Inferred cell count was calculated by multiplying the fold expansion following a stimulation cycle by the number of CAR$^+$ T cells resulting from previous stimulation. Data represented as mean ± SD, n=7. (C) Expression of CAR in CD3$^+$ T cells was determined 24 hours after electroporation of CAR and after 28 days of expansion by flow cytometry for the IgG portion of CAR. Data represented as mean, n=7. (D) Median fluorescence intensity of CAR expression was determined by flow cytometry for the IgG portion of CAR after 28 days of expansion. Data represented as mean ± SD, n=7.

Donor	Cetux-CAR %CD4	Cetux-CAR %CD8	Cetux-CAR Ratio (CD4/CD8)	Nimo-CAR %CD4	Nimo-CAR %CD8	Nimo-CAR Ratio (CD4/CD8)
1	46.7	42.9	1.09	18.8	73.1	0.26
2	83.0	17.3	4.80	88.4	7.17	12.3
3	2.5	96.2	0.03	0.4	97.9	0.01
4	62.0	24.9	2.49	38.7	48.8	0.79
5	35.5	47.6	0.75	20.8	57.6	0.36
6	78.5	17.1	4.59	82.3	11.3	7.29
7	44.0	49.2	0.89	31.9	60.1	0.53

Table 3. Ratio of CD4 and CD8 in Cetux-CAR$^+$ and Nimo CAR$^+$ T cells. Expression of CD4 and CD8 in Cetux-CAR$^+$ and Nimo-CAR$^+$ T cells after 28 days of expansion was determined by flow cytometry. Data from 7 independent donors.

population (**Figure 18B**). Likewise, markers for senescence CD57 and KLRG1 and the inhibitory receptor programmed death receptor 1 (PD-1) were found to be low and not statistically different between Cetux-CAR$^+$ and Nimo-CAR$^+$ T-cell populations ($p>0.05$) (**Figure 18C**). In aggregate, these findings indicate that Cetux-CAR$^+$ and Nimo-CAR$^+$ T cells have no detectable phenotypic differences, including CAR expression after electroporation and propagation, enabling direct comparison.

3.2.2 Cetux-CAR$^+$ and Nimo-CAR$^+$ T cells have equivalent capacity for CAR-dependent T-cell activation

To verify Cetux-CAR and Nimo-CAR were functional in response to stimulation with EGFR, we incubated CAR$^+$ T cells with A431 epidermoid carcinoma cell line, which is reported to express high levels of EGFR, about $1x10^6$ molecules of EGFR/cell (231). Cetux- and Nimo-CAR$^+$ T cells produced IFN-γ during co-culture with A431, which was reduced in the presence of anti-EGFR monoclonal antibody that blocks binding to EGFR (**Figure 19A**). To verify that Cetux-CAR and Nimo-CAR are equivalently capable of activating T cells, we generated targets that could be recognized by both CARs independent of the scFv domain. This was accomplished by expressing the scFv region of an activating antibody specific for the IgG4 region of CAR (CAR-L) on immortalized mouse T cell line EL4 (286). Activation of T cells by CAR-L$^+$ EL4 was compared to activation by an EL4 cell line expressing tEGFR. Quantitative flow cytometry was performed to measure the density of tEGFR expressed on EL4. In this method, intensity of fluorescence from microspheres with a known antibody binding capacity labeled with fluorescent antibody is measured by flow cytometry and used to derive a standard curve, which defines a linear relationship between known antibody binding capacity and mean fluorescence intensity (MFI). The standard curve can then be used to derive the mean density of antigen expression from the mean fluorescence intensity of an unknown sample labeled with the same fluorescent antibody. tEGFR$^+$ EL4 expressed tEGFR at a relatively low density, about 45,000 molecules/cell (**Figure 19B**). Cetux-CAR$^+$ and Nimo-CAR$^+$ CD8$^+$ T cells demonstrated statistically similar amounts of IFN-γ in response to CAR-L$^+$ EL4s, indicating equivalent capacity for CAR-dependent activation ($p>0.05$) (**Figure 19C**). While Cetux-CAR$^+$ T cells produced IFN-γ in response to EGFR$^+$, there was no appreciable IFN-γ production from Nimo-CAR$^+$ T cells (**Figure 19C**), which is consistent with the affinity of the scFv of CAR impacting T-cell activation in response to low antigen density. In addition to measuring cytokine production, we analyzed CD8$^+$ T cells for phosphorylation of molecules downstream of T-cell activation, Erk1/2 and p38. There was

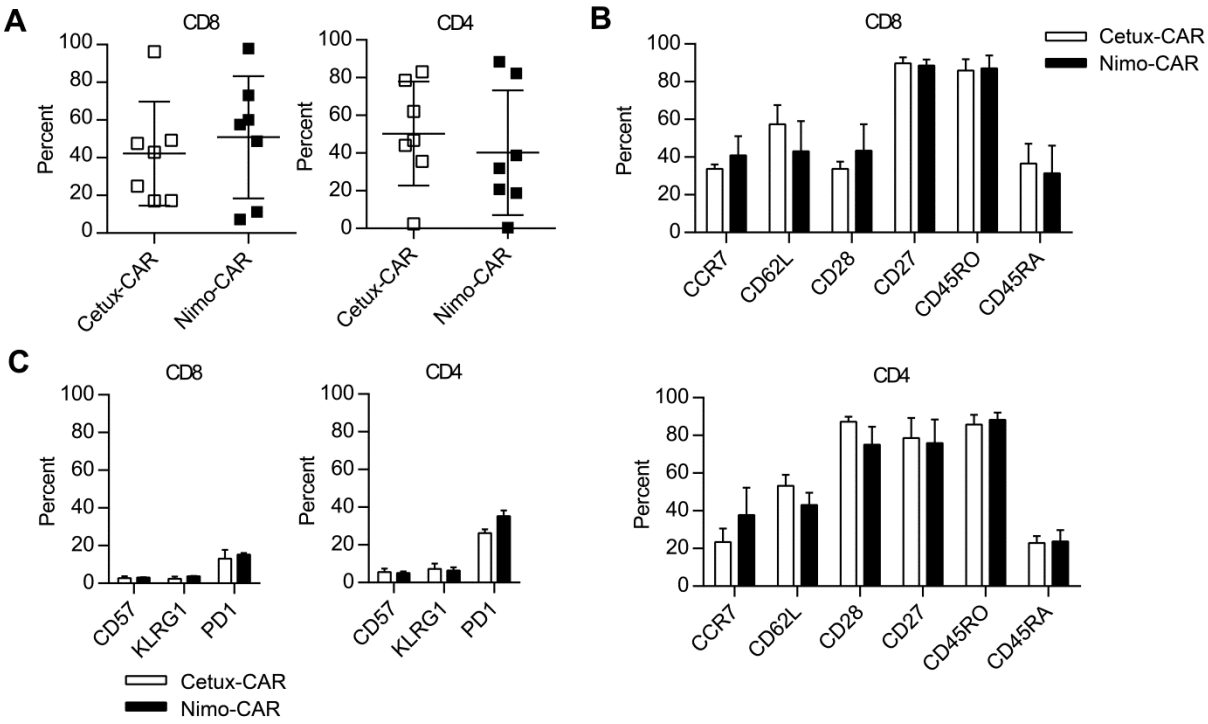

Figure 18. Cetux-CAR$^+$ and Nimo-CAR$^+$ T cells are phenotypically similar. (A) Proportion of CD4 and CD8 T cells in total T-cell population after 28 days of expansion measured by flow cytometry on gated CD3$^+$ CAR$^+$ cells. Data represented as mean ± SD, n=7. (B,C) Expression of T-cell memory and differentiation markers after 28 days of T-cell expansion measured by flow cytometry in gated CD4$^+$ and CD8$^+$ T-cell populations. Data represented as mean ± SD, n=4.

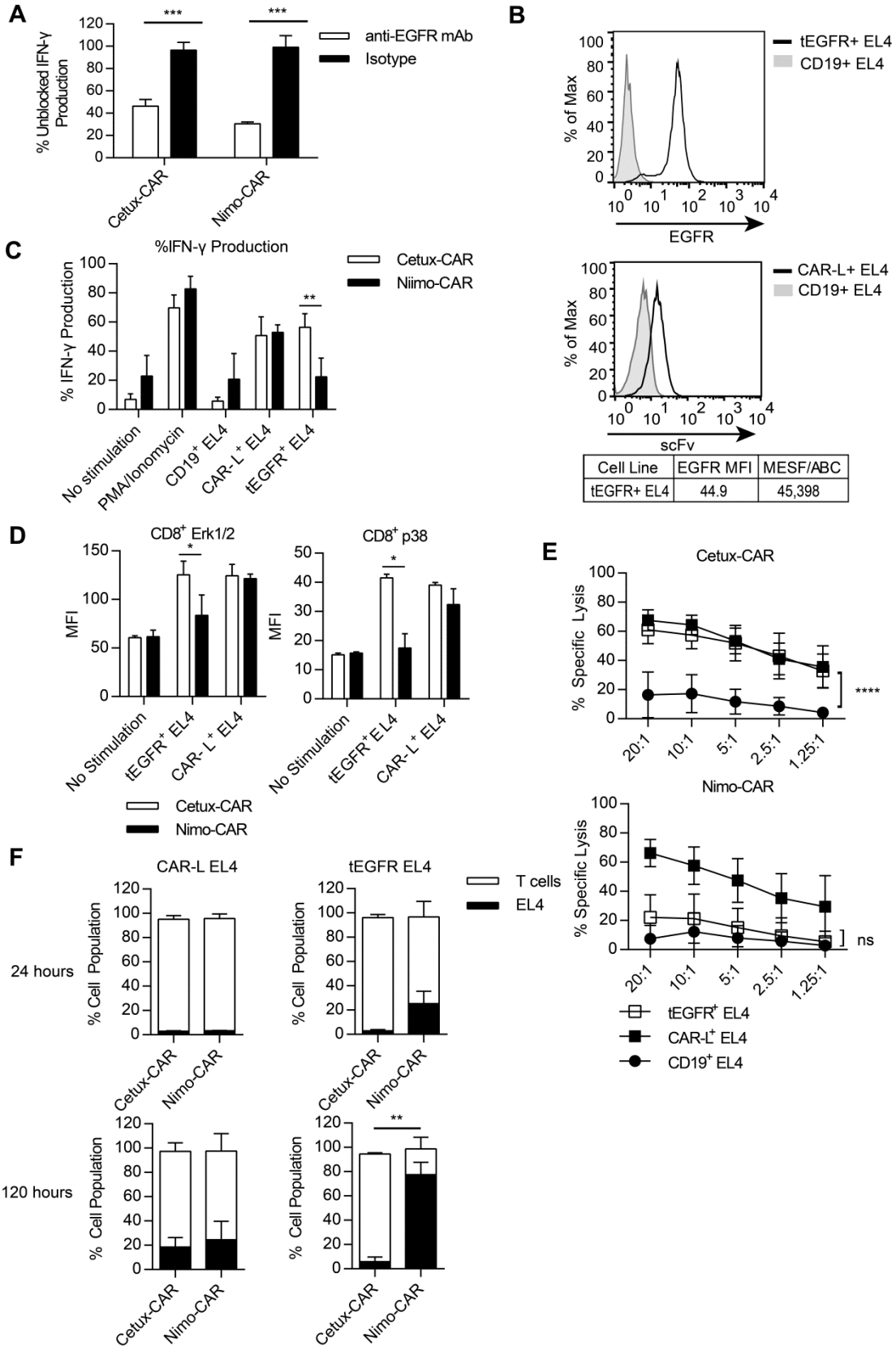

Figure 19. Cetux-CAR$^+$ and Nimo-CAR$^+$ T cells are activated equivalently through affinity-independent triggering of CAR. (A) Production of IFN-γ in response to EGFR$^+$ A431 in the presence of EGFR blocking monoclonal antibody. CAR$^+$ T cells were co-cultured with A431 with anti-EGFR blocking antibody or isotype control and IFN-γ production was measured by intracellular flow cytometry. Percent of production was calculated as mean fluorescence intensity of IFN-γ in gated CD8$^+$ T cells relative to unblocked CD8$^+$ T cell production. Data represented as mean ± SD, n=3, *** p<0.001, two-way ANOVA (Tukey's post-test). (B) Representative histograms of expression of tEGFR (top panel) and CAR-L (bottom panel) on EL4 cells relative to cell lines negative for antigen. Density of EGFR expression was determined by quantitative flow cytometry. (C) Production of IFN-γ by gated CD8$^+$ CAR$^+$ T cells after co-culture with CD19$^+$, tEGFR$^+$, or CARL$^+$ EL4 cells measured by intracellular staining and flow cytometry. Data represented as mean ± SD, n=4, ** p<0.01, two-way ANOVA (Tukey's post-test). (D) Phosphorylation of p38 and Erk1/2 by phosflow cytometry in gated CD8$^+$ CAR$^+$ T cells 30 minutes after co-culture with CD19$^+$, EGFR$^+$, or CARL$^+$ EL4 cells. Data represented as mean ± SD, n=2, * p<0.05, two-way ANOVA (Tukey's post-test). (E) Specific lysis of CD19$^+$, EGFR$^+$ and CARL$^+$ EL4 cells measured by standard 4-hour chromium release assay. Data represented as mean ± SD, n=4, **** p<0.0001, two-way ANOVA (Tukey's post-test). (F) Relative proportion of T cells to EL4 cells in long term co-culture. Fraction of co-culture containing T cells to EL4 cells measured by flow cytometry for human and murine CD3, respectively, with non-species cross reactive antibodies. Data represented as mean ± SD, n=4, ** p<0.01, two-way ANOVA (Tukey's post-test).

no statistical difference in phosphorylation of Erk1/2 ($p>0.05$) or p38 ($p>0.05$) between Cetux-CAR$^+$ and Nimo-CAR$^+$ T cells in response to CAR-L$^+$ EL4 (**Figure 19D**). While Cetux-CAR$^+$ T cells exhibited phosphorylation of Erk1/2 and p38 in response to tEGFR$^+$ EL4, Nimo-CAR$^+$ T cells failed to appreciably phosphorylate either molecule. Similarly, Cetux-CAR$^+$ and Nimo-CAR$^+$ T cells demonstrated equivalent specific lysis against CAR-L$^+$ EL4 (10:1 E:T ratio, Cetux-CAR = 64.5 ± 6.7%, Nimo-CAR = 57.5 ± 12.9%, mean ± SD, n=4)($p>0.05$). While Cetux-CAR$^+$ T cells demonstrated significant specific lysis in response to tEGFR$^+$ EL4 over non-specific lysis of irrelevant antigen expression on CD19$^+$ EL4 (tEGFR$^+$EL4 = 57.5 ± 9.4%, tCD19$^+$EL4 = 17.3 ± 13.0, mean ± SD, n=4) ($p<0.0001$), there was not significant lysis of tEGFR$^+$ EL4 by Nimo-CAR$^+$ T cells (tEGFR$^+$EL4 = 21.2 ± 16.9%, CD19$^+$EL4 = 12.3 ± 13.0, mean ± SD, n=4) ($p>0.05$) (**Figure 19E**). Endogenous, low-affinity T-cell responses may require longer interaction with antigen to achieve effector function (16), therefore, we evaluated the ability of CAR$^+$ T cells to control growth of tEGFR$^+$ and CAR-L$^+$ EL4 cells in an extended co-culture. Cetux-CAR$^+$ T cells and Nimo-CAR$^+$ T cells controlled growth of CAR-L$^+$ EL4s equivalently ($p>0.05$), as demonstrated by low proportion of CAR-L$^+$ EL4 cells in co-culture after 5 days **(Figure 19F**). Cetux-CAR$^+$ T cells controlled growth of tEGFR$^+$EL4, resulting in less than 10% of tEGFR$^+$ EL4 in the co-culture after 5 days. Nimo-CAR$^+$ T cells were less capable of controlling tEGFR$^+$ EL4 cell growth, resulting in tEGFR$^+$ EL4 accounting for 80% of the co-culture after 5 days, significantly more than co-culture with Cetux-CAR$^+$T cells ($p<0.01$). Therefore, reduced response by Nimo-CAR$^+$ T cells to low tEGFR density on tEGFR$^+$ EL4 is not likely due to insufficient time for activation. In sum, these data demonstrate that Cetux-CAR$^+$ and Nimo-CAR$^+$ T cells have functional specificity for EGFR and can be equivalently activated by CAR-dependent, scFv-independent stimulation. Cetux-CAR$^+$ T cells were capable of specific activation in response to low tEGFR density on tEGFR$^+$ EL4; however, this density of EGFR expression was not sufficient for activation Nimo-CAR$^+$ T cells to produce cytokine, phosphorylate downstream molecules Erk1/2 and p38, or initiate specific lysis.

3.2.3 Activation and functional response of Nimo-CAR$^+$ T cells is impacted by density of EGFR expression on target cells.

To investigate the impact of EGFR expression density on activation of Cetux-CAR$^+$ and Nimo-CAR$^+$ T cells, we compared T-cell function against cell lines with a range of EGFR expression density: NALM-6, U87, LN18, T98G, and A431. First, we evaluated EGFR expression density by quantitative flow cytometry (**Figure 20A**). NALM-6, a B-cell leukemia

cell line, expressed no EGFR. U87, a human glioblastoma cell line, expressed EGFR at low density (~30,000 molecule/cell). LN18 and T98G, both human glioblastoma cell lines, expressed EGFR at intermediate density (~160,000 and ~205,000 molecules/cell, respectively), and A431 was found to expression EGFR at high density (~780,000 molecules/cell), similar to previous reports (231). Cetux-CAR$^+$ and Nimo-CAR$^+$ CD8$^+$ T cells demonstrated statistically similar IFN-γ production in response to A431 with high EGFR density ($p>0.05$) and LN18 with intermediate EGFR density ($p>0.05$). However, Nimo-CAR$^+$ T cells demonstrated reduced IFN-γ production in response to T98G with intermediate EGFR density ($p<0.001$) and U87 with low EGFR density ($p<0.001$) relative to Cetux-CAR$^+$ T cells (**Figure 20B**). Similarly, while Cetux-CAR$^+$ and Nimo-CAR$^+$ T cells demonstrated statistically equivalent lysis of A431 cells (5:1 E:T ratio, $p>0.05$) and T98G cells (5:1 E:T ratio, $p>0.05$), Nimo-CAR$^+$ T cells demonstrated some reduced capacity for specific lysis of LN18 cells (5:1 E:T ratio, $p<0.05$) and reduced capacity for specific lysis of U87 cells (5:1 E:T ratio, $p< 0.01$) (**Figure 20C**). These data support that activation of Nimo-CAR$^+$ T cells is impacted by the density of EGFR expression.

3.2.4 Activation of function of Nimo-CAR$^+$ T cells is directly and positively correlated with EGFR expression density

Evaluating function against EGFR density in the context of different cellular backgrounds is not ideal since different cell lines may have different propensity for T-cell activation and susceptibility to T-cell mediated lysis. Therefore, to determine the impact of EGFR expression density on a syngeneic cellular background, we developed a series of U87 cell lines expressing varying densities of EGFR: unmodified, parental U87 (~30,000 molecules of EGFR/cell), U87^{low} (130,000 molecules of EGFR/cell), U87^{med} (340,000 molecules of EGFR/cell), and U87^{high} (630,000 molecules of EGFR/cell) (**Figure 21A**). To compare phosphorylation of Erk1/2 and p38 following scFv-dependent CAR stimulation, we ensured there was not a distinction in kinetics of phosphorylation between Nimo-CAR$^+$ T cells and Cetux-CAR$^+$ T cells following stimulation U87 and U87^{high}. Both CD8$^+$CAR$^+$ T cells demonstrated peak phosphorylation of Erk1/2 and p38 45 minutes after interaction and phosphorylation began to decrease by 120 minutes after interaction (**Figure 21B**). There was no appreciable distinction in phosphorylation kinetics between Cetux-CAR$^+$ T cells and Nimo-CAR$^+$ T cells and future experiments assessed phosphorylation of Erk1/2 and p38 45 minutes following interaction for all future experiments. Cetux-CAR$^+$ CD8$^+$ T cells

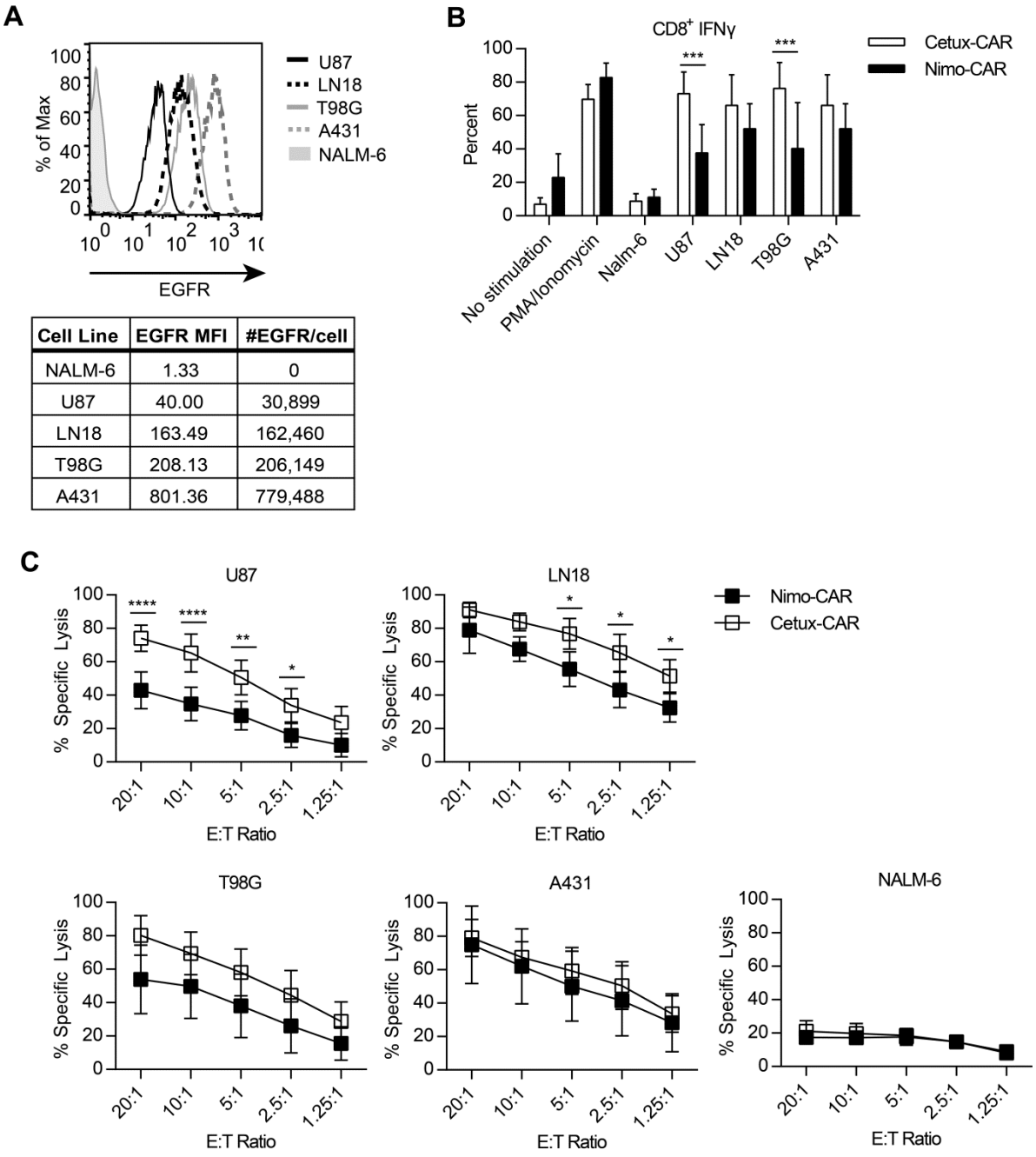

Cell Line	EGFR MFI	#EGFR/cell
NALM-6	1.33	0
U87	40.00	30,899
LN18	163.49	162,460
T98G	208.13	206,149
A431	801.36	779,488

Figure 20. Activation and functional response of Nimo CAR T cells is impacted by density of EGFR expression. (A) Representative histograms of EGFR expression on A431, T98G, LN18, U87 and NALM-6 cell lines measured by flow cytometry. Number of molecules per cell determined by quantitative flow cytometry. Data representative of three replicates. (B) Production of IFN-γ by $CD8^+CAR^+$ T cells in response to co-culture with A431, T98G, LN18, U87 and NALM-6 cell lines measured by intracellular flow cytometry gated on $CD8^+$ cells. Data represented as mean ± SD, n=4, *** p<0.001, two-way ANOVA (Tukey's post-test) (C) Specific lysis of A431, T98G, LN18, U87 and NALM-6 by CAR^+ T cells measured by standard 4 hour chromium release assay. Data represented as mean ± SD, n=4, **** p<0.0001, ** p<0.01, * p<0.05, two-way ANOVA (Tukey's post-test).

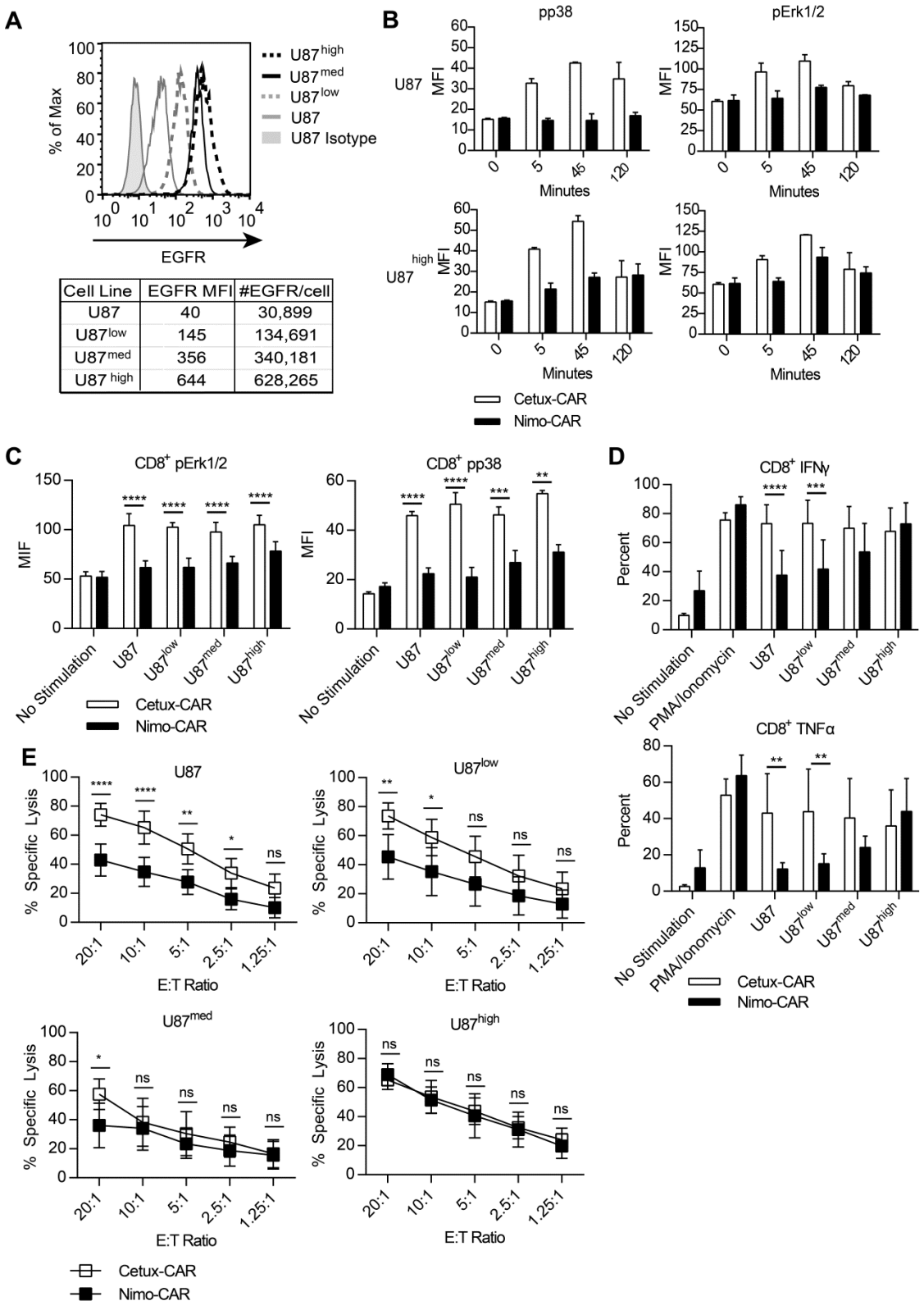

Cell Line	EGFR MFI	#EGFR/cell
U87	40	30,899
U87low	145	134,691
U87med	356	340,181
U87 high	644	628,265

Figure 21. Activation of function of Nimo-CAR$^+$ T cells is directly and positively correlated with EGFR expression density. (A) Representative histogram of EGFR expression on series of four U87-derived tumor cell lines (U87, U87^{low}, U87^{med}, and U87^{high}) measured by flow cytometry. Number of molecules per cell determined quantitative flow cytometry. Data representative of triplicate experiments. (B) Phosphorylation of Erk1/2 and p38 in gated CD8$^+$ T cells following co-culture with U87 or U87^{high} for 5, 45, and 120 minutes measured by phosflow cytometry. Data represented as mean fluorescence intensity ± SD, n=2. (C) Phosphorylation of Erk1/2 and p38 MAP kinase family members in gated CD8$^+$ T cells after 45 minutes of co-culture with U87 cell lines with increasing levels of EGFR measured by phosflow cytometry. Data represented as mean fluorescence intensity ± SD, n=4, **** p<0.0001, *** p<0.001, ** p<0.01, two-way ANOVA (Tukey's post-test). (D) Production of IFN-γ and TNF-α by gated CD8$^+$ CAR$^+$ T cells in response to co-culture with U87 cell lines with increasing levels of EGFR measured by intracellular staining and flow cytometry. Data represented as mean ± SD, n=4, **** p<0.0001, *** p<0.001, ** p<0.01, two-way ANOVA (Tukey's post-test). (E) Specific lysis of U87 cell lines with increasing density of EGFR by CAR$^+$ T cells measured by standard 4-hour chromium release assay. Data represented as mean ± SD, n=5, **** p<0.0001, ** p<0.01, * p<0.05, two-way ANOVA (Tukey's post-test).

phosphorylated Erk1/2 and p38 in response to all four U87 cell lines and showed no correlation with density of EGFR expression (one-way ANOVA with post-test for linear trend; Erk1/2, p=0.88; p38, p=0.09) (**Figure 21C**). In contrast, phosphorylation of Erk1/2 and p38 by Nimo-CAR$^+$ CD8$^+$ T cells directly correlated with EGFR expression density (one-way ANOVA with post-test for linear trend; Erk1/2, p = 0.0030 and p38, p=0.0044). We noted that Nimo-CAR$^+$ T cells demonstrated significantly less phosphorylation of Erk1/2 and p38 than Cetux-CAR$^+$ T cells, even in response to high EGFR density on U87^{high} (Erk1/2, p<0.0001; p38, p<0.01). Similarly, production of IFN-γ and TNF-α by Cetux-CAR$^+$ CD8$^+$ T cells in response to U87, U87^{low}, U87^{med} and U87^{high} did not correlate with EGFR density on target cells (one-way ANOVA with post-test for linear trend; IFN-γ, p=0.5703 and TNF-α, p=0.6189) (**Figure 21D**). In contrast, Nimo-CAR$^+$ CD8$^+$ T cells produced IFN-γ and TNF-α in direct correlation with EGFR expression density (one-way ANOVA with post-test for linear trend; IFN-γ, p=0.0124 and TNF-α, p=0.0006). Cetux-CAR$^+$ CD8$^+$ T cells produced significantly more cytokine than Nimo-CAR$^+$ CD8$^+$ T cells in response to stimulation with U87 (IFN-γ, p<0.0001; TNFα, p<0.01) or U87^{low} (IFN-γ, p<0.001; TNFα, p<0.01), however, Cetux-CAR$^+$ T cells and Nimo-CAR$^+$ T cells demonstrated statistically similar cytokine production in response to stimulation with U87^{med} (IFN-γ, p>0.05; TNFα, p>0.05) or U87^{high} (IFN-γ, p>0.05; TNFα, p>0.05). Likewise, Cetux-CAR$^+$ T cells demonstrated significantly more lysis of U87 (10:1 E:T ratio, p<0.0001) and U87^{low} (10:1 E:T ratio, p<0.05) than Nimo-CAR$^+$ T cells, but statistically similar lysis of U87^{med} (10:1 E:T ratio, p>0.05) and U87^{high} (10:1 E:T ratio, p>0.05) (**Figure 21E**). In sum, these data show that activation of Nimo-CAR$^+$ T cells is directly correlated to EGFR expression density on target. As a result, Cetux-CAR$^+$ and Nimo-CAR$^+$ T cells demonstrate equivalent T-cell activity in response to high EGFR density, but Nimo-CAR$^+$ T cells demonstrate significantly reduced activity in response to low EGFR density.

Because endogenous, low-affinity T-cell responses may require longer interaction with antigen to acquire effector function (16), we verified that the observed differences in T-cell activity between Cetux-CAR$^+$ T cells and Nimo-CAR$^+$ T cells was not due to a similar requirement for Nimo-CAR$^+$ T cells. Extending interaction of CAR$^+$ T cells with targets did not substantially increase cytokine production and did not alter the relationship of cytokine production between Cetux-CAR$^+$ and Nimo-CAR$^+$ CD8$^+$ T cells (**Figure 22A**). Similarly, we evaluated the ability of Cetux-CAR$^+$ and Nimo-CAR$^+$ T cells to control growth of U87 and U87^{high} over time and found that Cetux-CAR$^+$ and Nimo-CAR$^+$ T cells demonstrated

statistically similar ability to control the growth of U87^{high}, resulting in 80% reduction in cell number relative to controls grown in the absence of CAR$^+$ T cells ($p>0.05$). Cetux-CAR$^+$ T cells controlled growth of U87 with endogenously low EGFR expression, resulting in 40% reduction in cell number relative to controls grown in the absence of CAR$^+$ T cells. However, Nimo-CAR$^+$ T cells demonstrated significantly less control of U87 growth, with no apparent reduction in cell number ($p<0.001$) (**Figure 22B**). These data indicate that Nimo-CAR$^+$ T-cell activity in response to low EGFR on U87 is not improved by increasing interaction time of T cells with targets, making it unlikely that reduced activity of Nimo-CAR$^+$ T cells is due to a requirement for prolonged interaction to activate T cells.

Expression of CAR above a minimum density is required for CAR-dependent T-cell activation, and increasing density of CAR expression has been shown to impact sensitivity of CAR to antigen (123, 124). Therefore, to determine if expressing Nimo-CAR with higher density improves recognition of low EGFR density, we sought to overexpress Cetux-CAR and Nimo-CAR in human primary T cells. Load of DNA in electroporation transfection is limited due to toxicity of DNA to cells; however, transfer of RNA is relatively non-toxic and more amenable to overexpression by increasing amount of CAR RNA transcript delivered. Therefore, we *in vitro* transcribed Cetux-CAR and Nimo-CAR as RNA species and electro-transferred into human primary T cells. RNA transfer resulted in 2-5 fold increased expression of CAR when compared to donor-matched DNA-modified T cells (**Figure 23A**). Overexpression of CAR did not render Nimo-CAR$^+$ T cells more sensitive to low EGFR density on U87 and both Cetux-CAR and Nimo-CAR demonstrated similar cytokine production in response to U87^{high} (**Figure 23B**). Thus, increasing CAR density on Nimo-CAR$^+$ T cells does not restore sensitivity to low EGFR density.

3.2.5 Nimo-CAR$^+$ T cells have reduced activity in response to basal EGFR levels on normal renal epithelial cells

To determine if Nimo-CAR$^+$ T cells have reduced activation in response to low, basal EGFR density on normal cells, we evaluated activity of Nimo-CAR$^+$ T cells in response to normal human renal cortical epithelial cells, HRCE. HRCE express ~15,000 molecules of EGFR per cell, lower than expression on EGFR$^+$ tumor cell lines, including U87 (**Figure 24A**). While Cetux-CAR$^+$ T cells produced IFN-γ and TNF-α in response to HRCE, Nimo-CAR$^+$ T cells produced significantly less IFN-γ or TNF-α in response to HRCE (IFN-γ, $p<0.05$; TNF-α, $p<0.01$) (**Figure 24B**). In fact, Nimo-CAR$^+$ T cells did not demonstrate

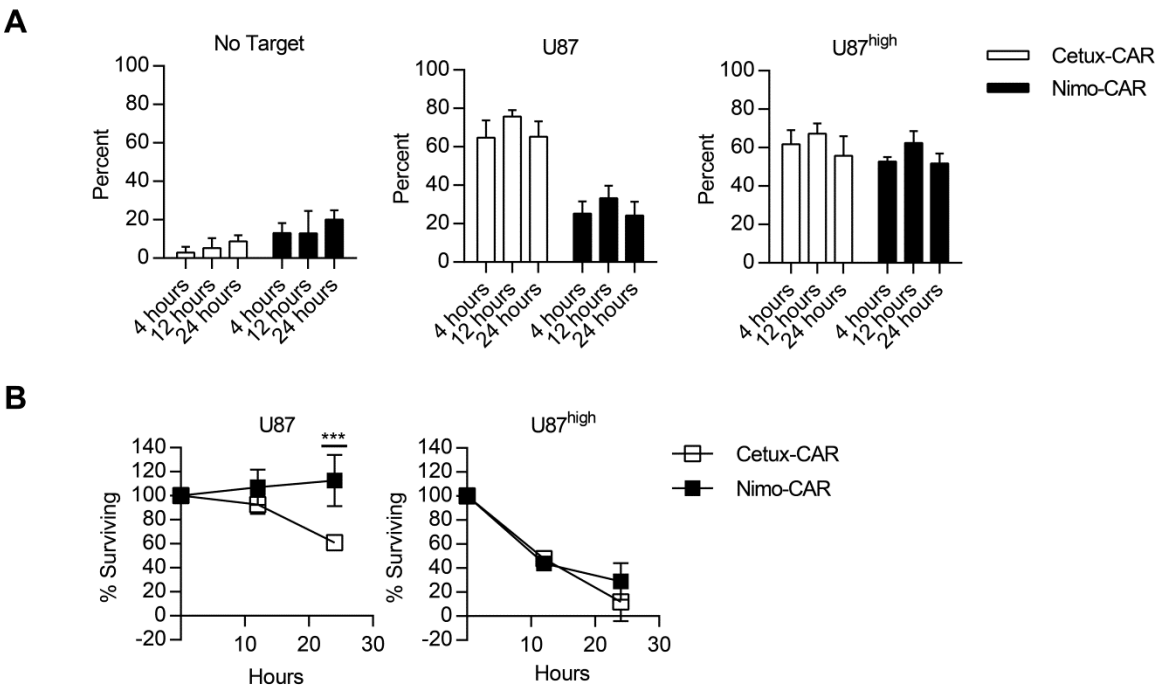

Figure 22. Increasing interaction time does not restore Nimo-CAR$^+$ T-cell function in response to low EGFR density. (A) Production of IFN-γ was measured by intracellular staining and flow cytometry following stimulation with U87 or U87^{high} over time in CD8$^+$ gated cells. Data represented as mean ± SD, n=3. (B) Fraction of U87 and U87^{high} cells remaining after co-culture with Cetux-CAR$^+$ or Nimo-CAR$^+$ T cells. U87 cell lines were co-cultured with CAR$^+$ T cells at an E:T ratio of 1:5 in triplicate. Suspension T cells were separated from adherent target cells, and adherent fraction was counted by trypan blue exclusion. Percent surviving was calculated as [cell number harvested after co-culture]/[cell number without T cells]*100. Data represented as mean ± SD, n=3, *** p<0.001, two-way ANOVA (Tukey's post-test).

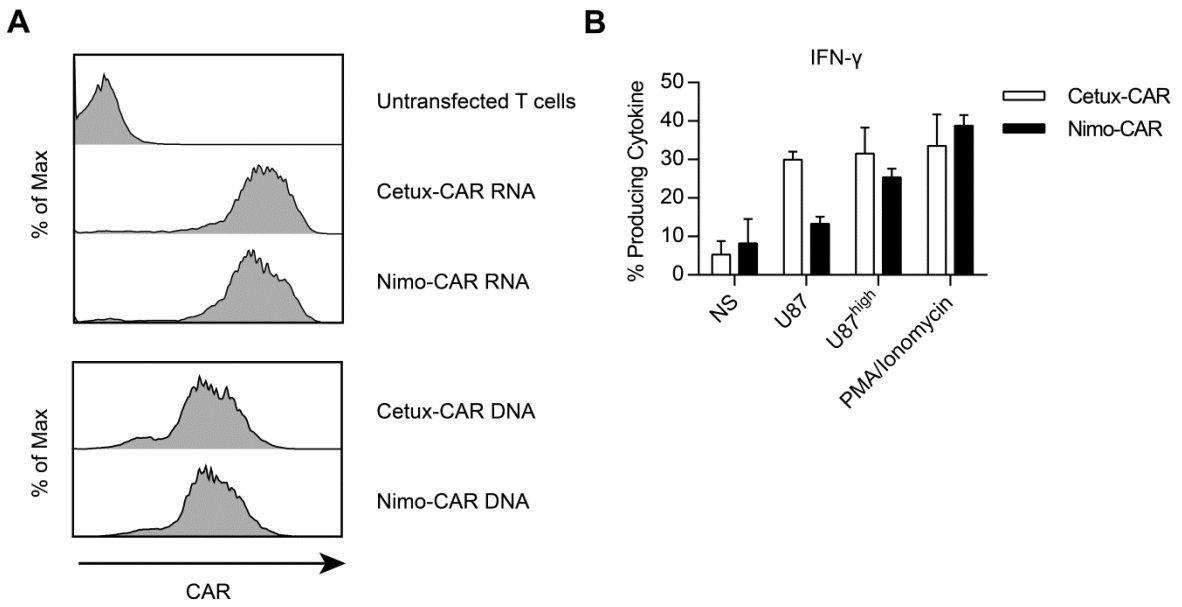

Figure 23. Increasing CAR density on T-cell surface does not restore sensitivity of Nimo-CAR$^+$ T cells to low density EGFR. A) Representative histograms of CAR expression in T cells modified by RNA transfer and traditional DNA electroporation via SB system. Data representative of 2 independent experiments. B) Production of IFN-γ in T cells overexpressing CAR by RNA electro-transfer in response to low and high antigen density. Production of IFN-γ was measured by intracellular flow cytometry in CD8$^+$ gated cells following stimulation with U87 or U87^{high} target cells. Data represented as mean ± SD, n=2.

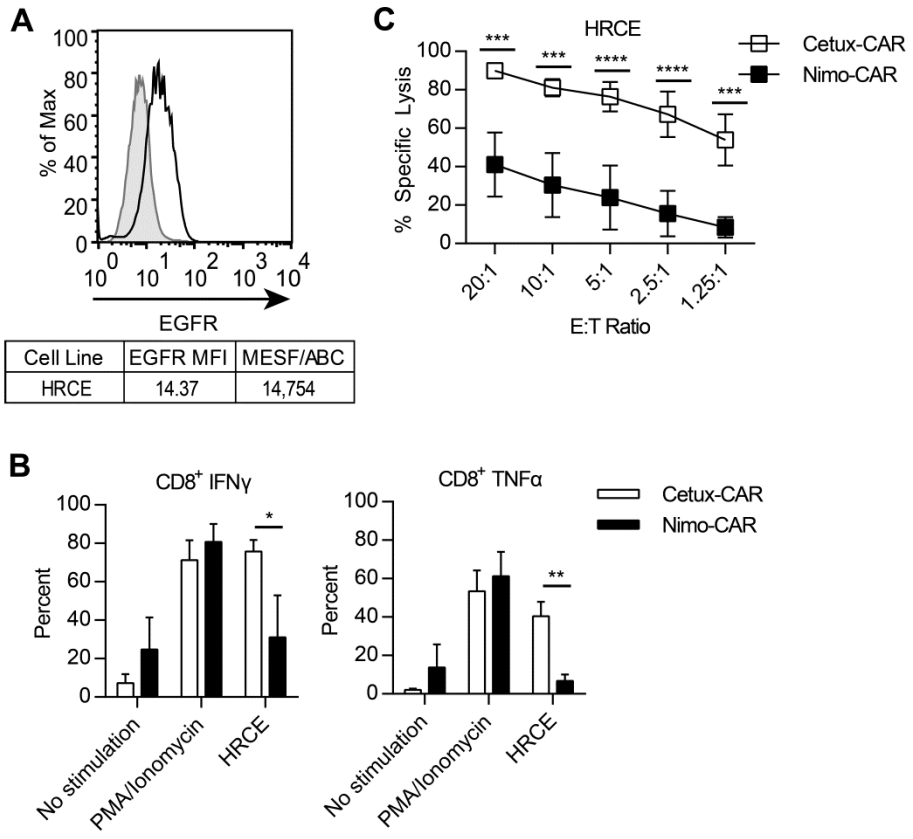

Figure 24. Nimo-CAR$^+$ T cells have less activity in response to basal EGFR levels on normal renal epithelial cells than Cetux-CAR$^+$ T cells. (A) Representative histogram of expression of EGFR on HRCE measured by flow cytometry. Number of molecules per cell determined by quantitative flow cytometry. Data representative of three replicates. (B) Production of IFN-γ and TNF-α by CD8$^+$ CAR$^+$ T cells after co-culture with HRCE measured by intracellular staining and flow cytometry gated on CD8$^+$ cells. Data represented as mean ± SD, n=4, ** p<0.01, * p<0.05, two-way ANOVA (Tukey's post-test). (C) Specific lysis of HRCE by CAR$^+$ T cells measured by standard 4-hour chromium release assay. Data represented as mean ± SD, n=3, **** p<0.0001, *** p<0.001, two-way ANOVA (Tukey's post-test).

significant production of IFN-γ or TNF-α above background production without stimulation (IFN-γ, $p>0.05$; TNF-α, $p>0.05$). Nimo-CAR$^+$ T cells displayed less than 50% of the specific lysis executed by Cetux-CAR$^+$ T cells in response to HRCE (Cetux-CAR = 81.1 ± 4.5%, Nimo-CAR = 30.4 ± 16.7%, mean ± SD, n=3), which was significantly less (10:1 E:T ratio, $p<0.001$) (**Figure 24C**). These findings indicate that Nimo-CAR$^+$ T cells have reduced T-cell function in response to cells with very low EGFR density compared to Cetux-CAR$^+$ T cells.

3.2.6 Cetux-CAR$^+$ T cells proliferate less following stimulation than Nimo-CAR$^+$ T cells, but do not have increased propensity for activation induced cell death (AICD)

Strength of endogenous TCR signal, impacted by affinity of binding and antigen density, can influence proliferation of T cells in response to antigenic stimulus (60, 61). To evaluate proliferative response of Cetux-CAR$^+$ T cells and Nimo-CAR$^+$ T cells following stimulation with antigen, we measured intracellular expression of Ki-67 by flow cytometry after two days of co-culture with U87 or U87^{high} in absence of exogenous cytokines. In response to low EGFR density on U87, Cetux-CAR$^+$ and Nimo-CAR$^+$ T cells demonstrated statistically similar proliferation ($p>0.05$) (**Figure 25A**). In response to U87^{high}, Nimo-CAR$^+$ T cells demonstrated increased proliferation over Cetux-CAR$^+$ ($p<0.01$), which did not show any statistical difference in proliferation in response to U87 and U87^{high} ($p>0.05$).

To determine if affinity of CAR or antigen density increases the propensity of CAR$^+$ T cells to undergo AICD, we co-cultured Cetux-CAR$^+$ and Nimo-CAR$^+$ T cells with U87 or U87^{high} in the absence of exogenous cytokines and evaluated T-cell viability by annexin V and 7-AAD staining. In response to U87, Cetux-CAR$^+$ T showed reduction in viability compared to unstimulated Cetux-CAR$^+$ T cells, however, Nimo-CAR$^+$ T cells did not show any appreciable change in viability (**Figure 25B**). In response to U87^{high}, Cetux-CAR$^+$ and Nimo-CAR$^+$ T cells demonstrated statistically similar reduction in viability relative to unstimulated CAR$^+$ T cells ($p>0.05$). We noted that Cetux-CAR$^+$ T cells stimulated with U87^{high} did not show any statistical difference in viability relative to Cetux-CAR$^+$ T cells stimulate with U87 ($p>0.05$). These data suggest that antigen density impact induction of AICD for Nimo-CAR$^+$ T cells, but not Cetux-CAR$^+$ T cells, supporting previous data that activity of Nimo-CAR is dependent on antigen density. However, in response to high antigen density that is capable of Cetux-CAR$^+$ T cells and Nimo-CAR$^+$ T-cell activation, affinity of scFv domain of CAR does not appear to impact the induction of AICD.

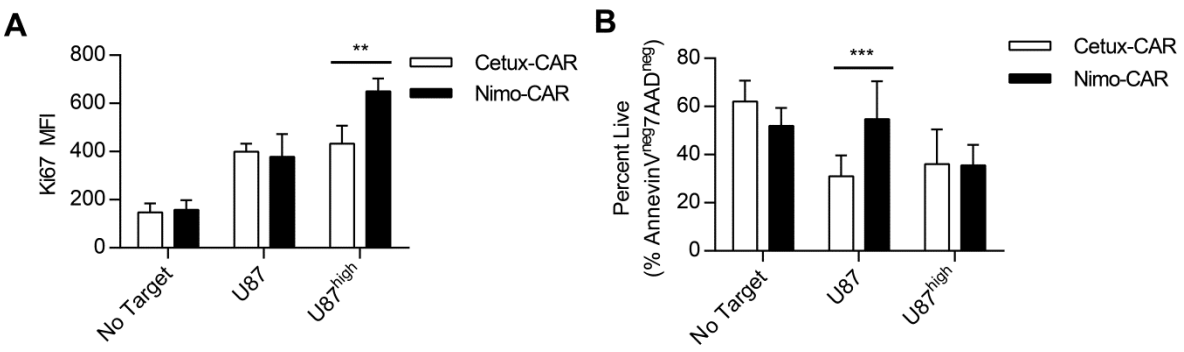

Figure 25. Cetux-CAR$^+$ T cells proliferate less following stimulation than Nimo-CAR$^+$ T cells, but do not have increased propensity for AICD. (A) Proliferation of CD8$^+$ CAR$^+$ T cells after stimulation with U87 or U87^{high} measured by intracellular flow cytometry for Ki-67 gated on CD8$^+$ cells. Data represented as mean fluorescence intensity ± SD, n=4, ** p<0.01, two-way ANOVA (Tukey's post-test). (B) Viability of T cells after stimulation with U87 or U87^{high} measured by flow cytometry for Annexin V and 7-AAD gated on CD8$^+$ cells. Percent live cells determined by percent Annevin V^{neg} 7-AAD^{neg}. Data represented as mean ± SD, n=4, *** p<0.001, two-way ANOVA (Tukey's post-test).

3.2.7 Cetux-CAR$^+$ T cells demonstrate enhanced downregulation of CAR

Endogenous TCR can be downregulated following interaction with antigen, and the degree of downregulation is influenced by the strength of TCR binding (20). Similarly, CAR can be downregulated following interaction with antigen, but the effect of affinity on CAR downregulation is unknown (117, 122). Therefore, we sought to determine if Cetux-CAR$^+$ T cells have a higher propensity for antigen-induced downregulation. To accomplish this, we co-cultured Cetux-CAR$^+$ T cells and Nimo-CAR$^+$ T cells with U87 or U87^{high} and monitored CAR expression relative to unstimulated controls. In response to low EGFR density on U87, Cetux-CAR expression was significantly less than Nimo-CAR following 12 hours of interaction (Cetux-CAR = 68.0 ± 27.8%, Nimo-CAR = 126.5 ± 34.9%, mean ± SD, n=3) ($p<0.05$) (**Figure 26A**, left panel). By 48 hours of interaction with low density EGFR, Cetux-CAR returned to the T-cell surface, and Cetux-CAR and Nimo-CAR were expressed in a statistically similar proportion of T cells (Cetux-CAR = 95.5 ± 40.7, Nimo-CAR = 94.4 ± 11.8%, mean ± SD, n=3) ($p>0.05$). In response to high EGFR density on U87^{high}, expression of Cetux-CAR was significantly reduced relative to Nimo-CAR, which showed no appreciable downregulation after 12 hours of interaction (Cetux-CAR = 37.4 ± 11.5%, Nimo-CAR= 124.4 ±1 5.3%, mean ± SD, n=3) ($p<0.01$) (12 hrs, $p<0.01$; 24 hrs, $p<0.01$; 48 hrs, $p<0.05$) (**Figure 26A**, right panel). However, in contrast to stimulation with low EGFR density, Cetux-CAR did not recover surface expression after 48 hours of interaction and remained reduced relative to Nimo-CAR expression (Cetux-CAR = 42.6 ± 5.9%, Nimo-CAR = 95.7 ± 11.6%, mean ± SD, n=3)($p<0.05$). Cetux-CAR and Nimo-CAR were both detected intracellularly following stimulation, even when Cetux-CAR was reduced from the T-cell surface, signifying that reduced CAR expression was due to internalization of CAR and not outgrowth of genetically unmodified T cells (**Figure 26B**). In response to CAR-dependent, scFv-independent stimulation by CAR-L$^+$ EL4, Cetux-CAR and Nimo-CAR showed mild and statistically similar downregulation of ~20% **(Figure 26C**). Similar to previous results, Cetux-CAR showed slight downregulation in response to tEGFR$^+$ EL4, whereas Nimo-CAR showed no appreciable downregulation. In sum, these data show that Cetux-CAR demonstrates rapid and prolonged downregulation relative to Nimo-CAR that is dependent on interaction of the scFv domain of CAR with antigen and antigen density.

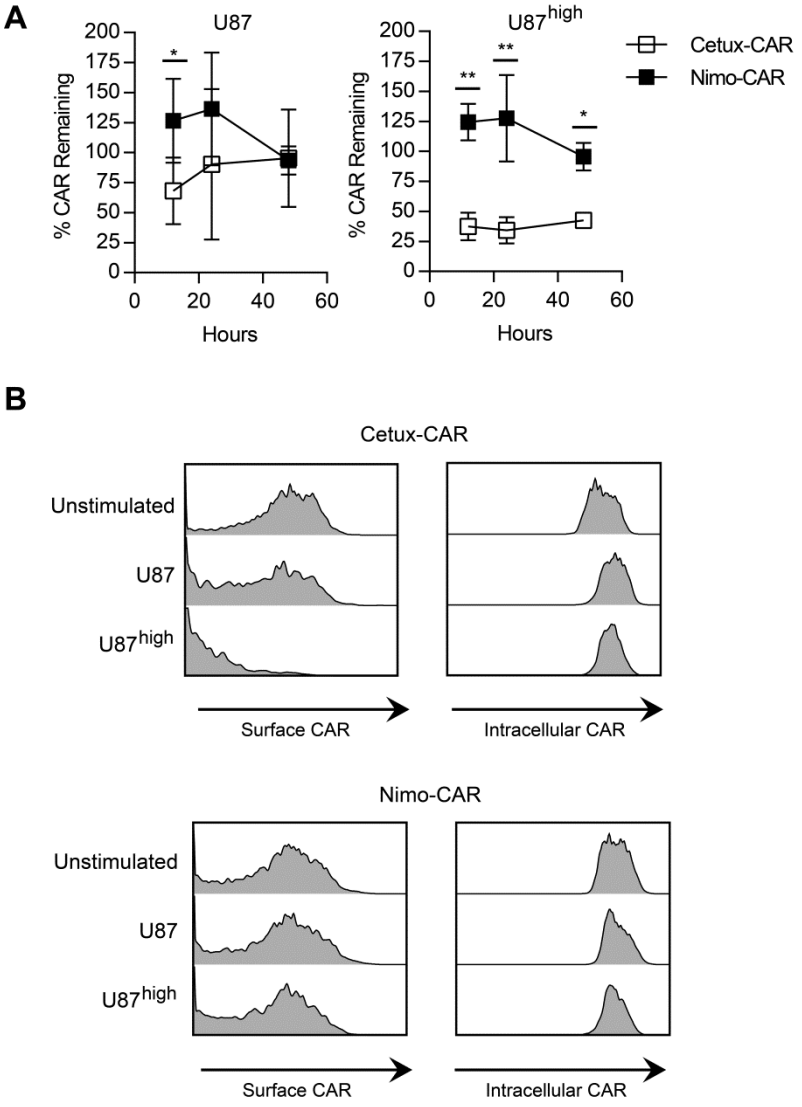

Figure 26. Cetux-CAR$^+$ T cells demonstrate enhanced downregulation of CAR. (A) Surface expression of CAR during co-culture (E:T 1:5) with U87 or U87^{high} measured by flow cytometry for IgG portion of CAR. Percent CAR remaining calculated as [%CAR$^+$ in co-culture] / [%CAR$^+$ in unstimulated culture] x 100. Data represented as mean ± SD, n=3, ** p<0.01. * p<0.05, two-way ANOVA (Tukey's post-test) (B) Representative histograms of Intracellular and surface expression of CAR determined by flow cytometry after 24 hours of co-culture with U87 or U87^{high} in CD8$^+$ gated T cells. Data representative of three independent donors. (C) Surface expression of CAR during co-culture (E:T 1:1) with EGFR$^+$ EL4 or CAR-L$^+$ EL4 measured by flow cytometry for Fc portion of CAR. Percent CAR remaining calculated as [%CAR$^+$ in co-culture] / [%CAR$^+$ in unstimulated culture] x 100. Data represented as mean, n=2, * p<0.05, two-way ANOVA (Tukey's post-test).

3.2.8 Cetux-CAR$^+$ T cells have reduced response to re-challenge with antigen

Strength of prior stimulus in endogenous CD8$^+$ T cell responses can be correlated with T-cell response upon re-challenge with antigen (287). Therefore, we evaluated the ability of Cetux-CAR$^+$ and Nimo-CAR$^+$ T cells to respond to antigen re-challenge. CAR$^+$ T cells were co-cultured with U87 or U87^{high} for 24 hours, then harvested and re-challenged with U87 or U87^{high} to assess production of IFN-γ. Following initial challenge with U87 and U87^{high}, Cetux-CAR$^+$ T cells had reduced production of IFN-γ in response to rechallenge with both U87 and U87^{high} (**Figure 27**) However, after initial challenge with U87 or U87^{high}, Nimo-CAR$^+$ T cells retained IFN-γ production in response to re-challenge with U87 and U87^{high}. As a result, Nimo-CAR$^+$ T cells demonstrated statistically similar IFN-γ production in response to U87 ($p>0.05$) and statistically more IFN-γ in response to rechallenge with U87^{high} (initial challenge with U87, $p<0.001$; initial challenge with U87^{high} $p<0.01$). This is in contrast to IFN-γ production in response to initial challenge, in which Nimo-CAR$^+$ T cells produce less IFN-γ in response to U87($p<0.05$) and demonstrate statistically similar IFN-γ production in response to U87^{high} ($p>0.05$). Thus, while Nimo-CAR$^+$ T cells retain their ability to recognize and respond to antigen, Cetux-CAR$^+$ T cells have reduced capacity to respond to subsequent encounter with antigen, which is likely to be at least partially due to downregulation of CAR and may indicate increased propensity for functional exhaustion of Cetux-CAR T$^+$ cells after initial antigen exposure.

3.3 Discussion

Recent clinical success in patients with CLL and ALL note persistent B-cell in patients with complete tumor response to CD19-CAR$^+$ T-cell therapy, but this toxicity is considered tolerable as CD19 is a lineage-restricted antigen and B cell aplasia is considered a tolerable toxicity in the setting of advanced lymphoma (111, 112). Serious adverse events in clinical trials targeting HER2 and CAIX with CAR-modified T cells makes obvious the need to control CAR$^+$ T-cell activity against normal tissue antigen expression in order to broaden the range of safely targetable antigens beyond lineage and tumor restricted antigens (140, 143). Aberrantly expressed TAAs are often overexpressed on tumor relative to normal tissue, such as EGFR expression in glioblastoma (180, 182, 199). We sought to develop a CAR specific to EGFR with reduced capacity to respond to low antigen density to minimize the potential for normal tissue, while maintaining adequate effector function in

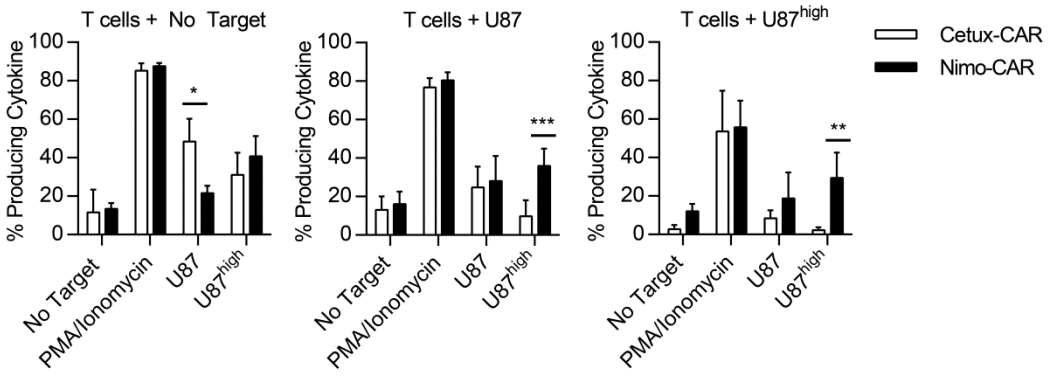

Figure 27. Cetux-CAR$^+$ T cells have reduced response to re-challenge with antigen. After 24-hours of incubation with U87 or U87^{high}, CAR$^+$ T cells were rechallenged with U87 or U87^{high} and production of IFN-γ CAR$^+$ T cells measured by intracellular staining and flow cytometry gated on CD8$^+$ cells. Data represented as mean ± SD, n=3, *** p<0.001, ** p<0.01, * p<0.05, two-way ANOVA (Tukey's post-test).

response to high antigen density. This was accomplished by developing an EGFR-specific CAR from nimotuzumab, a monoclonal antibody with a highly-overlapping epitope with cetuximab, yet reduced binding kinetics (223, 231). While Cetux-CAR$^+$ T cells are capable of targeting low and high EGFR density, Nimo-CAR$^+$ T cells are able to tune T-cell activity to antigen density and T-cell response is dependent on EGFR density on target cells. While Nimo-CAR$^+$ T cells demonstrate reduced activity relative to Cetux-CAR$^+$ T cells in response to low EGFR density on tumor cells and normal renal cells, they are capable of equivalent redirected specificity and function in response to high EGFR density. We observed that CAR affinity influenced proliferation after antigen challenge, Cetux-CAR$^+$ T cells demonstrated impaired proliferation when compared with Nimo-CAR$^+$ T cells after antigen challenge, but no increased propensity for AICD. Additionally, we observed that CAR affinity influences downregulation of CAR from T-cell surface after interaction with antigen. Cetux-CAR exhibited rapid and prolonged downregulation from the cell surface after interaction with high EGFR density, whereas Nimo-CAR did not appreciably downregulate from T-cell surface. Cetux-CAR$^+$ T cells had impaired ability to respond to re-challenge with antigen, which is likely due, at least in part, to downregulation of CAR, and may indicate functional exhaustion of Cetux-CAR$^+$ T cells (122, 287).

Complications in delineating the impact of scFv affinity on CAR-mediated T-cell function stem from considerable debate surrounding the biochemical parameter of endogenous TCR binding pepMHC that best predicts T-cell function. The kinetics of TCR binding can be described by the equation:

$$K_d = \frac{k_{off}}{k_{on}}$$

such that the dissociation constant, K_d, is equal to the ratio of the rate of dissociation (k_{off}) and the rate of association, (k_{on}) (14). Both the dissociation constant (K_d) and the dissociation rate (k_{off}) have been reported as important determinants of T-cell function following TCR recognition of pepMHC, however these two parameters are often strongly correlated, so it is difficult to separate their respective impact on T-cell function (15, 22, 23). The kinetic proofreading model of T-cell triggering states that k_{off} impact T-cell function, such that sufficiently long dwell time is required to trigger T-cell signaling and activation. This has been amended to include a window of optimal dwell time, in which prolonged dwell time may be detrimental to T-cell activation by impairing the ability of serial triggering of multiple TCR by a single pepMHC complex (27). However, these models are contradicted by reports of

very short dwell time interactions capable of producing functional T-cell responses (25, 26, 34, 60). Recent analysis aiming to reduce previous dataset bias by reducing the high degree of correlation between K_d and k_{off} values and expanding dynamic range of k_{on} values uncovered an important role in contribution of k_{on} to T-cell activation, encompassed in a T-cell confinement model of T-cell triggering, in which T-cell function is directly correlated with the duration of T-cell confinement derived from a mathematical relationship between rate of association, rate of dissociation, and diffusion of TCR and pepMHC in their relative membranes (25, 34). Interestingly, as k_{on} becomes low, TCR and pepMHC are able to diffuse in their relative membranes before rebinding, thus the duration of interaction reduces to the k_{off} value. In contrast, as k_{on} becomes high, the TCR is capable of rapid rebinding to extend the dwell time, and the duration of interaction and resulting T-cell function is best predicted by K_d. This ongoing debate to define role of TCR affinity components that control T-cell functional avidity cautions against universal models relying on one biochemical parameter of binding as a superior indicator of function over others. Instead, it is likely a combination of rates of association and dissociation as well as density of antigen freely moving through target cell membrane that defines functional response.

Endogenous TCR responses are generally described as much lower affinity than the binding of monoclonal antibodies, which are used to derive CARs (14). However, SPR techniques used to measure TCR binding affinity measure are typically performed in three dimensions, and do not recapitulate physiological interaction of a T cells with an antigen presenting cell, in which both binding partners are constrained in their respective membranes, increasing the probability of binding due to constrained intercellular space and proper molecule orientation (38). Measurement of TCR binding kinetics in 2D suggests that TCR binding is of higher affinity than suggested by 3D measurements characterized by increased rates of association and decreased rates of dissociation (37, 39). However, binding kinetics of other ligand/receptor pairs, such as ICAM-1 or LFA-1 did not show a difference between affinity measurements taken in 3D or 2D assays. Interestingly, ablation of cytoskeletal polymerization reduces measurements made in 2D to measurements to those made in 3D, highlighting the role of dynamic cellular and cytoskeletal processes in enhancing T-cell binding to antigen (39). Whether similar cytoskeletal interactions or enhancement of binding affinity of CAR occurs is currently unknown, and therefore, it is unclear if assumptions made about binding affinity of the scFv domain of CAR can be directly made from measurements of monoclonal antibody affinity in 3D assays. In addition,

several factors contribute to enhance overall T-cell binding avidity, such as co-receptor binding to MHC and TCR nanocluster and microcluster formation on the T-cell surface prior to and following T-cell activation (31, 40-42, 47). While it appears that CARs can be expressed in oligomeric form on the T cell surface, the degree of involvement of CAR with endogenous T cell signaling complexes in unclear. Reports of first generation CARs, signaling through only CD3-ζ demonstrate a requirement for association with endogenous CD3-ζ to achieve CAR-dependent T cell activation; however, second generation CARs signaling through transmembrane CD28 and intracellular CD28 and CD3-ζ demonstrate no difference in CAR-dependent activation ability when endogenous TCR-CD3 complexes are restricted from the T cell surface (125, 127). Therefore, the association of CAR with endogenous TCR signaling machinery may be dependent on CAR configuration. In sum, the contribution of dynamic cellular processes that occur during endogenous TCR activation to CAR-dependent T-cell activation requires further investigation. However, due to the contribution of these processes to enhancing avidity of T-cell interaction with antigen, the difference between CAR and TCR binding affinities may not be as disparate as initially thought.

Specific studies addressing the role of scFv affinity in CAR design are limited, and focus on contribution of the dissociation constant, $K_{d.}$ Recent studies with ROR1-specific CAR compared a with 6-fold lower K_d, thus higher affinity, resulting from both increased k_{on} and decreased k_{off} and demonstrated that higher affinity ROR-1 specific CAR increased T-cell function *in vitro*, including production of cytokines and specific lysis, without increased propensity for AICD (119). Additionally, high affinity ROR-1-specific CAR^+ T cells mediated superior anti-tumor activity *in vivo*. Similarly, we found the higher affinity of Cetux-CAR+ T cells did not increase propensity for AICD, and had increased T-cell function, including production of cytokines and specific lysis, in response to reduced EGFR density. However, a previous study of a series of CARs derived from a panel of affinity-matured HER2-specific monoclonal antibodies with a wide range of K_d values, found that an affinity threshold existed, below which CAR-dependent T-cell activation was impaired; however, above this threshold, activation of T cells in response to various levels of HER2 did not improve with increased affinity (120). In contrast, the present study identified different ability of high affinity CAR and low affinity CAR to target based on antigen density. Higher affinity Cetux-CAR^+ T cells were associated with increased cytokine production and specific lysis in response to reduced EGFR density relative to Nimo-CAR^+ T cells. While, Nimo-CAR is lower

affinity relative to Cetux-CAR, the K_d value of Nimo-CAR is above the affinity threshold and within the range predicted to have effector function by the previous study. Similar to studies with endogenous TCRs, these results indicate that descriptions of CAR affinity should not be described solely by the dissociation constant, and support that relationship between individual dissociation and association rates be taken into consideration for CAR design.

The contradictions between the influence of affinity on CAR function between studies may be explained by the distinct relationships of the biochemical parameters k_{off} and k_{on} that constitute the dissociation constant K_d. The HER2-specific CARs were derived from antibodies that displayed a wide range of K_d values differing primarily in k_{off}, with minimal correlation of k_{on} values (120). Thus, higher affinity interactions did not have increased rates of association, but increased duration of interaction with antigen. In contrast, the higher affinity of the ROR-1-specific CAR and Cetux-CAR were both influenced by increased association rates of binding. The higher affinity monoclonal antibody used to derive the ROR-1-specific CAR had a 6-fold lower K_d, from contributions of both increased k_{on} and decreased k_{off}, such that the higher affinity was characterized by both increased association rates and increased duration of interaction (119). The 10-fold difference in K_d between cetuximab and nimotuzumab is primarily impacted by a 59-fold increase in the k_{on} and a 5.3-fold increase in the k_{off} of cetuximab, such that cetuximab has greatly enhanced rate of association relative to nimotuzumab, but in contrast to most higher affinity interactions, a shorter duration of interaction (223). Therefore, altering association rate rather than the dissociation rate of scFv domain in CAR design may have a greater impact on CAR-mediated T-cell function.

Nimotuzumab with combination radiotherapy has been evaluated in clinical trial for the treatment of head and neck squamous cell carcinoma and high grade glioma and has demonstrated significant survival benefit for both malignancies (227, 288-290). Clinical trials have noted the absence of grade III/IV acneiform rash that is common in treatment with cetuximab, despite strongly overlapping epitopes of nimotuzumab and cetuximab and similar mechanisms of action (223, 228). *In vitro* studies have demonstrated that while cetuximab can bind any density of EGFR expression, nimotuzumab bindings directly correlates with EGFR density and at the highest EGFR density tested, nimotuzumab was able to bind EGFR with similar efficiency as cetuximab (231). Interestingly, when dissociated into monovalent fragments, cetuximab maintains ability to bind EGFR independent of expression density, but nimotuzumab binding to EGFR is completely abrogated. This

indicates that nimotuzumab has a requirement for bivalent recognition of antigen not present for cetuximab and attributed to the lower affinity of nimotuzumab. Thus, the low rate of association of nimotuzumab enforces a requirement for bivalent binding of EGFR that may be responsible for decreased sensitivity to low EGFR density.

While it appears the lower association rate of nimotuzumab relative to cetuximab may account for the reduced activity of Nimo-CAR in response to low density EGFR, it is possible that dissociation rate of nimotuzumab binding also plays a role. With all other things being equal, a lower dissociation rate (k_{off}) and therefore increased duration of interaction is typically associated with higher affinity interactions. In the case of cetuximab and nimotuzumab, however, the much lower association rate (k_{on}) overshadows the slightly lower dissociation rate of nimotuzumab, resulting in dissociation constant (K_d) that describes nimotuzumab as a lower affinity antibody, even though it has a longer duration of interaction. The k_{on} value is sufficiently low that rapid rebinding is not likely to occur to amplify T cell signal. Thus, according to the T-cell confinement model of T-cell triggering (34), a sufficiently long duration of interaction from low k_{off} may be necessary in the setting of low k_{on} for CAR^+ T cells to adequately initiate and sustain signaling cascades for T-cell activation. Therefore, it is unclear that this time which biochemical parameters are responsible for the ability of nimotuzumab to discriminate based on tissue antigen density. Future work, including mutation of the scFvs of nimotuzumab and cetuximab to alter k_{on} and k_{off}, may elucidate whether a single biochemical parameter or a more complex interaction of multiple biochemical parameters of binding can account for reduced ability to bind low density EGFR. Determining the precise biochemical parameter or relationship between biochemical parameters that imparts the ability of nimotuzumab to discriminate between low and high EGFR density may aid in identification of other monoclonal antibodies with potential to discriminate between high and low antigen density to apply this CAR design strategy to other TAAs.

Previous studies have established that a minimum CAR density is required for T-cell activation, below which T-cell activation is abrogated (122). However, sufficiently high antigen expression can mitigate this requirement and achieve CAR-dependent T-cell activation when CAR is expressed at low density (117, 122, 123). The interplay between CAR expression density, antigen density and CAR affinity and impact on CAR^+ T cell function were evaluated in a study using high and low affinity HER2-specific CARs. This study reported that reduced T-cell function of T cells with low CAR density in response to

low antigen density was only apparent when T cells expressed a higher affinity HER2-specific CAR (124). However, when CAR was expressed at higher density, CAR-mediated cytotoxicity was irrespective of affinity or antigen density. The authors attributed the reduced response of high affinity CAR when expressed low density to low HER2 density to a failure to induce serial triggering. Although it has been reported that CARs to do not serially trigger as endogenous TCRs do (122), it is possible that this is specific to individual CARs, and that different transmembrane regions, endodomains, and scFv affinity may impact ability to serially trigger. We did not observe any defect in Cetux-CAR$^+$ T cells in initial response to low antigen density, however, the level of CAR expression culled out through repetitive stimulation on EGFR$^+$ aAPC may select for an optimum CAR density, with T cells expressing suboptimal levels of CAR failing to expand and thus falling out of the repertoire. Our findings suggest that the lower affinity Nimo-CAR$^+$ T cells demonstrate reduced sensitivity to low antigen expression, but increasing density of Nimo-CAR did not restore Nimo-CAR$^+$ T cell sensitivity to low antigen, thus it is likely controlled by a different mechanism. Although expression CAR at low density can reduce sensitivity to antigen, this is not likely to be an optimal strategy selectively target high antigen density *in vivo,* primarily because CAR expressed at low density demonstrate reduced sensitivity to all levels of antigen, and therefore the potential for reduced anti-tumor activity (122, 123). Additionally, CAR downregulates from the T-cell surface at a constant number of CAR molecules per antigen molecule (122). Thus, T cells expressing CAR at lower density are more susceptible to downregulation below the minimum density to achieve T-cell activation.

T-cell function can be influenced by antigen quality, dictated by the affinity of the interaction, and antigen quantity, or the density of antigen expression (17). While increasing quantity of low affinity antigen can increase T-cell proliferation, it does not restore IL-2 production, highlighting the distinct regulation of T-cell responses by quality and quantity of signal (60). Distinction between quality and quantity of signaling between Cetux-CAR and Nimo-CAR is evident by reduced phosphorylation of Erk1/2 and p38, enhanced proliferation, and reduced CAR downregulation of Nimo-CAR$^+$ T cells in response to high EGFR density, in spite of comparable functional responses. Efficient phosphorylation by CAR-L$^+$ EL4 cells indicates that Nimo-CAR$^+$ T cells have equivalent capacity for phosphorylation as Cetux-CAR$^+$ T cells when triggering in a CAR-dependent but scFv-independent manner. Endogenous, low-affinity TCRs can accumulate signal through transient and undetectable phosphorylation intermediates to culminate in functional T-cell responses (60). This may be

an explanation for functional response of Nimo-CAR$^+$ T cells even when phosphorylation of Erk1/2 and p38 is lacking.

Superior proliferation of Nimo-CAR$^+$ T cells over Cetux-CAR$^+$ T cells in response to high EGFR density in the absence of exogenous cytokine support may be due to reduced stimulation to Cetux-CAR$^+$ T cells following CAR downregulation, or may indicate functional exhaustion of Cetux-CAR$^+$ T cells. In endogenous T-cell responses, downregulation of TCR is enhanced in response to strong stimulation as a mechanism to regulated T-cell responses. Thus, reduced expression of Cetux-CAR may be responsible for reduced proliferation of Cetux-CAR$^+$ T cells. Although cell surface markers for differentiation and exhaustion showed no difference between Cetux-CAR$^+$ T cells and Nimo-CAR$^+$ T cells, it is possible that reiterative stimulation with aAPC through Cetux-CAR with higher affinity could drive a more exhausted or anergic phenotype. Future studies to profile expression of gene transcripts important in T-cell biology will determine potential differences in Cetux-CAR$^+$ and Nimo-CAR$^+$ T cell phenotype throughout *ex vivo* culture.

Cetux-CAR$^+$ T cells were less capable of responding to re-challenge with antigen, which may be a result of downregulated CAR expression following antigen exposure or functional exhaustion. A similar finding was reported in studies with CD22-specific CAR, in which downregulation of CAR was correlated with antigen density, and impaired T-cell activity in response to antigen re-challenge (122). However, impairment of lytic activity was noted at antigen densities that induced minimal CAR downregulation, therefore, the authors concluded that both CAR downregulation and functional impairment after antigenic exposure contributed to impairment of T-cell response to antigen re-challenge. Whether due to reduced CAR expression or functional exhaustion, reduced response of Cetux-CAR$^+$ T cells to re-challenge with antigen may indicate reduced ability of Cetux-CAR$^+$ T cells serially kill tumor cells, resulting in potentially reduced anti-tumor efficacy.

In summary, affinity of scFv in CAR design and impact CAR-mediated T-cell function. In this study, Nimo-CAR, predicted to have lower affinity due to reduced association rate of binding relative to Cetux-CAR, mediated T-cell activation that directly correlated with EGFR expression density and reduced activity in response to low EGFR density. Additionally, Nimo-CAR$^+$ T cells showed enhanced proliferation and reduced CAR downregulation relative to Cetux-CAR$^+$ T cells. Targeting EGFR on glioblastoma by Nimo-CAR$^+$ T cells has

the potential to mediate anti-tumor activity while reducing the potential for on-target, off-tissue toxicity.

CHAPTER 4

In vivo anti-tumor efficacy of Cetux-CAR$^+$ and Nimo-CAR$^+$ T cells in an intracranial glioma model

4.1 Introduction

In Chapter 3, we acknowledged that some tumors, such as glioblastoma, overexpress EGFR at a higher density relative to normal tissue expression and hypothesized that altering the scFv domain of CAR to reduce binding affinity could preferentially activate T cells in the presence of high EGFR density but reduce T-cell activity in the presence of low EGFR density. Cetux-CAR and Nimo-CAR bind overlapping epitopes on EGFR with distinct affinities and binding kinetics, such that Cetux-CAR has a 5.3-fold lower dissociation constant, and therefore higher affinity, characterized by a 59-fold higher rate of association. *In vitro* studies also demonstrated Cetux-CAR had reduced proliferation in response to antigen in the absence of exogenous cytokine, enhanced downregulation of CAR that was dependent on scFv domain of CAR binding EGFR and density of EGFR, and impaired cytokine production in response to re-challenge with antigen.

Previous studies have reported that affinity of TCRs up to a threshold increase effector functions *in vitro* and *in vivo* (23, 62). In contrast, high affinity TCRs have also been described to have impaired function *in vivo*, characterized by deletion in tumor and periphery, failure to infiltrate tumor, and loss of cytotoxic effector functions despite potent *in vitro* function (65-67). Therefore, *in vitro* function does not necessarily correlate with effective treatment of *in vivo* tumor models.(65)

To determine if *in vitro* findings that Nimo-CAR$^+$ T cells are cytotoxic in response to high EGFR density, but have reduced activity in response to low EGFR density, extend to *in vivo* observations, we compared Cetux-CAR$^+$ T cells and Nimo-CAR$^+$ T cells delivered intratumorally in the treatment of intracranial glioma xenografts with low or intermediate EGFR density. We *hypothesized* that Nimo-CAR$^+$ T cells would be equally capable of *in vivo* activity against xenograft with intermediate EGFR density, but reduced anti-tumor activity against xenograft with low EGFR density.

4.2 Results

4.2.1 Establishment of an intracranial glioma model using U87 cells in NSG mice

To evaluate anti-tumor efficacy of Cetux-CAR$^+$ T cells and Nimo-CAR$^+$ T cells *in vivo*, we elected to establish an intracranial glioma xenograft of U87 cells modified to express firefly luciferase (ffLuc) reporter for serial, non-invasive imaging of relative tumor burden by bioluminescence (BLI). We adopted the previously described guide-screw method for directed infusion of tumor and T cells (291). The guide screw was implanted into the right frontal lobe of the cranium of NOD/*Scid*/IL2Rg$^{-/-}$ (NSG) mice and mice recovered for two weeks (**Figure 28A**). A timeline from guide screw implantation through T-cell treatment and evaluation of relative tumor burden by BLI is depicted in **Figure 28B**. 250,000 U87 cells with endogenously low EGFR or intermediate EGFR expression through enforced expression of tEGFR were injected through the center of the guide screw at depth of 2.5mm. Mice were imaged prior to T-cell treatment to evaluate tumor burden and mice were stratified to evenly distribute tumor burden into three groups: mice to receive no treatment, Cetux-CAR$^+$ T cells, or Nimo-CAR$^+$ T cells. Five days after injection of tumor, the initial dose of 4x10^6 T cells was injected intratumorally through the center of the guide screw. Subsequent T-cell doses were administered through the guide screw weekly for a total of three T-cell doses. Measurement of BLI six days after each T-cell treatment was used to assess relative tumor burden. Following treatment, mice were evaluated for end point criteria, including rapid weight loss of greater than 5% of body mass in a 24 hour period, progressive weight loss of more than 25% of body mass, or obvious clinical signs of illness, including ataxia, labored respiration, and hind-limb paralysis. Mice were sacrificed when end-point criteria were met, suggesting imminent animal death, and survival of Cetux-CAR$^+$ T-cell treated mice and Nimo-CAR$^+$ T-cell treated mice relative to mice receiving no treatment was assessed.

4.2.2 Nimo-CAR$^+$ T cells inhibit growth of xenografts with moderate EGFR density similar to Cetux-CAR$^+$ T cells, but without T-cell related toxicity.

Four days after injection of U87^{med}, mice were imaged by BLI to assess tumor burden (**Figure 29A**). Mice were distributed into three groups to evenly distribute relative tumor burden and then randomly assigned treatment: no treatment, Cetux-CAR$^+$ T cells, or Nimo-CAR$^+$ T cells (**Figure 29B**). On the day of T-cell treatment, CAR$^+$ T cells that had

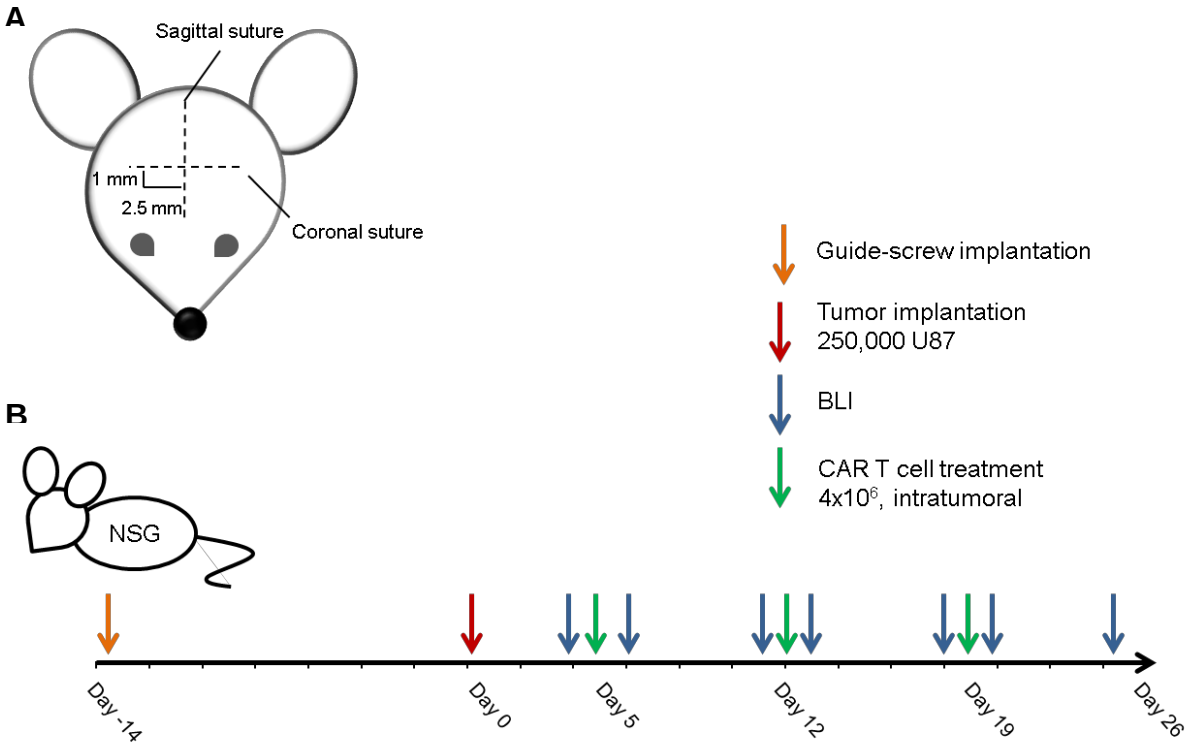

Figure 28. Schematic of animal model and treatment schedule. (A) Schematic of guide screw placement. A 1-mm hole is drilled for insertion of guide screw in the right frontal lobe, 1 mm from the coronal suture and 2.5 mm from the sagittal suture. (B) Timeline of treatment schedule. Guide-screw is implanted into the right frontal lobe of mice no less than 14 days prior to injection of tumor. Injection of tumor is designated as day 0 of study. Tumor was imaged by BLI four days after injection, which was the day prior to initiation of T-cell treatment. CAR^+ T cells were administered intracranially through the guide-screw weekly for three weeks. Tumor growth was assessed by BLI the prior to and following T-cell treatment while mice were actively receiving treatments, then weekly throughout remainder of experiment.

undergone 3 rounds of stimulation and numeric expansion on $EGFR^+$ aAPC were phenotyped by flow cytometry to determine expression of CAR and ratio of $CD8^+$ and $CD4^+$ T cells (**Figure 29C**). CAR expression was similar between Cetux-CAR^+ T cells and Nimo-CAR^+ T cells (92% and 85%, respectively). Both Cetux-CAR^+ and Nimo-CAR^+ T cells contained a mixture of $CD4^+$ and $CD8^+$ T cells, however, Cetux-CAR^+ T cells contained about 20% fewer $CD8^+$ T cells than Nimo-CAR^+ T cells (31.8% and 51.2%, respectively). Cetux-CAR^+ T cells and Nimo-CAR^+ T cells were both capable of inhibiting tumor growth as assayed by BLI (day 18; Cetux-CAR, $p<0.01$ and Nimo-CAR, $p<0.05$) (**Figure 30A,B**). There was no difference between the ability of Cetux-CAR^+ T cells and Nimo-CAR^+ T cells to control tumor growth ($p>0.05$). Reduced tumor burden assessed by BLI was evident in 3/7 mice treated with Cetux-CAR^+ T cells and 4/7 mice treated with Nimo-CAR^+ T cells past 100 days post-tumor injection, when all mice which did not receive treatment had succumbed to disease.

Cetux-CAR^+ T-cell treated mice showed significant toxicity resulting in death of 6/14 mice from two independent experiments within 7 days of T-cell treatment ($p=0.0006$) (**Figure 31A**). Overall, Cetux-CAR^+ T-cell treatment did not statistically improve survival compared to untreated mice, possibly due to early deaths soon after T-cell treatment (untreated median survival = 88 days, Cetux-CAR median survival = 105 days, $p=0.19$) (**Figure 31B**). Interestingly, the survival curve depicts an inflection point, before which Cetux-CAR^+ T-cell treatment results in reduced survival compared to untreated mice, and after which mice surviving initial T-cell toxicity show improved survival. When only considering mice surviving initial T-cell related toxicity, Cetux-CAR^+ T cells improve survival in 3/4 mice, relative to untreated mice ($p=0.0065$). In contrast, Nimo-CAR^+ T cells mediate effective tumor regression and extend survival in 4/7 of mice without any noted toxicity (untreated median survival = 88 days, Nimo-CAR median survival = 158 days, $p=0.0269$). These results indicate that Cetux-CAR^+ T cells and Nimo-CAR^+ T cells are effective at controlling growth of tumor with intermediate antigen density, however Cetux-CAR^+ T cells demonstrate notable toxicity soon after T-cell treatment.

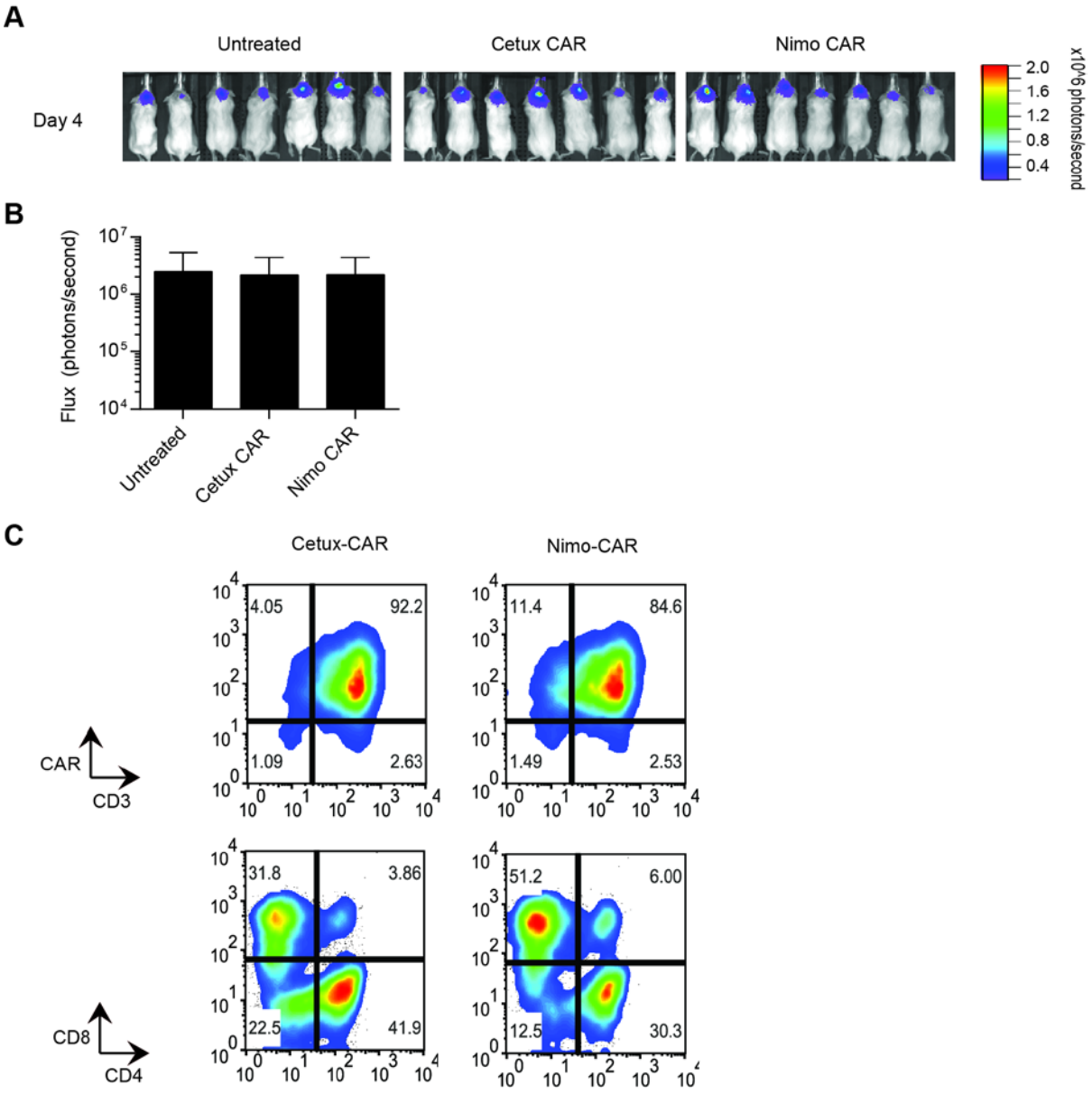

Figure 29. Engraftment of U87^{med} and CAR^{+} T-cell phenotype prior to T-cell treatment. (A) Four days after tumor injection, tumors were imaged by BLI following injection with D-luciferin and 10 minute incubation. (B) Mice were divided into three groups to evenly distribute relative tumor burden as determined by day 4 BLI measurements. (C) Cetux-CAR^{+} and Nimo-CAR^{+} T cells expanded through 3 stimulation cycles were evaluated for CAR expression and CD4/CD8 ratio by flow cytometry.

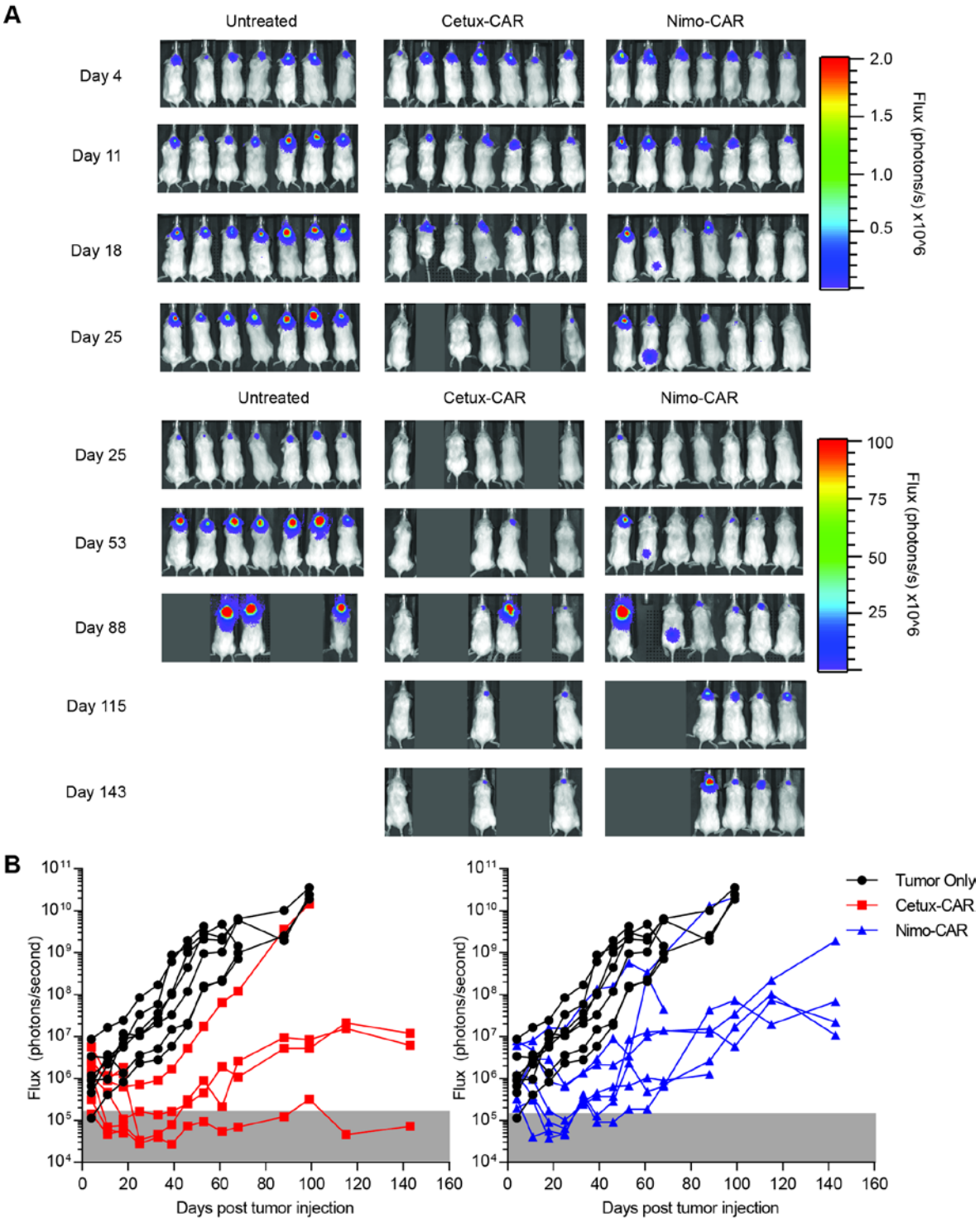

Figure 30. Cetux-CAR$^+$ and Nimo-CAR$^+$ T cells inhibit growth of U87^{med} intracranial xenografts. (A) Serial BLI assessed relative size of tumor. (B) Relative tumor growth as assessed by serial BLI of tumor. Background luminescence (gray shading) was defined by BLI of mice with no tumors. Significant difference in BLI between mice with no treatment vs. treatment (n=7) with Cetux-CAR$^+$ T cells (n=7, $p<0.01$) and no treatment (n=7) vs. treatment with Nimo-CAR$^+$ T cells (n=7, $p<0.05$) at day 18, two-way ANOVA (Sidak's post-test).

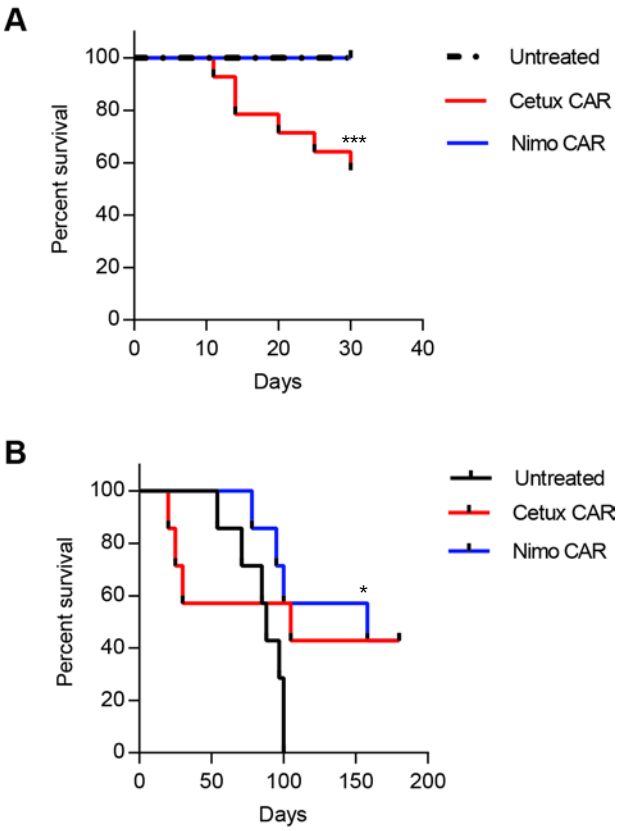

Figure 31. Survival of mice bearing U87^{med} intracranial xenografts treated with Cetux-CAR^{+} and Nimo-CAR^{+} T cells. (A) Survival of mice with U87^{med}-ffLuc-mKate intracranial xenografts from two independent experiments within 7 days of T-cell treatment. Significant reduction in survival in Cetux-CAR^{+} T cell treated mice 8/14 surviving) relative to untreated mice (14/14 surviving) determined by Mantel-Cox log-rank test, p=0.0006. (B) Survival of mice with U87med-ffLuc-mKate intracranial xenografts receiving no treatment, Cetux-CAR^{+} T cells or Nimo-CAR^{+} T cells. Significant extension in survival in Nimo-CAR^{+} T cell treatment group determined by Mantel-Cox log-rank test, p=0.0269.

4.2.3 Cetux-CAR$^+$ T cells, but not Nimo-CAR$^+$ T cells, inhibit growth of xenografts with low EGFR density

Because Nimo-CAR$^+$ T cells are predicted to have reduced T-cell activity in response to targets with low EGFR density, we evaluated activity of T cells in response to U87 with endogenous, low density EGFR expression. Mice were injected with U87, then four days later relative tumor burden was assessed by BLI (**Figure 32A**). Relative tumor burden was evenly distributed into three groups and randomly assigned treatment: no treatment, Cetux-CAR$^+$ T cells, or Nimo-CAR$^+$ T cells (**Figure 32B**). On the day of T-cell treatment, CAR$^+$ T cells that had undergone 3 rounds of stimulation and numeric expansion on EGFR$^+$ aAPC were phenotyped by flow cytometry to determine expression of CAR and ratio of CD8$^+$ and CD4$^+$ T cells (**Figure 32C**). CAR expression was similar between Cetux-CAR$^+$ T cells and Nimo-CAR$^+$ T cells (92% and 85%, respectively). Both Cetux-CAR$^+$ and Nimo-CAR$^+$ T cells contained a mixture of CD4$^+$ and CD8$^+$ T cells, however, Cetux-CAR$^+$ T cells contained about 20% fewer CD8$^+$ T cells than Nimo-CAR$^+$ T cells (31.8% and 51.2%, respectively).

Mice received T-cell treatment and tumor was assessed by BLI as previously described (**Figure 28B**). Treatment of mice with Cetux-CAR$^+$ T cells resulted in significant reduction of tumor burden compared to untreated mice (day 25, $p< 0.01$) (**Figure 33A and 33B**). In contrast, treatment with Nimo-CAR$^+$ T cells did not significantly reduce tumor burden compared to untreated mice (Nimo-CAR, $p>0.05$). Reduced tumor burden in mice treated with Cetux-CAR$^+$ T cells was transient, however, and following cessation of T-cell treatment, tumors resumed growth.

Cetux-CAR$^+$ T cell treatment significantly extended survival in 3/6 mice compared to mice receiving no treatment (untreated median survival = 38.5 days, Cetux-CAR median survival = 53 days, $p=0.0150$) (**Figure 34**). In contrast, treatment with Nimo-CAR$^+$ T cells did not significantly improve survival (untreated median survival 38.5 days, Nimo-CAR median survival 46 days, $p=0.0969$). These data indicate that while Cetux-CAR$^+$ T cells are effective against low EGFR density, Nimo-CAR$^+$ T cells do not mediate significant activity against xenografts with low EGFR density.

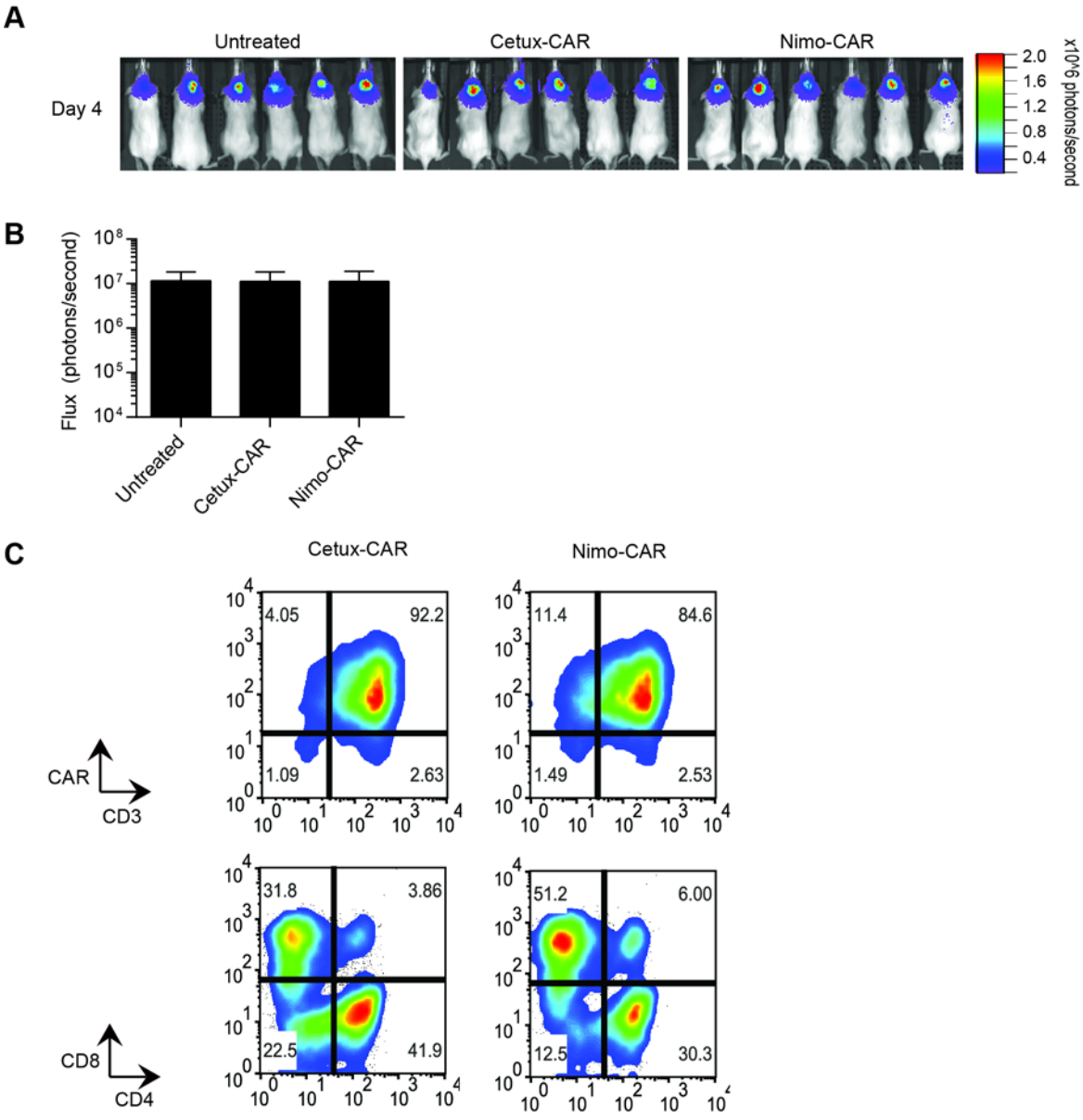

Figure 32. Engraftment of U87 and CAR$^+$ T-cell phenotype prior to T-cell treatment. (A) Four days after tumor injection, tumors were imaged by BLI following injection with D-luciferin and 10 minute incubation. (B) Mice were divided into three groups to evenly distribute relative tumor burden as determined by day 4 BLI flux measurements. (C) Cetux-CAR$^+$ and Nimo-CAR$^+$ T cells expanded through 3 stimulation cycles were evaluated for CAR expression and CD4/CD8 ratio by flow cytometry.

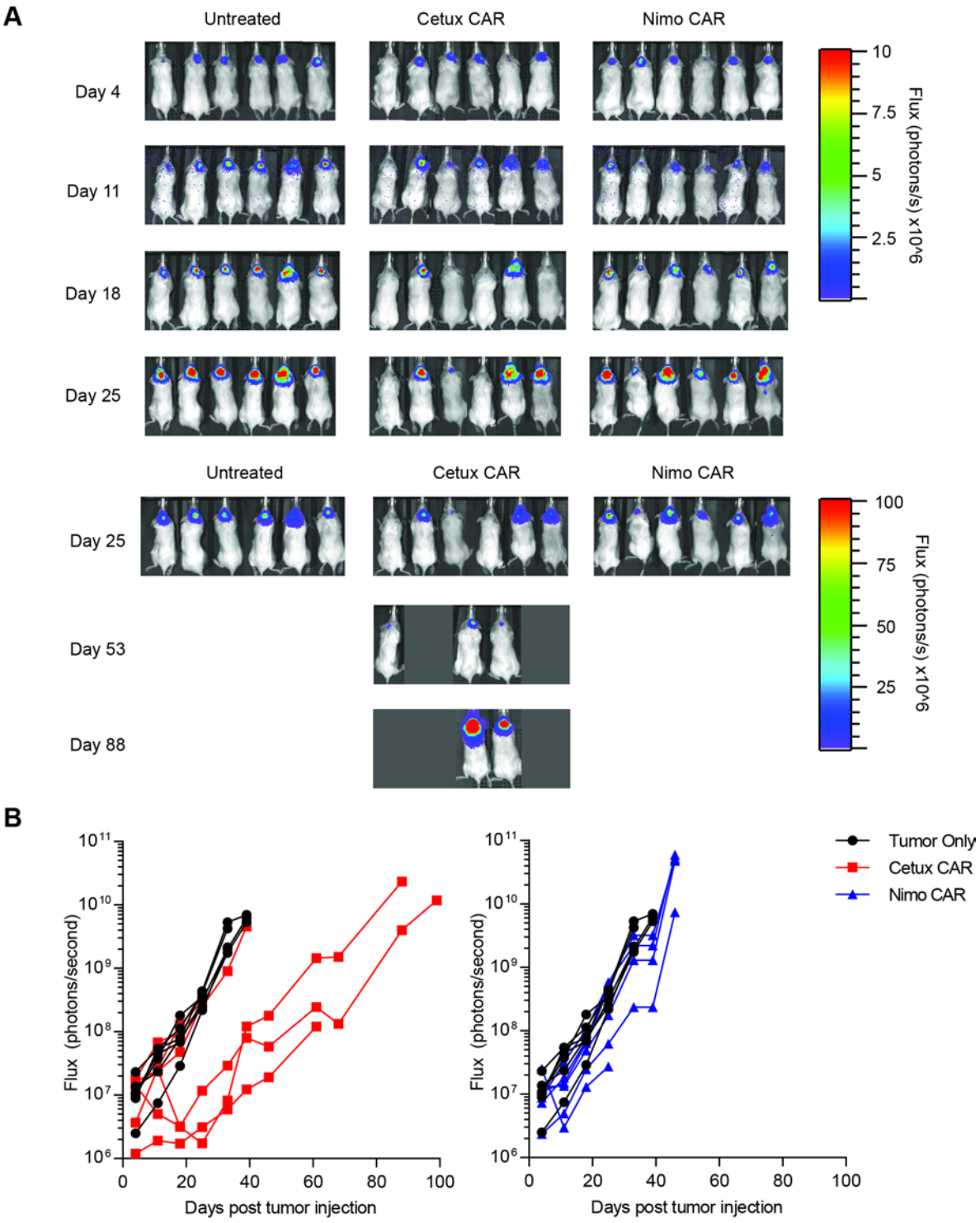

Figure 33. Cetux-CAR$^+$, but not Nimo-CAR$^+$ T cells inhibit growth of U87 intracranial xenografts(A) Serial BLI assessed relative size of tumor. (B) Relative tumor growth as assessed by serial BLI of tumor. Significant difference in BLI between mice with no treatment vs. treatment (n=6) with Cetux-CAR$^+$ T cells (n=6, $p<0.01$) reached at day 25, two-way ANOVA (Sidak's post-test).

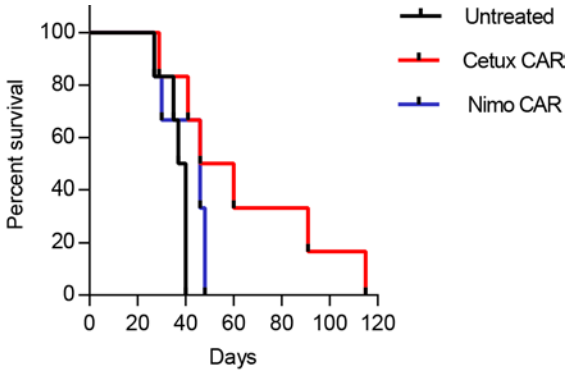

Figure 34. Survival of mice bearing U87 intracranial xenografts treated with Cetux-CAR$^+$ and Nimo-CAR$^+$ T cells. Survival of mice with U87-ffLuc-mKate intracranial xenografts receiving no treatment, Cetux-CAR$^+$ T cells or Nimo-CAR$^+$ T cells. Significant extension in survival in Cetux-CAR$^+$ T cell treatment group determined by Mantel-Cox log-rank test, p=0.0150.

4.3 Discussion

Evaluation of efficacy of Cetux-CAR$^+$ and Nimo-CAR$^+$ T cells in treatment of intracranial glioma xenografts supported *in vitro* conclusions by demonstrating that Cetux-CAR$^+$ T cells and Nimo-CAR$^+$ T cells can mediate anti-tumor activity against U87^{med}, expressing intermediate EGFR density, but only Cetux-CAR$^+$ T cells demonstrated anti-tumor activity against U87 with endogenously low EGFR density.

Some studies have demonstrated that higher affinity TCR interactions can result in superior *in vivo* activity (23, 62), however, it has been demonstrated that *in vitro* T-cell activity does not always mirror *in vivo* efficacy (65, 67). High affinity T cells with high potency *in vitro* have been shown to have attenuated responses *in vivo*, characterized by decreased signaling, expansion, and T-cell mediated function (63). Similarly, low affinity interaction have been demonstrated to have curtailed T-cell expansion *in vivo*, resulting in fewer T cells present at each stage of the immune response (64). Models assessing the role of TCR affinity in anti-tumor efficacy have demonstrated that high affinity TCR interactions have impaired anti-tumor function, characterized by decreased presence in tumor and impaired cytolytic function (65-67). Thus, it has been suggested that T cells with intermediate affinity may better control tumor growth relative to high affinity T cells (63, 67). Combining these observation with *in vitro* observations that Cetux-CAR$^+$ T cells have decreased proliferative capacity when stimulated in the absence of exogenous cytokine, enhanced CAR downregulation following engagement with antigen, and reduced ability to respond to re-challenge with antigen, it is reasonable to expect that Cetux-CAR$^+$ T cells may have reduced anti-tumor efficacy *in vivo*. We did not observe impaired anti-tumor efficacy relative to Nimo-CAR$^+$ T cells, however, the fate of CAR$^+$ after intratumoral injection was not followed, and therefore, differences *in vivo* T-cell expansion were not assessed. Intratumoral injection of CAR$^+$ T cells was chosen to avoid the confounding variable of disparate abilities of CAR$^+$ T cells to home to tumor when evaluating anti-tumor activity; however, it is possible that Cetux-CAR$^+$ T cells may have reduced tumor infiltration due to retention in tumor periphery. Therefore, future studies in which CAR$^+$ T cells are labeled and their fate, including tumor infiltration and *in vivo* expansion, should be undertaken. Additionally, isolating T cells following tumor infiltration and evaluating their retained cytotoxic capacity may provide interesting information about the role of the scFv domain affinity in CAR design and function *in vivo*.

Nimo-CAR$^+$ T-cell treatment did not significantly reduce tumor burden or improve the survival of mice relative to untreated mice in response to low EGFR density on U87, which is about 2-fold higher than EGFR density measured on normal renal epithelial cells (**Figure 21 and Figure 24**). In contrast, Cetux-CAR$^+$ T cells demonstrated tumor control and extended survival in 3/6 mice with low EGFR density. While Nimo-CAR$^+$ T-cell treatment may have reduced cytotoxic potential against normal tissue with very low EGFR density, they also have the potential for tumor escape variants expressing low EGFR density. Due to the substantial heterogeneity in glioblastoma, it is unlikely for a single target to be expressed on all of the tumor cells within a given patient (237, 292). Treatment of experimental glioblastoma models with HER2-specific CAR$^+$ T cells has also demonstrated escape of HER2^{null} tumor cells (257, 259). Profiling patient tumors can identify combinations of antigens to target the maximum number of cells in a given tumor, and targeting multiple antigens by CAR$^+$ T cells has been shown to improve treatment efficacy of treatment of CAR$^+$ T cells with single specificity (259). *In vivo* experimentation with U87 with uniform EGFR density does not recapitulate antigen heterogeneity in patient tumors, therefore, evaluation of Cetux-CAR$^+$ T cells or Nimo-CAR$^+$ T cells in combination with CAR$^+$ T cells of different specificities can be evaluated against glioblastoma specimens derived from patients that may better recapitulate tumor heterogeneity *in vivo* (257).

Unexpectedly, Cetux-CAR$^+$ T cells showed significant toxicity within 7 days of T-cell treatment, with 6/14 mice dying within 7 days of a T-cell injection. Previously, an EGFR-specific CAR has been reported to have no detectable *in vivo* toxicity by measurement of liver enzymes 48 hours after T-cell infusion in mice bearing no tumor (293). Because this CAR was derived from a murine antibody, it is unlikely that the EGFR-specific CAR would recognize murine EGFR on normal tissue. Additionally, measurement of toxicity in the absence of antigen does not replicate physiologic CAR$^+$ T-cell activation in patients expressing antigen on tumors, as these cells will activate, proliferate, and produce cytokine in response to tumor lysis, which could all contribute to measureable toxicity (158). In fact, in the present study, treatment of mice with Cetux-CAR$^+$ T cells bearing low antigen tumor or no tumor did not result in detectable toxicity (**Figure 7** and unpublished observations), highlighting the role of *in vivo* T-cell activation to observed T-cell toxicity.

Because cetuximab does not recognize murine EGFR, on-target, off-tissue toxicity is not likely a cause of Cetux-CAR$^+$ T cell-related toxicity (294). Possible mechanisms for Cetux-CAR mediated toxicity in this model include cytokine-related toxicity resulting from T-

cell activation or possibly enhanced avidity of Cetux-CAR due to clustering, immune synapse formation or association with T-cell cytoskeleton that reduces antigenic-specificity, as has been described in the contribution of CD8 coreceptor binding to enhance avidity of high affinity TCRs, resulting in loss of specificity (295).

Although tumor xenografts in immunosuppressed mice are the standard in the field to assess efficacy of CAR-modified T-cell therapies due to their readiness to accept human grafts, this model is limited in ability to measure toxicity responses. The inability of human CAR^+ T cells to recognize murine EGFR makes this model incapable of determining the potential of on-target, off-tissue toxicity from CAR^+ T cells. In addition, because these mice are immunosuppressed, the interaction of Cetux-CAR^+ T cells with other components of the immune system, such as the effect of secreted cytokines from CAR^+ T cells, which have been attributed with significant toxicity in clinical trials, cannot be fully assessed. Additionally, a recent clinical trial has demonstrated the potential for anaphylaxis in response to CAR^+ T cell treatment when multiple doses of T cells are given, hypothesized to be due to development of IgE antibodies specific to CAR moieties (160). Therefore, evaluation of EGFR-specific CAR in an immunocompetent host in which EGFR on normal tissue is capable of recognition is necessary for adequate pre-clinical evaluation of occurrence and mechanism of T-cell mediated toxicity.

Expression of a fully murine CAR specific EGFRvIII expressed in murine T cells was able to mediate complete tumor regression against syngeneic intracranial, orthotopic murine glioblastoma in an immune competent mouse model (296). Interestingly, following regression of EGFRvIII-expressing glioblastoma, immunocompetent mice showed protection against challenge with syngeneic $EGFRvIII^{null}$ tumor cells, providing evidence of antigen-spreading against unindentified epitopes. Likewise, a recent clinical trial of mesothelin-specific CAR^+ T cells for the treatment of mesolthelioma have demonstrated development of novel anti-self antibodies following CAR^+ T cell therapy, indicative of antigen-spreading when CAR^+ T cells function in the context of a complete immune response (266). Thus, evaluation of CAR^+ T cell activity in an immunocompetent model may demonstrate additional anti-tumor efficacy through interaction with an intact immune system.

Because cetuximab and nimotuzumab do not bind murine EGFR, the Cetux-CAR and Nimo-CAR are not amenable to testing in a fully murine, immunocompetent model. However, canines develop spontaneous glioma that overexpress EGFR and because

canine EGFR is highly homologous to human EGFR and cross-reactive with cetuximab, a trial with owner-initiated treatment of canine patients diagnosed with glioblastoma with a chimeric Cetux-CAR or Nimo-CAR to include canine signaling endodomains expressed in canine T cells may be a good preclinical model to evaluate complex pre-clinical issues surrounding EGFR-specific CARs (297, 298). However, initial steps to ensure that affinity of Cetux-CAR and Nimo-CAR binding to canine EGFR maintain their equivalent kinetic parameters will be of primary importance to ensure translatability to human treatment.

In summary, Nimo-CAR$^+$ T cells demonstrate anti-tumor activity and improved survival comparable to higher affinity Cetux-CAR$^+$ T cells in an intracranial orthotopic xenograft model, without T-cell related toxicity associated with Cetux-CAR$^+$ T cells. In contrast, Cetux-CAR$^+$ T cells, but not Nimo-CAR$^+$ T cells demonstrate anti-tumor activity against tumor with low EGFR density. These findings are consistent with *in vitro* observations that Nimo-CAR$^+$ T cells have reduced activity in response to low EGFR density. Future experiments tracking CAR$^+$ T cells *in vivo*, evaluating the potential for tumor escape variants, and evaluation of efficacy and toxicity in an immunocompetent canine model may provide further distinction between the in vivo anti-tumor activity of Cetux-CAR$^+$ and Nimo-CAR$^+$ T cells.

CHAPTER 5

General Discussion and Future Directions

5.1 Dissertation Summary

Adoptive immunotherapy with CAR^+ T cells is proving to be a promising treatment modality for B-cell lineage malignancies in clinical trials (111, 112, 132), however, persistent B-cell aplasia demonstrates the longevity of CAR^+ T-cell responses and limits applicability to TAA with widespread normal tissue expression, such as EGFR. EGFR is overexpressed on many tumor types, including glioblastoma, but also is expressed on many epithelial surfaces throughout the body at low basal levels (185, 201). Therefore, targeting EGFR with EGFR-specific CAR^+ T cells poses the potential risk of toxicity to normal tissue expressing low density EGFR. Two strategies were evaluated to limit recognition of EGFR on normal tissue by EGFR-specific CAR^+ T cells: (i) temporally limiting CAR expression through transient modification of T cell with RNA, and (ii) tuning CAR sensitivity to antigen density through scFv domain with lower affinity and reduced capacity to bind low density EGFR.

RNA-modification of T cells resulted in transient expression of Cetux-CAR, an EGFR-specific CAR derived from the monoclonal antibody cetuximab. Comparing Cetux-CAR^+ T cells modified by DNA or RNA transfer revealed that DNA-modified T cells were superior in production of cytokines IFN-γ and TNF-α in response to EGFR-expressing tumor cells, likely due to the enhanced proportion of effector memory/effector phenotype T cells in DNA-modified T cells relative to RNA-modified T cells. However, RNA-modified T cells demonstrated similar specific lysis after RNA transfer in response to EGFR-expressing tumor cells as DNA-modified CAR^+ T cells. Cetux-CAR expressed by RNA transfer was gradually lost over time, with very low CAR expression detected 4-5 days following RNA transfer, and the loss of CAR expression in RNA-modified T cells was accelerated by T-cell stimulation with cytokine or antigen. Concomitant with loss of CAR, T cells lost ability to mediate cytotoxicity of EGFR-expressing tumor cells. While this strategy can reduce normal tissue toxicity by temporally limiting CAR expression, it does not endow CAR^+ T cells the ability to distinguish normal tissue from malignant tissue and when CAR^+ T cells lose CAR expression, they lose the ability to target tumor as well as normal tissue antigen. Moreover, transient expression of CAR does not protect normal tissue from short-term targeting of EGFR-expressing normal tissue upon infusion of CAR^+ T cells. Because of these limitations, we sought to develop an EGFR-specific CAR that could be stably expressed, but could

distinguish malignant cells from normal cells based on increased EGFR density on malignant tissue to prevent normal tissue toxicity while maintaining anti-tumor activity.

To achieve this, another EGFR-specific CAR was developed from the monoclonal antibody nimotuzumab, termed Nimo-CAR. Relative to cetuximab, nimotuzumab has a 1-log lower affinity but is specific to an epitope on EGFR that highly overlaps with that of cetuximab (223, 231). In clinical trials, nimotuzumab has demonstrated a low toxicity profile relative to cetuximab, with notable absence of the grade III/IV skin rash associated with cetuximab treatment (230, 289, 299). Nimo-CAR$^+$ and Cetux-CAR$^+$ T cells demonstrated equivalent capability of T-cell activation, measured by phosphorylation of Erk1/2 and p38, production of IFN-γ, and specific lysis, when stimulated in a CAR-dependent, scFv-independent manner. By measuring activity of Nimo-CAR$^+$ T cells and Cetux-CAR$^+$ T cells in response to U87 cells expressing graded EGFR densities, we demonstrated the capacity of Nimo-CAR$^+$ T cells to phosphorylate signaling molecules, produce cytokine and induce specific lysis of targets was directly correlated with density of EGFR expression, whereas Cetux-CAR$^+$ T cells demonstrated equivalent activity against all EGFR-expressing U87 cell lines, regardless of density of EGFR expression. In response to low EGFR density on normal renal cells, Nimo-CAR$^+$ T cells were unable to produce significant amounts of IFN-γ and had 50% less specific lytic activity than Cetux-CAR$^+$ T cells, which produced IFN-γ and exhibited efficient specific lysis of normal human renal epithelial cells. In addition to having reduced sensitivity to low EGFR density, Nimo-CAR$^+$ T cells also demonstrated increased proliferation following stimulation in cytokine-free conditions, reduced downregulation of CAR following stimulation with antigen, and increased capacity to produce cytokine in response to secondary encounter with antigen in comparison to Cetux-CAR$^+$ T cells.

In vitro observations were supported by *in vivo* observations in an intracranial xenograft model in which Nimo-CAR$^+$ T cells demonstrated equivalent anti-tumor efficacy as measured by relative tumor BLI in response to moderate EGFR density as Cetux-CAR$^+$ T cells, resulting in significant extension of survival. Cetux-CAR$^+$ T cells were associated with significant toxicity soon after T-cell treatment, which was notably absent in mice treated with Nimo-CAR$^+$ T cells. However, in response to low EGFR density on U87, which is still twice the density measured on normal human renal cortical epithelial cells, only Cetux-CAR$^+$ T cells and not Nimo-CAR$^+$ T cells were capable of anti-tumor activity and significant extension of survival. In sum, we described a novel method of reducing T-cell activity to normal tissue by tuning CAR sensitivity to antigen density such that CAR-dependent T-cell activation

occurs in the presence of high antigen density on tumor tissue, but is reduced in the presence of low antigen density on normal tissue.

5.2 Safely expanding repertoire of antigens for CAR$^+$ T-cell therapy

Methods developed to achieve safety of CAR$^+$ T cells can be categorized into three main strategies: (i) restricting CAR$^+$ T cells to tumor tissue, (ii) limiting CAR expression/T cell persistence, and (iii) restricting CAR-mediated T-cell activation to tumor (**Figure 35**). Co-expression of homing molecules with CAR in T cells to home to site of the tumor, such as CCR2, CCR4 and CXCR2, has been described to sequester CAR$^+$ T cells to site of the tumor (154, 156, 157). While CAR$^+$ T cells are enriched in tumor tissue when compared with CAR$^+$ T cells without homing receptors, it is unclear what percentage of CAR$^+$ T cells expressing homing receptors do not efficiently home to the tumor and could, therefore, target normal tissue. Likewise, chemokines secreted by tumors can also be secreted in normal tissue during tissue trauma and healing. Therefore, combining these treatments with other treatment modalities, such as surgery, chemotherapy and radiation would risk attracting T cells to normal tissue non-specifically injured during treatment. Development of CAR preferentially expressed in hypoxic condition, common in many tumors, has been achieved by fusing CAR to an oxygen-dependent degradation domain to limit CAR expression and capacity to target tissue in normoxia (unpublished data, O. Ang) (300). Because CAR degradation in T cells moving from hypoxia to normoxia may take minutes to hours, it is feasible for on-target, off-tissue toxicity may occur prior to CAR degradation. In addition, while the center of many tumors are hypoxic, well-vascularized peripheral tumor regions may have sufficient oxygen concentration to degrade CAR, protecting peripheral regions from CAR-mediated T-cell activity (301).

Strategies to temporally limit CAR$^+$ T-cell presence include suicide gene modification of T cells, such as expression of CAR as a transient RNA species, and introduction of iCaspase9 suicide switch, which is specifically activated by a chemical inducer of dimerization (CID) to result in T-cell death (152, 163, 164, 167, 168). Both methods have high penetrance and result in almost complete abrogation of CAR$^+$ T cells, either after induction of apoptosis by drug delivery or loss of RNA transgene expression over time. Because both strategies permanently ablate CAR$^+$ T cells, they also limit therapeutic efficacy against tumor while protecting normal tissue. One limitation of these strategies is that before CAR reduction or T cell ablation, potent activity against normal cells exists, and

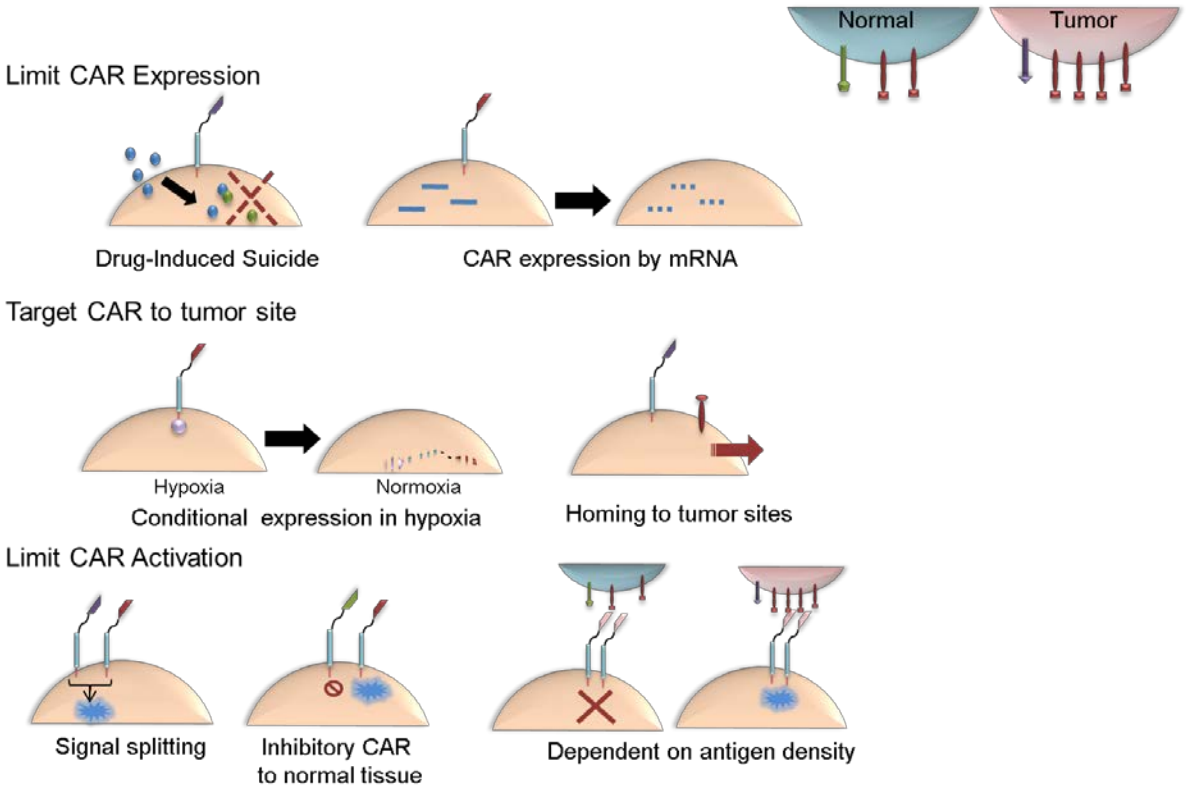

Figure 35. Summary of strategies to safely expand repertoire of antigens for CAR$^+$ T cell therapy. Strategies fall into three main categories: (i) limiting CAR expression by drug-induced suicide or transient CAR expression, (ii) targeting CAR to tumor site by limiting expression to hypoxic regions or co-expressing homing receptors, and (iii) limiting CAR activation by splitting signals to require two antigens to recognize tumor, expressing an inhibitory CAR to prevent activation to normal tissue, or expressing CAR conditionally activated by high antigen density.

there is no short-term limitation of toxicity. Serious adverse events from T-cell therapy can progress rapidly from onset of clinical symptoms, therefore, it is desirable to have a strategy to protect normal tissue from the moment of CAR^+ T-cell infusion (111, 112).

Dual-specific, complementary CARs have achieved selective activation in response to co-expression of two antigens mutually expressed only on tumor by dissociating signaling domains and expressing two chimeric receptors with two specificities. In this strategy, one specificity is fused to CD3ζ to express a first generation CAR and a different, complementary specificity is fused to costimulation endodomains, termed a chimeric costimulation receptor (CCR), such that full activation and T-cell function is only attained with simultaneous engagement of CAR and CCR by co-expression of by antigens (302-304). This approach has been piloted with different pairs of CAR and CCR with redirected specificities towards HER2 and MUC1 for breast cancer, PSMA and PSCA for prostate cancer and mesothelin and α-folate receptor for ovarian cancer treatment. Early studies have demonstrated that T-cell activation and lytic function can occur against single antigen expressing targets via first generation CAR expression in the absence of CCR activation. Although this cytotoxicity is lower than that observed with second generation CARs, there is still some residual risk of CAR targeting normal tissue expressing single antigen (302, 303). One strategy to overcome this limitation is to develop a first generation CAR with suboptimal affinity, such that it barely renders T-cell function when activated by single antigen and toxicity is only rescued by ligation of CCR (304). However, this strategy functions by blunting T-cell sensitivity to tumor antigen. While this strategy prevents recognition and targeting of single antigen expression tissue, thereby potentially reduced normal tissue toxicity, it also reduces anti-tumor activity. Additionally, the requirement for two antigens to be expressed for efficient T-cell activation and tumor elimination reduces the fraction of tumor capable of CAR activation and increases the potential for the development of tumor escape variants.

An inhibitory CAR (iCAR) fusing specificity for antigen found only on normal tissue, and not on tumor to PD-1 signaling endodomains is capable of significantly inhibiting T-cell-mediated killing and cytokine production in response to binding normal tissue antigen (305). Impressively, iCAR inhibition of T-cell function is reversible, and T cells are capable of subsequent functionally productive responses upon encounter with tumor antigen. The success of this strategy is dependent of stoichiometry of CAR, iCAR and both antigens. Therefore, it is reasonable to predict that normal tissue toxicity could occur if iCAR expression or antigen is insufficient in the presence of overwhelming CAR/tumor antigen

expression. This stoichiometric parameter must evaluated and tightly control for each set of antigens for this strategy to be successful.

We add to this array of methods to reduce normal tissue toxicity a novel method to control T-cell activation to the site of tumor based on the affinity of the scFv used in CAR design to mitigate activation of CAR^+ T cells in response to low density of EGFR on normal tissue while mediating T-cell cytotoxicity in response to high EGFR density on tumor tissue. Advantages of this method are that (i) reduction of normal tissue toxicity is not associated with mitigated T-cell activity in response to tumor and (ii) activation/inhibition of T cells does not require recognition of multiple antigens, for which the stoichiometry of expression and binding to relative receptors must be tightly controlled. Additionally, requiring multiple antigens for T cell activation further reduces the proportion of a tumor that will be efficiently targeted. None of the methods to restrict T-cell on-target, off-tissue tissue toxicity are mutually exclusive, and combinations of multiple strategies may provide improve avoidance of normal tissue destruction.

5.3 Clinical implications

Glioblastoma patients may be an ideal patient population for initial evaluation of safety of T cells specific for EGFR for cancer immunotherapy. EGFR is overexpressed in 40-50% of patients with glioblastoma (176, 181), and EGFR expression is not reported in normal CNS tissue (201). Because EGFR is widespread on normal epithelial surfaces, intracavitary delivery of T cells following tumor resection can maximize anti-tumor potential while minimizing the potential for interaction with epithelial surfaces outside of the CNS. Following initial safety evaluation in patients with glioblastoma, it may be possible to extend EGFR-specific CAR^+ T cell therapy to other EGFR-expressing malignancies, which include breast, ovarian, lung, head and neck, colorectal, and renal cell carcinoma (184).

Although transient expression of CAR through RNA modification of T cells may result in reduced anti-tumor efficacy due to limited presence of CAR^+ T cells, multiple infusions of RNA-modified T cells, particularly with a weighted initial dose, may overcome these potential limitations, as previously demonstrated with CD19 CAR^+ T cells modified by RNA transfer in an advanced leukemia murine model (168). While clinical trials with mesothelin-specific CAR transferred by RNA expression have demonstrated the potential for anaphylaxis attributed to the development of IgE antibody responses specific for CAR moieties in response to repeated CAR infusions, a dosing strategy with no more than 10 days between

CAR^+ T cell infusions and treatment to be completed over a course of 21 days has been proposed to avoid isotype switching of IgG antibodies to IgE antibodies and is currently being evaluated (160). Despite these challenges, there are many attractive advantage of RNA modification to express CAR in clinical application. First, RNA-modification of T cells does not involve genomic integration of transgenes, and thus have the potential for less cumbersome processes for regulatory approval, which may shorten the preclinical development period for CAR^+ T-cell therapy. In addition, generation of CAR-modified T cells by RNA transfer is much quicker than DNA-modification using the Sleeping Beauty transposon/transposase system, resulting in >90% CAR^+ T cells in about half of the *ex vivo* culture time as is required for DNA-modification of T cells. Improving the speed of regulatory approval processes and *ex vivo* manufacture time could result in getting new CAR^+ T cell therapies to the clinic faster, quicken the communication time from bench-to-bedside and back to mediate improved efficiency in fine-tuning these therapies for clinical application.

RNA-modification may also provide a platform to test transiently modified T cells specific to widely expressed normal tissue antigens, such as EGFR, in patients to determine safety profiles of CAR structures prior to evaluating permanently integrated CARs as an additional measure of safety. Because Cetux-CAR demonstrates T-cell activation and lytic activity in response to low EGFR density, DNA-modification of T cells to permanently express Cetux-CAR is not likely to be a viable clinical strategy due to the high risk of normal tissue toxicity. However, initial clinical evaluation of Nimo-CAR^+ T cells modified by RNA transfer may determine the capacity of Nimo-CAR^+ T cells to mediate normal tissue toxicity with the additional safety feature of transient CAR expression to alleviate concerns of long-term normal tissue toxicity.

While the reduced capacity of Nimo-CAR^+ T cells to mediate cytotoxicity against low density EGFR functions to reduce normal tissue toxicity, it also may reduce effectiveness against tumors that express low density EGFR, increasing the potential for outgrowth of tumor escape variants expressing EGFR at low density. In contrast, specific lytic activity of Cetux-CAR^+ T cells against all levels of EGFR expression may reduce the risk of outgrowth of low EGFR expressing tumor escape variants, but does so at the expense of potential toxicity against normal tissue with low EGFR expression. In addition, Cetux-CAR^+ T cells appear to mediate some degree of T-cell related toxicity independent of targeting normal tissue expressing EGFR, as demonstrated in treatment of intracranial U87 expressing moderate density of EGFR, perhaps due to enhanced cytokine production or induction of

local inflammation. The relationship between Cetux-CAR$^+$ and Nimo-CAR$^+$ T cells highlight the balance that must be achieved between safety and efficacy of gene-modified T-cell therapies. Choosing which strategy might have better clinical outcome, Cetux-CAR$^+$ T cells with increased risk of toxicity but potential for greater tumor control or Nimo-CAR$^+$ T cells with reduced risk of toxicity, but greater potential for development of tumor escape variants, does not have a simple solution. One potential clinical strategy for coping with this balance may be infusing Nimo-CAR$^+$ T cells modified by DNA for stable control of high EGFR-expressing tumor variants combined with multiple infusions of Cetux-CAR$^+$ T cells modified by RNA to eliminate low EGFR-expressing tumor cells.

5.4 Future directions

It is currently unclear how CARs are similar or dissimilar from TCRs in mechanisms of action. For example, it is unknown if CARs cluster after initiation of signaling, are involved in formation of immunological synapses, or interact with the actinomysoin cytoskeleton during signaling as endogenous TCRs do. Each of these processes contributes to enhancing avidity of interaction with antigen, and therefore, extrapolating findings from studies of TCR affinity to designing CARs with desirable attributes is difficult. Wild-type endogenous TCRs have monomeric affinities orders of magnitude lower than monomeric affinities of CARs, and yet are often characterized by enhanced sensitivity relative to CARs, requiring few complexes of peptide in the context of MHC and few TCRs triggered to activate cytolytic T-cell responses, highlighting the likelihood of some distinction in mechanism of action. Reduced sensitivity of CAR$^+$ T cells can be explained by reports that they fail to induce serial triggering, where one antigen molecule can activate many molecules of CAR, potentially due to the reduced dissociation rate resulting in longer interactions with antigen than observed with wild-type TCR. Questions of whether CARs form functional immune synapses and whether they interact with actin cytoskeleton of T cells to enhance avidity of interaction as endogenous TCRs do remain to be answered. Better understanding of these basic mechanisms of CAR function can inform rational design of CAR structures for future clinical evaluation.

The stromal microenvironment of glioblastoma is immunosuppressive, and may reduce the effectiveness of T-cell immunotherapy strategies for treatment. Murine xenograft models for glioblastoma do not recapitulate the stromal environment of glioblastoma, and therefore, it is difficult to determine its impact on CAR$^+$ T cells in preclinical studies.

Manipulation of the microenvironment to potentiate T-cell therapy can be achieved by combining therapies that modulate T cell function with CAR^+ T cell therapy. For example, PD-L1 is expressed on ~60% of glioblastoma and binds to PD-1 expressed on T cells to inhibit function (249). Blockade the interaction of PD-L1 and PD-1 has demonstrated promising results in early phase clinical studies in patients with non-small cell lung carcinoma, melanoma, and renal cell carcinoma, and has extended survival in a murine model of glioma (243, 306). Combination of PD-L1 blockade with CAR^+ T cell therapy may improve T-cell function to overcome immunosuppression through this pathway. TGF-β is also secreted in the glioblastoma microenvironment and linked to immune suppression and poor outcomes in glioblastoma patients (307). Clinical trials inhibiting TGF-β with the chemical inhibitor trabesdersin has demonstrated some improvement in tumor control relative to patients receiving chemotherapy (308). Treatment of a model of spontaneous arising prostate cancer in transgenic mice engineered to express SV40 antigen demonstrated that treatment with SV40-specific TCR transgenic T cells was significantly improved by coexpression of a dominant negative TGF-β receptor (309). Co-expression of a dominant negative TGF-β receptor on Cetux-CAR^+ or Nimo-CAR^+ T cells may overcome immunosuppressive effects of TGF-β in glioblastoma.

Due to the heterogeneous nature of glioblastoma, the risk of tumor escape variants null for EGFR expression is likely present regardless of complete elimination of tumor cells expressing all levels of EGFR density, due to the notorious complexity of glioblastoma. Kloss et. al. demonstrated that treatment of a glioblastoma cell line with a HER2-specific resulted in outgrowth of HER2 negative cells. For that reason, combination therapy targeting additional tumor antigens is an attractive strategy to prevent tumor escape. Other CARs for treatment of GBM with promising preclinical results have been described, targeting EphA2, HER2, and EGFRvIII, IL13Rα2, the latter three currently in phase I/II clinical trials (147-150, 257, 310, 311). Development of a bispecific CAR to able to target HER2 and IL13Rα2 in one transgenic receptor displayed dual specificity and synergistic enhancement of T-cell function upon simultaneous engagement with both antigens (259, 312). While targeting HER2 and IL13Rα2 improved GBM clearance over single modal therapy, a small, resistant population negative for antigen remained. Expanding repertoire of targetable antigens by including EGFR may contribute to finding combinations of two or more targetable antigens to account for all tumor cells. Because cetuximab and nimotuzumab are both capable of recognizing EGFRvIII with similar affinity as wild type EGFR (313, 314),

combination of Cetux-CAR$^+$ T cell or Nimo-CAR$^+$ T cell therapy should be evaluated with CARs specific for HER2, EphA2 and IL13Rα2. Additionally, mutually exclusive mosaic-like expression of PDGFRα and EGFR has been reported in glioblastoma patients. Thus, a combination of CARs targeting these two RTKs may be beneficial for covering a large proportion of tumor and should be evaluated, although, to date, preclinical studies evaluating PDGFR-α as a target for CAR therapy are lacking. Autologous glioblastoma patient samples can be used to establish intracranial xenografts in mice to evaluate T-cell therapies. While they do not recapitulate the host's immune interactions or the stromal microenvironment of the tumor, autologous models of glioblastoma do recapitulate intratumoral and intertumoral heterogeneity. Therefore, evaluation of target expression on patient glioblastoma samples and evaluation and combination therapies in an autologous murine model of glioblastoma may inform combinations of CARs worthy of clinical evaluation.

CHAPTER 6

Materials and Methods

6.1 Plasmids

6.1.1 Cetuximab-derived CAR transposon

Cetuximab-derived CAR is composed of the following: a signal peptide from human GMCSFR2 signal peptide (amino acid 1-22; NP_758452.1), variable light chain of cetuximab (PDB:1YY9_C) whitlow linker (AAE37780.1), variable heavy chain of cetuximab (PDB:1YY9_D), human IgG4 (amino acids 161-389, AAG00912.1), human CD28 transmembrane and signaling domains (amino acids 153-220, NP_006130), and human CD3-ζ intracellular domain (amino acids 52 through 164, NP_932170.1). Sequence of GMCSFR2, variable light chain, whitlow linker, variable heavy chain and partial IgG4 were human codon optimized and generated by GeneART (Regensburg, Germany) as 0700310/pMK. Previously described CD19CD28mZ(CoOp)/pSBSO under control of human elongation factor 1-alpha (HEF1α) promoter was selected as backbone for SB transposon. 0700310/pMK and previously described CD19CD28mZ/pSBSO (93, 94) underwent double digestion with *NheI* and *XmnI* restriction enzymes. CAR insert and transposon backbone were identified as DNA fragments of 1.3 kb and 5.2 kb, respectively, by agarose gel electrophoresis in a 0.8% agarose gel run at 150 volts for 45 minutes and stained with ethidium bromide for visualization under ultraviolet light exposure. Bands were excised and purified (Qiaquick Gel Extraction kit, Qiagen, Valencia, CA), then ligated using T4 DNA ligase (Promega, Madison, WI) at a molar ratio of insert to backbone of 3:1. Heat shock transformation of TOP10 chemically competent bacteria (Invitrogen, Grand Island, NY) and selection on kanamycin-containing agar plates cultured at 37ºC for 12-16 hours identified bacteria clones positive for transposon backbone. Six clones were selected for mini-culture in TB media with kanamycin selection at 37ºC for 8 hours. Preparation of DNA from mini-cultures was done via MiniPrep kit (Qiagen) and subsequent analytical digestion with restriction enzymes and analysis of fragment size by agarose gel electrophoresis identified clones positive for CetuxCD28mZ(CoOp)/pSBSO (**Figure 36A**). A positive clone was inoculated 1:1000 into large culture in TB media with kanamycin antibiotic selection and cultured on shaker at 37ºC for 16 hours, until log-phase growth was achieved. DNA was isolated from bacteria using EndoFree Maxi Prep kit (Qiagen). Spectrophotometer analysis of DNA verified purity by OD260/280 reading between 1.8 and 2.0.

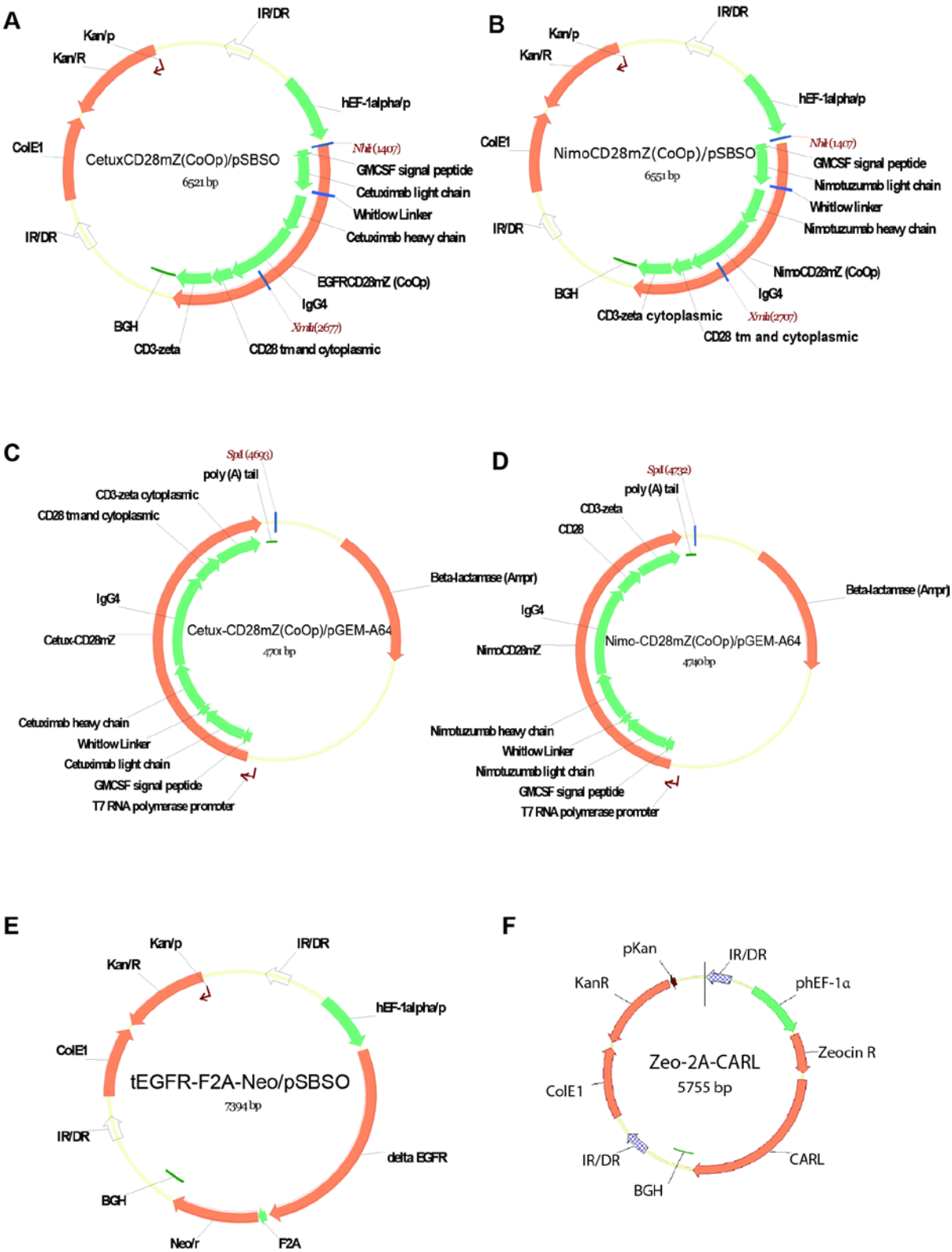

Figure 36. Vector maps of constructed plasmids. (A) Cetuximab-derived CAR transposon. Annotated as follows: HEF-1α/p: promoter for human elongation factor-1α; BGH: bovine growth hormone poly adenylation sequence; IR/DR: inverted repeat/direct repeat; ColE1: a minimal E.coli origin of replication; Kan/R: gene for kanamycin resistance; Kan/p: promoter for kanamycin resistance gene. (B) Nimotuzumab-derived CAR transposon. Annotated as follows: HEF-1α/p: promoter for human elongation factor-1α; BGH: bovine growth hormone poly adenylation sequence; IR/DR: inverted repeat/direct repeat; ColE1: a minimal E.coli origin of replication; Kan/R: gene for kanamycin resistance; Kan/p: promoter for kanamycin resistance gene.(C) Cetuximab-derived CAR/pGEM-A64 plasmid. Annotated as follows: amp/R: gene for ampicillin resistance, *SpeI:* restriction site for linearization. (D) Nimotuzumab-derived CAR/pGEM-A64 plasmid. Annotated as follows: amp/R: gene for ampicillin resistance, *SpeI:* restriction site for linearization. (E) tEGFR-F2A-Neo transposon. Annotated as follows: HEF-1α/p: promoter for human elongation factor-1α; BGH: bovine growth hormone poly adenylation sequence; F2A: self-cleavable peptide F2A; Neo/r: gene for neomycin resistance; IR/DR: inverted repeat/direct repeat; ColE1: a minimal E.coli origin of replication; Kan/R: gene for kanamycin resistance; Kan/p: promoter for kanamycin resistance gene. (F) CAR-L transposon. Annotated as follows: HEF-1α/p: promoter for human elongation factor-1α; Zeocin R: gene for zeomycin resistance; BGH: bovine growth hormone poly adenylation sequence; IR/DR: inverted repeat/direct repeat; ColE1: a minimal E.coli origin of replication; Kan/R: gene for kanamycin resistance; Kan/p: promoter for kanamycin resistance gene.

6.1.2 Nimotuzumab-derived CAR transposon

Nimotuzumab-derived CAR is composed of the following: a signal peptide from human GMCSFR2 signal peptide (amino acids 1-19, NP_001155003.1), variable light chain of nimotuzumab (PDB:3GKW_L) whitlow linker (GenBank: AAE37780.1), variable heavy chain of nimotuzumab (PDB:3GKW_H), human IgG4 (amino acids 161-389, AAG00912.1), human CD28 transmembrane and signaling domains (amino acids 153-220, NP_006130), and human CD3-ζ intracellular domain (amino acids 52 through 164, NP_932170.1). Sequence of GMCSFR2, variable light chain, whitlow linker, variable heavy chain and partial IgG4 were human codon optimized and generated by GeneART as 0841503/pMK. 08541503/pMK and previously described CD19CD28mZ/pSBSO (93, 94) underwent double digestion with *NheI* and *XmnI* restriction enzymes, ligation, transformation, large scale amplification and purification of plasmid NimoCD28mZ(CoOp)/pSBSO (**Figure 36B**) were performed as described above.

6.1.3 SB11 transposase

The hyperactive SB11 transposase under control of CMV promoter (Kan-CMV-SB11) was used as previously described (94, 315).

6.1.4 pGEM/GFP/A64

GFP under control of of a T7 promoter followed by 64 A-T base pairs and a *SpeI* site was use to *in vitro* transcribe GFP RNA. The cloning of pGEM/GFP/A64 has been previously described (316).

6.1.5 Cetuximab-derived CAR/pGEM-A64

Cetuximab-derived CAR was cloned into an intermediate vector, pSBSO-MCS, by *NheI* and *XmnI* double digestion of CetuxCD28mZ(CoOp)/pSBSO and CD19CD28mZ(CoOp)/pSBSO-MCS. Cetux-CAR insert and pSBSO-MCS backbone were isolated by extraction from agarose gel after electrophoresis and ligated, transformed, and amplified on large-scale as described in generation of CetuxCD28mZ(CoOp)/pSBSO. CetuxCD28mZ(CoOp) was cloned into pGEM/GFP/A64 plasmid to place Cetux-CAR under control of a T7 promoter for *in vitro* transcription of RNA with artificial poly-A tail 64 nucleotides in length. CetuxCD28mZ(CoOp)/pSBSO-MCS was digested with *NheI* and *EcoRV* at 37ºC while pGEM/GFP/A64 was sequentially digested with *XbaI* at 37ºC then *SmaI* at 25ºC. Digested Cetux-CAR insert and pGEM/A64 backbone were separated by

electrophoresis in 0.8% agarose gel run at 150 volts for 45 minutes and visualized by ethidium bromide staining and UV light exposure. Fragments were excised from gel and purified by Qiaquick Gel Extraction (Qiagen) and ligated using T4 DNA ligase (Promega) at 3:1 insert to vector molar ratio and incubated at 16ºC overnight. Dam -/- C2925 chemcially competent bacteria (Invitrogen) were transformed by heat shock and cultured overnight at 37ºC on ampicillin-containing agar for selection of clones containing pGEM/A64 backbone. Eight clones were selected for small-scale DNA amplification by inoculation in TB media with ampicillin antibiotic selection and cultured on a shaker at 37ºC for 8 hours. Purification of DNA was performed using MiniPrep kit (Qiagen) and analytical restriction enzyme digest and subsequent electrophoresis determined which clones expressed correct ligation product, CetuxCD28mZ/pGEM-A64 (**Figure 36C**). A positive clone was selected an inoculated 1:1000 in TB containing ampicillin. After 18 hours of culture at 37ºC, DNA was purified using EndoFree Plasmid Purification kit (Qiagen). Spectrophotometry analysis confirmed high quality DNA by OD260/280 ration between 1.8 and 2.0.

6.1.6 Nimotuzumab-derived CAR/pGEM-A64

NimoCD28mZ(CoOp)/pSBSO was digested sequentially with *NheI* at 37ºC and *SfiI* at 50ºC while pGEM/GFP/A64 was digested sequentially with *XbaI* at 37ºC and *SfiI* at 50ºC. NimoCD28mZ(CoOp) was cloned into pGEM/GFP/A64 plasmid to place Nimo-CAR under control of a T7 promoter for *in vitro* transcription of RNA with artificial polyA tail 64 nucleotides in length. Digested Nimo-CAR insert and pGEM/A64 backbone were separated by electrophoresis in 0.8% agarose gel run at 150 volts for 45 minutes and visualized by ethidium bromide staining and UV light exposure. Fragments were excised from gel and purified by Qiaquick Gel Extractions (Qiagen) and ligated using T4 DNA ligase (Promega) at 3:1 insert to vector molar ratio and incubated at 16ºC overnight. Dam-/- C2925 chemically competent bacteria (Invitrogen) were transformed by heat shock and cultured overnight at 37ºC on ampicillin-containing agar for selection of clones containing pGEM/A64 backbone. Eight clones were selected for small-scale DNA amplification by inoculation in TB media with ampicillin antibiotic selection and cultured on a shaker at 37ºC for 8 hours. Purification of DNA was performed using MiniPrep kit (Qiagen) and analytical restriction enzyme digest and subsequent electrophoresis determined which clones expressed correct ligation product, NimoCD28mZ/pGEM-A64 (**Figure 36D**). A positive clone was selected an inoculated 1:1000 in TB containing ampicillin. After 18 hours of culture at 37ºC, DNA was

purified using EndoFree Plasmid Purification kit (Qiagen). Spectrophotometry analysis confirmed high quality DNA by OD260/280 ration between 1.8 and 2.0.

6.1.7 Truncated EGFR transposon

Truncated EGFR was cloned into a SB transposon linked via self-cleavable peptide sequence F2A to a gene for neomycin resistance. A codon-optimized truncated form of human EGFR (accession NP_005219.2) containing only extracellular and transmembrane domains, 0909312 ErbB1/pMK-RQ, was synthesized by GeneArt (Regensburg, Germany). ErbB1/pMK-RQ was digested with *NheI* and *SmaI* at 37ºC while tCD19-F2A-Neo/pSBSO (produced by S. Olivares) was sequentially digested with *NheI* at 37ºC, then *NruI* at 37ºC with a purification step between (Qiaquick Gel Extraction kit, Qiagen). tEGFR insert and F2A-Neo/pSBSO backbone were separated by gel electrophoresis on 0.8% agarose gel run at 150 volts for 45 minutes. Bands of predicted sizes were isolated (Qiaquick Gel Extraction kit, Qiagen) and ligated with T4 DNA Ligase (Promega) overnight at 16ºC. TOP10 chemically competent cells (Invitrogen) were heat-shock transformed with ligation production and cultured overnight on agar containing kanamycin. Five clones were inoculated for small scale DNA amplification by culture in TB containing kanamycin for 8 hours. DNA purification by Mini Prep kit (Qiagen) and subsequent analytical restriction enzyme digest identified clones positive for tErbB1-F2A-Neo/pSBSO (**Figure 36E**). A positive clone was inoculated into culture at 1:1000 for large-scale DNA amplification and cultured on a shaker at 37ºC for 16 hours. Purification of DNA from bacteria in log-phase growth was performed using EndoFree Plasmid Purification kit (Qiagen) and spectrophotometry verified DNA purity by OD 260/280 reading between 1.8 and 2.0.

6.1.8 CAR-L transposon

A previously described 2D3 hybridoma (94) was used to derive the scFv sequence of CAR-L. Briefly, RNA was extracted from hybridoma by RNeasy Mini Kit (Qiagen), according to manufacturer's instructions. Reverse transcription via Superscript III First Strand kit (Invitrogen) generated a cDNA library. PCR using degenerate primers for the FR1 region amplified mouse variable heavy and light chains, which were subsequently ligated into TOPO TA vector. CAR-L was constructed as a codon optimized sequence, as follows: Following a human GMCSFR signal peptide (amino acid 1-22; NP_758452.1), 2D3-derived scFv was fused to human CD8α extracellular domain (amino acid 136-182; NP_001759.3) and transmembrane and intracellular domains of human CD28 (amino acid 56-123;

NP_001230006.1) and terminates in human intracellular domain of CD3ζ (amino acid. 48-163; NP_ 000725.1). The CAR-L protein was synthesized at GeneART, then excised and ligated into a SB transposon with a self-cleavable 2A peptide fused to a Zeomycin resistance gene, designated CAR-L-2A-Zeo (**Figure 36F**) (286) (Performed by D. Rushworth).

6.2 Cell lines: propagation and modification

All cell lines were maintained in complete media, defined as Dulbecco's modified eagle media (DMEM) (Life Technologies, Grand Island, NY), supplemented with 10% heat inactivated fetal bovine serum (FBS) (HyClone, ThermoScientific) and 2mM Glutamax-100 (Gibco, Life Technologies) at 5% CO_2, 95% humidity and 37ºC, unless otherwise noted. Adherent cell lines were routinely cultured to 70-80% confluency, then passaged 1:10 following dissociation with 0.05% Trypsin-EDTA (Gibco). Identity of cell lines was validated by STR DNA fingerprinting using the AmpF_STR Identifier kit according to manufacturer's instructions (Applied Biosystems, cat# 4322288). The STR profiles were compared to known ATCC fingerprints (ATCC.org), and to the Cell Line Integrated Molecular Authentication database (CLIMA) version 0.1.200808 (http://bioinformatics.istge.it/clima/) (Nucleic Acids Research 37:D925-D932 PMCID: PMC2686526). The STR profiles matched known DNA fingerprints.

6.2.1 OKT3-loaded K562 clone 4

K562 clone 4 was received as a gift from Carl June, M.D. at the University of Pennsylvania and has been previously described (95, 97). Clone 4 are modified to express tCD19, CD86, CD137L, CD64 and a membrane IL15-GFP fusion protein and have been manufactured as a working cell bank for pre-clinical and clinical studies under PACT. K562 clone 4 can be made to express anti-CD3 antibody, OKT3, through binding to the CD64 high affinity Fc receptor. To load OKT3 onto K562 clone 4, cells are cultured overnight in X-VIVO serum free media (Lonza, Cologne, Germany) with 2% N-acetylcysteine at a density of $1x10^6$ cells/mL. This step clears the Fc receptors for optimal binding of OKT3. The following day, cells are washed and resuspended at $1x10^6$ cells/mL in X-VIVO media with 2% N-acetylcysteine and irradiated at achieve 100 Gy. Cells are washed and resuspended at $1x10^6$ cells/mL in PBS and OKT3 (eBioscience, San Diego, CA) is added at a concentration of 1 mg/mL and incubated on roller at 4ºC for 30 minutes. Cells are washed again, stained

to verify expression of costimulatory molecules and OKT3 by flow cytometry, and cryopreserved.

6.2.2 tEGFR$^+$ K562 clone 27

K562 clone 27 was derived from K562 clone 9, gift from Carl June, M.D. at the University of Pennsylvania. K562 clone 9 was lentivirally transduced, as previously described (95, 97), to express tCD19, CD86, CD137L, and CD64. Clone 27 were modified from clone 9 to stably express a membrane tethered IL15-IL15Rα fusion protein (317) via SB transfection, cloned by limiting dilution, and verified to have high expression of all transgenes by flow cytometry (performed by L. Hurton). K562 clone 27 was modified to express truncated EGFR by SB transfection of tErbB1-F2A-Neo/pSBSO. K562 clone 27 expressing EGFR were incubated with PE-labeled EGFR-specific antibody (BD Biosciences, Carlsbad, CA, cat# 555997) and anti-PE beads (Miltenyi Biotec, Auburn, CA), then separated from non-labeled cells by flow through a magnetic column (Miltenyi Biotec). Following magnetic selection, tEGFR$^+$ K562 clone 27 were cultured in the presence of 1 mg/mL G418 (Invivogen, San Diego, CA) to maintain high EGFR expression.

6.2.3 EL4, CD19$^+$ EL4, tEGFR$^+$ EL4, and CAR-L$^+$ EL4

EL4 were obtained from ATCC and modified to express tCD19-F2A-Neo, tEGFR-F2A-Neo or CAR-L-F2A-Neo by SB non-viral gene modification. EL4 were electroporated in using Amaxa Nucelofector (Lonza) and primary mouse T cell kit (Lonza) according to manufacturer's instructions. Briefly, 2x10^6 EL4 cells were centrifuged at 90xg for 10 minutes and resuspended in 100 uL primary mouse T cell buffer with 3 ug transposon (tCD19-F2A-Neo, tEGFR-F2A-Neo, or CAR-L-2A-Zeo) and 2 ug SB11 transposase and electroporated using Amaxa program X-001. Following electroporation, cells were immediately transferred to pre-warmed and supplemented primary mouse T cell media, supplied with kit (Lonza). The following day, 1 mg/mL G418 was added to select for EL4 cells modified to express transgenes. Expression was verified by flow cytometry 7 days post-modification.

6.2.4 U87, U87^{low}, U87^{med}, and U87^{high}

U87, formally designated U87MG, were obtained from ATCC (Manassas, VA). U87^{low} and U87^{med} were generated to overexpress EGFR by modification with tErbB1-F2A-Neo/pSBSO and SB11 using Amaxa Nucleofector and cell line Nucleofector kit T (Lonza, cat#VACA-1002), according to manufacturer's instructions. Briefly, U87 cells were cultured to 80% confluency, then harvested by dissociation in 0.05% Trypsin-EDTA (Gibco) and

counted via trypan blue exclusion using and automated cell counter (Cellometer, Auto T4 Cell Counter, Nexcelcom, Lawrence, MA). $1x10^6$ U87 cells were suspended in 100 uL cell line kit T electroporation buffer in the presence of 3 ug of tErbB1-F2A-Neo/pSBSO transposon and 2 ug SB11 transposase, transferred to a cuvette and electroporated via program U-029. Immediately following electroporation, cells were transferred to 6-well plate and allowed to recover in complete DMEM media. The following day, 0.35 mg/mL G418 (Invivogen) was added to select for transgene expression. After propagation to at least $1x10^6$ cells, flow cytometry was performed to assess EGFR expression. Electroporated U87 cells demonstrated modest increase in EGFR expression relative to unmodified U87 and were designated $U87^{low}$. To generate $U87^{med}$ cells, U87 cells were lipofectamine-transferred with tErbB1-F2A-Neo and SB11 using Lipofectamine 2000 (Invitrogen) according to manufacturer's instructions. The following day, 0.35 mg/mL G418 was added to culture to select for neomycin resistance. After propagation of cells to significant number, flow cytometrey revealed a two-peak population, with mutually exclusive modest or high EGFR overexpression, relative to U87 cells. Cells were stained with anti-EGFR-PE and FACS sorted for the top 50% of highest peak. Careful subcloning when cells reached no greater than 70% confluence and flow cytometry analysis was routinely performed to ensure cells maintained EGFR expression. $U87^{high}$ are U87-172b cells overexpressing wtEGFR, and were a kind gift from Oliver Bölger, Ph.D.

6.2.5 U87-ffLuc-mKate and $U87^{med}$-ffLuc-mKate

U87 and $U87^{med}$ cells were lentivirally transduced to express ffLuc-mKate transgene (**Figure 37**), similar to a previously described protocol (318). Briefly, 293-METR packaging cells were transfected with pcMVR8.2, VSV-G and pLVU3GeffLuc-T2AmKates158A in the presence of Lipofectamine 2000 (Invitrogen), according to manufacturer's instructions. After 48 hours, virus-like particles (VLP) were harvested and concentrated on 100 kDa NMWL filters (Millipore, Billerica, MA). To transduce U87 and $U87^{med}$, cells were plated in 6 well plates until 70-80% confluent, then ffLucmKate VLPs were added in conjunction with 8 µg/mL polybrene. The plate was centrifuged at 1800 rpm for 1.5 hours, then incubated for 6 hours. Following incubation, supernatant was removed. Twenty-four hours after transduction, cells reached confluency and were subcultured and FACS sorted for cells expressing moderate levels of ffLuc-mKate (Performed by D. Deniger).

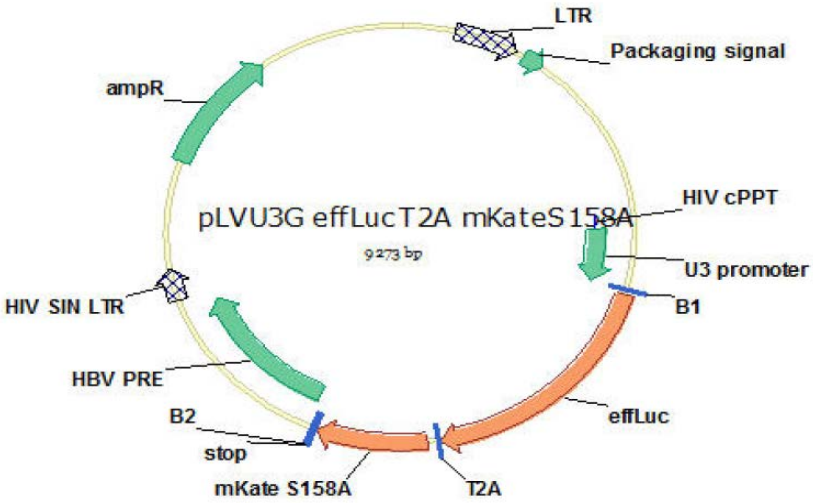

Figure 37. Vector map of pLVU3G-effLuc-T2A-mKateS158A. Annotations are as follows: B1: Gateway donor site B1; effLuc: enhanced firefly luciferase; T2A: T2A ribosomal slip site; mKateS158A: enhanced mKate red fluorescent protein; B2: Gateway donor site B2, HBV PRE: Hepatitis B post-translational regulatory element; HIV SIN LTR: HIV self-inactivating long terminal repeat; ampR: ampicillin resistance; LTR: long terminal repeat; HIV cPPT: HIV central polypurine tract.

6.2.6 Human renal cortical epithelial cells (HRCE)

HRCE were obtained from Lonza, described to be taken from proximal and distal renal tubules of healthy individuals, and were cultured in complete Renal Growth Media (Lonza, cat# CC-3190) supplemented with recombinant human epidermal growth factor (rhEGFR), epinephrine, insulin, triiodothyronine, hydrocortisone, transferrin, 10% heat-inactivated FBS (HyClone), and 2mM Glutamax-100 (Gibco). HRCE have finite lifespan *in vitro*, therefore, all assays were performed with cells that underwent less than 10 passages. Cells were cultured to 70-80% confluency, then detached by 0.05% Trypsin-EDTA (Gibco) and passaged 1:5 in fresh, complete Renal Growth Media.

6.2.7 NALM-6, T98G, LN18 and A431

NALM-6, T98G, LN18, and A431 were all obtained from ATCC and cultured as described for cell lines.

6.3 T cell modification and culture

Peripheral blood mononuclear cells were obtained from healthy donors from Gulf Coast Regional Blood Bank and isolated by Ficoll-Paque (GE Healthcare, Milwaukee, WI) and cryopreserved. All T-cell cultures were maintained in complete RPMI-1640 (HyClone), supplemented with 10% FBS (HyClone) and 2mM Glutamax (Gibco).

6.3.1 Electroporation with SB Transposon/Transposase

SB electroporation was performed as previously described (94). PBMC were thawed on the day of electroporation and rested in cytokine-free media complete RPMI-1640 at a density of $1x10^6$ cells/mL for 2 hours. Following resting period, cells were centrifuged at 200xg for 8 minutes, then resuspended in media and counted by trypan blue exclusion using an automated cell counter (Cellometer, Auto T4 Cell Counter, Nexcelcom). PBMC were centrifuged again and resuspended at $2x10^8$/mL in human T cell electroporation buffer (Lonza, cat# VPA-1002), then 100 µL of cell suspension was mixed with 15 µg transposon (either Cetux- or Nimo-CAR) and 5 µg SB11 transposase, transferred to electroporation cuvette, and electroporated via Amaxa Nucleofector (Lonza) using program U-014 for unstimulated human T cells. Following electroporation, cells were immediately transferred to phenol-free RPMI supplemented with 20% heat-inactivated FBS (HyClone), and 2 mM Glutamax-100 (Gibco) to recover overnight. The next day, cells were analyzed by flow cytometry for CD3 and Fc (IgG portion of CAR).

6.3.2 Stimulation and Culture of CAR^+ T cells

Twenty-four hours after electroporation, cells were stimulated with 100 Gy-irradiated $EGFR^+$ K562 clone 27 artificial antigen presenting cells (aAPC) at a ratio of 2 CAR^+ T cells:1 aAPC. T cells were restimulated every 7-9 days following evaluation of CAR expression by flow cytometry. Throughout culture period, T cells received 30 ng/mL IL-21 (Peprotech, Rocky Hill, NJ) added to culture every 2-3 days. IL-2 (Aldeleukin, Novartis, Switzerland) was added to culture after second stimulation cycle at 50 U/mL, every 2-3 days. At day 14, cultures were evaluated for the presence of NK cells, designated as $CD3^{neg}CD56^+$ cells present in culture. If NK cells represented >10% of cell population, NK cell depletion was performed by labeling NK cells with CD56-specific magnetic beads (Miltenyi Biotec) and sorting on LS column (Miltenyi Biotec). Flow cytometry of negative flow through containing CAR^+ T cells verified successful depletion of NK cell subset from culture. Cultures were evaluated for function when CAR was expressed on >85% of $CD3^+$ T cells, usually following 5 stimulation cycles.

6.3.3 *In vitro* transcription of RNA

CetuxCD28mZ/pGEM-A64, NimoCD28mZ/pGEM-A64, or GFP/pGEM-A64 was digested with *SpeI* at 37 ºC for 4 hours to provide linear template for *in vitro* RNA transcription. Complete linearization of template confirmed by agarose gel electrophoresis in 0.8% agarose gel and presence of single band and remaining digest purified by QiaQuick PCR Purification (Qiagen) and eluted in low volume to achieve concentration of 0.5 µg/µL. *In vitro* transcription reaction was performed using T7 mMACHINE mMESSAGE Ultra (Ambion, Life Technologies, cat# AM1345) according to manufacturer's protocol and incubated at 37ºC for 2 hours. After transcription of mRNA, DNA template was degraded by addition of supplied Turbo DNAse at 1 unit/µg DNA template and incubated an additional 30 minutes at 37ºC. Transcribed RNA was purified using RNeasy Mini kit (Qiagen). Concentration and purity (OD 260/280 value = 2.0-2.2) were determined by spectrophotometry and frozen in single-thaw aliquots at -80ºC. Quality of RNA product evaluated by gel electrophoresis on formaldehyde-containing agarose gel (1% agarose, 10% 10x MOPS Running Buffer, 6.7% formaldehyde) at 75 volts for 80 minutes in 1xMOPS Running Buffer and visualization of single, delineated band.

6.3.4 Polyclonal T-cell expansion

Numeric expansion of T cells independent of antigen was achieved by culture with 100 Gy-irradiated K562 clone 4 loaded with OKT3 delivering proliferative stimulus through cross-linking CD3. aAPC were added at a density of 10:1 or 1:2 (T cells: aAPC) every 7-10 days, 50 U/mL IL-2 was added every 2-3 days. Media changes were performed throughout culture to keep T cells at a density between 0.5-2x10^6 cells/mL.

6.3.5 RNA electro-transfer to T cells

T cells underwent stimulation 3-5 days prior to RNA transfer by co-culture with 100 Gy-irradiated OKT3-loaded K562 clone 4 as described above. Prior to electro-transfer, T cells were harvested and counted by trypan blue exclusion using an automated cell counter (Cellometer, Auto T4 Cell Counter, Nexcelcom). During preparation of cells, RNA was removed from -80ºC freezer and thawed on ice. T cells were centrifuged at 90xg for 10 minutes, and supernatant was carefully aspirated to ensure complete removal without disruption of cell pellet. T cells were suspended in P3 Primary Cell 4D-Nucleofector buffer (Lonza, cat # V4XP-3032) to a concentration of 1x10^8/mL and 20 µL of each T-cell suspension was mixed with 3 µg of *in vitro* transcribed RNA, then transferred to Nucleofector cuvette strip (Lonza, cat # V4XP-3032). Cells were electroporated in Amaxa 4D Nucleofector (Lonza) using program DQ-115, then allowed to rest in cuvette up to 15 minutes. Following rest period, warm recovery media, phenol-free RPMI 1640 (HyClone) supplemented with 2mM Glutamax-100 (Gibco) and 20% heat-inactivated FBS (HyClone), was added to cuvette and cells were gently transferred to 6 well plate containing recovery media and transferred to a tissue culture incubator. After 4 hours, 50 U/mL IL-2 and 30 ng/mL IL-21 were added to the T cells. Four to twenty-four hours after RNA transfer, T cells were analyzed for expression of CAR by flow cytometry for Fc. All functional assays were carried out at 24 hours post-RNA transfer.

6.4 Immunostaining and Flow Cytometry

6.4.1 Acquisiton and analysis:

Flow cytometry data were collected on FACS Calibur (BD Biosciences, San Jose, CA) and acquired using CellQuest software (version 3.3, BD Biosciences). Analysis of flow cytometry data was performed using FlowJo software (version x.0.6, TreeStar, Ashland, OR).

6.4.2 Surface Immunostaining and Antibodies:

Immunostaining of up to $1x10^6$ cells was performed with monoclonal antibodies conjugated to the following dyes at the following dilutions (unless otherwise stated): fluorescein (FITC, 1:25), phycoerythrin (PE, 1:40), peridinin chlorophyll protein conjugated to cyanine dye (PerCPCy5.5, 1:25), allophycocyanin (APC, 1:40), AlexaFluor488 (1:20), AlexaFluor647 (1:20). All antibodies were purchased from BD Biosciences, unless otherwise stated. Antibodies specific for the following were human-specific, unless otherwise noted: CD3 (clone SK7), CD3 (clone UCHT1), CD3 (hamster anti-mouse, clone 500A2), CD4 (clone RPA-T4), CD8 (clone SK1), CD19 (HIB19), CD27 (clone L128), CD28 (clone L293), CD45RA (clone HI100), CD45RO (clone HI100), CD56 (clone B159), CD62L (clone DREG-56), CCR7 (clone GD43H7, Biolegend, San Diego, CAR PerCPCy5.5 diluted 1:45), EGFR (clone EGFR.1, PE diluted 1:13.3), Fc (to detect CAR, clone HI10104, Invitrogen), IL15 (clone 34559, R&D Systems, Minneapolis, MN, PE diluted 1:20), murine F(ab')2 (to detect OKT3 loaded on K562, Jackson Immunoresearch, West Grove, PA, cat# 115-116-072, PE diluted 1:100), TNF-α (clone mAb11, PE diluted 1:40) and IFN-γ (clone 27, APC diluted 1:66.7), pErk1/2 (clone 20A, AlexaFluor 647), pp38 (clone 36/p38, PE) and Ki-67 (clone B56, FITC, 1:20, BD Biosciences). Surface molecules were stained in FACS buffer (PBS, 2% FBS, 0.5% sodium azide) for 30 minutes in the dark at 4ºC.

6.4.3 Quantitative Flow Cytometry:

Quantitative flow cytometry was performed using Quantum Simply Cellular polystyrene beads (Bangs Laboratories, Fishers, IN). Five bead populations are provided, four populations with increasing amounts of anti-murine IgG, and therefore a known antibody binding capacity (ABC) and one blank population. EGFR-PE (BD Biosciences, cat#555997) was incubated with beads at a saturated concentration (1:3 dilution, per manufacturer's recommendation) synchronously with immunostaining of target cells. MFI of EGFR-PE binding to microspheres was used to create a standard curve, to which a linear regression was fit using QuickCal Data Analysis Program (version 2.3, Bangs Laboratories) (**Figure 38**). Applying measured MFI of EGFR-PE binding to target cells, less the amount of background autofluroescence, to the linear regression yielded a mean number of EGFR molecules expressed per cell.

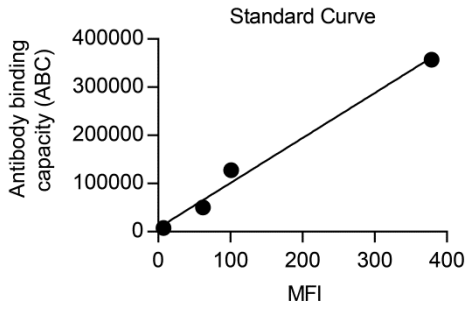

Figure 38. Standard curve for relating MFI to ABC for quantitative flow cytometry. Following incubation with saturating amounts anti-EGFR-PE, microsphere bead standard samples with known antibody binding capacity were acquired on flow cytometer. Standard curve was generated by plotting known antibody binding capacity against measured mean fluorescence intensity acquired by flow cytometry.

6.4.4 Intracellular cytokine staining and flow cytometry

T cells were co-cultured with target cells at a ratio of 1:1 for 4-6 hours in the presence of 4000 x diluted GolgiStop (BD Biosciences). Unstimulated T cells served as negative controls, while T cells treated with Leukocyte Activation Cocktail, containing PMA/Ionomycin and brefeldin A (BD Biosciences) diluted 1000x served as positive controls. An EGFR-specific monoclonal antibody (clone LA1, Millipore) was used to block interaction of CAR and EGFR interaction. Intracellular cytokine staining was performed after surface immunostaining by fixation/permeabilization in Cytofix/Cytoperm buffer (BD Biosciences) for 20 minutes in the dark at 4ºC, followed by staining of intracellular cytokine in 1x Perm/Wash Buffer (BD Biosciences) for 30 minutes, in the dark at 4ºC. Antibodies used were TNF-α (BD Biosciences, clone mAb11, PE diluted 1:40) and IFN-γ (BD Biosciences, clone 27, APC diluted 1:66.7). Following intracellular cytokine staining, cells were fixed with 0.5% paraformaldehyde (CytoFix, BD Biosciences) until samples were acquired on FACS Calibur.

6.4.5 Measuring phosphorylation by flow cytometry:

T cells were co-cultured with target cells at a ratio of 1:1 for 45 minutes, unless otherwise indicated. Following activation, T cells centrifuged 300xg for 5 min and supernatant decanted. T cells were lysed and fixed by addition of 20 volumes of 1x PhosFlow Lyse/Fix buffer (BD Biosciences), pre-warmed to 37ºC and incubated at 37ºC for 10 minutes. Following centrifugation, T cells are permeabilized by addition of ice-cold PhosFlow Perm III Buffer (BD Biosciences) while vortexing and incubated on ice in the dark for 20 minutes. After incubation, cells were washed with FACS Buffer and resuspended in 100 µL staining solution. Staining solution was composed of antibodies against CD4 (clone SK3, FITC), CD8 (clone SK1, PerCPCy5.5), pErk1/2 (clone 20A, AlexaFluor 647), pp38 (clone 36/p38, PE) and FACS buffer, all present at the same ratio and incubated for 20 minutes in the dark at room temperature. Cells were fixed with 0.5% paraformaldehyde and analyzed by flow cytometry within 24 hours.

6.4.6 Viability Staining

Staining for Annexin V (BD Biosciences) and 7-AAD (BD Biosciences) or propidium iodide (PI) (BD Biosciences) was used to determine cell viability and was performed in 1x Annexin Binding buffer, with staining for CD4 or CD8, for 20 minutes, in the dark, at room temperature. Percentage of viable cells was determined as %AnnexinV^{neg}7-AAD^{neg} or %AnnexinV^{neg}PI^{neg} in CD4 or CD8 gated T-cell population.

6.4.7 Staining for cellular proliferation marker Ki-67:

Proliferation marker Ki-67 was measured by intracellular flow cytometry. T cells were co-cultured with adherent target cells at a ratio of 1:5 for 36 hours, then T cells were harvested from culture by removing supernatant and centrifugation at 300xg. T cells were then fixed and permeabilized by drop-wise addition of ice-cold 70% ethanol while vortexing at high speed. T cells were then stored at -20ºC for 2-24 hours before staining. Cells were stained with Ki-67 (clone B56, FITC, 1:20, BD Biosciences), CD4 (clone RPA-T4), and CD8 (clone SK1) in 100 µL FACs Buffer for 30 min in the dark at room temperature, then immediately analyzed by flow cytometry.

6.5 T-cell functional assays

6.5.1 CAR downregulation:

CAR^+ T cells and targets were harvested and counted by trypan blue exclusion using an automated cell counter (Cellometer, Auto T4 Cell Counter, Nexcelcom), then mixed at a 1:1 ratio in a 12-well plate, and individual wells were harvested at each time point to measure CAR surface expression on T cells. Negative controls for downregulation were T cells plated without stimuli. Staining for T cells by CD3, CD4 and CD8 expression and co-staining for CAR by Fc was analyzed on flow cytometer. Percent downregulation of CAR was calculated as [CAR expression following stimuli]/[CAR expression without stimuli] x 100.

6.5.2 Secondary activation and cytokine production

CAR^+ T cells and adherent targets were harvested and counted by trypan blue exclusion using an automated cell counter (Cellometer, Auto T4 Cell Counter, Nexcelcom), then mixed at a ratio of 1:1 in a 12-well plate. After 24 hours of co-culture, T cells were harvested from culture by removing supernatant and washing adherent cells with PBS. T cells were spun at 300xg for 5 minutes, then resuspended in media and counted by trypan blue exclusion using an automated cell counter (Cellometer, Auto T4 Cell Counter, Nexcelcom). T cells were stimulated with targets at 1:1 ratio and intracellular cytokine production analysis as described above.

6.5.3 Long-term cytotoxicity assay

The day prior to initiation of assay, adherent U87 and $U87^{high}$ cells were harvested, counted, and 40,000 target cells were plated in each well of a 6-well plate in complete DMEM and incubated in tissue culture incubator overnight. On the day of assay, CAR^+ T

cells were harvested, counted by trypan blue exclusion, and added at a 1:5 E:T ratio to plated target cells. Negative control wells had no T cells added. At each assay time point, T cells were removed by discarding supernatant and washing the well with PBS. Adherent cells were dissociated from wells by 0.05% Trypsin-EDTA (Gibco). Microscopy was performed to visually ensure complete detachment of cells from well. Harvested cells were spun down and resuspended in 100 uL of media, then counted by trypan blue exclusion using a hemacytometer. Percent surviving cells was calculated as [cell number after T cell co-culture]/[cell number with no T cell co-culture] x 100.

Long-term co-culture with EL4 was performed by mixing T cells and either $tEGFR^+$ EL4 or $CAR\text{-}L^+$ EL4 at a ratio of 1:1 and monitoring relative proportion of CAR+ T cell to EL4 cell over time by flow cytometry. Human T cells were detected by anti-human CD3 antibody (clone UCHT1), not cross-reactive for murine CD3. EL4 cells were detected by anti-murine CD3 (clone 500A2), not cross-reactive for human CD3.

6.5.4 Chromium release assay

Specific cytotoxicity was assessed via standard 4-hour chromium release assay, as previously described (94). Target cells were harvested and counted by trypan blue exclusion using an automated cell counter (Cellometer, Auto T4 Cell Counter). No less than 250,000 cells were aliquoted, then centrifuged at 300xg for 5 minutes and supernatant was discarded. Next, 0.1 µCi of ^{51}Cr was added to each target and incubated for 1-1.5 hours in a tissue culture incubator at 37ºC. 100,000 T cells per well were plated in triplicate and serially diluted at 1:2 ratio to give a final effector to target (E:T) ratio of 20:1, 10:1, 5:1, 2.5:1 and 1.25:1 in a 96-well V-bottom plate (Corning, Corning, NY) and placed in a tissue culture incubator. Media only was placed in wells designated for minimum chromium release control. Following labeling with chromium, targets were washed three times with 10 mL PBS, then resuspended at a final concentration of 125,000 cells/mL, thoroughly mixed, and 100 µL was added to each row, included all T-cell containing rows, a minimum release row, and a maximum release row. Plates were centrifuged at 300xg for 3 minutes. Following centrifugation, 100 µL of 0.1% Triton X-100 (Sigma-Aldrich, St. Louis, MO) was added to maximum release row, and plates were placed in tissue culture incubator for 4 hours. Following incubation, plates were then harvested by removal of 50 µL supernatant, without disrupting cell pellet, which was transferred to LumaPlate-96 (Perkin-Elmer, Waltham, MA) and allowed to dry overnight. The following day, plates were sealed with Top-Seal (Perkin-Elmer) and scintillation measured on TopCount NXT (Perkin-Elmer). Percent specific lysis

was calculated as [(^{51}Cr released – minimum) / (maximum– minimum)] x 100 where maximum and minimum values were averaged for each triplicate.

6.6 High-throughput gene expression and CDR3 sequencing

6.6.1 Analysis of gene expression by direct imaging of mRNA transcripts

Direct imaging and quantification of mRNA molecules was performed as previously described (319-322). Cells prior to or following expansion were positively sorted for CD4 and CD8 expression by incubating with CD4 and CD8 magnetics beads (Miltenyi Biotec), respectively, and sorting on LS column. Flow cytometry was used to verify purity of CD4 and CD8 separated populations. 1x10^6 T cells were lysed in 165 µL of RLT Buffer (Qiagen) and frozen at -80ºC in single-thaw aliquots. RNA lysates were thawed and hybridized with multiplexed target-specific, color-coded reporter and biotinylated capture probes at 65ºC for 12 hours. Lymphocyte specific mRNA transcripts of interest were identified and two CodeSets were generated from RefSeq accessions were used to generate reporter and capture probe pairs, a Lymphocyte CodeSet, and TCR Vα and Vβ CodeSet (**Appendices A and B**). Following hybridization, samples were processed in nCounter Prep (NanoString Technologies, Seattle, WA), and analyzed in nCounter Digital Analyzer (NanoString Technologies). Reference genes were identified that span wide range of RNA expression levels: ACTB, G6PD, OA21, POLR1B, RPL27, RPS13, and TBP and were used to normalize data. Normalization to positive-, negative-, and house-keeping genes was using nCounter RCC Collector (version 1.6.0, NanoString Technologies). A statistical test developed for digital gene expression profiling was used to determine differential expression of genes between sample pairs (322, 323). After normalization, significant differential gene expression in the Lymphocyte CodeSet was identified by a combination of $p<0.01$ and a fold change greater than 1.5 in at least 2/3 pairs, as previously described (322). Heat-mapping of normalized values for differentially RNA transcripts was performed by hierarchical clustering and TreeView software, version 1.1 (324). After normalization, percentage of TCR Vα and Vβ were derived from count data as previously described (319).

6.6.2 High-throughput CDR3 deep-sequencing

TCRβ CDR3 regions were amplified and sequenced from DNA extracted from 1x10^6 T cells (Qiagen DNeasy Blood and Tissue Kit, Qiagen) and carried out on ImmunoSEQ platform (Adaptive Technologies, Seattle, WA), as previously described (325).

6.7 *In vivo* evaluation of T cells in intracranial glioma xenograft murine model

All animal experiments were carried out under guidance and regulation from the Institutional Animal Care and Use Committee (IACUC) at MD Anderson Cancer Center under the approved animal protocol ACUF 11-11-13131. All mice used were 7-8 week old female NOD.Cg-Prkdc^{scid}IL2Rγ^{tm1Wjl}/Sz strain (NSG) (Jackson Laboratory, Bar Harbor, ME).

6.7.1 Implantation of guide-screw

Mice aged 7-8 weeks were anesthetized using ketamine/xylazine cocktail (10 mg/mL ketamine, 0.5 mg/mL xylazine) dosed at 0.1 mL/10 g. Implantation of guide-screw was performed as previously described (291). Once unresponsive to stimuli, surgical area on head was prepared by shaving fur and treating with povidone-iodine (polyvinylpyrrolidone complexed with elemental iodine) antiseptic solution. Using surgically ascpetic technique, a 1 cm incision was made down the middle of the cranium. An opening was made using a 1 mm drill bit (DH#60, Plastics One, Roanoke, VA) extending 1 mm from drill (DH-0, Plastics One) using firm circular pressure in the right frontal lobe, 1 mm from coronal suture and 2.5 mm from the sagittal suture.. A guide-screw (Plastics One, cat # C212SG) with a 0.50 mm opening in the center and a 1.57 mm shaft diameter was inserted into the drill site using a screwdriver (SD-80, Plastics One). Incision sites were sutured and mice were given 0.01mg/mL buprenorphine dosed at 0.1 mL/10 grams as post-surgical analgesic. Mice recovered from surgery on low-power heat source until full mobility was regained.

6.7.2 Implantation of U87-ffLucm-Kate or U87^{med}-ffLuc-mKate tumor cells

Mice recovered from guide-screw implantation for 2-3 weeks before intracranial tumors were established, as previously described (291). U87-ffLuc-mKate or U87^{med}-ffLuc-mKate were dissociated from tissue culture vessel following 10 minute incubation with Cell Dissociation Buffer, enzyme-free, PBS (Gibco) at room temperature. Cells were counted by trypan blue exclusion using hemacytometer and centrifuged at 200xg for 8 minutes. Following centrifugation, cells were resuspended in sterile PBS to a final concentration of 50,000 cells/µL. Mice were anesthetized with isoflurane (2-chloro-2-(difluoromethoxy)-1,1,1-trifluoro-ethane), and prepared for incision as described above. While mice were undergoing surgical preparation, 26 gauge, 10 µL Hamilton syringes with blunt needle (Hamilton Company, Reno, NV cat# 80300) were prepared by placing plastic guard 2.5 mm from the end of syringe and loading 5 µL of cell suspension containing 250,000 cells. After incision site was opened, syringes were inserted into guide screw opening and cells were injected

with constant slow pressure. After completion of injection, syringes were held in place an additional 30 seconds to allow intracranial pressure to dissipate, then slowly removed. Incisions were sutured and mice were removed from isoflurane exposure. Day of implantation is designated as day 0 of study. On day 1 and 4 tumors were imaged via non-invasive bioluminescent imaging, as described above to ensure successful tumor engraftment. Mice were then divided into three groups to evenly distribute relative tumor flux, and then randomly assigned to receive Cetux-CAR$^+$ T-cell treatment, Nimo-CAR$^+$ T-cell treatment and no treatment.

6.7.3 Non-invasive bioluminescent imaging of U87-ffLuc-mKate or U87^{med}-ffLuc-mKate

Intracranial glioma was non-invasively and serially imaged and used as a measure of relative tumor burden. Ten minutes after sub-cutaneous injection of 215 µg D-luciferin potassium salt (Caliper Life Sciences, Perkin-Elmer), tumor flux (photons/s/cm^2/steradian) was measured using Xenogen Spectrum (Caliper Life Sciences, Perkin-Elmer) and Living Image software (version 2.50, Caliper Life Sciences, Perkin-Elmer). Tumor flux was measured in a delineated region of interest encompassing entire cranial region of mice.

6.7.4 Delivery of CAR$^+$ T cells to intracranially established U87-ffLuc-mKate or U87^{med}-ffLuc-mKate glioma

Treatment of intracranial glioma xenografts began on day 5 of tumor establishment and continued weekly for a total of 3 T cell injections. CAR$^+$ T cells having completed 3 stimulation cycles were confirmed to be >85% CAR-expressing by flow cytometry, then viable cells were counted by trypan blue exclusion using an automated cell counter (Cellometer, Auto T4 Cell Counter, Nexcelcom). CAR$^+$ T cells were spun at 300xg for 5 minutes, and resuspended at a concentration of $0.6x10^6$/µL in sterile PBS. Mice were prepared for cranial incision as described above, and anesthetized by isoflurane exposure. While mice were being prepared, 26 gauge, 10 µL Hamilton syringes with blunt needle (Hamilton Company, cat# 80300) were prepared by placing plastic guard 2.5 mm from the end of syringe and loading 5 µL of cell suspension containing $3x10^6$ T cells. Syringes were inserted into the guide-screw, extending 2.5 mm into intracranial space, and injected with slow, constant pressure. After syringe was emptied, it was held in place an addition 30 seconds to allow intracranial pressure to dissipate. Following injection, incisions were sutured closed and mice were removed from isoflurane exposure.

6.7.5 Assessing survival of mice

Mice were sacrificed when they displayed progressive weight loss (>25% of body mass), rapid weight loss (>10% loss of body mass within 48 hours) or hind limb paralysis, or any two of the following clinical symptoms of illness: ataxia, hunched posture, irregular respiration rate, ulceration of exposed tumor, or palpable tumor diameter exceeding 1.5 cm.

6.8 Statistics

All statistical analyses were performed in GraphPad Prism, version 6.03. Statistical analyses of all *in vitro* cell culture experimentation, including flow cytometry analysis of cytokine production, viability, proliferation, and surface phenotype, kinetics of cell expansion, long term cytotoxicity, and chromium release assay by two-way ANOVA with donor-matching and Tukey's post-test for multiple comparisons. Correlation of function with antigen density was performed by one-way ANOVA with post-test for linear trend. Analyses of *in vivo* bioluminescent imaging of tumor were performed using two-way ANOVA with repeated measures and Sidak's post-test for multiple comparisons. Statistical analysis of animal survival data was performed by log-rank (Mantel-Cox) test. Significance of findings defined as follows: * $p<0.05$, ** $p<0.01$, *** $p<0.001$, **** $p<0.0001$.

APPENDICES

Appendix A: Lymphocyte-specific CodeSet

Gene Name	Accession	Target Region	Target Sequence
ABCB1	NM_000927.3	3910-4010	TATAGCACTAAAGTAGGAGACAAAGGAACTCAGCTCTCTGGTGGCCAGAAACAAC GCATTGCCATAGCTCGTGCCCTTGTTAGACAGCCTCATATTTTGC
ABCG2	NM_004827.2	285-385	AGGATTTAGGAACGCACCGTGCACATGCTTGGTGGTCTTGTTAAGTGGAAACTGC TGCTTTAGAGTTTGTTTGGAAGGTCCGGGTGACTCATCCCAACAT
ACTB	NM_001101.2	1010-1110	TGCAGAAGGAGATCACTGCCCTGGCACCCAGCACAATGAAGATCAAGATCATTGC TCCTCCTGAGCGCAAGTACTCCGTGTGGATCGGCGGCTCCATCCT
ADAM19	NM_023038.3	1690-1790	GAGAAGGTGAATGTGGCAGGAGACACCTTTGGAAACTGTGGAAAGGACATGAAT GGTGAACACAGGAAGTGCAACATGAGAGATGCGAAGTGTGGGAAGA
AGER	NM_001136.3	340-440	GAAAGGAGACCAAGTCCAACTACCGAGTCCGTGTCTACCAGATTCCTGGGAAGC CAGAAATTGTAGATTCTGCCTCTGAACTCACGGCTGGTGTTCCCAA
AHNAK	NM_001620.1	15420-15520	GGATTTGACCTGAATGTTCCTGGGGGTGAAATTGATGCCAGCCTCAAGGCTCCG GATGTAGATGTCAACATCGCAGGGCCGGATGCTGCACTCAAAGTCG
AIF1	NM_032955.1	315-415	AAAAGCGAGAGAAAAGGAAAAGCCAACAGGCCCCCCAGCCAAGAAAGCTATCTC TGAGTTGCCCTGATTTGAAGGGAAAAGGGATGATGGGATTGAAGGG
AIM2	NM_004833.1	607-707	ACGTGCTGCACCAAAAGTCTCTCCTCATGTTAAGCCTGAACAGAAACAGATGGTG GCCCAGCAGGAATCTATCAGAGAAGGGTTTCAGAAGCGCTGTTTG
AIMP2	NM_006303.3	507-607	CCCTCTCCCTGCTTGTGCTGCACAGGCTGCTCTGTGAGCACTTCAGGGTCCTGTC CACGGTGCACACGCACTCCTCGGTCAAGAGCGTGCCTGAAAACCT
AKIP1	NM_020642.3	570-670	GAACATCTCTAAGGACCTCTACATAGAAGTATATCCAGGGACCTATTCTGTCACTG TGGGCTCAAATGACTTAACCAAGAAGACTCATGTGGTAGCAGTT
AKT1	NM_005163.2	1772-1872	TTCTTTGCCGGTATCGTGTGGCAGCACGTGTACGAGAAGAAGCTCAGCCCACCCT TCAAGCCCCAGGTCACGTCGGAGACTGACACCAGGTATTTTGATG
ALDH1A1	NM_000689.3	11-111	ATTGCTGAGCCAGTCACCTGTGTTCCAGGAGCCGAATCAGAAATGTCATCCTCAG GCACGCCAGACTTACCTGTCCTACTCACCGATTTGAAGATTCAAT
ANXA1	NM_000700.1	515-615	GAAATCAGAGACATTAACAGGGTCTACAGAGAGGAACTGAAGAGAGATCTGGCCA AAGACATAACCTCAGACACATCTGGAGATTTTCGGAACGCTTTGC
ANXA2P2	NR_003573.1	257-357	ATATTGTCTTCTCCTACCAGAGAAGGACCAAAAAGGAACTTGCATCAGCACTGAA GTCAGCCTTATCTGGCCACCTGGAGACGGTGATTTTGGGCCTATT
APAF1	NM_181869.1	1160-1260	TTCTGATGAAACTGCAGAATCTTTGCACACGGTTGGATCAGGATGAGAGTTTTTCC CAGAGGCTTCCACTTAATATTGAAGAGGCTAAAGACCGTCTCCG
ARG1	NM_000045.2	505-605	AAGGAACTAAAAGGAAAGATTCCCGATGTGCCAGGATTCTCCTGGGTGACTCCCT GTATATCTGCCAAGGATATTGTGTATATTGGCTTGAGAGACGTGG
ARRB2	NM_004313.3	1652-1752	CATTAATTTTTTGACTGCAGCTCTGCTTCTCCAGCCCCGCCGTGGGTGGCAAGCT GTGTTCATACCTAAATTTTCTGGAAGGGGACAGTGAAAAGAGGAG
ATF3	NM_001030287.2	600-700	GGCTCAGAATGGGAGGACTCCAGAAGATGAGAGAAACCTCTTTATCCAACAGATA AAAGAAGGAACATTGCAGAGCTAAGCAGTCGTGGTATGGGGGCGA
ATM	NM_000051.3	30-130	ACGCTAAGTCGCTGGCCATTGGTGGACATGGCGCAGGCGCGTTTGCTCCGACGG GCCGAATGTTTTGGGGCAGTGTTTTGAGCGCGGAGACCGCGTGATA
ATP2B4	NM_001684.3	7640-7740	CTTCCCATAGTATCATCTGTCCTCTGGAATGACTCTCCTGTCCCTAAAGGGGTTAA GAGAGAGATCACCTAGAAATCCCTCTGGACACTTGTGGGTTCTT
AXIN2	NM_004655.3	1035-1135	CTTGTCCAGCAAAACTCTGAGGGCCACGGCGAGTGTGAGGTCCACGGAAACTGT TGACAGTGGATACAGGTCCTTCAAGAGGAGCGATCCTGTTAATCCT
B2M	NM_004048.2	25-125	CGGGCATTCCTGAAGCTGACAGCATTCGGGCCGAGATGTCTCGCTCCGTGGCCT TAGCTGTGCTCGCGCTACTCTCTCTTTCTGGCCTGGAGGCTATCCA
B3GAT1	NM_018644.3	145-245	CTGGACAGCGACCCCTTCTCAGACTCCAGTTGGGCCGGACTCTCCAAACCTGCTT CCGCAATGGGTGGGTTGTGAGTGCTGGTAATGAGGAGCCGTGGGT
BACH2	NM_021813.2	3395-3495	TGTGGCACTGTTCATCTGCTGTCCCGAAGAAACCGAGAACACATTTGGTGCACAC TACAGCGGTCTTAGCAGCAATACTGTTCCGAAGTATCCTCTCCTC
BAD	NM_004322.2	195-295	CAGCTGTGCCTTGACTACGTAACATCTTGTCCTCACAGCCCAGAGCATGTTCCAG ATCCCAGAGTTTGAGCCGAGTGAGCAGGAAGACTCCAGCTCTGCA
BAG1	NM_004323.3	1490-1590	CTCTTGTGATCGTGTAGTCCCATAGCTGTAAAACCAGAATCACCAGGAGGTTGCA CCTAGTCAGGAATATTGGGAATGGCCTAGAACAAGGTGTTTGGCA
BATF	NM_006399.3	825-925	CACTGTGGGTTGCAGGCCCAATGCAGAAGAGTATTAAGAAAGATGCTCAAGTCCC ATGGCACAGAGCAAGGCGGGCAGGGAACGGTTATTTTTCTAAATA
BAX	NM_138761.2	694-794	ATTTTTCTGGGAGGGGTGGGGATTGGGGGACATGGGCATTTTTCTTACTTTTGTA ATTATTGGGGGGTGTGGGGAAGAGTGGTCTTGAGGGGGTAATAAA
BCL10	NM_003921.2	1250-1350	TGAAAATACCATCTTCTCTTCAACTACACTTCCCAGACCTGGGGACCCAGGGGCT CCTCCTTTGCCACCAGATCTACAGTTAGAAGAAGAAGGAACTTGT
BCL11B	NM_022898.1	3420-3520	GAGATGTAGCACTCATGTCGTCCCGAGTCAAGCGGCCTTTTCTGTGTTGATTTCG GCTTTCATATTACATAAGGGAAACCTTGAGTGGTGGTGCTGGGGG
BCL2	NM_000633.2	1525-1625	CCAAGCACCGCTTCGTGTGGCTCCACCTGGATGTTCTGTGCCTGTAAACATAGAT TCGCTTTCCATGTTGTTGGCCGGATCACCATCTGAAGAGCAGACG

BCL2L1	NM_138578.1	1560-1660	CTAAGAGCCATTTAGGGGCCACTTTTGACTAGGGATTCAGGCTGCTTGGGATAAA GATGCAAGGACCAGGACTCCCTCCTCACCTCTGGACTGGCTAGAG
BCL2L1	NM_001191.2	260-360	ATCTTGGCTTTGGATCTTAGAAGAGAATCACTAACCAGAGACGAGACTCAGTGAG TGAGCAGGTGTTTTGGACAATGGACTGGTTGAGCCCATCCCTATT
BCL2L11	NM_138621.2	2825-2925	TGTTGGCACCAGAACTTAAAGCGATGACTGGATGTCTCTGTACTGTATGTATCTG GTTATCAAGATGCCTCTGTGCAGAAAGTATGCCTCCCGTGGGTAT
BCL2L11	NM_138621.4	257-357	CGGACTGAGAAACGCAAGAAAAAAAGACCAAATGGCAAAGCAACCTTCTGATGTA AGTTCTGAGTGTGACCGAGAAGGTAGACAATTGCAGCCTGCGGAG
BCL6	NM_001706.2	675-775	GTTGTGGACACTTGCCGGAAGTTTATTAAGGCCAGTGAAGCAGAGATGGTTTCTG CCATCAAGCCTCCTCGTGAAGAGTTCCTCAACAGCCGGATGCTGA
BCL6B	NM_181844.3	2135-2235	CTTTATTTGTTCTAGGGCAGCTCTGGGAACATGCGGGATTGTGGAATTGGGTCAG GAACCCTCTCTGGTATTCTGGATGTTGTAGGTTCTCTAGCAGTCT
BHLHE41	NM_030762.2	655-755	CGCCCATTCAGTCCGACTTGGATGCGTTCCACTCGGGATTTCAAACATGCGCCAA AGAAGTCTTGCAATACCTCTCCCGGTTTGAGAGCTGGACACCCAG
BID	NM_197966.1	2095-2195	GCTTAGCTTTAGAAACAGTGCAACACTGGTCTGCTGTTCCAGTGGTAAGCTATGT CCCAGGAATCAGTTTAAAAGCACGACAGTGGATGCTGGGTCCATA
BIRC2	NM_001166.3	1760-1860	TGGGATCCACCTCTAAGAATACGTCTCCAATGAGAAACAGTTTTGCACATTCATTA TCTCCCACCTTGGAACATAGTAGCTTGTTCAGTGGTTCTTACTC
BLK	NM_001715.2	990-1090	AGCTTCTTGCTCCAATCAACAAGGCCGGCTCCTTTCTTATCAGAGAGAGTGAAAC CAACAAAGGTGCCTTCTCCCTGTCTGTGAAGGATGTCACCACCCA
BMI1	NM_005180.5	1145-1245	CCTGGAGAAGGAATGGTCCACTTCCATTGAAATACAGAGTTCGACCTACTTGTAA AAGAATGAAGATCAGTCACCAGAGAGATGGACTGACAAATGCTGG
BNIP3	NM_004052.2	325-425	CACCTCGCTCGCAGACACCACAAGATACCAACAGGGCTTCTGAAACAGATACCCA TAGCATTGGAGAGAAAAACAGCTCACAGTCTGAGGAAGATGATAT
BTLA	NM_001085357.1	890-990	GCACCAACAGAATATGCATCCATATGTGTGAGGAGTTAAGTCTGTTTCTGACTCCA ACAGGGACCATTGAATGATCAGCATGTTGACATCATTGTCTGGG
C21orf33	NM_004649.5	1340-1440	TTGAGTTAATCAGCGTAAGGGGATTTCTAAAGCAGGCAATCCCTGTAGCCGCAGA GAATAAACGCCTTCCCAAAATGGCAACTTCCCACAGCCACATTTC
CA2	NM_000067.2	575-675	AGCTGTGCAGCAACCTGATGGACTGGCCGTTCTAGGTATTTTTTTGAAGGTTGGC AGCGCTAAACCGGGCCTTCAGAAAGTTGTTGATGTGCTGGATTCC
CA9	NM_001216.2	960-1060	CAGGTCCCAGGACTGGACATATCTGCACTCCTGCCCTCTGACTTCAGCCGCTACT TCCAATATGAGGGGTCTCTGACTACACCGCCCTGTGCCCAGGGTG
CARD9	NM_052813.2	1850-1950	CGCTGACTTGGCCTGGAACGAGGAATCTGGTGCCCTGAAAGGCCCAGCCGGACT GCCGGGCATTGGGGCCGTTTGTTAAGCGGCACTCATTTTGCGGAGG
CASP1	NM_033292.2	575-675	ACAGGCATGACAATGCTGCTACAAAATCTGGGGTACAGCGTAGATGTGAAAAAAA ATCTCACTGCTTCGGACATGACTACAGAGCTGGAGGCATTTGCAC
CAT	NM_001752.2	1130-1230	ATGCTTCAGGGCCGCCTTTTTGCCTATCCTGACACTCACCGCCATCGCCTGGGAC CCAATTATCTTCATATACCTGTGAACTGTCCCTACCGTGCTCGAG
CBLB	NM_170662.3	3195-3295	TAATGTCGAAGTTGCCCGGAGCATCCTCCGAGAATTTGCCTTCCCTCCTCCAGTA TCCCCACGTCTAAATCTATAGCAGCCAGAACTGTAGACACCAAAA
CCBP2	NM_001296.3	1345-1445	GAACAGATGGGAACCAGCTCAATTGGGTGTCCACTCAAAGTGCTCTCTCCAGGG GCCTCAGTGACTGTGTTGCTAAACCCAGTGGTCAGTTCTCAGTTCT
CCL3	NM_002983.2	681-781	CTGTGTAGGCAGTCATGGCACCAAAGCCACCAGACTGACAAATGTGTATCGGATG CTTTTGTTCAGGGCTGTGATCGGCCTGGGGAAATAATAAAGATGC
CCL4	NM_002984.2	35-135	TTCTGCAGCCTCACCTCTGAGAAAACCTCTTTGCCACCAATACCATGAAGCTCTGC GTGACTGTCCTGTCTCTCCTCATGCTAGTAGCTGCCTTCTGCTC
CCL5	NM_002985.2	280-380	AGTGTGTGCCAACCCAGAGAAGAAATGGGTTCGGGAGTACATCAACTCTTTGGAG ATGAGCTAGGATGGAGAGTCCTTGAACCTGAACTTACACAAATTT
CCNB1	NM_031966.2	715-815	AACTTGAGGAAGAGCAAGCAGTCAGACCAAAATACCTACTGGGTCGGGAAGTCA CTGGAAACATGAGAGCCATCCTAATTGACTGGCTAGTACAGGTTCA
CCND1	NM_053056.2	690-790	TTGAACACTTCCTCTCCAAAATGCCAGAGGCGGAGGAGAACAAACAGATCATCCG CAAACACGCGCAGACCTTCGTTGCCCTCTGTGCCACAGATGTGAA
CCR1	NM_001295.2	535-635	CATCATTTGGGCCCTGGCCATCTTGGCTTCCATGCCAGGCTTATACTTTTCCAAGA CCCAATGGGAATTCACTCACCACACCTGCAGCCTTCACTTTCCT
CCR2	NM_001123041.2	20-120	ACATTCTGTTGTGCTCATATCATGCAAATTATCACTAGTAGGAGAGCAGAGAGTGG AAATGTTCCAGGTATAAAGACCCACAAGATAAAGAAGCTCAGAG
CCR4	NM_005508.4	35-135	GGTCCTTCTTAGCATCGTGCTTCCTGAGCAAGCCTGGCATTGCCTCACAGACCTT CCTCAGAGCCGCTTTCAGAAAAGCAAGCTGCTTCTGGTTGGGCCC
CCR5	NM_000579.1	2730-2830	TAGGAACATACTTCAGCTCACACATGAGATCTAGGTGAGGATTGATTACCTAGTAG TCATTTCATGGGTTGTTGGGAGGATTCTATGAGGCAACCACAGG
CCR6	NM_031409.2	935-1035	CTTTAACTGCGGGATGCTGCTCCTGACTTGCATTAGCATGGACCGGTACATCGCC ATTGTACAGGCGACTAAGTCATTCCGGCTCCGATCCAGAACACTA
CCR7	NM_001838.2	1610-1710	TTCCGAAAACCAGGCCTTATCTCCAAGACCAGAGATAGTGGGGAGACTTCTTGGC TTGGTGAGGAAAAGCGGACATCAGCTGGTCAAACAAACTCTCTGA
CD160	NM_007053.2	500-600	TTGATGTTCACCATAAGCCAAGTCACACCGTTGCACAGTGGGACCTACCAGTGTT GTGCCAGAAGCCAGAAGTCAGGTATCCGCCTTCAGGGCCATTTTT
CD19	NM_001770.4	1770-1870	AGATTCACACCTGACTCTGAAATCTGAAGACCTCGAGCAGATGATGCCAACCTCT GGAGCAATGTTGCTTAGGATGTGTGCATGTGTGTAAGTGTGTGTG
CD19R-scfv	SCFV013.1	204-304	GGCACCGACTACAGCCTGACCATCTCCAACCTGGAGCAGGAGGACATCGCCACC TACTTTTGCCAGCAGGGCAACACACTGCCCTACACCTTTGGCGGCG

CD19RCD28	MDA_00002.1	2-102	CAGGTGTTCCTGAAGATGAACAGCCTGCAGACCGACGACACCGCCATCTACTACT GTGCCAAGCACTACTACTACGGCGGCAGCTACGCCATGGACTACT
CD2	NM_001767.2	1400-1500	TGGGTCTCACTACAAGCAGCCTATCTGCTTAAGAGACTCTGGAGTTTCTTATGTGC CCTGGTGGACACTTGCCCACCATCCTGTGAGTAAAAGTGAAATA
CD20-scfv (rutuximab)	SCFV002.1	8-108	GCTGTCCCAGAGCCCCGCCATCCTGAGCGCCAGCCCTGGCGAGAAGGTGACCA TGACCTGCCGGGCCAGCAGCTCTGTGAGCTACATGCACTGGTATCAG
CD226	NM_006566.2	163-263	TAAACAGGATACGATAAAAGTCCTTAACCAAGACGCAGATGGGAAGAAGCGTTAG AGCGAGCAGCACTCACATCTCAAGAACCAGCCTTTCAAACAGTTT
CD244	NM_016382.2	1150-1250	AAGAGGAACCACAGCCCTTCCTTCAATAGCACTATCTATGAAGTGATTGGAAAGA GTCAACCTAAAGCCCAGAACCCTGCTCGATTGAGCCGCAAAGAGC
CD247	NM_198053.1	1490-1590	TGGCAGGACAGGAAAAACCCGTCAATGTACTAGGATACTGCTGCGTCATTACAGG GCACAGGCCATGGATGGAAAACGCTCTCTGCTCTGCTTTTTTTCT
CD27	NM_001242.4	330-430	CCAGATGTGTGAGCCAGGAACATTCCTCGTGAAGGACTGTGACCAGCATAGAAA GGCTGCTCAGTGTGATCCTTGCATACCGGGGGTCTCCTTCTCTCCT
CD274	NM_014143.2	684-784	TAGGAGATTAGATCCTGAGGAAAACCATACAGCTGAATTGGTCATCCCAGAACTA CCTCTGGCACATCCTCCAAATGAAAGGACTCACTTGGTAATTCTG
CD276	NM_001024736.1	2120-2220	ACATTTCTTAGGGACACAGTACACTGACCACATCACCACCCTCTTCTTCCAGTGCT GCGTGGACCATCTGGCTGCCTTTTTTCTCCAAAAGATGCAATAT
CD28	NM_006139.1	305-405	GCTTGTAGCGTACGACAATGCGGTCAACCTTAGCTGCAAGTATTCCTACAATCTCT TCTCAAGGGAGTTCCGGGCATCCCTTCACAAAGGACTGGATAGT
CD300A	NM_007261.2	0-100	CGGGGAAGTGAGAGTCGGGGATCAGTCCTGCAAGCTACGGAGTCACTACAGGGA GAGGTCTCATCACTAGAAATAGCCGAAGAACCTGCAGCCTCAACCA
CD38	NM_001775.2	1035-1135	CCTTGACTCCTTGTGGTTTATGTCATCATACATGACTCAGCATACCTGCTGGTGCA GAGCTGAAGATTTTGGAGGGTCCTCCACAATAAGGTCAATGCCA
CD3D	NM_000732.4	110-210	TATCTACTGGATGAGTTCCGCTGGGAGATGGAACATAGCACGTTTCTCTCTGGCC TGGTACTGGCTACCCTTCTCTCGCAAGTGAGCCCCTTCAAGATAC
CD3E	NM_000733.2	75-175	AAGTAACAGTCCCATGAAACAAAGATGCAGTCGGGCACTCACTGGAGAGTTCTGG GCCTCTGCCTCTTATCAGTTGGCGTTTGGGGGCAAGATGGTAATG
CD4	NM_000616.3	835-935	AGACATCGTGGTGCTAGCTTTCCAGAAGGCCTCCAGCATAGTCTATAAGAAAGAG GGGGAACAGGTGGAGTTCTCCTTCCCACTCGCCTTTACAGTTGAA
CD40LG	NM_000074.2	1225-1325	GCATTTGATTTATCAGTGAAGATGCAGAAGGGAAATGGGGAGCCTCAGCTCACAT TCAGTTATGGTTGACTCTGGGTTCCTATGGCCTTGTTGGAGGGGG
CD44	NM_000610.3	2460-2560	GTGGGCAGAAGAAAAAGCTAGTGATCAACAGTGGCAATGGAGCTGTGGAGGACA GAAAGCCAAGTGGACTCAACGGAGAGGCCAGCAAGTCTCAGGAAAT
CD45R-scfv	SCFV006.1	222-322	TTCACCCTGAACATCCACCCCGTGGAGGAAGAGGACGCCGCCACCTACTACTGC CAGCACAGCAGAGAGCTGCCCTTCACCTTCGGCTCCGGCACCAAGC
CD47	NM_001777.3	897-997	GCCATATTGGTTATTCAGGTGATAGCCTATATCCTCGCTGTGGTTGGACTGAGTCT CTGTATTGCGGCGTGTATACCAATGCATGGCCCTCTTCTGATTT
CD56R-scfv	SCFV008.1	197-297	ATTCAGCGGCTCTGGCTCCGGCACCGACTTCACTCTGATGATCTCTCGGGTGGA GGCCGAGGACCTGGGCGTGTACTACTGCTTTCAGGGCAGCCACGTG
CD58	NM_001779.2	478-578	GTGCTTGAGTCTCTTCCATCTCCCACACTAACTTGTGCATTGACTAATGGAAGCAT TGAAGTCCAATGCATGATACCAGAGCATTACAACAGCCATCGAG
CD63	NM_001780.4	350-450	GTCATCATCGCAGTGGGTGTCTTCCTCTTCCTGGTGGCTTTTGTGGGCTGCTGCG GGGCCTGCAAGGAGAACTATTGTCTTATGATCACGTTTGCCATCT
CD69	NM_001781.1	460-560	AGGACATGAACTTTCTAAAACGATACGCAGGTAGAGAGGAACACTGGGTTGGACT GAAAAAGGAACCTGGTCACCCATGGAAGTGGTCAAATGGCAAAGA
CD7	NM_006137.6	440-540	CCTACACCTGCCAGGCCATCACGGAGGTCAATGTCTACGGCTCCGGCACCCTGG TCCTGGTGACAGAGGAACAGTCCCAAGGATGGCACAGATGCTCGGA
CD80	NM_005191.3	1288-1388	AAAGATCTGAAGGTCCCACCTCCATTTGCAATTGACCTCTTCTGGGAACTTCCTCA GATGGACAAGATTACCCCACCTTGCCCTTTACGTATCTGCTCTT
CD86	NM_006889.3	146-246	TATGGGACTGAGTAACATTCTCTTTGTGATGGCCTTCCTGCTCTCTGGTGCTGCTC CTCTGAAGATTCAAGCTTATTTCAATGAGACTGCAGACCTGCCA
CD8A	NM_001768.5	1320-1420	GCTCAGGGCTCTTTCCTCCACACCATTCAGGTCTTTCTTTCCGAGGCCCCTGTCT CAGGGTGAGGTGCTTGAGTCTCCAACGGCAAGGGAACAAGTACTT
CDH1	NM_004360.2	1230-1330	CGATAATCCTCCGATCTTCAATCCCACCACGTACAAGGGTCAGGTGCCTGAGAAC GAGGCTAACGTCGTAATCACCACACTGAAAGTGACTGATGCTGAT
CDK2	NM_001798.2	220-320	TCGCTGGCGCTTCATGGAGAACTTCCAAAAGGTGGAAAAGATCGGAGAGGGCAC GTACGGAGTTGTGTACAAAGCCAGAAACAAGTTGACGGGAGAGGTG
CDK4	NM_000075.2	1055-1155	ACTTTTAACCCACACAAGCGAATCTCTGCCTTTCGAGCTCTGCAGCACTCTTATCT ACATAAGGATGAAGGTAATCCGGAGTGAGCAATGGAGTGGCTGC
CDKN1A	NM_000389.2	1975-2075	CATGTGTCCTGGTTCCCGTTTCTCCACCTAGACTGTAAACCTCTCGAGGGCAGGG ACCACACCCTGTACTGTTCTGTGTCTTTCACAGCTCCTCCCACAA
CDKN1B	NM_004064.2	365-465	GCTTCCGAGAGGGGTTCGGGCCGCGTAGGGGCGCTTTGTTTTGTTCGGTTTTGT TTTTTTGAGAGTGCGAGAGAGGCGGTCGTGCAGACCCGGGAGAAAG
CDKN2A	NM_000077.3	975-1075	AAGCGCACATTCATGTGGGCATTTCTTGCGAGCCTCGCAGCCTCCGGAAGCTGT CGACTTCATGACAAGCATTTTGTGAACTAGGGAAGCTCAGGGGGGT
CDKN2C	NM_001262.2	1295-1395	ATAATGTAAACGTCAATGCACAAAATGGATTTGGAAGGACTGCGCTGCAGGTTAT GAAACTTGGAAATCCCGAGATTGCCAGGAGACTGCTACTTAGAGG
CEBPA	NM_004364.2	1320-1420	GAGCTGGGAGCCCGGCAACTCTAGTATTTAGGATAACCTTGTGCCTTGGAAATGC AAACTCACCGCTCCAATGCCTACTGAGTAGGGGGAGCAAATCGTG

CFLAR	NM_003879.3	445-545	CAAGACCCTTGTGAGCTTCCCTAGTCTAAGAGTAGGATGTCTGCTGAAGTCATCC ATCAGGTTGAAGAAGCACTTGATACAGATGAGAAGGAGATGCTGC
CFLAR	NM_001127183.1	653-753	TAGAGTGCTGATGGCAGAGATTGGTGAGGATTTGGATAAATCTGATGTGTCCTCA TTAATTTTCCTCATGAAGGATTACATGGGCCGAGGCAAGATAAGC
CHPT1	NM_020244.2	1303-1403	GATATGGTGATATACTTTAGTGCTTTGTGCCTGCAAATTTCAAGACACCTTCATCT AAATATATTCAAGACTGCATGTCATCAAGCACCTGAACAGGTTC
CIITA	NM_000246.3	470-570	GCCTGAGCAAGGACATTTTCAAGCACATAGGACCAGATGAAGTGATCGGTGAGA GTATGGAGATGCCAGCAGAAGTTGGGCAGAAAAGTCAGAAAAGACC
CITED2	NM_006079.3	965-1065	AGGAGCTGCCCGAACTCTGGCTGGGGCAAAACGAGTTTGATTTTATGACGGACTT CGTGTGCAAACAGCAGCCCAGCAGAGTGAGCTGTTGACTCGATCG
CLIC1	NM_001288.4	310-410	GTGATGGGGCCAAGATTGGGAACTGCCCATTCTCCCAGAGACTGTTCATGGTACT GTGGCTCAAGGGAGTCACCTTCAATGTTACCACCGTTGACACCAA
CLNK	NM_052964.2	1108-1208	GAAGGAGAACAAGGATGGTAGTTTCTTGGTCCGAGATTGTTCCACAAAATCCAAG GAAGAGCCCTATGTTTTGGCTGTGTTTTATGAGAACAAAGTCTAC
c-MET-scfv	SCFV004.1	138-238	CTGATCTACGCCGCCAGCAGCCTGAAGAGCGGCGTGCCCAGCCGGTTTAGCGG CTCTGGCTCTGGCGCCGACTTCACCCTGACCATCAGCAGCCTGCAGC
CREB1	NM_004379.3	4855-4955	TTTGATGGTAGGTCAGCAGCAGTGCTAGTCTCTGAAAGCACAATACCAGTCAGGC AGCCTATCCCATCAGATGTCATCTGGCTGAAGTTTATCTCTGTCT
CREM	NM_001881.2	260-360	CTCCACCTCCTCGCGTCCGTAATCAGTGACGAGGTCCGCTACGTAAATCCCTTTG CGGCGGACAAATGACCATGGAAACAGTTGAATCCCAGCATGATGG
CRIP1	NM_001311.4	269-369	CAACCACCCCTGCTACGCAGCCATGTTTGGGCCTAAAGGCTTTGGGCGGGGCGG AGCCGAGAGCCACACTTTCAAGTAAACCAGGTGGTGGAGACCCCAT
CRLF2	NM_022148.2	1420-1520	CAAGGCAGCACGTCCAAAATGCTGTAAAACCATCTTCCCACTCTGTGAGTCCCCA GTTCCGTCCATGTACCTGTTCCATAGCATTGGATTCTCGGAGGAT
CSAD	NM_015989.4	205-305	TCAAATTCTTCTGCCTAGCCTTAGCCATTAGAGAGAGGTCCTGCTAAAGATGGACT GCAAATGCGCTTGATGGAAGGAGATGTCAATTCCACTGAAGTCC
CSF2	NM_000758.2	475-575	AGATGAGGCTGGCCAAGCCGGGGAGCTGCTCTCTCATGAAACAAGAGCTAGAAA CTCAGGATGGTCATCTTGGAGGGACCAAGGGGTGGGCCACAGCCAT
CSNK2A1	NM_177559.2	1930-2030	CCATTCCCACCATTGTTCCTCCACCGTCCCACACTTTAGGGGGTTGGTATCTCGT GCTCTTCTCCAGAGATTACAAAAATGTAGCTTCTCAGGGGAGGCA
CTGF	NM_001901.2	1100-1200	ACCACCCTGCCGGTGGAGTTCAAGTGCCCTGACGGCGAGGTCATGAAGAAGAAC ATGATGTTCATCAAGACCTGTGCCTGCCATTACAACTGTCCCGGAG
CTLA4	NM_005214.3	405-505	AGTCTGTGCGGCAACCTACATGATGGGGAATGAGTTGACCTTCCTAGATGATTCC ATCTGCACGGGCACCTCCAGTGGAAATCAAGTGAACCTCACTATC
CTNNA1	NM_001903.2	75-175	TCGCCCAGCTAGCCGCAGAAATGACTGCTGTCCATGCAGGCAACATAAACTTCAA GTGGGATCCTAAAAGTCTAGAGATCAGGACTCTGGCAGTTGAGAG
CTNNB1	NM_001098210.1	1815-1915	TCTTGCCCTTTGTCCCGCAAATCATGCACCTTTGCGTGAGCAGGGTGCCATTCCA CGACTAGTTCAGTTGCTTGTTCGTGCACATCAGGATACCCAGCGC
CTNNBL1	NM_030877.3	855-955	TGATGCCAACAAACTGTATTGCAGTGAAGTGCTGGCCATATTGCTCCAGGACAAT GATGAAAACAGGGAATTGCTTGGGGAGCTGGATGGAATCGATGTG
CTSC	NM_001114173.1	260-360	TGCTCGGTTATGGGACCACAAGAAAAAAAAGTAGTGGTGTACCTTCAGAAGCTGG ATACAGCATATGATGACCTTGGCAATTCTGGCCATTTCACCATCA
CTSD	NM_001909.3	1495-1595	GAAGCCGGCGGCCCAAGCCCGACTTGCTGTTTTGTTCTGTGGTTTTCCCCTCCCT GGGTTCAGAAATGCTGCCTGCCTGTCTGTCTCTCCATCTGTTTGG
CX3CL1	NM_002996.3	140-240	AGCACCACGGTGTGACGAAATGCAACATCACGTGCAGCAAGATGACATCAAAGAT ACCTGTAGCTTTGCTCATCCACTATCAACAGAACCAGGCATCATG
CX3CR1	NM_001337.3	1040-1140	GGGCGCTCAGTCCACGTTGATTTCTCCTCATCTGAATCACAAAGGAGCAGGCATG GAAGTGTTCTGAGCAGCAATTTTACTTACCACACGAGTGATGGAG
CXCL10	NM_001565.1	40-140	GCAGAGGAACCTCCAGTCTCAGCACCATGAATCAAACTGCGATTCTGATTTGCTG CCTTATCTTTCTGACTCTAAGTGGCATTCAAGGAGTACCTCTCTC
CXCL12	NM_199168.2	505-605	GGGCCTGAGGTTTGCCAGCATTTAGACCCTGCATTTATAGCATACGGTATGATATT GCAGCTTATATTCATCCATGCCCTGTACCTGTGCACGTTGGAAC
CXCL9	NM_002416.1	1975-2075	CACCATCTCCCATGAAGAAAGGGAACGGTGAAGTACTAAGCGCTAGAGGAAGCA GCCAAGTCGGTTAGTGGAAGCATGATTGGTGCCCAGTTAGCCTCTG
CXCR1	NM_000634.2	1950-2050	GCAGCCACCAGTCCATTGGGCAGGCAGATGTTCCTAATAAAGCTTCTGTTCCGTG CTTGTCCCTGTGGAAGTATCTTGGTTGTGACAGAGTCAAGGGTGT
CXCR3	NM_001504.1	80-180	GTGAGTGACCACCAAGTGCTAAATGACGCCGAGGTTGCCGCCCTCCTGGAGAAC TTCAGCTCTTCCTATGACTATGGAGAAAACGAGAGTGACTCGTGCT
CXCR4	NM_001008540.1	135-235	GTCACTATGGGAAAAGATGGGGAGGAGAGTTGTAGGATTCTACATTAATTCTCTT GTGCCCTTAGCCCACTACTTCAGAATTTCCTGAAGAAAGCAAGCC
DAPL1	NM_001017920.2	190-290	CGAGAAAACAAGTGCCATTGCAAATGTTGCCAAAATACAGACACTGGATGCCCTG AATGACGCACTGGAGAAGCTCAACTATAAATTTCCAGCAACAGTG
DEC1	NM_017418.2	190-290	AGGCCTTACTTTCCAGATCCAGATCCTTGTGCATACAACTGACTTGTGTGGGTGA GGCTTGCAGAAAAAATCAGCTAGAACAGCCTTGGGGGTAGTGGCA
DECTIN-1R	SCFV010.1	270-370	CTGAAGATCGACAGCAGCAACGAGCTGGGCTTCATCGTGAAGCAGGTGTCCAGC CAGCCCGACAACTCCTTCTGGATCGGCCTGAGCAGGCCCCAGACCG
DGKA	NM_001345.4	1375-1475	TTCCTAACACCCACCCACTTCTCGTCTTTGTCAATCCTAAGAGTGGCGGGAAGCA GGGGCAAAGGGTGCTCTGGAAGTTCCAGTATATATTAAACCCTCG
DOCK5	NM_024940.6	630-730	TGCGAGATGACAATGGGAACATCCTAGACCCTGACGAAACCAGCACCATTGCCCT CTTCAAGGCCCATGAGGTGGCCTCCAAAAGGATTGAGGAAAAGAT

DOK2	NM_003974.2	650-750	GCCAGGGACCCAGCTGTACGACTGGCCCTACAGGTTTCTGCGGCGCTTTGGGCG GGACAAGGTAACCTTTTCCTTTGAGGCAGGCCGTCGCTGCGTCTCT
DPP4	NM_001935.3	2700-2800	CAGCAGTCAGCTCAGATCTCCAAAGCCCTGGTCGATGTTGGAGTGGATTTCCAGG CAATGTGGTATACTGATGAAGACCATGGAATAGCTAGCAGCACAG
DUSP16	NM_030640.2	615-715	ATGGGTTTAACTCTCCTTTTGCCAGTCACCACCAGCCTGACCTCATACACTTTTAG TACAATGGAGTGGCTGAGCCTTTGAGCACACCACCATTACATCA
EGFR-scfv_ (NIMO CAR)	SCFV015.1	7-107	AGATGACCCAGAGCCCTAGCAGCCTGAGCGCCAGCGTGGGCGACAGAGTGACC ATCACCTGCCGGTCCAGCCAGAACATCGTGCACAGCAACGGCAACAC
EGLN1	NM_022051.1	3975-4075	AGCAGCATGGACGACCTGATACGCCACTGTAACGGGAAGCTGGGCAGCTACAAA ATCAATGGCCGGACGAAAGCCATGGT
EGLN3	NM_022073.3	800-900	AAGCTACATGGTGGGATCCTGCGGATATTTCCAGAGGGGAAATCATTCATAGCAG ATGTGGAGCCCATTTTTGACAGACTCCTGTTCTTCTGGTCAGATC
EIF1	NM_005801.3	869-969	CCTGAACAGTCCTCGGTGAATCTGAGAGGAGAGGATGGGGTAAGGCAGAAGCAC CAGCTGTACTACTAGAAGGGAGCTTTTGGTGGTAGATCCCCTGGTG
ELF4	NM_001421.3	335-435	AGCTCTGGAGGGCTCTGATAATCCCGTTGTCAGCTCTCTGAAAAGACAGCATGGC TATTACCCTACAGCCCAGTGACCTGATCTTTGAGTTCGCAAGCAA
ELOF1	NM_032377.3	125-225	AGACCCAGTTCACCTGCCCCTTCTGCAACCACGAGAAATCCTGTGATGTGAAAAT GGACCGTGCCCGCAACACCGGAGTCATCTCTTGTACCGTGTGCCT
ENTPD1	NM_001776.4	225-325	TTCGAGTAACTTTAGGAAAATGAGCTGCTGGACTCCTCAGTCAATCTGTCCTTTCT AGTCAATGAAAAAGACAGGGTTTGAGGTTCCTTCCGAAACGGGG
EOMES	NM_005442.2	1670-1770	ATCCCATGCCCTGGGGTATTACCCAGACCCAACCTTTCCTGCAATGGCAGGGTG GGGAGGTCGAGGTTCTTACCAGAGGAAGATGGCAGCTGGACTACCA
EPHA2	NM_004431.2	1525-1625	GAGCCGAGTGTGGAAGTACGAGGTCACTTACCGCAAGAAGGGAGACTCCAACAG CTACAATGTGCGCCGCACCGAGGGTTTCTCCGTGACCCTGGACGAC
EPHA4	NM_004438.3	20-120	GCAGCGTTGGCACCGGCGAACCATGGCTGGGATTTTCTATTTCGCCCTATTTTCG TGTCTCTTCGGGATTTGCGACGCTGTCACAGGTTCCAGGGTATAC
EPHB2	NM_017449.2	785-885	CAAAGCAGGCTTCGAGGCCGTTGAGAATGGCACCGTCTGCCGAGGTTGTCCATC TGGGACTTTCAAGGCCAACCAAGGGGATGAGGCCTGTACCCACTGT
ETV6	NM_001987.4	3840-3940	GTATGAATATGAAATCAGAGACCAGGGCATGATGTTGCTAGGATTAGAGCCTCTC AGTCTGGCCTCTTCACCCAAGTGCAAGAACTCAGTCTCTTACTGT
FADD	NM_003824.2	1560-1660	TGAGACTGCTAAGTAGGGGCAGTGATGGTTGCCAGGACGAATTGAGATAATATCT GTGAGGTGCTGATGAGTGATTGACACACAGCACTCTCTAAATCTT
FAM129A	NM_052966.2	3526-3626	TGCCCAATAGATTCAAGAGAAGCTAAGCGGAAATGGAGGGTGGAAGGTGTGATC TGTGGGACTGTCTGGGCCTGTTACTCATCCTGCTATCAATTTCTTA
FANCC	NM_000136.2	2130-2230	GACTCAGTCAGACATGTTCACTAATGACTCAAGTGAGCCTTCGGTACTCCTGGTG CCCGCCCGGCCAGACCGTCAGCTTGATAATTACTAAAGCAAAGGC
FAS	NM_000043.3	90-190	CACCGGGGCTTTTCGTGAGCTCGTCTCTGATCTCGCGCAAGAGTGACACACAGG TGTTCAAAGACGCTTCTGGGGAGTGAGGGAAGCGGTTTACGAGTGA
FASLG	NM_000639.1	625-725	TCCATGCCTCTGGAATGGGAAGACACCTATGGAATTGTCCTGCTTTCTGGAGTGA AGTATAAGAAGGGTGGCCTTGTGATCAATGAAACTGGGCTGTACT
FCGR3B	NM_000570.3	73-173	CCTATTCCTGTTCTATGGTGGGGCTCCATTGCGAGACTTCAGATTGAGAAATCAG ATGAAGTTTCAAGAAAAGGAAACTGGCAGGTGACAGAGATGGGTG
FGL2	NM_006682.2	250-350	CAATTCAGCAGGATCGAGGAGGTGTTCAAAGAAGTCCAAAACCTCAAGGAAATCG TAAATAGTCTAAAGAAATCTTGCCAAGACTGCAAGCTGCAGGCTG
FLT1	NM_002019.2	5615-5715	TTCAACTGCTTTGAAACTTGCCTGGGGTCTGAGCATGATGGGAATAGGGAGACAG GGTAGGAAAGGGCGCCTACTCTTCAGGGTCTAAAGATCAAGTGGG
FLT3LG	NM_001459.2	927-1027	CCTCCCCAGAATGGAGGCAACGCCAGAATCCAGCACCGGCCCCATTTACCCAAC TCTGTACAAAGCCCTTGTCCCCATGAAATTGTATATAAATCATCCT
FOS	NM_005252.2	1475-1575	ACTCAAGTCCTTACCTCTTCCGGAGATGTAGCAAAACGCATGGAGTGTGTATTGTT CCCAGTGACACTTCAGAGAGCTGGTAGTTAGTAGCATGTTGAGC
FOXO1	NM_002015.3	1526-1626	TCTCATCACCAACATCATTAACTGTTTCGACCCAGTCCTCACCTGGCACCATGATG CAGCAGACGCCGTGCTACTCGTTTGCGCCACCAAACACCAGTTT
FOXO3	NM_001455.2	1860-1960	CCGGAACGTGATGCTTCGCAATGATCCGATGATGTCCTTTGCTGCCCAGCCTAAC CAGGGAAGTTTGGTCAATCAGAACTTGCTCCACCACCAGCACCAA
FOXP1	NM_032682.5	6758-6858	CCTGAAAATCAGATTTACAATGCTGAAGGCATTTCTTGGGCCCAGTGTAGCTCAC GCAATCTCTGCTACCCATAAGCCTTGATGAAGATGATACAGTCCG
FOXP3	NM_014009.3	1230-1330	GGGCCATCCTGGAGGCTCCAGAGAAGCAGCGGACACTCAATGAGATCTACCACT GGTTCACACGCATGTTTGCCTTCTTCAGAAACCATCCTGCCACCTG
FYN	NM_002037.3	765-865	GTCTTTGGAGGTGTGAACTCTTCGTCTCATACGGGGACCTTGCGTACGAGAGGA GGAACAGGAGTGACACTCTTTGTGGCCCTTTATGACTATGAAGCAC
FZD1	NM_003505.1	2430-2530	GTGCCAATCCTGACATCTCGAGGTTTCCTCACTAGACAACTCTCTTTCGCAGGCT CCTTTGAACAACTCAGCTCCTGCAAAAGCTTCCGTCCCTGAGGCA
G6PD	NM_000402.2	1155-1255	ACAACATCGCCTGCGTTATCCTCACCTTCAAGGAGCCCTTTGGCACTGAGGGTCG CGGGGGCTATTTCGATGAATTTGGGATCATCCGGGACGTGATGCA
GABPA	NM_002040.3	1160-1260	GACCAAGTCCTGCATTGGGTGGTTTGGGTAATGAAGGAATTCAGCATGACCGATA TAGACCTCACCACACTCAACATTTCGGGGAGAGAATTATGTAGTC
GADD45A	NM_001924.2	865-965	GTTACTCCCTACACTGATGCAAGGATTACAGAAACTGATGCCAAGGGGCTGAGTG AGTTCAACTACATGTTCTGGGGGCCCGGAGATAGATGACTTTGCA
GADD45B	NM_015675.2	365-465	TGTGGACCCAGACAGCGTGGTCCTCTGCCTCTTGGCCATTGACGAGGAGGAGGA GGATGACATCGCCCTGCAAATCCACTTCACGCTCATCCAGTCCTTC

GAL3ST4	NM_024637.4	1140-1240	CGAGCCCAAACCCTCAATCCCAATGCCCTCATCCATCCTGTTTCCACTGTTACTGA TCATCGCAGCCAGATATCAAGCCCTGCCTCTTTCGATTTGGGGT
GAS2	NM_005256.3	915-1015	GATCTCCCGTGTGGATGGCAAAACATCCCCTATCCAAAGCAAATCTCCAACTCTA AAGGACATGAATCCAGATAACTACTTGGTGGTCTCTGCCAGTTAT
GATA2	NM_032638.3	1495-1595	GAAGAAGGAAGGGATCCAGACTCGGAACCGGAAGATGTCCAACAAGTCCAAGAA GAGCAAGAAAGGGGCGGAGTGCTTCGAGGAGCTGTCAAAGTGCATG
GATA3	NM_001002295.1	2835-2935	AAGAGTCCGGCGGCATCTGTCTTGTCCCTATTCCTGCAGCCTGTGCTGAGGGTA GCAGTGTATGAGCTACCAGCGTGCATGTCAGCGACCCTGGCCCGAC
gBAD-1R-scfv	SCFV001.1	1-101	AGACAGACACCCTGCTCCTCTGGGTGTCCGGCCACCTGTGGCGACATCGTGATGA GCAGAAGCCCCAGCAGCCTGGCCGTGTCCGTGGGCGAGAAAGTGAC
GEMIN2	NM_001009182.1	537-637	ACAAGCAACAGTAACTAGTGTCTTGGAATATCTGAGTAATTGGTTTGGAGAAAGAG ACTTTACTCCAGAATTGGGAAGATGGCTTTATGCTTTATTGGCT
GFI1	NM_005263.2	2235-2335	TCATCACTGGAGGTAAAAGCACAAGCAATGCCTGTGGACAAGATGTCATTCATTC ACTCAGCAAATGTTCATGGATCACCGGCTACCAAGGTACCAGGCA
GLIPR1	NM_006851.2	255-355	CTGCGTTCGAATCCATAACAAGTTCCGATCAGAGGTGAAACCAACAGCCAGTGAT ATGCTATACATGACTTGGGACCCAGCACTAGCCCAAATTGCAAAA
GLO1	NM_006708.1	1240-1340	GGAAATGATATGGTACCCAGACACTGGGCTAGGCTGCAACTTTATCTCATTTAATA CTCCCAGCTGTCATGTGAGAAAGAAAGCAGGCTAGGCATGTGAA
GNLY	NM_006433.2	305-405	CAGGAGCTGGGCCGTGACTACAGGACCTGTCTGACGATAGTCCAAAAACTGAAG AAGATGGTGGATAAGCCCACCCAGAGAAGTGTTTCCAATGCTGCGA
GSK3B	NM_002093.2	925-1025	ACTGATTATACCTCTAGTATAGATGTATGGTCTGCTGGCTGTGTGTTGGCTGAGCT GTTACTAGGACAACCAATATTTCCAGGGGATAGTGGTGTGGATC
GZMA	NM_006144.2	155-255	AGACCCTACATGGTCCTACTTAGTCTTGACAGAAAAACCATCTGTGCTGGGGCTT TGATTGCAAAAGACTGGGTGTTGACTGCAGCTCACTGTAACTTGA
GZMB	NM_004131.3	540-640	ACACTACAAGAGGTGAAGATGACAGTGCAGGAAGATCGAAAGTGCGAATCTGACT TACGCCATTATTACGACAGTACCATTGAGTTGTGCGTGGGGGACC
GZMH	NM_033423.3	705-805	AAAAAAGGGACACCTCCAGGAGTCTACATCAAGGTCTCACACTTCCTGCCCTGGA TAAAGAGAACAATGAAGCGCCTCTAACAGCAGGCATGAGACTAAC
HCST	NM_001007469.1	132-232	ATCCTCTTCCTGCTTTTGCTCCCAGTGGCTGCAGCTCAGACGACTCCAGGAGAGA GATCATCACTCCCTGCCTTTTACCCTGGCACTTCAGGCTCTTGTT
HDAC1	NM_004964.2	785-885	CAAGCCGGTCATGTCCAAAGTAATGGAGATGTTCCAGCCTAGTGCGGTGGTCTTA CAGTGTGGCTCAGACTCCCTATCTGGGGATCGGTTAGGTTGCTTC
HDAC2	NM_001527.1	930-1030	AAGCCTATTATCTCAAAGGTGATGGAGATGTATCAACCTAGTGCTGTGGTATTACA GTGTGGTGCAGACTCATTATCTGGTGATAGACTGGGTTGTTTCA
HER2-scfv	SCFV014.1	64-164	CCTGCAGCGCCAGCAGCAGCGTGTCCTACATGCACTGGTATCAGCAGAAGTCCG GCACTAGCCCCAAGCGGTGGATCTACGACACCTACAAGCTCGCCAG
HERV-K 6H5-scfv	SCFV012.1	137-237	CGGCGGCACCAGCTACAACCAGAAGTTCAAGGACAAGGCCATCCTGACCGTGGA CAAGAGCAGCAGCACCGCCTACATGGAACTGCGGAGCCTGACCAGC
HLA-A	NM_002116.5	1000-1100	GGAAGAGCTCAGATAGAAAAGGAGGGAGTTACACTCAGGCTGCAAGCAGTGACA GTGCCCAGGGCTCTGATGTGTCCCTCACAGCTTGTAAAGTGTGAGA
HMGB2	NM_001130688.1	125-225	CTGTCAACATGGGTAAAGGAGACCCCAACAAGCCGCGGGGCAAAATGTCCTCGT ACGCCTTCTTCGTGCAGACCTGCCGGGAAGAGCACAAGAAGAAACA
HOPX	NM_001145460.1	1117-1217	AACAATAGGAAGCTATGTGTATCTTCTGTGTAAAGCAGTGGCTTCACTGGAAAAAT GGTGTGGCTAGCATTTCCCTTTGAGTCATGATGACAGATGGTGT
HOXA10	NM_018951.3	1503-1603	TTCTATAGAGATAGATATTGTCCTAAGTGTCAAGTCCTGACTGGGCTGGGTTTGCT GTCTTGGGGTCCCACTGCTCGAAATGGCCCCTGTCTTCGGCCGA
HOXA9	NM_152739.3	1015-1115	GGCTCTAAACCTCAGGCCACATCTTTTCCAAGGCAAACCCTGTTCAGGCTGGCTC GTAGGCCTGCCGCTTTGATGGAGGAGGTATTGTAAGCTTTCCATT
HOXB3	NM_002146.4	60-160	TGTCCGTTTAAATGCTGCTGGGAGACTCGTAAAAAAATCATCGTGGACCTGGAGG ATGAGAGGGGCGAGCTTTATTTCGGTCGGATTGCGGTGTGGTGGT
HOXB4	NM_024015.4	1340-1440	CCTTTCTTTGTCCCCCACTCCCGATACCCAGCGAAAGCACCCTCTGACTGCCAGA TAGTGCAGTGTTTTGGTCACGGTAACACACACACACTCTCCCTCA
HPRT1	NM_000194.1	240-340	TGTGATGAAGGAGATGGGAGGCCATCACATTGTAGCCCTCTGTGTGCTCAAGGG GGGCTATAAATTCTTTGCTGACCTGCTGGATTACATCAAAGCACTG
HRH1	NM_000861.2	3055-3155	GTGGCAGCTCAAAATGATATGTTTGAGTAGACGAACAGCTGACATGGAGTTCCCG TGCACCTACGGAAGGGGACGCTTTGAAGGAACCAAGTGCATTTTT
HRH2	NM_022304.1	600-700	GCGGTCCTCATCCTCATCACCGTTGCTGGCAATGTGGTCGTCTGTCTGGCCGTG GGCTTGAACCGCCGGCTCCGCAACCTGACCAATTGTTTCATCGTGT
Human CD19R-scfv	SCFV009.1	215-315	CTTCACCATCAGCAGCCTGCAGCCCGAGGACATCGCCACCTACTACTGCCAGCA GTACCAGAGCCTGCCCTACACCTTCGGCCAGGGCACCAAGCTGCAG
ICOS	NM_012092.2	640-740	AACTCTGGCACCCAGGCATGAAGCACGTTGGCCAGTTTTCCTCAACTTGAAGTGC AAGATTCTCTTATTTCCGGGACCACGGAGAGTCTGACTTAACTAC
ICOSLG	NM_015259.4	1190-1290	CTGCTGGCGTTGGCTGTGATCCTGGAATGAGGCCCTTTCAAAAGCGTCATCCACA CCAAAGGCAAATGTCCCCAAGTGAGTGGGCTCCCCGCTGTCACTG
ID2	NM_002166.4	505-605	CGGATATCAGCATCCTGTCCTTGCAGGCTTCTGAATTCCCTTCTGAGTTAATGTCA AATGACAGCAAAGCACTGTGTGGCTGAATAAGCGGTGTTCATGA
ID3	NM_002167.3	195-295	AGGAAGCCTGTTTGCAATTTAAGCGGGCTGTGAACGCCCAGGGCCGGCGGGGG CAGGGCCGAGGCGGGCCATTTTGAATAAAGAGGCGTGCCTTCCAGGC
IDO1	NM_002164.3	50-150	CTATTATAAGATGCTCTGAAAACTCTTCAGACACTGAGGGGCACCAGAGGAGCAG ACTACAAGAATGGCACACGCTATGGAAAACTCCTGGACAATCAGT

IFNA1	NM_024013.1	585-685	ATCCCTCTCTTTATCAACAAACTTGCAAGAAAGATTAAGGAGGAAGGAATAACATC TGGTCCAACATGAAAACAATTCTTATTGACTCATACACCAGGTC
IFNG	NM_000619.2	970-1070	ATACTATCCAGTTACTGCCGGTTTGAAAATATGCCTGCAATCTGAGCCAGTGCTTT AATGGCATGTCAGACAGAACTTGAATGTGTCAGGTGACCCTGAT
IFNGR1	NM_000416.1	1140-1240	CCCGGGCAGCCATCTGACTCCAATAGAGAGAGAGAGTTCTTCACCTTTAAGTAGT AACCAGTCTGAACCTGGCAGCATCGCTTTAAACTCGTATCACTCC
IGF1R	NM_000875.2	455-555	TCGGGGGGCCATCAGGATTGAGAAAAATGCTGACCTCTGTTACCTCTCCACTGTG GACTGGTCCCTGATCCTGGATGCGGTGTCCAATAACTACATTGTG
IKZF1	NM_006060.3	4485-4585	CCGCTGTGTACTACTGTGTGCCTAGATTCCATGCACTCTCGTTGTGTTTGAAGTAA ATATTGGAGACCGGAGGGTAACAGGTTGGCCTGTTGATTACAGC
IKZF2	NM_001079526.1	945-1045	CCATGTACCTCCTATGGAAGATTGTAAGGAACAAGAGCCTATTATGGACAACAATA TTTCTCTGGTGCCTTTTGAGAGACCTGCTGTCATAGAGAAGCTC
IL10	NM_000572.2	230-330	AAGGATCAGCTGGACAACTTGTTGTTAAAGGAGTCCTTGCTGGAGGACTTTAAGG GTTACCTGGGTTGCCAAGCCTTGTCTGAGATGATCCAGTTTTACC
IL10RA	NM_001558.2	150-250	TGCCCAGCCCTCCGTCTGTGTGGTTTGAAGCAGAATTTTTCCACCACATCCTCCA CTGGACACCCATCCCAAATCAGTCTGAAAGTACCTGCTATGAAGT
IL12A	NM_000882.2	775-875	CTTTCTAGATCAAAACATGCTGGCAGTTATTGATGAGCTGATGCAGGCCCTGAATT TCAACAGTGAGACTGTGCCACAAAAATCCTCCCTTGAAGAACCG
IL12B	NM_002187.2	1435-1535	GCAAGGCTGCAAGTACATCAGTTTTATGACAATCAGGAAGAATGCAGTGTTCTGA TACCAGTGCCATCATACACTTGTGATGGATGGGAACGCAAGAGAT
IL12RB1	NM_005535.1	1292-1392	AGGAAAAGTGTTACTACATTACCATCTTTGCCTCTGCGCACCCCGAGAAGCTCAC CTTGTGGTCTACGGTCCTGTCCACCTACCACTTTGGGGGCAATGC
IL12RB2	NM_001559.2	1315-1415	CCTCCGTGGGACATTAGAATCAAATTTCAAAAGGCTTCTGTGAGCAGATGTACCC TTTATTGGAGAGATGAGGGACTGGTACTGCTTAATCGACTCAGAT
IL13	NM_002188.2	516-616	TTTCTTTCTGATGTCAAAAATGTCTTGGGTAGGCGGGAAGGAGGGTTAGGGAGGG GTAAAATTCCTTAGCTTAGACCTCAGCCTGTGCTGCCCGTCTTCA
IL15	NM_172174.1	1685-1785	AGGGTGATAGTCAAATTATGTATTGGTGGGGCTGGGTACCAATGCTGCAGGTCAA CAGCTATGCTGGTAGGCTCCTGCCAGTGTGGAACCACTGACTACT
IL15RA	NM_002189.2	39-139	CGCTCGCCCGGGGAGTCCAGCGGTGTCCTGTGGAGCTGCCGCCATGGCCCCGC GGCGGGCGCGCGGCTGCCGGACCCTCGGTCTCCCGGCGCTGCTACTG
IL17A	NM_002190.2	240-340	TACTACAACCGATCCACCTCACCTTGGAATCTCCACCGCAATGAGGACCCTGAGA GATATCCCTCTGTGATCTGGGAGGCAAAGTGCCGCCACTTGGGCT
IL17F	NM_052872.3	210-310	GCCCGCCTGTGCCAGGAGGTAGTATGAAGCTTGACATTGGCATCATCAATGAAAA CCAGCGCGTTTCCATGTCACGTAACATCGAGAGCCGCTCCACCTC
IL17RA	NM_014339.4	3020-3120	CTACTATGTGGCGGGCATTTGGGATACCAAGATAAATTGCATGCGGCATGGCCCC AGCCATGAAGGAACTTAACCGCTAGTGCCGAGGACACGTTAAACG
IL18	NM_001562.2	48-148	GACAGTCAGCAAGGAATTGTCTCCCAGTGCATTTTGCCCTCCTGGCTGCCAACTC TGGCTGCTAAAGCGGCTGCCACCTGCTGCAGTCTACACAGCTTCG
IL18R1	NM_003855.2	2025-2125	GAATGAGGGGATTTTAAGTGTCTGAAGAGGCATTTTCTAGGGACCAGTGGGTGAC TGAGTAACTGAAATGCTGCTTTCACTCCCTAACACCATGGATCTG
IL18RAP	NM_003853.2	2412-2512	GCTTGATGGACAATGGAGTGGGATTGAGACTGTGGTTTAGAGCCTTTGATTTCCT GGACTGGACTGACGGCGAGTGAATTCTCTAGACCTTGGGTACTTT
IL1A	NM_000575.3	1085-1185	ACTCCATGAAGGCTGCATGGATCAATCTGTGTCTCTGAGTATCTCTGAAACCTCTA AAACATCCAAGCTTACCTTCAAGGAGAGCATGGTGGTAGTAGCA
IL1B	NM_000576.2	840-940	GGGACCAAAGGCGGCCAGGATATAACTGACTTCACCATGCAATTTGTGTCTTCCT AAAGAGAGCTGTACCCAGAGAGTCCTGTGCTGAATGTGGACTCAA
IL2	NM_000586.2	300-400	AGGATGCAACTCCTGTCTTGCATTGCACTAAGTCTTGCACTTGTCACAAACAGTGC ACCTACTTCAAGTTCTACAAAGAAAACACAGCTACAACTGGAGC
IL21R	NM_021798.2	2080-2180	CGTGTTTGTGGTCAACAGATGACAACAGCCGTCCTCCCTCCTAGGGTCTTGTGTT GCAAGTTGGTCCACAGCATCTCCGGGGCTTTGTGGGATCAGGGCA
IL22	NM_020525.4	319-419	CTATCTGATGAAGCAGGTGCTGAACTTCACCCTTGAAGAAGTGCTGTTCCCTCAA TCTGATAGGTTCCAGCCTTATATGCAGGAGGTGGTGCCCTTCCTG
IL23A	NM_016584.2	411-511	CAGGGACAACAGTCAGTTCTGCTTGCAAAGGATCCACCAGGGTCTGATTTTTTAT GAGAAGCTGCTAGGATCGGATATTTTCACAGGGGAGCCTTCTCTG
IL23R	NM_144701.2	710-810	AACTGCAAATTCACCTGGATGATATAGTGATACCTTCTGCAGCCGTCATTTCCAGG GCTGAGACTATAAATGCTACAGTGCCCAAGACCATAATTTATTG
IL27	NM_145659.3	143-243	CAGGAGCTGCGGAGGGAGTTCACAGTCAGCCTGCATCTCGCCAGGAAGCTGCTC TCCGAGGTTCGGGGCCAGGCCCACCGCTTTGCGGAATCTCACCTGC
IL2RA	NM_000417.1	1000-1100	CTTGGTAAGAAGCCGGGAACAGACAACAGAAGTCATGAAGCCCAAGTGAAATCAA AGGTGCTAAATGGTCGCCCAGGAGACATCCGTTGTGCTTGCCTGC
IL2RB	NM_000878.2	1980-2080	GTCCTGCTGCCCGAGCCAGGAACTGTGTGTGTTGCAGGGGGGCAGTAACTCCCC AACTCCCTCGTTAATCACAGGATCCCACGAATTTAGGCTCAGAAGC
IL2RG	NM_000206.1	595-695	CCACAGCTGGACTGAACAATCAGTGGATTATAGACATAAGTTCTCCTTGCCTAGT GTGGATGGGCAGAAACGCTACACGTTTCGTGTTCGGAGCCGCTTT
IL4	NM_000589.2	625-725	GACACTCGCTGCCTGGGTGCGACTGCACAGCAGTTCCACAGGCACAAGCAGCTG ATCCGATTCCTGAAACGGCTCGACAGGAACCTCTGGGGCCTGGCGG
IL4R	NM_000418.2	705-805	ATCATCTCACCTATGCAGTCAACATTTGGAGTGAAAACGACCCGGCAGATTTCAG AATCTATAACGTGACCTACCTAGAACCCTCCCTCCGCATCGCAGC
IL5	NM_000879.2	105-205	CCACAGAAATTCCCACAAGTGCATTGGTGAAAGAGACCTTGGCACTGCTTTCTAC TCATCGAACTCTGCTGATAGCCAATGAGACTCTGAGGATTCCTGT

IL6	NM_000600.1	220-320	TGACAAACAAATTCGGTACATCCTCGACGGCATCTCAGCCCTGAGAAAGGAGACA TGTAACAAGAGTAACATGTGTGAAAGCAGCAAAGAGGCACTGGCA
IL6R	NM_000565.2	993-1093	CTTTCTACATAGTGTCCATGTGCGTCGCCAGTAGTGTCGGGAGCAAGTTCAGCAA AACTCAAACCTTTCAGGGTTGTGGAATCTTGCAGCCTGATCCGCC
IL7R	NM_002185.2	1610-1710	TTGCTTTGACCACTCTTCCTGAGTTCAGTGGCACTCAACATGAGTCAAGAGCATC CTGCTTCTACCATGTGGATTTGGTCACAAGGTTTAAGGTGACCCA
IL9	NM_000590.1	300-400	AAGTACTAAAGAACAACAAGTGTCCATATTTTTCCTGTGAACAGCCATGCAACCAA ACCACGGCAGGCAACGCGCTGACATTTCTGAAGAGTCTTCTGGA
IRF1	NM_002198.1	510-610	CTGTGCGAGTGTACCGGATGCTTCCACCTCTCACCAAGAACCAGAGAAAAGAAAG AAAGTCGAAGTCCAGCCGAGATGCTAAGAGCAAGGCCAAGAGGAA
IRF2	NM_002199.2	1375-1475	CAGTACCTGGAGCTTCTCTTTAACTCAGGACTCCAGCCCATTGGTAGACGTGTGT TTCTAGAGCCTGCTGGATCTCCCAGGGCTACTCACTCAAGTTCAA
IRF4	NM_002460.1	325-425	GGGCACTGTTTAAAGGAAAGTTCCGAGAAGGCATCGACAAGCCGGACCCTCCCA CCTGGAAGACGCGCCTGCGGTGCGCTTTGAACAAGAGCAATGACTT
ITCH	NM_031483.4	155-255	ACTGTGAGAACTTCAGGTTTTCCAACCTATTGGTGGTATGTCTGACAGTGGATCAC AACTTGGTTCAATGGGTAGCCTCACCATGAAATCACAGCTTCAG
ITGA1	NM_181501.1	1875-1975	AAGTGGCAAGACTATAAGGAAAGAGTATGCACAACGTATTCCATCAGGTGGGGAT GGTAAGACACTGAAATTTTTTGGCCAGTCTATCCACGGAGAAATG
ITGA4	NM_000885.4	975-1075	GCCCACTGCCAACTGGCTCGCCAACGCTTCAGTGATCAATCCCGGGGCGATTTA CAGATGCAGGATCGGAAAGAATCCCGGCCAGACGTGCGAACAGCTC
ITGA5	NM_002205.2	925-1025	AGAAGACTTTGTTGCTGGTGTGCCCAAAGGGAACCTCACTTACGGCTATGTCACC ATCCTTAATGGCTCAGACATTCGATCCCTCTACAACTTCTCAGGG
ITGAL	NM_002209.2	3905-4005	GTGAGGGCTTGTCATTACCAGACGGTTCACCAGCCTCTCTTGGTTTCCTTCCTTG GAAGAGAATGTCTGATCTAAATGTGGAGAAACTGTAGTCTCAGGA
ITGAM	NM_000632.3	515-615	GCCCTCCGAGGGTGTCCTCAAGAGGATAGTGACATTGCCTTCTTGATTGATGGCT CTGGTAGCATCATCCCACATGACTTTCGGCGGATGAAGGAGTTTG
ITGAX	NM_000887.3	700-800	CCCCTCAGCCTGTTGGCTTCTGTTCACCAGCTGCAAGGGTTTACATACACGGCCA CCGCCATCCAAAATGTCGTGCACCGATTGTTCCATGCCTCATATG
ITGB1	NM_033666.2	2000-2100	TTTTAACATTACCAAGGTAGAAAGTCGGGACAAATTACCCCAGCCGGTCCAACCT GATCCTGTGTCCCATTGTAAGGAGAAGGATGTTGACGACTGTTGG
ITGB7	NM_000889.1	1278-1378	CAACGTGGTACAGCTCATCATGGATGCTTATAATAGCCTGTCTTCCACCGTGACC CTTGAACACTCTTCACTCCCTCCTGGGGTCCACATTTCTTACGAA
ITK	NM_005546.3	3430-3530	GCCAGTAAAGAAGTCAGTATAGAACCACTAGCGAATAGTGTTGCTCTGGCACAGA CCACTGTGGTTGATGGCATGGCCCTCCAACTTGGAATAGGATTTT
JAK1	NM_002227.1	285-385	GAGAACACCAAGCTCTGGTATGCTCCAAATCGCACCATCACCGTTGATGACAAGA TGTCCCTCCGGCTCCACTACCGGATGAGGTTCTATTTCACCAATT
JAK2	NM_004972.2	455-555	CTCCTCCCGCGACGGCAAATGTTCTGAAAAAGACTCTGCATGGGAATGGCCTGC CTTACGATGACAGAAATGGAGGGAACATCCACCTCTTCTATATATC
JAK3	NM_000215.2	1715-1815	GTGCTGCTGAAGGTCATGGATGCCAAGCACAAGAACTGCATGGAGTCATTCCTG GAAGCAGCGAGCTTGATGAGCCAAGTGTCGTACCGGCATCTCGTGC
JUN	NM_002228.3	140-240	ACACAGCCAGCCAGCCAGGTCGGCAGTATAGTCCGAACTGCAAATCTTATTTTCT TTTCACCTTCTCTCTAACTGCCCAGAGCTAGCGCCTGTGGCTCCC
JUNB	NM_002229.2	1155-1255	GCGCGCCTGGAGGACAAGGTGAAGACGCTCAAGGCCGAGAACGCGGGGCTGTC GAGTACCGCCGGCCTCCTCCGGGAGCAGGTGGCCCAGCTCAAACAGA
KIR2DL1	NM_014218.2	881-981	GCAGGAAACAGAACAGCGAATAGCGAGGACTCTGATGAACAAGACCCTCAGGAG GTGACATACACACAGTTGAATCACTGCGTTTTCACACAGAGAAAAA
KIR2DL2	NM_014219.2	814-914	TCTCCTTCATCGCTGGTGCTCCAACAAAAAAAATGCTGCGGTAATGGACCAAGAG TCTGCAGGGAACAGAACAGCGAATAGCGAGGACTCTGATGAACAA
KIR2DL3	NM_015868.2	741-841	CTCCGAAACCGGTAACCCCAGACACCTGCATGTTCTGATTGGGACCTCAGTGGTC ATCATCCTCTTCATCCTCCTCCTCTTCTTTCTCCTTCATCGCTGG
KIR2DL4	NM_002255.5	15-115	GCGTCCTGGCAGCAGAAGCTGCACCATGTCCATGTCACCCACGGTCATCATCCT GGCATGTCTTGGGTTCTTCTTGGACCAGAGTGTGTGGGCACACGTG
KIR2DL5A	NM_020535.3	1451-1551	GACACGTGCTGTTCCACCTTCCCTCATGCTGTTTCACCTTTCCTCAGACTATTTTC CAGCCTTCTGTCAGTCAGCAGTGAAACTTATAAAATTTTTTGTG
KIR2DS1	NM_014512.1	698-798	CTTCACCCACTGAACCAAGCTCCGAAACCGGTAACCCCAGACACCTACATGTTCT GATTGGGACCTCAGTGGTCAAAATCCCTTTCACCATCCTCCTCTT
KIR2DS2	NM_012312.2	856-956	CAAGAGCCTGCAGGGAACAGAACAGTGAACAGCGAGGATTCTGATGAACAAGAC CATCAGGAGGTGTCATACGCATAATTGGATCACTGTGTTTTCACAC
KIR2DS3	NM_012313.1	693-793	GGCCTTCACCCACTGAACCAAGCTCCAAAACCGGTAACCCCAGACACCTACACGT TCTGATTGGGACCTCAGTGGTCAAACTCCCTTTCACCATCCTCCT
KIR2DS4	NM_012314.3	1427-1527	ACATACAAGAGGCTGCCTCTTAACACAGCACTTAGACACGTGCTGTTCCACCTCC CTTCAGACTATCTTTCAGCCTTCTGCCAGCAGTAAAACTTATAAA
KIR2DS5	NM_014513.2	204-304	CTTCCTTCTGCACAGAGAGGGGACGTTTAACCACACTTTGCGCCTCATTGGAGAG CACATTGATGGGGTCTCCAAGGGCAACTTCTCCATCGGTCGCATG
KIR3DL1	NM_013289.2	1054-1154	CCAAATCTGGTAACCCCAGACACCTGCACATTCTGATTGGGACCTCAGTGGTCAT CATCCTCTTCATCCTCCTCCTCTTCTTTCTCCTTCATCTCTGGTG
KIR3DL2	NM_006737.2	884-984	TGCCACCCACGGAGGGACCTACAGATGCTTCGGCTCTTTCCGTGCCCTGCCCTG CGTGTGGTCAAACTCAAGTGACCCACTGCTTGTTTCTGTCACAGGA
KIR3DL3	NM_153443.3	508-608	CCTTGCGCCTCGTTGGACAGCTCCACGATGCGGGTTCCCAGGTCAACTATTCCAT GGGTCCCATGACACCTGCCCTTGCAGGGACCTACAGATGCTTTGG

KIR3DS1	NM_001083539.1	1000-1100	CTCCAAATCTGGTAACCTCAGACACCTGCACATTCTGATTGGGACCTCAGTGGTC AAAATCCCTTTCACCATCCTCCTCTTCTTTCTCCTTCATCGCTGG
KIT	NM_000222.1	5-105	CATCGCAGCTACCGCGATGAGAGGCGCTCGCGGCGCCTGGGATTTTCTCTGCGT TCTGCTCCTACTGCTTCGCGTCCAGACAGGCTCTTCTCAACCATCT
KLF10	NM_005655.1	570-670	GCTCAGGCAACAAGTGTGATTCGTCATACAGCTGATGCCCAGCTATGTAACCACC AGACCTGCCCAATGAAAGCAGCCAGCATCCTCAACTATCAGAACA
KLF2	NM_016270.2	1015-1115	GGAAGTTTGCGCGCTCAGACGAGCTCACGCGCCACTACCGAAAGCACACGGGCC ACCGGCCATTCCAGTGCCATCTGTGCGATCGTGCCTTCTCGCGCTC
KLF4	NM_004235.4	1980-2080	CGAGCATTTTCCAGGTCGGACCACCTCGCCTTACACATGAAGAGGCATTTTTAAA TCCCAGACAGTGGATATGACCCACACTGCCAGAAGAGAATTCAGT
KLF6	NM_001008490.1	1165-1265	GGGATGCGTGTTCCAGCCAAAGCATGCCGTTCTGCACCCTACCCAGTTGCCTCC AGGGCCTCTCCTTGGAAGGTCTTTTGAGGGCTAAAAAGGTCCTGTA
KLF7	NM_001270943.1	1546-1646	GTACTATTGAGATCTTTCGCGTCGATCCCAACGGCCTTAGCGGCGGCAGACTGG AATAACACCTTACACCTTTCTGGCCTGCATTTCTGTAGACTTCACT
KLRAP1	NR_028045.1	414-514	CCTTCAGAGTCACAGAATAGATTAAGGCCTGATGATACTCAAAGGCCTGGGAAAA CTGATGACAAAGAATTTTCAGTGCCCTGGCACCTCATTGCAGTGA
KLRB1	NM_002258.2	85-185	TGAGTTAAACTTACCCACAGACTCAGGCCCAGAAAGTTCTTCACCTTCATCTCTTC CTCGGGATGTCTGTCAGGGTTCACCTTGGCATCAATTTGCCCTG
KLRC1	NM_002259.3	335-435	ACCTATCACTGCAAAGATTTACCATCAGCTCCAGAGAAGCTCATTGTTGGGATCCT GGGAATTATCTGTCTTATCTTAATGGCCTCTGTGGTAACGATAG
KLRC2	NM_002260.3	942-1042	TATGTGAGTCAGCTTATAGGAAGTACCAAGAACAGTCAAACCCATGGAGACAGAA AGTAGAATAGTGGTTGCCAATGTCTCAGGGAGGTTGAAATAGGAG
KLRC3	NM_002261.2	760-860	ACTCCTGAGCTCAAGAAATCAACACATCTTGGCCTCCCAAGTTGCTGGGATTACT GACACAAGCCACCGCCCCTGAGTGCTCATGTACCATTTAGCTTGT
KLRC4	NM_013431.2	29-129	TTATATTGGTCAACAGCAAAATGAACATTACTACTCAGCCTCCAACACATGCAGTT TGCCTATACCAGGGATCCTGTCAAAATATACACCACTTATAGCT
KLRD1	NM_002262.3	542-642	AGCCTGCTTCAGCTTCAAAACACAGATGAACTGGATTTTATGAGCTCCAGTCAACA ATTTTACTGGATTGGACTCTCTTACAGTGAGGAGCACACCGCCT
KLRF1	NM_016523.1	275-375	AAAAAGGAAGTTGTTCAAATGCCACTCAGTATGAGGACACTGGAGATCTAAAAGT GAATAATGGCACAAGAAGAAATATAAGTAATAAGGACCTTTGTGC
KLRG1	NM_005810.3	45-145	TGCCTACGGCAACCCAAGCCCAGAATGACTATGGACCACAGCAAAAATCTTCCTC TTCCAGGCCTTCTTGTTCTTGCCTTGTGGCAATAGCTTTGGGGCT
KLRK1	NM_007360.1	760-860	GGACCAGGATTTACTTAAACTGGTGAAGTCATATCATTGGATGGGACTAGTACAC ATTCCAACAAATGGATCTTGGCAGTGGGAAGATGGCTCCATTCTC
LAG3	NM_002286.5	1735-1835	CTTTTGGTGACTGGAGCCTTTGGCTTTCACCTTTGGAGAAGACAGTGGCGACCAA GACGATTTTCTGCCTTAGAGCAAGGGATTCACCCTCCGCAGGCTC
LAIR1	NM_002287.3	1195-1295	GCACCTGAGGGTAGAAAGTCACTCTAGGAAAAGCCTGAAGCAGCCATTTGGAAG GCTTCCTGTTGGATTCCTCTTCATCTAGAAAGCCAGCCAGGCAGCT
LAT	NM_001014987.1	1290-1390	TGTGTAATAGAATAAAGGCCTGCGTGTGTCTGTGTTGAGCGTGCGTCTGTGTGTG CCTGTGTGCGAGTCTGAGTCAGAGATTTGGAGATGTCTCTGTGTG
LAT2	NM_014146.3	1863-1963	TGCAGAGCTGATTAAACAGTGTTGTGACTGTCTCATGGGAAGAGCTGGGGCCCA GAGGGACCTTGAGTCAGAAATGTTGCCAGAAAAAGTATCTCCTCCA
LCK	NM_005356.2	1260-1360	ATTAAGTGGACAGCGCCAGAAGCCATTAACTACGGGACATTCACCATCAAGTCAG ATGTGTGGTCTTTTGGGATCCTGCTGACGGAAATTGTCACCCACG
LDHA	NM_005566.1	985-1085	CAGAATGGAATCTCAGACCTTGTGAAGGTGACTCTGACTTCTGAGGAAGAGGCCC GTTTGAAGAAGAGTGCAGATACACTTTGGGGGATCCAAAAGGAGC
LEF1	NM_016269.3	1165-1265	CCGTCACACATCCCATCAGATGTCAACTCCAAACAAGGCATGTCCAGACATCCTC CAGCTCCTGATATCCCTACTTTTTATCCCTTGTCTCCGGGTGGTG
LGALS1	NM_002305.3	60-160	GGTGCGCCTGCCCGGGAACATCCTCCTGGACTCAATCATGGCTTGTGGTCTGGT CGCCAGCAACCTGAATCTCAAACCTGGAGAGTGCCTTCGAGTGCGA
LGALS3	NM_002306.2	120-220	CAGCCGTCCGGAGCCAGCCAACGAGCGGAAAATGGCAGACAATTTTTCGCTCCA TGATGCGTTATCTGGGTCTGGAAACCCAAACCCTCAAGGATGGCCT
LIFR	NM_002310.3	2995-3095	CCTATTGTCCACCCATCATTGAGGAAGAAATACCAAACCCAGCCGCAGATGAAGC TGGAGGGACTGCACAGGTTATTTACATTGATGTTCAGTCGATGTA
LILRB1	NM_001081637.1	2332-2432	AGCTGAGAAAACTAAGTCAGAAAGTGCATTAAACTGAATCACAATGTAAATATTAC ACATCAAGCGATGAAACTGGAAAACTACAAGCCACGAATGAATG
LOC282997	NR_026932.1	665-765	TGATCACATTCTACCTGGCATTATTTCATCTGAGTCCCTGTCCTAGCCCTTCTGCC CATTAGACTGTAACCTTGTTTAGGGAAAGACCTGTGTCTTACTC
LRP5	NM_002335.1	2515-2615	TGGACACCAACATGATCGAGTCGTCCAACATGCTGGGTCAGGAGCGGGTCGTGA TTGCCGACGATCTCCCGCACCCGTTCGGTCTGACGCAGTACAGCGA
LRP6	NM_002336.1	2185-2285	CTTAGATTATCCAGAAGGCATGGCAGTAGACTGGCTTGGGAAGAACTTGTACTGG GCAGACACAGGAACGAATCGAATTGAGGTGTCAAAGTTGGATGGG
LRRC32	NM_005512.2	3470-3570	CACCCTGGTGTGGGTTCTCCTGTTCTCTCTGTGCTCTTGCATTCTCTCATTCCCTT TTCCTCTATTGAGCAGAGCCTGGAGTTTGAGACTATGGAATCCA
LTA	NM_000595.2	885-985	CTGATCAAGTCACCGGAGCTTTCAAAGAAGGAATTCTAGGCATCCCAGGGGACCA CACCTCCCTGAACCATCCCTGATGTCTGTCTGGCTGAGGATTTCA
LTBR	NM_002342.1	1435-1535	CTAACAGGGGCCCAAGGAACCAATTTATCACCCATGACTGACGGAGTCTGAGAAA AGGCAGAAGAAGGGGGGCACAAGGGCACTTTCTCCCTTGAGGCTG
LYN	NM_002350.1	1285-1385	TCCTGAAGAGCGATGAAGGTGGCAAAGTGCTGCTTCCAAAGCTCATTGACTTTTC TGCTCAGATTGCAGAGGGAATGGCATACATCGAGCGGAAGAACTA

MAD1L1	NM_003550.2	306-406	GAAGACCTGGGGGAAAACACCATGGTTTTATCCACCCTGAGATCTTTGAACAACT TCATCTCTCAGCGTGTGGAGGGAGGCTCTGGACTGGATATTTCTA
MAP2K1	NM_002755.2	970-1070	ACGGAATGGACAGCCGACCTCCCATGGCAATTTTTGAGTTGTTGGATTACATAGT CAACGAGCCTCCTCCAAAACTGCCCAGTGGAGTGTTCAGTCTGGA
MAPK14	NM_001315.1	450-550	TGGGCTCTGGCGCCTATGGCTCTGTGTGTGCTGCTTTTGACACAAAAACGGGGTT ACGTGTGGCAGTGAAGAAGCTCTCCAGACCATTTCAGTCCATCAT
MAPK3	NM_002746.2	580-680	AACGTGCTCCACCGAGATCTAAAGCCCTCCAACCTGCTCATCAACACCACCTGCG ACCTTAAGATTTGTGATTTCGGCCTGGCCCGGATTGCCGATCCTG
MAPK8	NM_139049.1	945-1045	TCTCTGTAGATGAAGCTCTCCAACACCCGTACATCAATGTCTGGTATGATCCTTCT GAAGCAGAAGCTCCACCACCAAAGATCCCTGACAAGCAGTTAGA
MBD2	NM_003927.3	2015-2115	ATTTACATTCAACTCTGATCCCTGGGCCTTAGGTTTGACATGGAGGTGGAGGAAG ATAGCGCATATATTTGCAGTATGAACTATTGCCTCTGGACGTTGT
MCL1	NM_021960.3	1260-1360	GCTGTAACTTCCTAGAGTTGCACCCTAGCAACCTAGCCAGAAAAGCAAGTGGCAA GAGGATTATGGCTAACAAGAATAAATACATGGGAAGAGTGCTCCC
MIF	NM_002415.1	319-419	TCCTACAGCAAGCTGCTGTGCGGCCTGCTGGCCGAGCGCCTGCGCATCAGCCC GGACAGGGTCTACATCAACTATTACGACATGAACGCGGCCAATGTGG
MMP14	NM_004995.2	1470-1570	GACAAGATTGATGCTGCTCTCTTCTGGATGCCCAATGGAAAGACCTACTTCTTCC GTGGAAACAAGTACTACCGTTTCAACGAAGAGCTCAGGGCAGTGG
MPL	NM_005373.2	895-995	CAGTGGCACTTGGACTGCAATGCTTTACCTTGGACCTGAAGAATGTTACCTGTCA ATGGCAGCAACAGGACCATGCTAGCTCCCAAGGCTTCTTCTACCA
MTOR	NM_004958.2	5095-5195	TTAGTGTTGCTCCTGGGAGTTGATCCGTCTCGGCAACTTGACCATCCTCTGCCAA CAGTTCACCCTCAGGTGACCTATGCCTACATGAAAAACATGTGGA
MXD1	NM_002357.2	880-980	GAGAATAAAGCTGCAGGACAGTCACAAGGCGTGTCTTGGTCTCTAAGAGAGTGG GCACTGCGGCTGTCTCCTTGAAGGTTCTCCCTGTTGGTTCTGATTA
MYB	NM_005375.2	3145-3245	AACTGTTGCATGGATCCTGTGTTTGCAACTGGGGAGACAGAAACTGTGGTTGATA GCCAGTCACTGCCTTAAGAACATTTGATGCAAGATGGCCAGCACT
MYC	NM_002467.3	1610-1710	TCGGACACCGAGGAGAATGTCAAGAGGCGAACACACAACGTCTTGGAGCGCCAG AGGAGGAACGAGCTAAAACGGAGCTTTTTTGCCCTGCGTGACCAGA
MYO6	NM_004999.3	6655-6755	AAGTTGGGGAGATGGCACCTTCTCAGAGGATTGTGAAAATATGAGGAAGAAACAA AACAGTGCATGTAGGAGCACAGGGCCACACAAAGGCATTCTATTG
NANOG	NM_024865.2	1100-1200	CTACTCCATGAACATGCAACCTGAAGACGTGTGAAGATGAGTGAAACTGATATTA CTCAATTTCAGTCTGGACACTGGCTGAATCCTTCCTCTCCCCTCC
NBEA	NM_015678.3	8645-8745	CTGAGAGCCCTTGAAGGACCAGAAAACTGCTTATTCCCACGCTTGATATCTGTCT CCAGCGAAGGCCACTGTATCATATACTATGAACGAGGGCGATTCA
NCAM1	NM_000615.5	1620-1720	GGTATTTGCCTATCCCAGTGCCACGATCTCATGGTTTCGGGATGGCCAGCTGCTG CCAAGCTCCAATTACAGCAATATCAAGATCTACAACACCCCCTCT
NCL	NM_005381.2	1492-1592	GAACAGAGATCGATGGGCGATCTATTTCCCTGTACTATACTGGAGAGAAAGGTCA AAATCAAGACTATAGAGGTGGAAAGAATAGCACTTGGAGTGGTGA
NCR1	NM_001145457.1	145-245	TTTCATGGTTCCAAAGGAAAAGCAAGTGACCATCTGTTGCCAGGGAAATTATGGG GCTGTTGAATACCAGCTGCACTTTGAAGGAAGCCTTTTTGCCGTG
NCR2	NM_004828.3	798-898	CTTCAACAGGTCACGGACCTTCCCTGGACCTCAGTTTCCTCACCTGTAGAGAGAG AAATATTATATCACACTGTTGCAAGGACTAAGATAAGCGATGATG
NCR3	NM_147130.1	50-150	GCATCTGTCCTCTCTCCTCAGGGAGGCAAGCATTTGATGCTCGAGGTCCCTGGCA GTTGTGGTCCTTGGCAAGTGATGTGTGAGTCCCGTGTGTCATAGG
NCRNA00185	NR_001544.2	143-243	GAGGCTGTCTGCCAACATCTTTCATCACTCTGCCTGCAACTATGAAAAATTTAGTT CTAAAAAATGCAACCTTGCTAAATTGAGTACTAATAGGATTGGT
NEIL1	NM_024608.2	1675-1775	TTAGCAGGAGGCTCTCCTTGCTTGCACTCACCCTTTCTTATTGTCTTGCCCTGCAT CTGGGGGTCTGAATTTTTGGGAGCAGGCAATATCTGAAGGTGCA
NEIL2	NM_145043.2	2570-2670	GCCCGGTGGTGTGTAGAGAAAAGCTGCTTGTTTACTCCTTAAGTCAATGTATTGG TGACTGTTGATTTGTTGAACAATTCAGGAATCAAGGGCTGTGGAG
NFAT5	NM_173214.1	3290-3390	CCCTGACAACTATTCAAACCCAGGACATCTCACAGCCTGGTACTTTTCCAGCAGTT TCTGCTTCTAGTCAGCTGCCCAACAGCGATGCACTATTGCAGCA
NFATC1	NM_172390.1	2510-2610	CCAGTACCAGCGTTTCACCTACCTTCCCGCCAACGGTAACGCCATCTTTCTAACC GTAAGCCGTGAACATGAGCGCGTGGGGTGCTTTTTCTAAAGACGC
NFATC2	NM_012340.3	1815-1915	GACGGACATTGGAAGAAAGAACACGCGGGTGAGACTGGTTTTCCGAGTTCACAT CCCAGAGTCCAGTGGCAGAATCGTCTCTTTACAGACTGCATCTAAC
NFATC3	NM_004555.2	2190-2290	GTCCTTGAAGTTCCTCCATATCATAACCCAGCAGTTACAGCTGCAGTGCAGGTGC ACTTTTATCTTTGCAATGGCAAGAGGAAAAAAAGCCAGTCTCAAC
NFKB1	NM_001165412.1	2305-2405	CTTGGGTAACTCTGTTTTGCACCTAGCTGCCAAAGAAGGACATGATAAAGTTCTCA GTATCTTACTCAAGCACAAAAAGGCAGCACTACTTCTTGACCAC
NOS2	NM_000625.4	605-705	TTGCCTGGGGTCCATTATGACTCCCAAAAGTTTGACCAGAGGACCCAGGGACAAG CCTACCCCTCCAGATGAGCTTCTACCTCAAGCTATCGAATTTGTC
NOTCH1	NM_017617.3	735-835	CTGCCAGGCTTCACCGGCCAGAACTGTGAGGAAAATATCGACGATTGTCCAGGA AACAACTGCAAGAACGGGGGTGCCTGTGTGGACGGCGTGAACACCT
NR3C1	NM_001018077.1	1665-1765	GCTTTCTCCTCTGGCGGGAGAAGACGATTCATTCCTTTTGGAAGGAAACTCGAAT GAGGACTGCAAGCCTCTCATTTTACCGGACACTAAACCCAAAATT
NR4A1	NM_002135.3	155-255	CGGCCGGGTAGGGTGCAGCCTGAGGCTTGTTCAGCAGAACAGGTGCAAGCCAC ATTGTTGCCAAGACCTGCCTGAAGCCGGATTCTCCCCACTGCCTCCT
NREP	NM_001142474.1	990-1090	AAACTCATTGTTTCCTTGTGGTAAGTGACCGAGATGCTGCCACAGGACCTGAGAC ACTGATGAATGGTGCTATTTTGGACTTTCAACATGCTCCTTGGCG

NRIP1	NM_003489.2	335-435	TGACTCATGGAGAAGAGCTTGGCTCTGATGTGCACCAGGATTCTATTGTTTTAACT TACCTAGAAGGATTACTAATGCATCAGGCAGCAGGGGGATCAGG
NRP1	NM_003873.5	370-470	GCCTCGCTGCTTTCTTTTCTCCAAGACGGGCTGAGGATTGTACAGCTCTAGGCGG AGTTGGGGCTCTTCGGATCGCTTAGATTCTCCTCTTTGCTGCATT
NT5E	NM_002526.2	1214-1314	ATTCGGGTTTTGAAATGGATAAACTCATCGCTCAGAAAGTGAGGGGTGTGGACGT CGTGGTGGGAGGACACTCCAACACATTTCTTTACACAGGCAATCC
OAZ1	NM_004152.2	313-413	GGTGGGCGAGGGAATAGTCAGAGGGATCACAATCTTTCAGCTAACTTATTCTACT CCGATGATCGGCTGAATGTAACAGAGGAACTAACGTCCAACGACA
OPTN	NM_001008211.1	625-725	TGAAGCTAAATAATCAAGCCATGAAAGGGAGATTTGAGGAGCTTTCGGCCTGGAC AGAGAAACAGAAGGAAGAACGCCAGTTTTTTGAGATACAGAGCAA
P2RX7	NM_002562.4	340-440	AGTTGGTGCACAGTGTCTTTGACACCGCAGACTACACCTTCCCTTTGCAGGGGAA CTCTTTCTTCGTGATGACAAACTTTCTCAAAACAGAAGGCCAAGA
PAX5	NM_016734.1	2288-2388	CTCCAAGAGGAGCACACTTTGGGGAGATGTCCTGGTTTCCTGCCTCCATTTCTCT GGGACCGATGCAGTATCAGCAGCTCTTTTCCAGATCAAAGAACTC
PDCD1	NM_005018.1	175-275	CTTCTTCCCAGCCCTGCTCGTGGTGACCGAAGGGGACAACGCCACCTTCACCTG CAGCTTCTCCAACACATCGGAGAGCTTCGTGCTAAACTGGTACCGC
PDCD1LG2	NM_025239.3	235-335	TGTGGAGCTGTGGCAAGTCCTCATATCAAATACAGAACATGATCTTCCTCCTGCTA ATGTTGAGCCTGGAATTGCAGCTTCACCAGATAGCAGCTTTATT
PDE3A	NM_000921.3	3010-3110	CTGGCCAACCTTCAGGAATCCTTCATCTCTCACATTGTGGGGCCTCTGTGCAACT CCTATGATTCAGCAGGACTAATGCCTGGAAAATGGGTGGAAGACA
PDE4A	NM_001111307.1	3855-3955	AATAATGGTGTATACCCTCATTCTCATTCCTGGGCAGCCCTTCCTTCCACCCTGGC ACCAAAATAATTTCTCCTCCATCCGTACCTTGCCTAGCCTCTCC
PDE7A	NM_002604.2	2210-2310	GTAGCTCAACAAGGAATAGAGGGAGGAGTGTAATTTTGGTAGCTGGTGTTGAATA GGGCCTTTGAGAATCAGACTGAACACAGTGAAATATGTGCCCAAA
PDK1	NM_002610.3	1170-1270	TGGATTGCCCATATCACGTCTTTACGCACAATACTTCCAAGGAGACCTGAAGCTG TATTCCCTAGAGGGTTACGGGACAGATGCAGTTATCTACATTAAG
PDXK	NM_003681.3	580-680	TCCCGGAGGACCTCCTTCCCGTCTACAAAGAAAAAGTGGTGCCGCTTGCAGACAT TATCACGCCCAACCAGTTTGAGGCCGAGTTACTGAGTGGCCGGAA
PECAM1	NM_000442.3	1365-1465	ATCTGCACTGCAGGTATTGACAAAGTGGTCAAGAAAAGCAACACAGTCCAGATAG TCGTATGTGAAATGCTCTCCCAGCCCAGGATTTCTTATGATGCCC
PHACTR2	NM_001100164.1	8350-8450	GGCAGAATGCCACTCTACCCTCAGGTCAATTTTATGGTATATGAAAATGCCAGTAA TATTTGTGCCACTTGCCAACTCGGGGGAGGAGGGGCTTTTCCCT
PHC1	NM_004426.2	2905-3005	ATACAGCTCCACCTACACCGGAATTACATGGCATCAACCCTGTGTTCCTGTCCAG TAATCCCAGCCGTTGGAGTGTAGAGGAGGTGTACGAGTTTATTGC
POLR1B	NM_019014.3	3320-3420	GGAGAACTCGGCCTTAGAATACTTTGGTGAGATGTTAAAGGCTGCTGGCTACAAT TTCTATGGCACCGAGAGGTTATATAGTGGCATCAGTGGGCTAGAA
POLR2A	NM_000937.2	3775-3875	TTCCAAGAAGCCAAAGACTCCTTCGCTTACTGTCTTCCTGTTGGGCCAGTCCGCT CGAGATGCTGAGAGAGCCAAGGATATTCTGTGCCGTCTGGAGCAT
POP5	NM_015918.3	560-660	GCTTCAGGCCCACTTGTTGAACAGAACAATCTGGGTAGCAACAGCATCTTCCACA GTTTTCCAAACTGGATAGCTGCCAACCAGCAGACATTACCCACTT
POU5F1	NM_002701.4	1225-1325	AAGTTCTTCATTCACTAAGGAAGGAATTGGGAACACAAAGGGTGGGGGCAGGGG AGTTTGGGGCAACTGGTTGGAGGGAAGGTGAAGTTCAATGATGCTC
PPARA	NM_001001928.2	5220-5320	GGGTGTGTTTGCTATACGAACATAATGGACGTGAAGTGGGGCAGAAACCCAGAA CTCAGCATTCAAGGATGCCCAGGAGAGCTGTCCCTGTTTTAAAGAG
PPP2R1A	NM_014225.3	1440-1540	AACTTAACTCCTTGTGCATGGCCTGGCTTGTGGATCATGTATATGCCATCCGCGA GGCAGCCACCAGCAACCTGAAGAAGCTAGTGGAAAAGTTTGGGAA
PRDM1	NM_182907.1	310-410	CATCCCTGCCAACCAGGAACTTCTTGTGTGGTATTGTCGGGACTTTGCAGAAAGG CTTCACTACCCTTATCCCGGAGAGCTGACAATGATGAATCTCACA
PRF1	NM_005041.3	2120-2220	ACTGTTTTTCAGGGAGGTGGCTGGGTTTACACGCTAATCCCGATTCACCCTGTCC AAACTGCCTAAGCCCTCCGCCATTCTCAAGCCCTGCAGTCACAGC
PRKAA2	NM_006252.2	975-1075	ATAGTGGTGACCCTCAAGACCAGCTTGCAGTGGCTTATCATCTTATCATTGACAAT CGGAGAATAATGAACCAAGCCAGTGAGTTCTACCTCGCCTCTAG
PRKCQ	NM_006257.2	1325-1425	GATGGACGATGATGTTGAGTGCACGATGGTAGAGAAGAGAGTTCTTTCCTTGGCC TGGGAGCATCCGTTTCTGACGCACATGTTTTGTACATTCCAGACC
PROM1	NM_006017.1	925-1025	AGCCTGCGGTCATCTCTCAATGACCCTCTGTGCTTGGTGCATCCATCAAGTGAAA CCTGCAACAGCATCAGATTGTCTCTAAGCCAGCTGAATAGCAACC
PTGER2	NM_000956.2	1410-1510	GTCAGAAGGAGCTACAAAACCTACCCTCAGTGAGCATGGTACTTGGCCTTTGGAG GAACAATCGGCTGCATTGAAGATCCAGCTGCCTATTGATTTAAGC
PTK2	NM_005607.3	1005-1105	GGTTCAAGCTGGATTATTTCAGTGGAACTGGCAATCGGCCCAGAAGAAGGAATCA GTTACCTAACGGACAAGGGCTGCAATCCCACACATCTTGCTGACT
PTPN11	NM_002834.3	4650-4750	TAGTCCCTAGGTTGCTACGGCTTATCATGTGCTTGGTAAAAGGTGATCGCAGGTT CTCAGACGAGTTTACTTTACATGAGATGGAATCAGGCAGAGAGGC
PTPN4	NM_002830.2	705-805	TCGAGGCTTTTTTTCTCCAGCCGAGAGGACGCGGCTGTGATATACGAAGACTTTG TGTGGACAGTAATGACCTCACGTTTCCGATTGCCTGCTGGCAGAA
PTPN6	NM_002831.5	1734-1834	TGGTGCAGACGGAGGCGCAGTACAAGTTCATCTACGTGGCCATCGCCCAGTTCA TTGAAACCACTAAGAAGAAGCTGGAGGTCCTGCAGTCGCAGAAGGG
PTPRK	NM_001135648.1	4315-4415	GTGATCAACCGGATTTTTAGGATATGCAATCTAACAAGACCACAGGAAGGTTATCT GATGGTGCAACAGTTTCAGTACCTAGGATGGGCTTCTCATCGAG
RAB31	NM_006868.3	3800-3900	TTTTGTAAAGAGCTTCCATCTGGGCTGGACCCAGTTCTTGCACATACAAGACACC GCTGCAGTCAGCTAGGACCTTTCCGCCATGTATTCTATTCTGTAG

RAC1	NM_198829.1	1250-1350	AAAGACCTTCGTCTTTGAGAAGACGGTAGCTTCTGCAGTTAGGAGGTGCAGACAC TTGCTCTCCTATGTAGTTCTCAGATGCGTAAAGCAGAACAGCCTC
RAC2	NM_002872.3	1069-1169	GCTGCCACAACTTGTGTACCTTCAGGGATGGGGCTCTTACTCCCTCCTGAGGCCA GCTGCTCTAATATCGATGGTCCTGCTTGCCAGAGAGTTCCTCTAC
RAF1	NM_002880.2	1990-2090	CCTATGGCATCGTATTGTATGAACTGATGACGGGGGAGCTTCCTTATTCTCACATC AACAACCGAGATCAGATCATCTTCATGGTGGGCCGAGGATATGC
RAP1GAP2	NM_015085.4	4140-4240	CCCACGGCTGGAAAGAGGCCTGTACGTTCTGGACGCGTTTTGTTGGCTGGGCTT CTGGAGGCACTGGCAAGGTCAAACTGCATTTCTTTAAGAACAGTTG
RARA	NM_000964.2	115-215	AGCCACCTAGCTGGGGCCCATCTAGGAGTGGCATCTTTTTTGGTGCCCTGAAGG CCAGCTCTGGACCTTCCCAGGAAAAGTGCCAGCTCACAGAACTGCT
RBPMS	NM_001008710.1	842-942	AAACAGCCTGTAGGTTTTGTCAGTTTTGACAGTCGCTCAGAAGCAGAGGCTGCAA AGAATGCTTTGAATGGCATCCGCTTCGATCCTGAAATTCCGCAAA
RHOA	NM_001664.2	1230-1330	GGTACTCTGGTGAGTCACCACTTCAGGGCTTTACTCCGTAACAGATTTTGTTGGC ATAGCTCTGGGGTGGGCAGTTTTTTGAAAATGGGCTCAACCAGAA
RNF125	NM_017831.3	790-890	GCAAGGTGTGTATGTCCCTTTTGTCAGAGGGAACTGTATGAAGACAGCTTGCTGG ATCATTGTATTACTCATCACAGATCGGAACGGAGGCCTGTGTTCT
RORA	NM_134261.2	1715-1815	AAAATTAACCGAGACACTTTATATGGCCCTGCACAGACCTGGAGCGCCACACACT GCACATCTTTTGGTGATCGGGGTCAGGCAAAGGAGGGGAAACAAT
RORC	NM_001001523.1	1350-1450	CTCATCAATGCCCATCGGCCAGGGCTCCAAGAGAAAAGGAAAGTAGAACAGCTG CAGTACAATCTGGAGCTGGCCTTTCATCATCATCTCTGCAAGACTC
RPL27	NM_000988.3	23-123	GGGCCGGGTGGTTGCTGCCGAAATGGGCAAGTTCATGAAACCTGGGAAGGTGGT GCTTGTCCTGGCTGGACGCTACTCCGGACGCAAAGCTGTCATCGTG
RPS13	NM_001017.2	331-431	GCATCTTGAGAGGAACAGAAAGGATAAGGATGCTAAATTCCGTCTGATTCTAATA GAGAGCCGGATTCACCGTTTGGCTCGATATTATAAGACCAAGCGA
RUNX1	NM_001754.4	635-735	CAGCCATGAAGAACCAGGTTGCAAGATTTAATGACCTCAGGTTTGTCGGTCGAAG TGGAAGAGGGAAAAGCTTCACTCTGACCATCACTGTCTTCACAAA
RUNX2	NM_004348.3	1850-1950	GAAGCCACAGCAGTTCCCCAACTGTTTTGAATTCTAGTGGCAGAATGGATGAATC TGTTTGGCGACCATATTGAAATTCCTCAGCAGTGGCCCAGTGGTA
RUNX3	NM_004350.1	2085-2185	GTGGTCTCATAATTCCATTTGTGGAGAGAACAGGAGGGCCAGATAGATAGGTCCT AGCAGAAGGCATTGAGGTGAGGGATCATTTTGGGTCAGACATCAA
S100A4	NM_002961.2	263-363	CAGGGACAACGAGGTGGACTTCCAAGAGTACTGTGTCTTCCTGTCCTGCATCGCC ATGATGTGTAACGAATTCTTTGAAGGCTTCCCAGATAAGCAGCCC
S100A6	NM_014624.3	539-639	TTCCTGGGGGCCTTGGCTTTGATCTACAATGAAGCCCTCAAGGGCTGAAAATAAA TAGGGAAGATGGAGACACCCTCTGGGGGTCCTCTCTGAGTCAAAT
SATB1	NM_001131010.1	1335-1435	TTCCGAAATCTACCAGTGGGTACGCGATGAACTGAAACGAGCAGGAATCTCCCAG GCGGTATTTGCACGTGTGGCTTTTAACAGAACTCAGGGCTTGCTT
SCML1	NM_001037540.1	925-1025	GCAACGTATGGTTCTTCTTCAGGGCTCTGCCTTGGCAACCCTCGGGCTGACAGCA TCCACAACACTTACTCAACTGACCATGCTTCTGCAGCACCACCTT
SCML2	NM_006089.2	360-460	ATTGGAAGCCCGTGACCCTCGCAATGCCACTTCAGTATGTATTGCTACGGTTATT GGAATTACTGGGGCCAGGTTACGGTTACGACTGGATGGTAGTGAC
SEL1L	NM_005065.4	980-1080	GGGCAATCTAATAGCCCACATGGTTTTGGGTTACAGATACTGGGCTGGCATCGGC GTCCTCCAGAGTTGTGAATCTGCCCTGACTCACTATCGTCTTGTT
SELL	NM_000655.3	110-210	CTCCCTTTGGGCAAGGACCTGAGACCCTTGTGCTAAGTCAAGAGGCTCAATGGG CTGCAGAAGAACTAGAGAAGGACCAAGCAAAGCCATGATATTTCCA
SELPLG	NM_003006.3	2297-2397	CATGGGCTGTTAGGTTGACTTCAGTTTTGCCTCTTGGACAACAGGGGGTCTTGTA CATCCTTGGGTGACCAGGAAAAGTTCAGGCTATGGGGGGCCAAAG
SERPINE2	NM_006216.2	240-340	CGCTGCCTTCCATCTGCTCCCACTTCAATCCTCTGTCTCTCGAGGAACTAGGCTC CAACACGGGGATCCAGGTTTTCAATCAGATTGTGAAGTCGAGGCC
SH2B3	NM_005475.2	4285-4385	CCTCCAGCCAGAAGTTAAACATCTGGGATATGACGTCTTCATGCCAGGGGCACTC ATTTCTTAGCAGCCTCTCTACATACATCTCTCAGGTGGTGCCAAG
SH2D2A	NM_001161443.1	341-441	TGCTGGAGCCCAAGCCTCAGGGGTGCTACTTGGTGCGGTTCAGCGAGAGCGCG GTGACCTTCGTGCTGACTTACAGGAGCCGGACTTGCTGCCGCCACTT
SIT1	NM_014450.2	720-820	GCCCCAGCCCCCCGTAGCAGGGGCATGACTGTTTCCCAACCAGCACCCAAAGAC GGGCGCCATTGCCAAGTCACAGGATGTGATCTACCCCGGACTTCCT
SKAP1	NM_003726.3	1360-1460	AAGTGGGAAGAGGCACGTTCATCAAACCTGTTACTAAACCAGCCTAGTCATAGCT CATCCCCATCTCTAAATGTGTCCACACAACCACATCTGCCTTTTC
SKAP2	NM_003930.3	3374-3474	TTTTACAGTTAATCCAGGAGAGGGAGTCCTTTGCCAACTGATGACCAACAGTTCC AAGCCAGATAGTCTCGTGAACAGTGACAATACAGAAATAAGGTGT
SLA2	NM_032214.2	1640-1740	AAAGGAAAGCTGAGATGATGTCTTACCGTAGCAGCAGATCTTGGATGGTCCAGGC TCTATGTGACCTCCAGAGCAAAGAGAAAGACTTCGGACAGTCTAG
SLAMF1	NM_003037.2	580-680	GTGTCTCTTGATCCATCCGAAGCAGGCCCTCCACGTTATCTAGGAGATCGCTACA AGTTTTATCTGGAGAATCTCACCCTGGGGATACGGGAAAGCAGGA
SLAMF7	NM_021181.3	215-315	GGGCACTATCATAGTGACCCAAAATCGTAATAGGGAGAGAGTAGACTTCCCAGAT GGAGGCTACTCCCTGAAGCTCAGCAAACTGAAGAAGAATGACTCA
SLC2A1	NM_006516.2	2500-2600	AGGCTCCATTAGGATTTGCCCCTTCCCATCTCTTCCTACCCAACCACTCAAATTAA TCTTTCTTTACCTGAGACCAGTTGGGAGCACTGGAGTGCAGGGA
SMAD3	NM_005902.3	4220-4320	TTAAAGGACAGTTGAAAAGGGCAAGAGGAAACCAGGGCAGTTCTAGAGGAGTGC TGGTGACTGGATAGCAGTTTTAAGTGGCGTTCACCTAGTCAACACG
SMAD4	NM_005359.3	1370-1470	AGGTTGCACATAGGCAAAGGTGTGCAGTTGGAATGTAAAGGTGAAGGTGATGTTT GGGTCAGGTGCCTTAGTGACCACGCGGTCTTTGTACAGAGTTACT

SNAI1	NM_005985.2	63-163	GACCACTATGCCGCGCTCTTTCCTCGTCAGGAAGCCCTCCGACCCCAATCGGAA GCCTAACTACAGCGAGCTGCAGGACTCTAATCCAGAGTTTACCTTC
SOCS1	NM_003745.1	1025-1125	TTAACTGTATCTGGAGCCAGGACCTGAACTCGCACCTCCTACCTCTTCATGTTTAC ATATACCCAGTATCTTTGCACAAACCAGGGGTTGGGGGAGGGTC
SOCS3	NM_003955.3	1870-1970	GGAGGATGGAGGAGACGGGACATCTTTCACCTCAGGCTCCTGGTAGAGAAGACA GGGGATTCTACTCTGTGCCTCCTGACTATGTCTGGCTAAGAGATTC
SOD1	NM_000454.4	35-135	GCCTATAAAGTAGTCGCGGAGACGGGGTGCTGGTTTGCGTCGTAGTCTCCTGCA GCGTCTGGGGTTTCCGTTGCAGTCCTCGGAACCAGGACCTCGGCGT
SOX13	NM_005686.2	3039-3139	ATTTATTGAGTGCCCACTACGTGCCAGGCACTGTTGCTGAGTTCCTGTGGGTGTG TCTCTCGATGCCACTCCTGCTTCTCTGGGGGCCTCTTTCTGTGCT
SOX2	NM_003106.2	151-251	CTTAAGCCTTTCCAAAAAATAATAATAACAATCATCGGCGGCGGCAGGATCGGCC AGAGGAGGAGGGAAGCGCTTTTTTTGATCCTGATTCCAGTTTGCC
SOX4	NM_003107.2	3040-3140	GTTCACGGTCAAACTGAAATGGATTTGCACGTTGGGGAGCTGGCGGCGGCGGCT GCTGGGCCTCCGCCTTCTTTTCTACGTGAAATCAGTGAGGTGAGAC
SOX5	NM_152989.2	1885-1985	TAGCCATGCAATGATGGATTTCAATCTGAGTGGAGATTCTGATGGAAGTGCTGGA GTCTCAGAGTCAAGAATTTATAGGGAATCCCGAGGGCGTGGTAGC
SPI1	NM_003120.1	730-830	CTCCGCAGCGGCGACATGAAGGACAGCATCTGGTGGGTGGACAAGGACAAGGG CACCTTCCAGTTCTCGTCCAAGCACAAGGAGGCGCTGGCGCACCGCT
SPN	NM_001030288.1	2798-2898	AAGCCAGGCTTCATGGAAAGATCGTATGTGTGACCCAAATATGAGTTCTTCAGCT CAGCCATGGTAATCCCTTCCTTGAAGTCTCCATTTCTGCAGTACA
SPRY2	NM_005842.2	85-185	AAAGAGGAAATACTCCGCGTGCGCTTGTAGAAGGGGAGTCGTCTCCAGCTCCGA ACCCCGGAGTGTTCATCAGCGGGGAATCTGGCTCCGAATTCTCTTT
STAT1	NM_007315.2	205-305	TTTGCTGTATGCCATCCTCGAGAGCTGTCTAGGTTAACGTTCGCACTCTGTGTATA TAACCTCGACAGTCTTGGCACCTAACGTGCTGTGCGTAGCTGCT
STAT3	NM_139276.2	4535-4635	AGACTTGGGCTTACCATTGGGTTTAAATCATAGGGACCTAGGGCGAGGGTTCAGG GCTTCTCTGGAGCAGATATTGTCAAGTTCATGGCCTTAGGTAGCA
STAT4	NM_003151.2	789-889	AGACAATGGATCAGAGTGACAAGAATAGTGCCATGGTGAATCAGGAAGTTTTGAC ACTGCAGGAAATGCTTAACAGCCTCGATTTCAAGAGAAAGGAGGC
STAT5A	NM_003152.2	3460-3560	GAGACAGAGAGAGAGAAAGAGAGAGTGTGTGGGTCTATGTAAATGCATCTGTCCT CATGTGTTGATGTAACCGATTCATCTCTCAGAAGGGAGGCTGGGG
STAT5B	NM_012448.3	200-300	AAGGAGAAGCCCTTCATCAGATGCAAGCGTTATATGGCCAGCATTTTCCCATTGA GGTGCGGCATTATTTATCCCAGTGGATTGAAAGCCAAGCATGGGA
STAT6	NM_003153.3	2030-2130	AGAACATCCAGCCATTCTCTGCCAAAGACCTGTCCATTCGCTCACTGGGGGACCG AATCCGGGATCTTGCTCAGCTCAAAAATCTCTATCCCAAGAAGCC
STMN1	NM_203401.1	287-387	CGTGGGTGGCGGCAGGACTTTCCTTATCCCAGTTGATTGTGCAGAATACACTGCC TGTCGCTTGTCTTCTATTCACCATGGCTTCTTCTGATATCCAGGT
SYK	NM_003177.3	1685-1785	CGGACTCTCCAAAGCACTGCGTGCTGATGAAAACTACTACAAGGCCCAGACCCAT GGAAAGTGGCCTGTCAAGTGGTACGCTCCGGAATGCATCAACTAC
TAL1	NM_003189.2	4635-4735	ACAGCATCTGTAGTCAGCCGACAACTATTTCGGCCTTTTGGGGGTGGGTCTGGCC GTACTTGTGATTTCGATGGTACGTGACCCTCTGCTGAAGACTTGC
TBP	NM_003194.3	25-125	CGCCGGCTGTTTAACTTCGCTTCCGCTGGCCCATAGTGATCTTTGCAGTGACCCA GCAGCATCACTGTTTCTTGGCGTGTGAAGATAACCCAAGGAATTG
TBX21	NM_013351.1	890-990	ACACAGGAGCGCACTGGATGCGCCAGGAAGTTTCATTTGGGAAACTAAAGCTCAC AAACAACAAGGGGGCGTCCAACAATGTGACCCAGATGATTGTGCT
TBXA2R	NM_001060.3	385-485	CACACGCGCTCCTCCTTCCTCACCTTCCTCTGCGGCCTCGTCCTCACCGACTTCC TGGGGCTGCTGGTGACCGGTACCATCGTGGTGTCCCAGCACGCCG
TCF12	NM_207037.1	1105-1205	CACATGACCGCTTGAGTTATCCTCCACACTCAGTTTCACCAACAGACATAAACACG AGTCTTCCACCAATGTCCAGCTTTCATCGCGGCAGTACCAGCAG
TCF3	NM_003200.2	4325-4425	ATACGTGTCAACACAGCTGGCTGGATGATTGGGACTTTAAAACGACCCTCTTTCA GGTGGATTCAGAGACCTGTCCTGTATATAACAGCACTGTAGCAAT
TCF7	NM_003202.2	2420-2520	ATTCCATTTCCAGTTCATCTATGGCAGTCCAGCCAGCTCCTGGGCAGCTTGAGAG GGCAAACCCAAAACCTCATGACAGCCAGAGCCTGTCTTTCAGCAT
TDGF1	NM_003212.2	1567-1667	AAGGAAAGAAAACATCTTTAAGGGGAGGAACCAGAGTGCTGAAGGAATGGAAGT CCATCTGCGTGTGTGCAGGGAGACTGGGTAGGAAAGAGGAAGCAAA
TDO2	NM_005651.1	0-100	AAGGTCAATGATAGCATCTGCCTAGAGTCAAACCTCCGTGCTTCTCAGACAGTGC CTTTTCACCATGAGTGGGTGCCCATTTTTAGGAAACAACTTTGGA
TEK	NM_000459.2	615-715	CGAGTTCGAGGAGAGGCAATCAGGATACGAACCATGAAGATGCGTCAACAAGCT TCCTTCCTACCAGCTACTTTAACTATGACTGTGGACAAGGGAGATA
TERF1	NM_003218.3	1037-1137	CTGAAAGCAGAATACCTGTTTCAAAGAGTCAGCCGGTAACTCCTGAAAAACATCG AGCTAGAAAAAGACAGGCATGGCTTTGGGAAGAAGACAAGAATTT
TERT	NM_198253.1	2570-2670	GGCTTCAAGGCTGGGAGGAACATGCGTCGCAAACTCTTTGGGGTCTTGCGGCTG AAGTGTCACAGCCTGTTTCTGGATTTGCAGGTGAACAGCCTCCAGA
TF	NM_001063.2	640-740	CTGCTCCACCCTTAACCAATACTTCGGCTACTCGGGAGCCTTCAAGTGTCTGAAG GATGGTGCTGGGGATGTGGCCTTTGTCAAGCACTCGACTATATTT
TFRC	NM_003234.1	1220-1320	CAGTTTCCACCATCTCGGTCATCAGGATTGCCTAATATACCTGTCCAGACAATCTC CAGAGCTGCTGCAGAAAAGCTGTTTGGGAATATGGAAGGAGACT
TGFA	NM_003236.2	780-880	TGCCACAGACCTTCCTACTTGGCCTGTAATCACCTGTGCAGCCTTTTGTGGGCCT TCAAAACTCTGTCAAGAACTCCGTCTGCTTGGGGTTATTCAGTGT
TGFB1	NM_000660.3	1260-1360	TATATGTTCTTCAACACATCAGAGCTCCGAGAAGCGGTACCTGAACCCGTGTTGC TCTCCCGGGCAGAGCTGCGTCTGCTGAGGCTCAAGTTAAAAGTGG

TGFB2	NM_003238.2	1125-1225	AAGCCAGAGTGCCTGAACAACGGATTGAGCTATATCAGATTCTCAAGTCCAAAGA TTTAACATCTCCAACCCAGCGCTACATCGACAGCAAAGTTGTGAA
TGFBR1	NM_004612.2	4280-4380	GGGGAAATACGACTTAGTGAGGCATAGACATCCCTGGTCCATCCTTTCTGTCTCC AGCTGTTTCTTGGAACCTGCTCTCCTGCTTGCTGGTCCCTGACGC
Thymidine Kinase	SCFV007.1	100-200	TCTACGTACCCGAGCCGATGACTTACTGGCAGGTGCTGGGGGCTTCCGAGACAA TCGCGAACATCTACACCACACAACACCGCCTCGACCAGGGTGAGAT
TIE1	NM_005424.2	2610-2710	CATCGGGGAGGGGAACTTCGGCCAGGTCATCCGGGCCATGATCAAGAAGGACG GGCTGAAGATGAACGCAGCCATCAAAATGCTGAAAGAGTATGCCTCT
TLR2	NM_003264.3	180-280	CTGCTTTCAACTGGTAGTTGTGGGTTGAAGCACTGGACAATGCCACATACTTTGT GGATGGTGTGGGTCTTGGGGGTCATCATCAGCCTCTCCAAGGAAG
TLR8	NM_138636.3	2795-2895	GACAAAAACGTTCTCCTTTGTCTAGAGGAGAGGGATTGGGATCCGGGATTGGCCA TCATCGACAACCTCATGCAGAGCATCAACCAAAGCAAGAAAACAG
TNF	NM_000594.2	1010-1110	AGCAACAAGACCACCACTTCGAAACCTGGGATTCAGGAATGTGTGGCCTGCACA GTGAAGTGCTGGCAACCACTAAGAATTCAAACTGGGGCCTCCAGAA
TNFRSF14	NM_003820.2	916-1016	CTCAGGGAGCCTCGTCATCGTCATTGTTTGCTCCACAGTTGGCCTAATCATATGT GTGAAAAGAAGAAAGCCAAGGGGTGATGTAGTCAAGGTGATCGTC
TNFRSF18	NM_004195.2	445-545	AGGGGAAATTCAGTTTTGGCTTCCAGTGTATCGACTGTGCCTCGGGGACCTTCTC CGGGGGCCACGAAGGCCACTGCAAACCTTGGACAGACTGCACCCA
TNFRSF1B	NM_001066.2	835-935	CCCAGCTGAAGGGAGCACTGGCGACTTCGCTCTTCCAGTTGGACTGATTGTGGG TGTGACAGCCTTGGGTCTACTAATAATAGGAGTGGTGAACTGTGTC
TNFRSF4	NM_003327.2	200-300	CCGTGCGGGCCGGGCTTCTACAACGACGTGGTCAGCTCCAAGCCGTGCAAGCC CTGCACGTGGTGTAACCTCAGAAGTGGGAGTGAGCGGAAGCAGCTGT
TNFRSF9	NM_001561.4	255-355	AGATTTGCAGTCCCTGTCCTCCAAATAGTTTCTCCAGCGCAGGTGGACAAAGGAC CTGTGACATATGCAGGCAGTGTAAAGGTGTTTTCAGGACCAGGAA
TNFSF10	NM_003810.2	115-215	GGGGGGACCCAGCCTGGGACAGACCTGCGTGCTGATCGTGATCTTCACAGTGCT CCTGCAGTCTCTCTGTGTGGCTGTAACTTACGTGTACTTTACCAAC
TNFSF11	NM_003701.2	490-590	TACCTGATTCATGTAGGAGAATTAAACAGGCCTTTCAAGGAGCTGTGCAAAAGGA ATTACAACATATCGTTGGATCACAGCACATCAGAGCAGAGAAAGC
TNFSF14	NM_003807.2	270-370	ATTTTCAGAAGCCTCTGGAAAGTCGTGCACAGCCCAGGAGTGTTGAGCAATTTCG GTTTCCTCTGAGGTTGAAGGACCCAGGCGTGTCAGCCCTGCTCCA
TOX	NM_014729.2	3950-4050	AATGAGCAGCTTTGACTTTGACAGGCGGTTTGTGCAGGAAAGCACAGTGCCGTGT TGTTTACAGCTTTTCTAGAGCAGCTGTGCGACCAGGGTAGAGAGT
TP53	NM_000546.2	1330-1430	GGGGAGCAGGGCTCACTCCAGCCACCTGAAGTCCAAAAAGGGTCAGTCTACCTC CCGCCATAAAAAACTCATGTTCAAGACAGAAGGGCCTGACTCAGAC
TRAF1	NM_005658.3	3735-3835	CGAGTGATGGGTCTAGGCCCTGAAACTGATGTCCTAGCAATAACCTCTTGATCCC TACTCACCGAGTGTTGAGCCCAAGGGGGGATTTGTAGAACAAGCC
TRAF2	NM_021138.3	1325-1425	GTGGCCCTTCAACCAGAAGGTGACCTTAATGCTGCTCGACCAGAATAACCGGGA GCACGTGATTGACGCCTTCAGGCCCGACGTGACTTCATCCTCTTTT
TRAF3	NM_145725.1	1795-1895	ATATGATGCCCTGCTTCCTTGGCCGTTTAAGCAGAAAGTGACACTCATGCTGATG GATCAGGGGTCCTCTCGACGTCATTTGGGAGATGCATTCAAGCCC
TSC22D3	NM_198057.2	1400-1500	TTAAGCAGAGGCAACCTCTCTCTTCTCCTCTGTTTCGTGAAGGCAGGGGACACAG ATGGGAGAGATTGAGCCAAGTCAGCCTTCTGTTGGTTAATATGGT
TSLP	NM_033035.3	395-495	CCGTCTCTTGTAGCAATCGGCCACATTGCCTTACTGAAATCCAGAGCCTAACCTTC AATCCCACCGCCGGCTGCGCGTCGCTCGCCAAAGAAATGTTCGC
TXK	NM_003328.1	800-900	ATGACTCGTCTCCGATATCCAGTTGGGCTGATGGGCAGTTGTTTACCAGCCACAG CTGGGTTTAGCTACGAAAAGTGGGAGATAGATCCATCTGAGTTGG
TYK2	NM_003331.3	485-585	TCATCGCTGACAGCTGAGGAAGTCTGCATCCACATTGCACATAAAGTTGGTATCA CTCCTCCTTGCTTCAATCTCTTTGCCCTCTTCGATGCTCAGGCCC
TYROBP	NM_003332.2	457-557	CTGCACCTCATTCCAACTCCTACCGCGATACAGACCCACAGAGTGCCATCCCTGA GAGACCAGACCGCTCCCCAATACTCTCCTAAAATAAACATGAAGC
UBASH3A	NM_001001895.1	1970-2070	GAGATGCTGCTGTTTCCAGAGGCGTCTTAGTCTCACCCAATGTGATTTGTAGAAG CACGAGACGCACTTTTATATCCCGGAATATTTCCCTCCGGCTTTC
VAX2	NM_012476.2	871-971	CAGCGCCAGCAGCTGCAAGAAAGCTAACACTTAAGACTCCCACCCTGTGACACTG AGTCCCGAGCACAGCACCTTCCCAGTCTCCTGTGCCCCAGCGGAC
VEGFA	NM_001025366.1	1325-1425	GAGTCCAACATCACCATGCAGATTATGCGGATCAAACCTCACCAAGGCCAGCACA TAGGAGAGATGAGCTTCCTACAGCACAACAAATGTGAATGCAGAC
WEE1	NM_003390.2	5-105	TGCGTTTGAGTTTGCCGCGAGCCGGGCCAATCGGTTTTGCCAACGCATGCCCAC GTGCTGGCGAACAAATGTAAACACGGAGATCGTGTGCCGGGCACTT
XBP1	NM_005080.2	440-540	GGAGTTAAGACAGCGCTTGGGGATGGATGCCCTGGTTGCTGAAGAGGAGGCGG AAGCCAAGGGGAATGAAGTGAGGCCAGTGGCCGGGTCTGCTGAGTCC
XBP1	NM_001079539.1	935-1035	ATTCATTGTCTCAGTGAAGGAAGAACCTGTAGAAGATGACCTCGTTCCGGAGCTG GGTATCTCAAATCTGCTTTCATCCAGCCACTGCCCAAAGCCATCT
YY1AP1	NM_139118.2	755-855	ATGGGAGCTATGCAGCTGATTGAAGACTTCAGCACACATGTCAGCATTGACTGCA GCCCTCATAAAACTGTCAAGAAGACTGCCAATGAATTTCCCTGTT
ZAP70	NM_001079.3	1175-1275	GGAGCTCAAGGACAAGAAGCTCTTCCTGAAGCGCGATAACCTCCTCATAGCTGAC ATTGAACTTGGCTGCGGCAACTTTGGCTCAGTGCGCCAGGGCGTG
ZBTB16	NM_006006.4	1585-1685	TCCTGGATAGTTTGCGGCTGAGAATGCACTTACTGGCTCATTCAGCGGGTGCCAA AGCCTTTGTCTGTGATCAGTGCGGTGCACAGTTTTCGAAGGAGGA
ZC2HC1A	NM_016010.2	665-765	ACGATTACCGCAGCCAAGTGGCGCTGGCAAAACTGTTGTAGGTGTTCCTTCAGGT AAAGTGTCTTCAAGTAGCAGCTCTTTGGGAAACAAACTTCAGACC

ZEB2	NM_014795.2	20-120	TCCCAGAGAGAAACTTGGCGATCACGTTTTCACATGATGCTCACGCTCAGGGCGC TTCAATTATCCCTCCCCACAAAGATAGGTGGCGCGTGTTTCAGGG
ZNF516	NM_014643.2	4830-4930	GGTGGGGGACGGCTTCATATACCTCTTCCTCAGTAATGCAAATGCGAGTTTTTGT GGTGGGGGTTAAGGCCCATAACAAAGGATCTTAAACCATGCAGTG

Appendix B: TCRVα and TCRBβ CodeSet

TCRVα genes	Target region	Target sequence
TRAV1-1	192-292	TACAATGCTCTGGATGGTTTGGAGGAGACAGGTCGTTTTTCTTCATTCCT TAGTCGCTCTGATAGTTATGGTTACCTCCTTCTACAGGAGCTCCAGATGA
TRAV1-2	187-287	TGTCTTACAATGTTCTGGATGGTTTGGAGGAGAAAGGTCGTTTTTCTTCA TTCCTTAGTCGGTCTAAAGGGTACAGTTACCTCCTTTTGAAGGAGCTCCA
TRAV2	177-277	TACCTTCACTTCCCGGGATGTGCACCAAGACTCCTTGTTAAAGGCTCAAA GCCTTCTCAGCAGGGACGATACAACATGACCTATGAACGGTTCTCTTCAT
TRAV3	6-106	TCTGCACCCATCTCGATGCTTGCGATGCTCTTCACATTGAGTGGGCTGAGA GCTCAGTCAGTGGCTCAGCCGGAAGATCAGGTCAACGTTGCTGAAGGGA
TRAV4	159-259	CAACAGTTTCCCAGCCAAGGACCACGATTTATTATTCAAGGATACAAGAC AAAAGTTACAAACGAAGTGGCCTCCCTGTTTATCCCTGCCGACAGAAAGT
TRAV5	118-218	TTATAAACTGCACTTACACAGACAGCTCCTCCACCTACTTATACTGGTAT AAGCAAGAACCTGGAGCAGGTCTCCAGTTGCTGACGTATATTTTTTCAAA
TRAV6	183-283	AGAGGCCCTGTTTTCTTGCTACTCATACGTGAAAATGAGAAAGAAAAAAG GAAAGAAAGACTGAAGGTCACCTTTGATACCACCCTTAAACAGAGTTTGT
TRAV7	126-226	AGCTGCACGTACTCTGTCAGTCGTTTTAACAATTTGCAGTGGTACAGGCA AAATACAGGGATGGGTCCCAAACACCTATTATCCATGTATTCAGCTGGAT
TRAV8-1	108-208	TCACTGGAGTTGGGATGCAACTATTCCTATGGTGGAACTGTTAATCTCTT CTGGTATGTCCAGTACCCTGGTCAACACCTTCAGCTTCTCCTCAAGTACT
TRAV8-2	206-306	CACATCAGCGGCCACCCTGGTTAAAGGCATCAACGGTTTTGAGGCTGAAT TTAAGAAGAGTGAAACCTCCTTCCACCTGACGAAACCCTCAGCCCATATG
TRAV8-3	49-149	CTGCCAGAGCCCAGTCAGTGACCCAGCCTGACATCCACATCACTGTCTCT GAAGGAGCCTCACTGGAGTTGAGATGTAACTATTCCTATGGGGCAACACC
TRAV8-6	206-306	TTTATCAGGATCCACCCTGGTTAAAGGCATCAACGGTTTTGAGGCTGAAT TTAACAAGAGTCAAACTTCCTTCCACTTGAGGAAACCCTCAGTCCATATA
TRAV9-1	49-149	GAATCAATGGAGATTCAGTGGTCCAGACAGAAGGCCAAGTGCTCCCCTCT GAAGGGGATTCCCTGATTGTGAACTGCTCCTATGAAACCACACAGTACCC
TRAV9-2	31-131	TACTCTTACTGCTTGGAAGAACCCGTGGAAATTCAGTGACCCAGATGGAA GGGCCAGTGACTCTCTCAGAAGAGGCCTTCCTGACTATAAACTGCACGTA
TRAV10	164-264	GTGGTATAAGCAAGATACTGGGAGAGGTCCTGTTTCCCTGACAATCATGA CTTTCAGTGAGAACACAAAGTCGAACGGAAGATATACAGCAACTCTGGAT
TRAV11	135-235	TATCAGGAGAGAACACTCTTCAATTTCCACTGGTTCCGGCAGGATCCGGG GAGAAGACTTGTGTCTTTGACCTTAATTCAATCAAGCCAGAAGGAGCAGG
TRAV12-1	140-240	CAACAGTGCTTCTCAGTCTTTCTTCTGGTACAGACAGGATTGCAGGAAAG AACCTAAGTTGCTGATGTCCGTATACTCCAGTGGTAATGAAGATGGAAGG
TRAV12-2	116-216	CATTGCCTCTCTCAACTGCACTTACAGTGACCGAGGTTCCCAGTCCTTCT TCTGGTACAGACAATATTCTGGGAAAAGCCCTGAGTTGATAATGTTCATA
TRAV12-3	99-199	AGTGTTCCAGAGGGAGCCATTGTTTCTCTCAACTGCACTTACAGCAACAG TGCTTTTCAATACTTCATGTGGTACAGACAGTATTCCAGAAAAGGCCCTG
TRAV13-1	189-289	CAGCTTATTATAGACATTCGTTCAAATGTGGGCGAAAAGAAAGACCAACG AATTGCTGTTACATTGAACAAGACAGCCAAACATTTCTCCCTGCACATCA
TRAV13-2	99-199	CAGGAGGGTGACAACTCTATTATCAACTGTGCTTATTCAAACAGCGCCTC AGACTACTTCATTTGGTACAAGCAAGAATCTGGAAAAGGTCCTCAATTCA
TRAV14	232-332	ATGCAACAGAAGGTCGCTACTCATTGAATTTCCAGAAGGCAAGAAAATCC GCCAACCTTGTCATCTCCGCTTCACAACTGGGGGACTCAGCAATGTATTT
TRAV16	222-322	ATCAAAGGCTTCACTGCTGACCTTAACAAAGGCGAGACATCTTTCCACCT GAAGAAACCATTTGCTCAAGAGGAAGACTCAGCCATGTATTACTGTGCTC
TRAV17	201-301	TTAATACGTTCAAATGAAAGAGAGAAACACAGTGGAAGATTAAGAGTCAC GCTTGACACTTCCAAGAAAAGCAGTTCCTTGTTGATCACGGCTTCCCGGC
TRAV18	198-298	CTGAAAAGTTCAGAAAACCAGGAGACGGACAGCAGAGGTTTTCAGGCCAG TCCTATCAAGAGTGACAGTTCCTTCCACCTGGAGAAGCCCTCGGTGCAGC
TRAV19	227-237	GCAAAATGAAATAAGTGGTCGGTATTCTTGGAACTTCCAGAAATCCACCA GTTCCTTCAACTTCACCATCACAGCCTCACAAGTCGTGGACTCAGCAGTA
TRAV20	136-236	ACACAGTCAGCGGTTTAAGAGGGCTGTTCTGGTATAGGCAAGATCCTGGG AAAGGCCCTGAATTCCTCTTCACCCTGTATTCAGCTGGGGAAGAAAAGGA

TRAV21	176-276	TGGGAAAGGTCTCACATCTCTGTTGCTTATTCAGTCAAGTCAGAGAGAGC AAACAAGTGGAAGACTTAATGCCTCGCTGGATAAATCATCAGGACGTAGT
TRAV22	183-283	CAGCTCATCAACCTGTTTTACATTCCCTCAGGGACAAAACAGAATGGAAG ATTAAGCGCCACGACTGTCGCTACGGAACGCTACAGCTTATTGTACATTT
TRAV23	159-259	GAGAACACTGCGTTTGACTACTTTCCATGGTACCAACAATTCCCTGGGAA AGGCCCTGCATTATTGATAGCCATACGTCCAGATGTGAGTGAAAAGAAAG
TRAV24	88-188	CTCAGTCACTGCATGTTCAGGAGGGAGACAGCACCAATTTCACCTGCAGC TTCCCTTCCAGCAATTTTTATGCCTTACACTGGTACAGATGGGAAACTGC
TRAV25	43-143	CACAGGTGAATGGACAACAGGTAATGCAAATTCCTCAGTACCAGCATGTA CAAGAAGGAGAGGACTTCACCACGTACTGCAATTCCTCAACTACTTTAAG
TRAV26-1	106-206	ACCTGCCTTGTAATCACTCTACCATCAGTGGAAATGAGTATGTGTATTGG TATCGACAGATTCACTCCCAGGGGCCACAGTATATCATTCATGGTCTAAA
TRAV26-2	11-111	GACAAGCATTACTGTACTCCTATCTTTGGGTATTATGGGTGATGCTAAGA CCACACAGCCAAATTCAATGGAGAGTAACGAAGAAGAGCCTGTTCACTTG
TRAV27	69-169	CAGAGCCCTCAGTTTCTAAGCATCCAAGAGGGAGAAAATCTCACTGTGTA CTGCAACTCCTCAAGTGTTTTTTCCAGCTTACAATGGTACAGACAGGAGC
TRAV29	193-293	ACCCTGCTGAAGGTCCTACATTCCTGATATCTATAAGTTCCATTAAGGAT AAAAATGAAGATGGAAGATTCACTGTCTTCTTAAACAAAAGTGCCAAGCA
TRAV30	141-241	GCTTTATATTCTGTACACTGGTACAGGCAGAAGCATGGTGAAGCACCCGT CTTCCTGATGATATTACTGAAGGGTGGAGAACAGAAGGGTCATGAAAAAA
TRAV34	169-269	AAAAGTATGGTGAAGGTCTTATCTTCTTGATGATGCTACAGAAAGGTGGG GAAGAGAAAAGTCATGAAAAGATAACTGCCAAGTTGGATGAGAAAAAGCA
TRAV35	216-316	TTGACCTCAAATGGAAGACTGACTGCTCAGTTTGGTATAACCAGAAAGGA CAGCTTCCTGAATATCTCAGCATCCATACCTAGTGATGTAGGCATCTACT
TRAV36	156-256	AGCCTACTATGGTACAAGCAGGAAAAGAAAGCTCCCACATTTCTATTTAT GCTAACTTCAAGTGGAATTGAAAAGAAGTCAGGAAGACTAAGTAGCATAT
TRAV38-1	250-350	TCTCTGTGAACTTCCAGAAAGCAGCCAAATCCTTCAGTCTCAAGATCTCA GACTCACAGCTGGGGGGACACTGCGATGTATTTCTGTGCTTTCATGAAGCA
TRAV38-2	249-349	TTCTCTGTGAACTTCCAGAAAGCAGCCAAATCCTTCAGTCTCAAGATCTCA GACTCACAGCTGGGGGATGCCGCGATGTATTTCTGTGCTTATAGGAGCG
TRAV39	49-149	GTGGAGAGCTGAAAGTGGAACAAAACCCTCTGTTCCTGAGCATGCAGGA GGGAAAAAACTATACCATCTACTGCAATTATTCAACCACTTCAGACAGACT
TRAV40	6-106	TCCTCTCTGGACTTTCTAATTCTGATCTTAATGTTTGGAGGAACCAGCAGC AATTCAGTCAAGCAGACGGGCCAAATAACCGTCTCGGAGGGAGCATCTG
TRAV41	38-138	GCTTCAGCTAAGCTGTGTAAGTGCCGCCAAAAATGAAGTGGAGCAGAGTC CTCAGAACCTGACTGCCCAGGAAGGAGAATTTATCACAATCAACTGCAGT

TCRVβ genes	Target region	Target sequence
TRBV2	220-320	CAGAGAAGTCTGAAATATTCGATGATCAATTCTCAGTTGAAAGGCCTGATG GATCAAATTTCACTCTGAAGATCCGGTCCACAAAGCTGGAGGACTCAGC
TRBV3-1	86-186	AATACCTGGTCACACAGATGGGAAACGACAAGTCCATTAAATGTGAACAA AATCTGGGCCATGATACTATGTATTGGTATAAACAGGACTCTAAGAAATT
TRBV4-1	143-243	CAGGGCTATGTATTGGTACAAGCAGAAAGCTAAGAAGCCACCGGAGCTC ATGTTTGTCTACAGCTATGAGAAACTCTCTATAAATGAAAGTGTGCCAAGT
TRBV4-2	138-238	GGGCATAACGCTATGTATTGGTACAAGCAAAGTGCTAAGAAGCCACTGG AGCTCATGTTTGTCTACAACTTTAAAGAACAGACTGAAAACAACAGTGTGC
TRBV4-3	138-238	GGTCATAACGCTATGTATTGGTACAAGCAAAGTGCTAAGAAGCCACTGGA GCTCATGTTTGTCTACAGTCTTGAAGAACGGGTTGAAAACAACAGTGTGC
TRBV5-1	194-298	TTTGAATACTTCAGTGAGACACAGAGAAACAAAGGAAACTTCCCTGGTCG ATTCTCAGGGCGCCAGTTCTCTAACTCTCGCTCTGAGATGAATGTGAGCA
TRBV5-4	151-251	CAACACTGTGTCCTGGTACCAACAGGCCCTGGGTCAGGGGCCCCAGTTTA TCTTTCAGTATTATAGGGAGGAAGAGAATGGCAGAGGAAACTTCCCTCCT
TRBV5-5	148-248	AGAGTGTGTCCTGGTACCAACAGGTCCTGGGTCAGGGGCCCCAGTTTATC TTTCAGTATTATGAGAAAGAAGAGAGAGGAAGAGGAAACTTCCCTGATCG
TRBV5-6	145-245	ACACTGTGTCCTGGTACCAACAGGCCCTGGGTCAGGGGCCCCAGTTTATC TTTCAGTATTATGAGGAGGAAGAGAGACAGAGAGGCAACTTCCCTGATCG
TRBV5-8	131-231	TATCTCTGGGCACACCAGTGTGTACTGGTACCAACAGGCCCTGGGTCTGG GCCTCCAGTTCCTCCTTTGGTATGACGAGGGTGAAGAGAGAAACAGAGGA

TRBV6-1	124-224	GTGCCCAGGATATGAACCATAACTCCATGTACTGGTATCGACAAGACCCA GGCATGGGACTGAGGCTGATTTATTACTCAGCTTCTGAGGGTACCACTGA
TRBV6-2	150-250	ATGTACTGGTATCGACAAGACCCAGGCATGGGGCTGAGGCTGATTCATTA CTCAGTTGGTGAGGGTACAACTGCCAAAGGAGAGGTCCCTGATGGCTACA
TRBV6-4	181-281	GGCTAAGGCTCATCCATTATTCAAATACTGCAGGTACCACTGGCAAAGGA GAAGTCCCTGATGGTTATAGTGTCTCCAGAGCAAACACAGATGATTTCCC
TRBV6-5	142-242	ATGAATACATGTCCTGGTATCGACAAGACCCAGGCATGGGGCTGAGGCTG ATTCATTACTCAGTTGGTGCTGGTATCACTGACCAAGGAGAAGTCCCCAA
TRBV6-6	159-259	TATCGACAAGACCCAGGCATGGGGCTGAAGCTGATTTATTATTCAGTTGG TGCTGGTATCACTGATAAAGGAGAAGTCCCGAATGGCTACAACGTATCTG
TRBV6-8	133-233	ATATGAACCATGGATACATGTCCTGGTATCGACAAGACCCAGGCATGGGG CTGAGACTGATTTACTACTCAGCTGCTGCTGGTACTACTGACAAAGAAGT
TRBV6-9	164-264	GGCATGGGGCTGAGGCGCATTCATTACTCAGTTGCTGCTGGTATCACTGA CAAAGGAGAAGTCCCCGATGGCTACAATGTATCCAGATCAAACACAGAGG
TRBV7-2	117-217	CTCAGGTGTGATCCAATTTCAGGTCATACTGCCCTTTACTGGTACCGACA GAGCCTGGGGCAGGGCCTGGAGTTTTTAATTTACTTCCAAGGCAACAGTG
TRBV7-3	163-263	GACAAAGCCTGGGGCAGGGCCCAGAGTTTCTAATTTACTTCCAAGGCACG GGTGCGGCAGATGACTCAGGGCTGCCCAACGATCGGTTCTTTGCAGTCAG
TRBV7-4	125-225	TGATTCAATTTCGGGTCATGTAACCCTTTATTGGTACCGACAGACCCTGGG GCAGGGCTCAGAGGTTCTGACTTACTCCCAGAGTGATGCTCAACGAGAC
TRBV7-6	76-176	CTCCCAGGTACAAAGTCACAAAGAGGGGACAGGATGTAGCTCTCAGGTGT GATCCAATTTCGGGTCATGTATCCCTTTATTGGTACCGACAGGCCCTGGG
TRBV7-7	74-174	GTCTCCCAGGTACAAAGTCACAAAGAGGGGACAGGATGTAACTCTCAGGT GTGATCCAATTTCGAGTCATGCAACCCTTTATTGGTATCAACAGGCCCTG
TRBV7-8	194-294	GACTTATTTCCAGAATGAAGCTCAACTAGACAAATCGGGGCTGCCCAGTG ATCGCTTCTTTGCAGAAAGGCCTGAGGGATCCGTCTCCACTCTGAAGATC
TRBV7-9	13-113	TCCTCTGCTGGATGGCCCTGTGTCTCCTGGGGGCAGATCACGCAGATACT GGAGTCTCCCAGAACCCCAGACACAAGATCACAAAGAGGGGACAGAATGT
TRBV9	175-275	ACCAGGGCCTCCAGTTCCTCATTCAGTATTATAATGGAGAAGAGAGAGCA AAAGGAAACATTCTTGAACGATTCTCCGCACAACAGTTCCCTGACTTGCA
TRBV10-1	176-276	ACATGGGCTGAGGCTGATCCATTACTCATATGGTGTTCAAGACACTAACA AAGGAGAAGTCGCTGCCTCCTCCCAGACATCTGTATATTTCTGCGCCAGC
TRBV10-2	62-162	TGGAATCACCCAGAGCCCAAGATACAAGATCACAGAGACAGGAAGGCAG GTGACCTTGATGTGTCACCAGACTTGGAGCCACAGCTATATGTTCTGGTAT
TRBV10-3	192-292	ATCCATTACTCATATGGTGTTAAAGATACTGACAAAGGAGAAGTCTCAGA TGGCTATAGTGTCTCTAGATCAAAGACAGAGGATTTCCTCCTCACTCTGG
TRBV11-1	131-231	TATTTCTGGCCATGCTACCCTTTACTGGTACCGGCAGATCCTGGGACAGG GCCCGGAGCTTCTGGTTCAATTTCAGGATGAGAGTGTAGTAGATGATTCA
TRBV11-2	131-231	TATATCTGGCCATGCTACCCTTTACTGGTACCAGCAGATCCTGGGACAGG GCCCAAAGCTTCTGATTCAGTTTCAGAATAACGGTGTAGTGGATGATTCA
TRBV11-3	73-173	AGTCTCCCAGATATAAGATTATAGAGAAAAAACAGCCTGTGGCTTTTTGG TGCAATCCTATTTCTGGCCACAATACCCTTTACTGGTACCTGCAGAACTT
TRBV12-3	150-250	CTTTTCTGGTACAGACAGACCATGATGCGGGGACTGGAGTTGCTCATTTA CTTTAACAACAACGTTCCGATAGATGATTCAGGGATGCCCGAGGATCGAT
TRBV12-5	120-220	AGATGTCAGCCAATTTTAGGCCACAATACTGTTTTCTGGTACAGACAGAC CATGATGCAAGGACTGGAGTTGCTGGCTTACTTCCGCAACCGGGCTCCTC
TRBV13	87-187	GCTGCTGGAGTCATCCAGTCCCCAAGACATCTGATCAAAGAAAAGAGGGA AACAGCCACTCTGAAATGCTATCCTATCCCTAGACACGACACTGTCTACT
TRBV14	233-333	TATGCCCAACAATCGATTCTTAGCTGAAAGGACTGGAGGGACGTATTCTA CTCTGAAGGTGCAGCCTGCAGAACTGGAGGATTCTGGAGTTTATTTCTGT
TRBV15	187-287	CCCAAAGCTGCTGTTCCACTACTATGACAAAGATTTTAACAATGAAGCAG ACACCCCTGATAACTTCCAATCCAGGAGGCCGAACACTTCTTTCTGCTTT
TRBV16	194-294	GATTTCCTTCCAGAATGAAAATGTCTTTGATGAAACAGGTATGCCCAAGG AAAGATTTTCAGCTAAGTGCCTCCCAAATTCACCCTGTAGCCTTGAGATC
TRBV18	156-256	TGGTATCGGCAGCTCCCAGAGGAAGGTCTGAAATTCATGGTTTATCTCCA GAAAGAAAATATCATAGATGAGTCAGGAATGCCAAAGGAACGATTTTCTG
TRBV19	195-295	TACTACTCACAGATAGTAAATGACTTTCAGAAAGGAGATATAGCTGAAGG GTACAGCGTCTCTCGGGAGAAGAAGGAATCCTTTCCTCTCACTGTGACAT

TRBV20-1	95-195	CAGAGAAGTCTGAAATATTCGATGATCAATTCTCAGTTGAAAGGCCTGAT GGATCAAATTTCACTCTGAAGATCCGGTCCACAAAGCTGGAGGACTCAGC
TRBV24-1	124-224	AATACCTGGTCACACAGATGGGAAACGACAAGTCCATTAAATGTGAACAA AATCTGGGCCATGATACTATGTATTGGTATAAACAGGACTCTAAGAAATT
TRBV25-1	181-281	CAGGGCTATGTATTGGTACAAGCAGAAAGCTAAGAAGCCACCGGAGCTC ATGTTTGTCTACAGCTATGAGAAACTCTCTATAAATGAAAGTGTGCCAAGT
TRBV27	162-262	GGGCATAACGCTATGTATTGGTACAAGCAAAGTGCTAAGAAGCCACTGG AGCTCATGTTTGTCTACAACTTTAAAGAACAGACTGAAAACAACAGTGTGC
TRBV28	47-147	GGTCATAACGCTATGTATTGGTACAAGCAAAGTGCTAAGAAGCCACTGGA GCTCATGTTTGTCTACAGTCTTGAAGAACGGGTTGAAAACAACAGTGTGC
TRBV29-1	190-290	TTTGAATACTTCAGTGAGACACAGAGAAACAAAGGAAACTTCCCTGGTCG ATTCTCAGGGCGCCAGTTCTCTAACTCTCGCTCTGAGATGAATGTGAGCA
TRBV30	5-105	CAACACTGTGTCCTGGTACCAACAGGCCCTGGGTCAGGGGCCCCAGTTTA TCTTTCAGTATTATAGGGAGGAAGAGAATGGCAGAGGAAACTTCCCTCCT

BIBLIOGRAPHY

1. Smith-Garvin, J. E., G. A. Koretzky, and M. S. Jordan. 2009. T cell activation. Annual review of immunology 27:591-619.
2. Call, M. E., J. Pyrdol, M. Wiedmann, and K. W. Wucherpfennig. 2002. The organizing principle in the formation of the T cell receptor-CD3 complex. Cell 111:967-979.
3. Krogsgaard, M., Q. J. Li, C. Sumen, J. B. Huppa, M. Huse, and M. M. Davis. 2005. Agonist/endogenous peptide-MHC heterodimers drive T cell activation and sensitivity. Nature 434:238-243.
4. Stone, J. D., and L. J. Stern. 2006. CD8 T cells, like CD4 T cells, are triggered by multivalent engagement of TCRs by MHC-peptide ligands but not by monovalent engagement. J Immunol 176:1498-1505.
5. Brownlie, R. J., and R. Zamoyska. 2013. T cell receptor signalling networks: branched, diversified and bounded. Nature reviews. Immunology 13:257-269.
6. Dustin, M. L., and D. Depoil. 2011. New insights into the T cell synapse from single molecule techniques. Nature reviews. Immunology 11:672-684.
7. Beemiller, P., and M. F. Krummel. 2010. Mediation of T-cell activation by actin meshworks. Cold Spring Harbor perspectives in biology 2:a002444.
8. Nguyen, K., N. R. Sylvain, and S. C. Bunnell. 2008. T cell costimulation via the integrin VLA-4 inhibits the actin-dependent centralization of signaling microclusters containing the adaptor SLP-76. Immunity 28:810-821.
9. Campi, G., R. Varma, and M. L. Dustin. 2005. Actin and agonist MHC-peptide complex-dependent T cell receptor microclusters as scaffolds for signaling. The Journal of experimental medicine 202:1031-1036.
10. Varma, R., G. Campi, T. Yokosuka, T. Saito, and M. L. Dustin. 2006. T cell receptor-proximal signals are sustained in peripheral microclusters and terminated in the central supramolecular activation cluster. Immunity 25:117-127.
11. Tan, Y. X., B. N. Manz, T. S. Freedman, C. Zhang, K. M. Shokat, and A. Weiss. 2014. Inhibition of the kinase Csk in thymocytes reveals a requirement for actin remodeling in the initiation of full TCR signaling. Nature immunology 15:186-194.
12. Blin, G., E. Margeat, K. Carvalho, C. A. Royer, C. Roy, and C. Picart. 2008. Quantitative analysis of the binding of ezrin to large unilamellar vesicles containing phosphatidylinositol 4,5 bisphosphate. Biophysical journal 94:1021-1033.

13. Gambhir, A., G. Hangyas-Mihalyne, I. Zaitseva, D. S. Cafiso, J. Wang, D. Murray, S. N. Pentyala, S. O. Smith, and S. McLaughlin. 2004. Electrostatic sequestration of PIP2 on phospholipid membranes by basic/aromatic regions of proteins. Biophysical journal 86:2188-2207.
14. Stone, J. D., A. S. Chervin, and D. M. Kranz. 2009. T-cell receptor binding affinities and kinetics: impact on T-cell activity and specificity. Immunology 126:165-176.
15. Kersh, G. J., E. N. Kersh, D. H. Fremont, and P. M. Allen. 1998. High- and low-potency ligands with similar affinities for the TCR: the importance of kinetics in TCR signaling. Immunity 9:817-826.
16. Rosette, C., G. Werlen, M. A. Daniels, P. O. Holman, S. M. Alam, P. J. Travers, N. R. Gascoigne, E. Palmer, and S. C. Jameson. 2001. The impact of duration versus extent of TCR occupancy on T cell activation: a revision of the kinetic proofreading model. Immunity 15:59-70.
17. Hemmer, B., I. Stefanova, M. Vergelli, R. N. Germain, and R. Martin. 1998. Relationships among TCR ligand potency, thresholds for effector function elicitation, and the quality of early signaling events in human T cells. J Immunol 160:5807-5814.
18. Chen, J. L., A. J. Morgan, G. Stewart-Jones, D. Shepherd, G. Bossi, L. Wooldridge, S. L. Hutchinson, A. K. Sewell, G. M. Griffiths, P. A. van der Merwe, E. Y. Jones, A. Galione, and V. Cerundolo. 2010. Ca2+ release from the endoplasmic reticulum of NY-ESO-1-specific T cells is modulated by the affinity of TCR and by the use of the CD8 coreceptor. J Immunol 184:1829-1839.
19. Jenkins, M. R., A. Tsun, J. C. Stinchcombe, and G. M. Griffiths. 2009. The strength of T cell receptor signal controls the polarization of cytotoxic machinery to the immunological synapse. Immunity 31:621-631.
20. Cai, Z., H. Kishimoto, A. Brunmark, M. R. Jackson, P. A. Peterson, and J. Sprent. 1997. Requirements for peptide-induced T cell receptor downregulation on naive CD8+ T cells. The Journal of experimental medicine 185:641-651.
21. Rabinowitz, J. D., C. Beeson, C. Wulfing, K. Tate, P. M. Allen, M. M. Davis, and H. M. McConnell. 1996. Altered T cell receptor ligands trigger a subset of early T cell signals. Immunity 5:125-135.
22. McKeithan, T. W. 1995. Kinetic proofreading in T-cell receptor signal transduction. Proceedings of the National Academy of Sciences of the United States of America 92:5042-5046.

23. Nauerth, M., B. Weissbrich, R. Knall, T. Franz, G. Dossinger, J. Bet, P. J. Paszkiewicz, L. Pfeifer, M. Bunse, W. Uckert, R. Holtappels, D. Gillert-Marien, M. Neuenhahn, A. Krackhardt, M. J. Reddehase, S. R. Riddell, and D. H. Busch. 2013. TCR-ligand koff rate correlates with the protective capacity of antigen-specific CD8+ T cells for adoptive transfer. Science translational medicine 5:192ra187.

24. Ely, L. K., K. J. Green, T. Beddoe, C. S. Clements, J. J. Miles, S. P. Bottomley, D. Zernich, L. Kjer-Nielsen, A. W. Purcell, J. McCluskey, J. Rossjohn, and S. R. Burrows. 2005. Antagonism of antiviral and allogeneic activity of a human public CTL clonotype by a single altered peptide ligand: implications for allograft rejection. J Immunol 174:5593-5601.

25. Tian, S., R. Maile, E. J. Collins, and J. A. Frelinger. 2007. CD8+ T cell activation is governed by TCR-peptide/MHC affinity, not dissociation rate. J Immunol 179:2952-2960.

26. Govern, C. C., M. K. Paczosa, A. K. Chakraborty, and E. S. Huseby. 2010. Fast on-rates allow short dwell time ligands to activate T cells. Proceedings of the National Academy of Sciences of the United States of America 107:8724-8729.

27. Kalergis, A. M., N. Boucheron, M. A. Doucey, E. Palmieri, E. C. Goyarts, Z. Vegh, I. F. Luescher, and S. G. Nathenson. 2001. Efficient T cell activation requires an optimal dwell-time of interaction between the TCR and the pMHC complex. Nature immunology 2:229-234.

28. Carreno, L. J., S. M. Bueno, P. Bull, S. G. Nathenson, and A. M. Kalergis. 2007. The half-life of the T-cell receptor/peptide-major histocompatibility complex interaction can modulate T-cell activation in response to bacterial challenge. Immunology 121:227-237.

29. Valitutti, S., S. Muller, M. Cella, E. Padovan, and A. Lanzavecchia. 1995. Serial triggering of many T-cell receptors by a few peptide-MHC complexes. Nature 375:148-151.

30. Purbhoo, M. A., D. J. Irvine, J. B. Huppa, and M. M. Davis. 2004. T cell killing does not require the formation of a stable mature immunological synapse. Nature immunology 5:524-530.

31. Holler, P. D., and D. M. Kranz. 2003. Quantitative analysis of the contribution of TCR/pepMHC affinity and CD8 to T cell activation. Immunity 18:255-264.

32. Li, Y., R. Moysey, P. E. Molloy, A. L. Vuidepot, T. Mahon, E. Baston, S. Dunn, N. Liddy, J. Jacob, B. K. Jakobsen, and J. M. Boulter. 2005. Directed evolution of

human T-cell receptors with picomolar affinities by phage display. Nature biotechnology 23:349-354.

33. Gonzalez, P. A., L. J. Carreno, D. Coombs, J. E. Mora, E. Palmieri, B. Goldstein, S. G. Nathenson, and A. M. Kalergis. 2005. T cell receptor binding kinetics required for T cell activation depend on the density of cognate ligand on the antigen-presenting cell. Proceedings of the National Academy of Sciences of the United States of America 102:4824-4829.
34. Aleksic, M., O. Dushek, H. Zhang, E. Shenderov, J. L. Chen, V. Cerundolo, D. Coombs, and P. A. van der Merwe. 2010. Dependence of T cell antigen recognition on T cell receptor-peptide MHC confinement time. Immunity 32:163-174.
35. Wulfing, C., J. D. Rabinowitz, C. Beeson, M. D. Sjaastad, H. M. McConnell, and M. M. Davis. 1997. Kinetics and extent of T cell activation as measured with the calcium signal. The Journal of experimental medicine 185:1815-1825.
36. Lavoie, P. M., A. R. Dumont, H. McGrath, A. E. Kernaleguen, and R. P. Sekaly. 2005. Delayed expansion of a restricted T cell repertoire by low-density TCR ligands. International immunology 17:931-941.
37. Huang, J., V. I. Zarnitsyna, B. Liu, L. J. Edwards, N. Jiang, B. D. Evavold, and C. Zhu. 2010. The kinetics of two-dimensional TCR and pMHC interactions determine T-cell responsiveness. Nature 464:932-936.
38. Huppa, J. B., M. Axmann, M. A. Mortelmaier, B. F. Lillemeier, E. W. Newell, M. Brameshuber, L. O. Klein, G. J. Schutz, and M. M. Davis. 2010. TCR-peptide-MHC interactions in situ show accelerated kinetics and increased affinity. Nature 463:963-967.
39. Robert, P., M. Aleksic, O. Dushek, V. Cerundolo, P. Bongrand, and P. A. van der Merwe. 2012. Kinetics and mechanics of two-dimensional interactions between T cell receptors and different activating ligands. Biophysical journal 102:248-257.
40. Schamel, W. W., I. Arechaga, R. M. Risueno, H. M. van Santen, P. Cabezas, C. Risco, J. M. Valpuesta, and B. Alarcon. 2005. Coexistence of multivalent and monovalent TCRs explains high sensitivity and wide range of response. The Journal of experimental medicine 202:493-503.
41. Schamel, W. W., and B. Alarcon. 2013. Organization of the resting TCR in nanoscale oligomers. Immunological reviews 251:13-20.
42. Kumar, R., M. Ferez, M. Swamy, I. Arechaga, M. T. Rejas, J. M. Valpuesta, W. W. Schamel, B. Alarcon, and H. M. van Santen. 2011. Increased sensitivity of antigen-

experienced T cells through the enrichment of oligomeric T cell receptor complexes. Immunity 35:375-387.

43. Molnar, E., M. Swamy, M. Holzer, K. Beck-Garcia, R. Worch, C. Thiele, G. Guigas, K. Boye, I. F. Luescher, P. Schwille, R. Schubert, and W. W. Schamel. 2012. Cholesterol and sphingomyelin drive ligand-independent T-cell antigen receptor nanoclustering. The Journal of biological chemistry 287:42664-42674.
44. Boniface, J. J., J. D. Rabinowitz, C. Wulfing, J. Hampl, Z. Reich, J. D. Altman, R. M. Kantor, C. Beeson, H. M. McConnell, and M. M. Davis. 1998. Initiation of signal transduction through the T cell receptor requires the multivalent engagement of peptide/MHC ligands [corrected]. Immunity 9:459-466.
45. Irvine, D. J., M. A. Purbhoo, M. Krogsgaard, and M. M. Davis. 2002. Direct observation of ligand recognition by T cells. Nature 419:845-849.
46. Lee, K. H., A. D. Holdorf, M. L. Dustin, A. C. Chan, P. M. Allen, and A. S. Shaw. 2002. T cell receptor signaling precedes immunological synapse formation. Science 295:1539-1542.
47. Yokosuka, T., and T. Saito. 2010. The immunological synapse, TCR microclusters, and T cell activation. Current topics in microbiology and immunology 340:81-107.
48. Seminario, M. C., and S. C. Bunnell. 2008. Signal initiation in T-cell receptor microclusters. Immunological reviews 221:90-106.
49. Yokosuka, T., K. Sakata-Sogawa, W. Kobayashi, M. Hiroshima, A. Hashimoto-Tane, M. Tokunaga, M. L. Dustin, and T. Saito. 2005. Newly generated T cell receptor microclusters initiate and sustain T cell activation by recruitment of Zap70 and SLP-76. Nature immunology 6:1253-1262.
50. Sykulev, Y., M. Joo, I. Vturina, T. J. Tsomides, and H. N. Eisen. 1996. Evidence that a single peptide-MHC complex on a target cell can elicit a cytolytic T cell response. Immunity 4:565-571.
51. Huppa, J. B., M. Gleimer, C. Sumen, and M. M. Davis. 2003. Continuous T cell receptor signaling required for synapse maintenance and full effector potential. Nature immunology 4:749-755.
52. Cemerski, S., J. Das, J. Locasale, P. Arnold, E. Giurisato, M. A. Markiewicz, D. Fremont, P. M. Allen, A. K. Chakraborty, and A. S. Shaw. 2007. The stimulatory potency of T cell antigens is influenced by the formation of the immunological synapse. Immunity 26:345-355.

53. Cemerski, S., J. Das, E. Giurisato, M. A. Markiewicz, P. M. Allen, A. K. Chakraborty, and A. S. Shaw. 2008. The balance between T cell receptor signaling and degradation at the center of the immunological synapse is determined by antigen quality. Immunity 29:414-422.
54. Lee, K. H., A. R. Dinner, C. Tu, G. Campi, S. Raychaudhuri, R. Varma, T. N. Sims, W. R. Burack, H. Wu, J. Wang, O. Kanagawa, M. Markiewicz, P. M. Allen, M. L. Dustin, A. K. Chakraborty, and A. S. Shaw. 2003. The immunological synapse balances T cell receptor signaling and degradation. Science 302:1218-1222.
55. Itoh, Y., B. Hemmer, R. Martin, and R. N. Germain. 1999. Serial TCR engagement and down-modulation by peptide:MHC molecule ligands: relationship to the quality of individual TCR signaling events. J Immunol 162:2073-2080.
56. Wherry, E. J., M. J. McElhaugh, and L. C. Eisenlohr. 2002. Generation of CD8(+) T cell memory in response to low, high, and excessive levels of epitope. J Immunol 168:4455-4461.
57. Henrickson, S. E., T. R. Mempel, I. B. Mazo, B. Liu, M. N. Artyomov, H. Zheng, A. Peixoto, M. P. Flynn, B. Senman, T. Junt, H. C. Wong, A. K. Chakraborty, and U. H. von Andrian. 2008. T cell sensing of antigen dose governs interactive behavior with dendritic cells and sets a threshold for T cell activation. Nature immunology 9:282-291.
58. Derby, M., M. Alexander-Miller, R. Tse, and J. Berzofsky. 2001. High-avidity CTL exploit two complementary mechanisms to provide better protection against viral infection than low-avidity CTL. J Immunol 166:1690-1697.
59. Viola, A., and A. Lanzavecchia. 1996. T cell activation determined by T cell receptor number and tunable thresholds. Science 273:104-106.
60. Gottschalk, R. A., M. M. Hathorn, H. Beuneu, E. Corse, M. L. Dustin, G. Altan-Bonnet, and J. P. Allison. 2012. Distinct influences of peptide-MHC quality and quantity on in vivo T-cell responses. Proceedings of the National Academy of Sciences of the United States of America 109:881-886.
61. Gottschalk, R. A., E. Corse, and J. P. Allison. 2010. TCR ligand density and affinity determine peripheral induction of Foxp3 in vivo. The Journal of experimental medicine 207:1701-1711.
62. Zhong, S., K. Malecek, L. A. Johnson, Z. Yu, E. Vega-Saenz de Miera, F. Darvishian, K. McGary, K. Huang, J. Boyer, E. Corse, Y. Shao, S. A. Rosenberg, N. P. Restifo, I. Osman, and M. Krogsgaard. 2013. T-cell receptor affinity and avidity defines

antitumor response and autoimmunity in T-cell immunotherapy. Proceedings of the National Academy of Sciences of the United States of America 110:6973-6978.

63. Corse, E., R. A. Gottschalk, M. Krogsgaard, and J. P. Allison. 2010. Attenuated T cell responses to a high-potency ligand in vivo. PLoS biology 8.

64. Zehn, D., S. Y. Lee, and M. J. Bevan. 2009. Complete but curtailed T-cell response to very low-affinity antigen. Nature 458:211-214.

65. Chervin, A. S., J. D. Stone, C. M. Soto, B. Engels, H. Schreiber, E. J. Roy, and D. M. Kranz. 2013. Design of T-cell receptor libraries with diverse binding properties to examine adoptive T-cell responses. Gene therapy 20:634-644.

66. Engels, B., A. S. Chervin, A. J. Sant, D. M. Kranz, and H. Schreiber. 2012. Long-term persistence of CD4(+) but rapid disappearance of CD8(+) T cells expressing an MHC class I-restricted TCR of nanomolar affinity. Molecular therapy : the journal of the American Society of Gene Therapy 20:652-660.

67. Janicki, C. N., S. R. Jenkinson, N. A. Williams, and D. J. Morgan. 2008. Loss of CTL function among high-avidity tumor-specific CD8+ T cells following tumor infiltration. Cancer research 68:2993-3000.

68. Holler, P. D., L. K. Chlewicki, and D. M. Kranz. 2003. TCRs with high affinity for foreign pMHC show self-reactivity. Nature immunology 4:55-62.

69. Zhao, Y., A. D. Bennett, Z. Zheng, Q. J. Wang, P. F. Robbins, L. Y. Yu, Y. Li, P. E. Molloy, S. M. Dunn, B. K. Jakobsen, S. A. Rosenberg, and R. A. Morgan. 2007. High-affinity TCRs generated by phage display provide CD4+ T cells with the ability to recognize and kill tumor cell lines. J Immunol 179:5845-5854.

70. Linette, G. P., E. A. Stadtmauer, M. V. Maus, A. P. Rapoport, B. L. Levine, L. Emery, L. Litzky, A. Bagg, B. M. Carreno, P. J. Cimino, G. K. Binder-Scholl, D. P. Smethurst, A. B. Gerry, N. J. Pumphrey, A. D. Bennett, J. E. Brewer, J. Dukes, J. Harper, H. K. Tayton-Martin, B. K. Jakobsen, N. J. Hassan, M. Kalos, and C. H. June. 2013. Cardiovascular toxicity and titin cross-reactivity of affinity-enhanced T cells in myeloma and melanoma. Blood 122:863-871.

71. Cameron, B. J., A. B. Gerry, J. Dukes, J. V. Harper, V. Kannan, F. C. Bianchi, F. Grand, J. E. Brewer, M. Gupta, G. Plesa, G. Bossi, A. Vuidepot, A. S. Powlesland, A. Legg, K. J. Adams, A. D. Bennett, N. J. Pumphrey, D. D. Williams, G. Binder-Scholl, I. Kulikovskaya, B. L. Levine, J. L. Riley, A. Varela-Rohena, E. A. Stadtmauer, A. P. Rapoport, G. P. Linette, C. H. June, N. J. Hassan, M. Kalos, and B. K. Jakobsen. 2013. Identification of a Titin-derived HLA-A1-presented peptide as a cross-reactive

target for engineered MAGE A3-directed T cells. Science translational medicine 5:197ra103.

72. Stromnes, I. M., T. M. Schmitt, A. G. Chapuis, S. R. Hingorani, and P. D. Greenberg. 2014. Re-adapting T cells for cancer therapy: from mouse models to clinical trials. Immunological reviews 257:145-164.

73. Dunn, G. P., L. J. Old, and R. D. Schreiber. 2004. The three Es of cancer immunoediting. Annual review of immunology 22:329-360.

74. Ruella, M., and M. Kalos. 2014. Adoptive immunotherapy for cancer. Immunological reviews 257:14-38.

75. Xing, Y., and K. A. Hogquist. 2012. T-cell tolerance: central and peripheral. Cold Spring Harbor perspectives in biology 4.

76. Cecco, S., E. Muraro, E. Giacomin, D. Martorelli, R. Lazzarini, P. Baldo, and R. Dolcetti. 2011. Cancer vaccines in phase II/III clinical trials: state of the art and future perspectives. Current cancer drug targets 11:85-102.

77. Leavy, O. 2010. Therapeutic antibodies: past, present and future. Nature reviews. Immunology 10:297.

78. Pardoll, D. M. 2012. The blockade of immune checkpoints in cancer immunotherapy. Nature reviews. Cancer 12:252-264.

79. Gross, S., A. Geldmacher, T. Sharav, F. Losch, and P. Walden. 2009. Immunosuppressive mechanisms in cancer: consequences for the development of therapeutic vaccines. Vaccine 27:3398-3400.

80. Rosenberg, S. A., J. R. Yannelli, J. C. Yang, S. L. Topalian, D. J. Schwartzentruber, J. S. Weber, D. R. Parkinson, C. A. Seipp, J. H. Einhorn, and D. E. White. 1994. Treatment of patients with metastatic melanoma with autologous tumor-infiltrating lymphocytes and interleukin 2. Journal of the National Cancer Institute 86:1159-1166.

81. Prieto, P. A., K. H. Durflinger, J. R. Wunderlich, S. A. Rosenberg, and M. E. Dudley. 2010. Enrichment of CD8+ cells from melanoma tumor-infiltrating lymphocyte cultures reveals tumor reactivity for use in adoptive cell therapy. J Immunother 33:547-556.

82. Dudley, M. E., J. R. Wunderlich, T. E. Shelton, J. Even, and S. A. Rosenberg. 2003. Generation of tumor-infiltrating lymphocyte cultures for use in adoptive transfer therapy for melanoma patients. J Immunother 26:332-342.

83. Tran, K. Q., J. Zhou, K. H. Durflinger, M. M. Langhan, T. E. Shelton, J. R. Wunderlich, P. F. Robbins, S. A. Rosenberg, and M. E. Dudley. 2008. Minimally cultured tumor-infiltrating lymphocytes display optimal characteristics for adoptive cell therapy. J Immunother 31:742-751.
84. Zhou, J., X. Shen, J. Huang, R. J. Hodes, S. A. Rosenberg, and P. F. Robbins. 2005. Telomere length of transferred lymphocytes correlates with in vivo persistence and tumor regression in melanoma patients receiving cell transfer therapy. J Immunol 175:7046-7052.
85. Cheadle, E. J., H. Gornall, V. Baldan, V. Hanson, R. E. Hawkins, and D. E. Gilham. 2014. CAR T cells: driving the road from the laboratory to the clinic. Immunological reviews 257:91-106.
86. Hanagiri, T., Y. Shigematsu, S. Shinohara, M. Takenaka, S. Oka, Y. Chikaishi, Y. Nagata, T. Baba, H. Uramoto, T. So, and S. Yamada. 2013. Clinical significance of expression of cancer/testis antigen and down-regulation of HLA class-I in patients with stage I non-small cell lung cancer. Anticancer research 33:2123-2128.
87. Yeung, J. T., R. L. Hamilton, K. Ohnishi, M. Ikeura, D. M. Potter, M. N. Nikiforova, S. Ferrone, R. I. Jakacki, I. F. Pollack, and H. Okada. 2013. LOH in the HLA class I region at 6p21 is associated with shorter survival in newly diagnosed adult glioblastoma. Clinical cancer research : an official journal of the American Association for Cancer Research 19:1816-1826.
88. Jena, B., G. Dotti, and L. J. Cooper. 2010. Redirecting T-cell specificity by introducing a tumor-specific chimeric antigen receptor. Blood 116:1035-1044.
89. Field, A. C., C. Vink, R. Gabriel, R. Al-Subki, M. Schmidt, N. Goulden, H. Stauss, A. Thrasher, E. Morris, and W. Qasim. 2013. Comparison of lentiviral and sleeping beauty mediated alphabeta T cell receptor gene transfer. PloS one 8:e68201.
90. Scholler, J., T. L. Brady, G. Binder-Scholl, W. T. Hwang, G. Plesa, K. M. Hege, A. N. Vogel, M. Kalos, J. L. Riley, S. G. Deeks, R. T. Mitsuyasu, W. B. Bernstein, N. E. Aronson, B. L. Levine, F. D. Bushman, and C. H. June. 2012. Decade-long safety and function of retroviral-modified chimeric antigen receptor T cells. Science translational medicine 4:132ra153.
91. Hacein-Bey-Abina, S., C. von Kalle, M. Schmidt, F. Le Deist, N. Wulffraat, E. McIntyre, I. Radford, J. L. Villeval, C. C. Fraser, M. Cavazzana-Calvo, and A. Fischer. 2003. A serious adverse event after successful gene therapy for X-linked

severe combined immunodeficiency. The New England journal of medicine 348:255-256.

92. Singh, H., H. Huls, P. Kebriaei, and L. J. Cooper. 2014. A new approach to gene therapy using Sleeping Beauty to genetically modify clinical-grade T cells to target CD19. Immunological reviews 257:181-190.

93. Singh, H., M. J. Figliola, M. J. Dawson, S. Olivares, L. Zhang, G. Yang, S. Maiti, P. Manuri, V. Senyukov, B. Jena, P. Kebriaei, R. E. Champlin, H. Huls, and L. J. Cooper. 2013. Manufacture of clinical-grade CD19-specific T cells stably expressing chimeric antigen receptor using Sleeping Beauty system and artificial antigen presenting cells. PloS one 8:e64138.

94. Singh, H., P. R. Manuri, S. Olivares, N. Dara, M. J. Dawson, H. Huls, P. B. Hackett, D. B. Kohn, E. J. Shpall, R. E. Champlin, and L. J. Cooper. 2008. Redirecting specificity of T-cell populations for CD19 using the Sleeping Beauty system. Cancer research 68:2961-2971.

95. Suhoski, M. M., T. N. Golovina, N. A. Aqui, V. C. Tai, A. Varela-Rohena, M. C. Milone, R. G. Carroll, J. L. Riley, and C. H. June. 2007. Engineering artificial antigen-presenting cells to express a diverse array of co-stimulatory molecules. Molecular therapy : the journal of the American Society of Gene Therapy 15:981-988.

96. Zhang, H., K. M. Snyder, M. M. Suhoski, M. V. Maus, V. Kapoor, C. H. June, and C. L. Mackall. 2007. 4-1BB is superior to CD28 costimulation for generating CD8+ cytotoxic lymphocytes for adoptive immunotherapy. J Immunol 179:4910-4918.

97. Paulos, C. M., M. M. Suhoski, G. Plesa, T. Jiang, S. Basu, T. N. Golovina, S. Jiang, N. A. Aqui, D. J. Powell, Jr., B. L. Levine, R. G. Carroll, J. L. Riley, and C. H. June. 2008. Adoptive immunotherapy: good habits instilled at youth have long-term benefits. Immunologic research 42:182-196.

98. Till, B. G., M. C. Jensen, J. Wang, E. Y. Chen, B. L. Wood, H. A. Greisman, X. Qian, S. E. James, A. Raubitschek, S. J. Forman, A. K. Gopal, J. M. Pagel, C. G. Lindgren, P. D. Greenberg, S. R. Riddell, and O. W. Press. 2008. Adoptive immunotherapy for indolent non-Hodgkin lymphoma and mantle cell lymphoma using genetically modified autologous CD20-specific T cells. Blood 112:2261-2271.

99. Lamers, C. H., S. Sleijfer, A. G. Vulto, W. H. Kruit, M. Kliffen, R. Debets, J. W. Gratama, G. Stoter, and E. Oosterwijk. 2006. Treatment of metastatic renal cell carcinoma with autologous T-lymphocytes genetically retargeted against carbonic

anhydrase IX: first clinical experience. Journal of clinical oncology : official journal of the American Society of Clinical Oncology 24:e20-22.

100. Kershaw, M. H., J. A. Westwood, L. L. Parker, G. Wang, Z. Eshhar, S. A. Mavroukakis, D. E. White, J. R. Wunderlich, S. Canevari, L. Rogers-Freezer, C. C. Chen, J. C. Yang, S. A. Rosenberg, and P. Hwu. 2006. A phase I study on adoptive immunotherapy using gene-modified T cells for ovarian cancer. Clinical cancer research : an official journal of the American Association for Cancer Research 12:6106-6115.

101. Savoldo, B., C. A. Ramos, E. Liu, M. P. Mims, M. J. Keating, G. Carrum, R. T. Kamble, C. M. Bollard, A. P. Gee, Z. Mei, H. Liu, B. Grilley, C. M. Rooney, H. E. Heslop, M. K. Brenner, and G. Dotti. 2011. CD28 costimulation improves expansion and persistence of chimeric antigen receptor-modified T cells in lymphoma patients. The Journal of clinical investigation 121:1822-1826.

102. Maher, J., R. J. Brentjens, G. Gunset, I. Riviere, and M. Sadelain. 2002. Human T-lymphocyte cytotoxicity and proliferation directed by a single chimeric TCRzeta /CD28 receptor. Nature biotechnology 20:70-75.

103. Loskog, A., V. Giandomenico, C. Rossig, M. Pule, G. Dotti, and M. K. Brenner. 2006. Addition of the CD28 signaling domain to chimeric T-cell receptors enhances chimeric T-cell resistance to T regulatory cells. Leukemia 20:1819-1828.

104. Kowolik, C. M., M. S. Topp, S. Gonzalez, T. Pfeiffer, S. Olivares, N. Gonzalez, D. D. Smith, S. J. Forman, M. C. Jensen, and L. J. Cooper. 2006. CD28 costimulation provided through a CD19-specific chimeric antigen receptor enhances in vivo persistence and antitumor efficacy of adoptively transferred T cells. Cancer research 66:10995-11004.

105. Brentjens, R. J., E. Santos, Y. Nikhamin, R. Yeh, M. Matsushita, K. La Perle, A. Quintas-Cardama, S. M. Larson, and M. Sadelain. 2007. Genetically targeted T cells eradicate systemic acute lymphoblastic leukemia xenografts. Clinical cancer research : an official journal of the American Association for Cancer Research 13:5426-5435.

106. Milone, M. C., J. D. Fish, C. Carpenito, R. G. Carroll, G. K. Binder, D. Teachey, M. Samanta, M. Lakhal, B. Gloss, G. Danet-Desnoyers, D. Campana, J. L. Riley, S. A. Grupp, and C. H. June. 2009. Chimeric receptors containing CD137 signal transduction domains mediate enhanced survival of T cells and increased

antileukemic efficacy in vivo. Molecular therapy : the journal of the American Society of Gene Therapy 17:1453-1464.

107. Hombach, A. A., J. Heiders, M. Foppe, M. Chmielewski, and H. Abken. 2012. OX40 costimulation by a chimeric antigen receptor abrogates CD28 and IL-2 induced IL-10 secretion by redirected CD4(+) T cells. Oncoimmunology 1:458-466.

108. Altvater, B., S. Landmeier, S. Pscherer, J. Temme, H. Juergens, M. Pule, and C. Rossig. 2009. 2B4 (CD244) signaling via chimeric receptors costimulates tumor-antigen specific proliferation and in vitro expansion of human T cells. Cancer immunology, immunotherapy : CII 58:1991-2001.

109. Song, D. G., Q. Ye, M. Poussin, G. M. Harms, M. Figini, and D. J. Powell, Jr. 2012. CD27 costimulation augments the survival and antitumor activity of redirected human T cells in vivo. Blood 119:696-706.

110. Shen, C. J., Y. X. Yang, E. Q. Han, N. Cao, Y. F. Wang, Y. Wang, Y. Y. Zhao, L. M. Zhao, J. Cui, P. Gupta, A. J. Wong, and S. Y. Han. 2013. Chimeric antigen receptor containing ICOS signaling domain mediates specific and efficient antitumor effect of T cells against EGFRvIII expressing glioma. Journal of hematology & oncology 6:33.

111. Grupp, S. A., M. Kalos, D. Barrett, R. Aplenc, D. L. Porter, S. R. Rheingold, D. T. Teachey, A. Chew, B. Hauck, J. F. Wright, M. C. Milone, B. L. Levine, and C. H. June. 2013. Chimeric antigen receptor-modified T cells for acute lymphoid leukemia. The New England journal of medicine 368:1509-1518.

112. Porter, D. L., B. L. Levine, M. Kalos, A. Bagg, and C. H. June. 2011. Chimeric antigen receptor-modified T cells in chronic lymphoid leukemia. The New England journal of medicine 365:725-733.

113. Tammana, S., X. Huang, M. Wong, M. C. Milone, L. Ma, B. L. Levine, C. H. June, J. E. Wagner, B. R. Blazar, and X. Zhou. 2010. 4-1BB and CD28 signaling plays a synergistic role in redirecting umbilical cord blood T cells against B-cell malignancies. Human gene therapy 21:75-86.

114. Hombach, A. A., and H. Abken. 2011. Costimulation by chimeric antigen receptors revisited the T cell antitumor response benefits from combined CD28-OX40 signalling. International journal of cancer. Journal international du cancer 129:2935-2944.

115. Wilkie, S., G. Picco, J. Foster, D. M. Davies, S. Julien, L. Cooper, S. Arif, S. J. Mather, J. Taylor-Papadimitriou, J. M. Burchell, and J. Maher. 2008. Retargeting of

human T cells to tumor-associated MUC1: the evolution of a chimeric antigen receptor. J Immunol 180:4901-4909.

116. Hombach, A. A., V. Schildgen, C. Heuser, R. Finnern, D. E. Gilham, and H. Abken. 2007. T cell activation by antibody-like immunoreceptors: the position of the binding epitope within the target molecule determines the efficiency of activation of redirected T cells. J Immunol 178:4650-4657.

117. James, S. E., P. D. Greenberg, M. C. Jensen, Y. Lin, J. Wang, B. G. Till, A. A. Raubitschek, S. J. Forman, and O. W. Press. 2008. Antigen sensitivity of CD22-specific chimeric TCR is modulated by target epitope distance from the cell membrane. J Immunol 180:7028-7038.

118. Guest, R. D., R. E. Hawkins, N. Kirillova, E. J. Cheadle, J. Arnold, A. O'Neill, J. Irlam, K. A. Chester, J. T. Kemshead, D. M. Shaw, M. J. Embleton, P. L. Stern, and D. E. Gilham. 2005. The role of extracellular spacer regions in the optimal design of chimeric immune receptors: evaluation of four different scFvs and antigens. J Immunother 28:203-211.

119. Hudecek, M., M. T. Lupo-Stanghellini, P. L. Kosasih, D. Sommermeyer, M. C. Jensen, C. Rader, and S. R. Riddell. 2013. Receptor affinity and extracellular domain modifications affect tumor recognition by ROR1-specific chimeric antigen receptor T cells. Clinical cancer research : an official journal of the American Association for Cancer Research 19:3153-3164.

120. Chmielewski, M., A. Hombach, C. Heuser, G. P. Adams, and H. Abken. 2004. T cell activation by antibody-like immunoreceptors: increase in affinity of the single-chain fragment domain above threshold does not increase T cell activation against antigen-positive target cells but decreases selectivity. J Immunol 173:7647-7653.

121. Alvarez-Vallina, L., and S. J. Russell. 1999. Efficient discrimination between different densities of target antigen by tetracycline-regulatable T bodies. Human gene therapy 10:559-563.

122. James, S. E., P. D. Greenberg, M. C. Jensen, Y. Lin, J. Wang, L. E. Budde, B. G. Till, A. A. Raubitschek, S. J. Forman, and O. W. Press. 2010. Mathematical modeling of chimeric TCR triggering predicts the magnitude of target lysis and its impairment by TCR downmodulation. J Immunol 184:4284-4294.

123. Weijtens, M. E., E. H. Hart, and R. L. Bolhuis. 2000. Functional balance between T cell chimeric receptor density and tumor associated antigen density: CTL mediated cytolysis and lymphokine production. Gene therapy 7:35-42.

124. Turatti, F., M. Figini, E. Balladore, P. Alberti, P. Casalini, J. D. Marks, S. Canevari, and D. Mezzanzanica. 2007. Redirected activity of human antitumor chimeric immune receptors is governed by antigen and receptor expression levels and affinity of interaction. J Immunother 30:684-693.

125. Bridgeman, J. S., R. E. Hawkins, S. Bagley, M. Blaylock, M. Holland, and D. E. Gilham. 2010. The optimal antigen response of chimeric antigen receptors harboring the CD3zeta transmembrane domain is dependent upon incorporation of the receptor into the endogenous TCR/CD3 complex. J Immunol 184:6938-6949.

126. Bridgeman, J. S., K. Ladell, V. E. Sheard, K. Miners, R. E. Hawkins, D. A. Price, and D. E. Gilham. 2013. CD3zeta-based chimeric antigen receptors mediate T-cell activation via cis- and trans-signalling mechanisms: implications for optimization of receptor structure for adoptive cell therapy. Clinical and experimental immunology.

127. Torikai, H., A. Reik, P. Q. Liu, Y. Zhou, L. Zhang, S. Maiti, H. Huls, J. C. Miller, P. Kebriaei, B. Rabinovitch, D. A. Lee, R. E. Champlin, C. Bonini, L. Naldini, E. J. Rebar, P. D. Gregory, M. C. Holmes, and L. J. Cooper. 2012. A foundation for universal T-cell based immunotherapy: T cells engineered to express a CD19-specific chimeric-antigen-receptor and eliminate expression of endogenous TCR. Blood 119:5697-5705.

128. Serrano, L. M., T. Pfeiffer, S. Olivares, T. Numbenjapon, J. Bennitt, D. Kim, D. Smith, G. McNamara, Z. Al-Kadhimi, J. Rosenthal, S. J. Forman, M. C. Jensen, and L. J. Cooper. 2006. Differentiation of naive cord-blood T cells into CD19-specific cytolytic effectors for posttransplantation adoptive immunotherapy. Blood 107:2643-2652.

129. Kochenderfer, J. N., and S. A. Rosenberg. 2013. Treating B-cell cancer with T cells expressing anti-CD19 chimeric antigen receptors. Nature reviews. Clinical oncology 10:267-276.

130. Jensen, M. C., L. Popplewell, L. J. Cooper, D. DiGiusto, M. Kalos, J. R. Ostberg, and S. J. Forman. 2010. Antitransgene rejection responses contribute to attenuated persistence of adoptively transferred CD20/CD19-specific chimeric antigen receptor redirected T cells in humans. Biology of blood and marrow transplantation : journal of the American Society for Blood and Marrow Transplantation 16:1245-1256.

131. Davila, M. L., I. Riviere, X. Wang, S. Bartido, J. Park, K. Curran, S. S. Chung, J. Stefanski, O. Borquez-Ojeda, M. Olszewska, J. Qu, T. Wasielewska, Q. He, M. Fink, H. Shinglot, M. Youssif, M. Satter, Y. Wang, J. Hosey, H. Quintanilla, E. Halton, Y. Bernal, D. C. Bouhassira, M. E. Arcila, M. Gonen, G. J. Roboz, P. Maslak, D. Douer,

M. G. Frattini, S. Giralt, M. Sadelain, and R. Brentjens. 2014. Efficacy and Toxicity Management of 19-28z CAR T Cell Therapy in B Cell Acute Lymphoblastic Leukemia. Science translational medicine 6:224ra225.

132. Brentjens, R. J., M. L. Davila, I. Riviere, J. Park, X. Wang, L. G. Cowell, S. Bartido, J. Stefanski, C. Taylor, M. Olszewska, O. Borquez-Ojeda, J. Qu, T. Wasielewska, Q. He, Y. Bernal, I. V. Rijo, C. Hedvat, R. Kobos, K. Curran, P. Steinherz, J. Jurcic, T. Rosenblat, P. Maslak, M. Frattini, and M. Sadelain. 2013. CD19-targeted T cells rapidly induce molecular remissions in adults with chemotherapy-refractory acute lymphoblastic leukemia. Science translational medicine 5:177ra138.

133. Brentjens, R. J., I. Riviere, J. H. Park, M. L. Davila, X. Wang, J. Stefanski, C. Taylor, R. Yeh, S. Bartido, O. Borquez-Ojeda, M. Olszewska, Y. Bernal, H. Pegram, M. Przybylowski, D. Hollyman, Y. Usachenko, D. Pirraglia, J. Hosey, E. Santos, E. Halton, P. Maslak, D. Scheinberg, J. Jurcic, M. Heaney, G. Heller, M. Frattini, and M. Sadelain. 2011. Safety and persistence of adoptively transferred autologous CD19-targeted T cells in patients with relapsed or chemotherapy refractory B-cell leukemias. Blood 118:4817-4828.

134. Brentjens, R., R. Yeh, Y. Bernal, I. Riviere, and M. Sadelain. 2010. Treatment of chronic lymphocytic leukemia with genetically targeted autologous T cells: case report of an unforeseen adverse event in a phase I clinical trial. Molecular therapy : the journal of the American Society of Gene Therapy 18:666-668.

135. Kochenderfer, J. N., M. E. Dudley, R. O. Carpenter, S. H. Kassim, J. J. Rose, W. G. Telford, F. T. Hakim, D. C. Halverson, D. H. Fowler, N. M. Hardy, A. R. Mato, D. D. Hickstein, J. C. Gea-Banacloche, S. Z. Pavletic, C. Sportes, I. Maric, S. A. Feldman, B. G. Hansen, J. S. Wilder, B. Blacklock-Schuver, B. Jena, M. R. Bishop, R. E. Gress, and S. A. Rosenberg. 2013. Donor-derived CD19-targeted T cells cause regression of malignancy persisting after allogeneic hematopoietic stem cell transplantation. Blood 122:4129-4139.

136. Kochenderfer, J. N., W. H. Wilson, J. E. Janik, M. E. Dudley, M. Stetler-Stevenson, S. A. Feldman, I. Maric, M. Raffeld, D. A. Nathan, B. J. Lanier, R. A. Morgan, and S. A. Rosenberg. 2010. Eradication of B-lineage cells and regression of lymphoma in a patient treated with autologous T cells genetically engineered to recognize CD19. Blood 116:4099-4102.

137. Kochenderfer, J. N., M. E. Dudley, S. A. Feldman, W. H. Wilson, D. E. Spaner, I. Maric, M. Stetler-Stevenson, G. Q. Phan, M. S. Hughes, R. M. Sherry, J. C. Yang, U.

S. Kammula, L. Devillier, R. Carpenter, D. A. Nathan, R. A. Morgan, C. Laurencot, and S. A. Rosenberg. 2012. B-cell depletion and remissions of malignancy along with cytokine-associated toxicity in a clinical trial of anti-CD19 chimeric-antigen-receptor-transduced T cells. Blood 119:2709-2720.

138. Kalos, M., B. L. Levine, D. L. Porter, S. Katz, S. A. Grupp, A. Bagg, and C. H. June. 2011. T cells with chimeric antigen receptors have potent antitumor effects and can establish memory in patients with advanced leukemia. Science translational medicine 3:95ra73.

139. Schroten, C., R. Kraaij, J. L. Veldhoven, C. A. Berrevoets, M. A. den Bakker, Q. Ma, M. Sadelain, C. H. Bangma, R. A. Willemsen, and R. Debets. 2010. T cell activation upon exposure to patient-derived tumor tissue: a functional assay to select patients for adoptive T cell therapy. Journal of immunological methods 359:11-20.

140. Lamers, C. H., S. Sleijfer, S. van Steenbergen, P. van Elzakker, B. van Krimpen, C. Groot, A. Vulto, M. den Bakker, E. Oosterwijk, R. Debets, and J. W. Gratama. 2013. Treatment of metastatic renal cell carcinoma with CAIX CAR-engineered T cells: clinical evaluation and management of on-target toxicity. Molecular therapy : the journal of the American Society of Gene Therapy 21:904-912.

141. Pule, M. A., B. Savoldo, G. D. Myers, C. Rossig, H. V. Russell, G. Dotti, M. H. Huls, E. Liu, A. P. Gee, Z. Mei, E. Yvon, H. L. Weiss, H. Liu, C. M. Rooney, H. E. Heslop, and M. K. Brenner. 2008. Virus-specific T cells engineered to coexpress tumor-specific receptors: persistence and antitumor activity in individuals with neuroblastoma. Nature medicine 14:1264-1270.

142. Louis, C. U., B. Savoldo, G. Dotti, M. Pule, E. Yvon, G. D. Myers, C. Rossig, H. V. Russell, O. Diouf, E. Liu, H. Liu, M. F. Wu, A. P. Gee, Z. Mei, C. M. Rooney, H. E. Heslop, and M. K. Brenner. 2011. Antitumor activity and long-term fate of chimeric antigen receptor-positive T cells in patients with neuroblastoma. Blood 118:6050-6056.

143. Morgan, R. A., J. C. Yang, M. Kitano, M. E. Dudley, C. M. Laurencot, and S. A. Rosenberg. 2010. Case report of a serious adverse event following the administration of T cells transduced with a chimeric antigen receptor recognizing ERBB2. Molecular therapy : the journal of the American Society of Gene Therapy 18:843-851.

144. Shirasu, N., H. Shibaguci, M. Kuroki, and H. Yamada. 2010. Construction and molecular characterization of human chimeric T-cell antigen receptors specific for carcinoembryonic antigen. Anticancer research 30:2731-2738.

145. Choi, B. D., C. M. Suryadevara, P. C. Gedeon, J. E. Herndon, 2nd, L. Sanchez-Perez, D. D. Bigner, and J. H. Sampson. 2014. Intracerebral delivery of a third generation EGFRvIII-specific chimeric antigen receptor is efficacious against human glioma. Journal of clinical neuroscience : official journal of the Neurosurgical Society of Australasia 21:189-190.

146. Morgan, R. A., L. A. Johnson, J. L. Davis, Z. Zheng, K. D. Woolard, E. A. Reap, S. A. Feldman, N. Chinnasamy, C. T. Kuan, H. Song, W. Zhang, H. A. Fine, and S. A. Rosenberg. 2012. Recognition of glioma stem cells by genetically modified T cells targeting EGFRvIII and development of adoptive cell therapy for glioma. Human gene therapy 23:1043-1053.

147. Bullain, S. S., A. Sahin, O. Szentirmai, C. Sanchez, N. Lin, E. Baratta, P. Waterman, R. Weissleder, R. C. Mulligan, and B. S. Carter. 2009. Genetically engineered T cells to target EGFRvIII expressing glioblastoma. Journal of neuro-oncology 94:373-382.

148. Kong, S., S. Sengupta, B. Tyler, A. J. Bais, Q. Ma, S. Doucette, J. Zhou, A. Sahin, B. S. Carter, H. Brem, R. P. Junghans, and P. Sampath. 2012. Suppression of human glioma xenografts with second-generation IL13R-specific chimeric antigen receptor-modified T cells. Clinical cancer research : an official journal of the American Association for Cancer Research 18:5949-5960.

149. Brown, C. E., R. Starr, B. Aguilar, A. F. Shami, C. Martinez, M. D'Apuzzo, M. E. Barish, S. J. Forman, and M. C. Jensen. 2012. Stem-like tumor-initiating cells isolated from IL13Ralpha2 expressing gliomas are targeted and killed by IL13-zetakine-redirected T Cells. Clinical cancer research : an official journal of the American Association for Cancer Research 18:2199-2209.

150. Kahlon, K. S., C. Brown, L. J. Cooper, A. Raubitschek, S. J. Forman, and M. C. Jensen. 2004. Specific recognition and killing of glioblastoma multiforme by interleukin 13-zetakine redirected cytolytic T cells. Cancer research 64:9160-9166.

151. Lanitis, E., M. Poussin, I. S. Hagemann, G. Coukos, R. Sandaltzopoulos, N. Scholler, and D. J. Powell, Jr. 2012. Redirected antitumor activity of primary human lymphocytes transduced with a fully human anti-mesothelin chimeric receptor. Molecular therapy : the journal of the American Society of Gene Therapy 20:633-643.

152. Zhao, Y., E. Moon, C. Carpenito, C. M. Paulos, X. Liu, A. L. Brennan, A. Chew, R. G. Carroll, J. Scholler, B. L. Levine, S. M. Albelda, and C. H. June. 2010. Multiple injections of electroporated autologous T cells expressing a chimeric antigen receptor mediate regression of human disseminated tumor. Cancer research 70:9053-9061.

153. Chinnasamy, D., E. Tran, Z. Yu, R. A. Morgan, N. P. Restifo, and S. A. Rosenberg. 2013. Simultaneous targeting of tumor antigens and the tumor vasculature using T lymphocyte transfer synergize to induce regression of established tumors in mice. Cancer research 73:3371-3380.

154. Peng, W., Y. Ye, B. A. Rabinovich, C. Liu, Y. Lou, M. Zhang, M. Whittington, Y. Yang, W. W. Overwijk, G. Lizee, and P. Hwu. 2010. Transduction of tumor-specific T cells with CXCR2 chemokine receptor improves migration to tumor and antitumor immune responses. Clinical cancer research : an official journal of the American Association for Cancer Research 16:5458-5468.

155. Craddock, J. A., A. Lu, A. Bear, M. Pule, M. K. Brenner, C. M. Rooney, and A. E. Foster. 2010. Enhanced tumor trafficking of GD2 chimeric antigen receptor T cells by expression of the chemokine receptor CCR2b. J Immunother 33:780-788.

156. Moon, E. K., C. Carpenito, J. Sun, L. C. Wang, V. Kapoor, J. Predina, D. J. Powell, Jr., J. L. Riley, C. H. June, and S. M. Albelda. 2011. Expression of a functional CCR2 receptor enhances tumor localization and tumor eradication by retargeted human T cells expressing a mesothelin-specific chimeric antibody receptor. Clinical cancer research : an official journal of the American Association for Cancer Research 17:4719-4730.

157. Di Stasi, A., B. De Angelis, C. M. Rooney, L. Zhang, A. Mahendravada, A. E. Foster, H. E. Heslop, M. K. Brenner, G. Dotti, and B. Savoldo. 2009. T lymphocytes coexpressing CCR4 and a chimeric antigen receptor targeting CD30 have improved homing and antitumor activity in a Hodgkin tumor model. Blood 113:6392-6402.

158. Barrett, D. M., D. T. Teachey, and S. A. Grupp. 2014. Toxicity management for patients receiving novel T-cell engaging therapies. Current opinion in pediatrics 26:43-49.

159. Davila, M. L., C. C. Kloss, G. Gunset, and M. Sadelain. 2013. CD19 CAR-targeted T cells induce long-term remission and B Cell Aplasia in an immunocompetent mouse model of B cell acute lymphoblastic leukemia. PloS one 8:e61338.

160. Maus, M. V., A. R. Haas, G. L. Beatty, S. M. Albelda, B. L. Levine, X. Liu, Y. Zhao, M. Kalos, and C. H. June. 2013. T cells expressing chimeric antigen receptors can cause anaphylaxis in humans. Cancer immunology research 1:26-31.

161. Berger, C., M. E. Flowers, E. H. Warren, and S. R. Riddell. 2006. Analysis of transgene-specific immune responses that limit the in vivo persistence of adoptively transferred HSV-TK-modified donor T cells after allogeneic hematopoietic cell transplantation. Blood 107:2294-2302.

162. Rettig, M. P., J. K. Ritchey, J. L. Prior, J. S. Haug, D. Piwnica-Worms, and J. F. DiPersio. 2004. Kinetics of in vivo elimination of suicide gene-expressing T cells affects engraftment, graft-versus-host disease, and graft-versus-leukemia after allogeneic bone marrow transplantation. J Immunol 173:3620-3630.

163. Di Stasi, A., S. K. Tey, G. Dotti, Y. Fujita, A. Kennedy-Nasser, C. Martinez, K. Straathof, E. Liu, A. G. Durett, B. Grilley, H. Liu, C. R. Cruz, B. Savoldo, A. P. Gee, J. Schindler, R. A. Krance, H. E. Heslop, D. M. Spencer, C. M. Rooney, and M. K. Brenner. 2011. Inducible apoptosis as a safety switch for adoptive cell therapy. The New England journal of medicine 365:1673-1683.

164. Budde, L. E., C. Berger, Y. Lin, J. Wang, X. Lin, S. E. Frayo, S. A. Brouns, D. M. Spencer, B. G. Till, M. C. Jensen, S. R. Riddell, and O. W. Press. 2013. Combining a CD20 Chimeric Antigen Receptor and an Inducible Caspase 9 Suicide Switch to Improve the Efficacy and Safety of T Cell Adoptive Immunotherapy for Lymphoma. PloS one 8:e82742.

165. Rabinovich, P. M., M. E. Komarovskaya, Z. J. Ye, C. Imai, D. Campana, E. Bahceci, and S. M. Weissman. 2006. Synthetic messenger RNA as a tool for gene therapy. Human gene therapy 17:1027-1035.

166. Yoon, S. H., J. M. Lee, H. I. Cho, E. K. Kim, H. S. Kim, M. Y. Park, and T. G. Kim. 2009. Adoptive immunotherapy using human peripheral blood lymphocytes transferred with RNA encoding Her-2/neu-specific chimeric immune receptor in ovarian cancer xenograft model. Cancer gene therapy 16:489-497.

167. Barrett, D. M., Y. Zhao, X. Liu, S. Jiang, C. Carpenito, M. Kalos, R. G. Carroll, C. H. June, and S. A. Grupp. 2011. Treatment of advanced leukemia in mice with mRNA engineered T cells. Human gene therapy 22:1575-1586.

168. Barrett, D. M., X. Liu, S. Jiang, C. H. June, S. A. Grupp, and Y. Zhao. 2013. Regimen-specific effects of RNA-modified chimeric antigen receptor T cells in mice with advanced leukemia. Human gene therapy 24:717-727.

169. Rabinovich, P. M., M. E. Komarovskaya, S. H. Wrzesinski, J. L. Alderman, T. Budak-Alpdogan, A. Karpikov, H. Guo, R. A. Flavell, N. K. Cheung, S. M. Weissman, and E. Bahceci. 2009. Chimeric receptor mRNA transfection as a tool to generate antineoplastic lymphocytes. Human gene therapy 20:51-61.

170. Johnson, D. R., and B. P. O'Neill. 2012. Glioblastoma survival in the United States before and during the temozolomide era. Journal of neuro-oncology 107:359-364.

171. Olar, A., and K. D. Aldape. 2014. Using the molecular classification of glioblastoma to inform personalized treatment. The Journal of pathology 232:165-177.

172. Kleihues, P., and H. Ohgaki. 1999. Primary and secondary glioblastomas: from concept to clinical diagnosis. Neuro-oncology 1:44-51.

173. Ohgaki, H., P. Dessen, B. Jourde, S. Horstmann, T. Nishikawa, P. L. Di Patre, C. Burkhard, D. Schuler, N. M. Probst-Hensch, P. C. Maiorka, N. Baeza, P. Pisani, Y. Yonekawa, M. G. Yasargil, U. M. Lutolf, and P. Kleihues. 2004. Genetic pathways to glioblastoma: a population-based study. Cancer research 64:6892-6899.

174. Schmidt, M. C., S. Antweiler, N. Urban, W. Mueller, A. Kuklik, B. Meyer-Puttlitz, O. D. Wiestler, D. N. Louis, R. Fimmers, and A. von Deimling. 2002. Impact of genotype and morphology on the prognosis of glioblastoma. Journal of neuropathology and experimental neurology 61:321-328.

175. Kim, B., J. K. Myung, J. H. Seo, C. K. Park, S. H. Paek, D. G. Kim, H. W. Jung, and S. H. Park. 2010. The clinicopathologic values of the molecules associated with the main pathogenesis of the glioblastoma. Journal of the neurological sciences 294:112-118.

176. Parsons, D. W., S. Jones, X. Zhang, J. C. Lin, R. J. Leary, P. Angenendt, P. Mankoo, H. Carter, I. M. Siu, G. L. Gallia, A. Olivi, R. McLendon, B. A. Rasheed, S. Keir, T. Nikolskaya, Y. Nikolsky, D. A. Busam, H. Tekleab, L. A. Diaz, Jr., J. Hartigan, D. R. Smith, R. L. Strausberg, S. K. Marie, S. M. Shinjo, H. Yan, G. J. Riggins, D. D. Bigner, R. Karchin, N. Papadopoulos, G. Parmigiani, B. Vogelstein, V. E. Velculescu, and K. W. Kinzler. 2008. An integrated genomic analysis of human glioblastoma multiforme. Science 321:1807-1812.

177. Liang, Y., M. Diehn, N. Watson, A. W. Bollen, K. D. Aldape, M. K. Nicholas, K. R. Lamborn, M. S. Berger, D. Botstein, P. O. Brown, and M. A. Israel. 2005. Gene expression profiling reveals molecularly and clinically distinct subtypes of glioblastoma multiforme. Proceedings of the National Academy of Sciences of the United States of America 102:5814-5819.

178. McNamara, M. G., S. Sahebjam, and W. P. Mason. 2013. Emerging biomarkers in glioblastoma. Cancers 5:1103-1119.
179. Kakkar, A., V. Suri, P. Jha, A. Srivastava, V. Sharma, P. Pathak, M. C. Sharma, M. S. Sharma, S. S. Kale, K. Chosdol, M. Phalak, and C. Sarkar. 2011. Loss of heterozygosity on chromosome 10q in glioblastomas, and its association with other genetic alterations and survival in Indian patients. Neurology India 59:254-261.
180. Smith, J. S., I. Tachibana, S. M. Passe, B. K. Huntley, T. J. Borell, N. Iturria, J. R. O'Fallon, P. L. Schaefer, B. W. Scheithauer, C. D. James, J. C. Buckner, and R. B. Jenkins. 2001. PTEN mutation, EGFR amplification, and outcome in patients with anaplastic astrocytoma and glioblastoma multiforme. Journal of the National Cancer Institute 93:1246-1256.
181. 2008. Comprehensive genomic characterization defines human glioblastoma genes and core pathways. Nature 455:1061-1068.
182. Hu, X., W. Miao, Y. Zou, W. Zhang, Y. Zhang, and H. Liu. 2013. Expression of p53, epidermal growth factor receptor, Ki-67 and O-methylguanine-DNA methyltransferase in human gliomas. Oncology letters 6:130-134.
183. Houillier, C., J. Lejeune, A. Benouaich-Amiel, F. Laigle-Donadey, E. Criniere, K. Mokhtari, J. Thillet, J. Y. Delattre, K. Hoang-Xuan, and M. Sanson. 2006. Prognostic impact of molecular markers in a series of 220 primary glioblastomas. Cancer 106:2218-2223.
184. Hynes, N. E., and H. A. Lane. 2005. ERBB receptors and cancer: the complexity of targeted inhibitors. Nature reviews. Cancer 5:341-354.
185. Kalman, B., E. Szep, F. Garzuly, and D. E. Post. 2013. Epidermal growth factor receptor as a therapeutic target in glioblastoma. Neuromolecular medicine 15:420-434.
186. Garrett, T. P., N. M. McKern, M. Lou, T. C. Elleman, T. E. Adams, G. O. Lovrecz, H. J. Zhu, F. Walker, M. J. Frenkel, P. A. Hoyne, R. N. Jorissen, E. C. Nice, A. W. Burgess, and C. W. Ward. 2002. Crystal structure of a truncated epidermal growth factor receptor extracellular domain bound to transforming growth factor alpha. Cell 110:763-773.
187. Ogiso, H., R. Ishitani, O. Nureki, S. Fukai, M. Yamanaka, J. H. Kim, K. Saito, A. Sakamoto, M. Inoue, M. Shirouzu, and S. Yokoyama. 2002. Crystal structure of the complex of human epidermal growth factor and receptor extracellular domains. Cell 110:775-787.

188. Yarden, Y., and M. X. Sliwkowski. 2001. Untangling the ErbB signalling network. Nature reviews. Molecular cell biology 2:127-137.

189. Taylor, T. E., F. B. Furnari, and W. K. Cavenee. 2012. Targeting EGFR for treatment of glioblastoma: molecular basis to overcome resistance. Current cancer drug targets 12:197-209.

190. Shinojima, N., K. Tada, S. Shiraishi, T. Kamiryo, M. Kochi, H. Nakamura, K. Makino, H. Saya, H. Hirano, J. Kuratsu, K. Oka, Y. Ishimaru, and Y. Ushio. 2003. Prognostic value of epidermal growth factor receptor in patients with glioblastoma multiforme. Cancer research 63:6962-6970.

191. Huang, H. S., M. Nagane, C. K. Klingbeil, H. Lin, R. Nishikawa, X. D. Ji, C. M. Huang, G. N. Gill, H. S. Wiley, and W. K. Cavenee. 1997. The enhanced tumorigenic activity of a mutant epidermal growth factor receptor common in human cancers is mediated by threshold levels of constitutive tyrosine phosphorylation and unattenuated signaling. The Journal of biological chemistry 272:2927-2935.

192. Schmidt, M. H., F. B. Furnari, W. K. Cavenee, and O. Bogler. 2003. Epidermal growth factor receptor signaling intensity determines intracellular protein interactions, ubiquitination, and internalization. Proceedings of the National Academy of Sciences of the United States of America 100:6505-6510.

193. Nishikawa, R., X. D. Ji, R. C. Harmon, C. S. Lazar, G. N. Gill, W. K. Cavenee, and H. J. Huang. 1994. A mutant epidermal growth factor receptor common in human glioma confers enhanced tumorigenicity. Proceedings of the National Academy of Sciences of the United States of America 91:7727-7731.

194. Ding, H., P. Shannon, N. Lau, X. Wu, L. Roncari, R. L. Baldwin, H. Takebayashi, A. Nagy, D. H. Gutmann, and A. Guha. 2003. Oligodendrogliomas result from the expression of an activated mutant epidermal growth factor receptor in a RAS transgenic mouse astrocytoma model. Cancer research 63:1106-1113.

195. Batra, S. K., S. Castelino-Prabhu, C. J. Wikstrand, X. Zhu, P. A. Humphrey, H. S. Friedman, and D. D. Bigner. 1995. Epidermal growth factor ligand-independent, unregulated, cell-transforming potential of a naturally occurring human mutant EGFRvIII gene. Cell growth & differentiation : the molecular biology journal of the American Association for Cancer Research 6:1251-1259.

196. Waha, A., A. Baumann, H. K. Wolf, R. Fimmers, J. Neumann, D. Kindermann, K. Astrahantseff, I. Blumcke, A. von Deimling, and U. Schlegel. 1996. Lack of prognostic relevance of alterations in the epidermal growth factor receptor-

transforming growth factor-alpha pathway in human astrocytic gliomas. Journal of neurosurgery 85:634-641.

197. Newcomb, E. W., H. Cohen, S. R. Lee, S. K. Bhalla, J. Bloom, R. L. Hayes, and D. C. Miller. 1998. Survival of patients with glioblastoma multiforme is not influenced by altered expression of p16, p53, EGFR, MDM2 or Bcl-2 genes. Brain Pathol 8:655-667.

198. Simmons, M. L., K. R. Lamborn, M. Takahashi, P. Chen, M. A. Israel, M. S. Berger, T. Godfrey, J. Nigro, M. Prados, S. Chang, F. G. Barker, 2nd, and K. Aldape. 2001. Analysis of complex relationships between age, p53, epidermal growth factor receptor, and survival in glioblastoma patients. Cancer research 61:1122-1128.

199. Galanis, E., J. Buckner, D. Kimmel, R. Jenkins, B. Alderete, J. O'Fallon, C. H. Wang, B. W. Scheithauer, and C. D. James. 1998. Gene amplification as a prognostic factor in primary and secondary high-grade malignant gliomas. International journal of oncology 13:717-724.

200. Bienkowski, M., S. Piaskowski, E. Stoczynska-Fidelus, M. Szybka, M. Banaszczyk, M. Witusik-Perkowska, E. Jesien-Lewandowicz, D. J. Jaskolski, A. Radomiak-Zaluska, D. Jesionek-Kupnicka, B. Sikorska, W. Papierz, P. Rieske, and P. P. Liberski. 2013. Screening for EGFR amplifications with a novel method and their significance for the outcome of glioblastoma patients. PloS one 8:e65444.

201. Yano, S., K. Kondo, M. Yamaguchi, G. Richmond, M. Hutchison, A. Wakeling, S. Averbuch, and P. Wadsworth. 2003. Distribution and function of EGFR in human tissue and the effect of EGFR tyrosine kinase inhibition. Anticancer research 23:3639-3650.

202. Moyer, J. D., E. G. Barbacci, K. K. Iwata, L. Arnold, B. Boman, A. Cunningham, C. DiOrio, J. Doty, M. J. Morin, M. P. Moyer, M. Neveu, V. A. Pollack, L. R. Pustilnik, M. M. Reynolds, D. Sloan, A. Theleman, and P. Miller. 1997. Induction of apoptosis and cell cycle arrest by CP-358,774, an inhibitor of epidermal growth factor receptor tyrosine kinase. Cancer research 57:4838-4848.

203. Halatsch, M. E., E. E. Gehrke, V. I. Vougioukas, I. C. Botefur, A. B. F, T. Efferth, E. Gebhart, S. Domhof, U. Schmidt, and M. Buchfelder. 2004. Inverse correlation of epidermal growth factor receptor messenger RNA induction and suppression of anchorage-independent growth by OSI-774, an epidermal growth factor receptor tyrosine kinase inhibitor, in glioblastoma multiforme cell lines. Journal of neurosurgery 100:523-533.

204. Lal, A., C. A. Glazer, H. M. Martinson, H. S. Friedman, G. E. Archer, J. H. Sampson, and G. J. Riggins. 2002. Mutant epidermal growth factor receptor up-regulates molecular effectors of tumor invasion. Cancer research 62:3335-3339.

205. D'Arcangelo, M., and F. Cappuzzo. 2013. Erlotinib in the first-line treatment of non-small-cell lung cancer. Expert review of anticancer therapy 13:523-533.

206. Kesavabhotla, K., C. D. Schlaff, B. Shin, L. Mubita, R. Kaplan, A. J. Tsiouris, S. C. Pannullo, P. Christos, E. Lavi, R. Scheff, and J. A. Boockvar. 2012. Phase I/II study of oral erlotinib for treatment of relapsed/refractory glioblastoma multiforme and anaplastic astrocytoma. Journal of experimental therapeutics & oncology 10:71-81.

207. Gallego, O., M. Cuatrecasas, M. Benavides, P. P. Segura, A. Berrocal, N. Erill, A. Colomer, M. J. Quintana, C. Balana, M. Gil, A. Gallardo, P. Murata, and A. Barnadas. 2014. Efficacy of erlotinib in patients with relapsed gliobastoma multiforme who expressed EGFRVIII and PTEN determined by immunohistochemistry. Journal of neuro-oncology 116:413-419.

208. Knight, L. A., F. Di Nicolantonio, P. Whitehouse, S. Mercer, S. Sharma, S. Glaysher, P. Johnson, and I. A. Cree. 2004. The in vitro effect of gefitinib ('Iressa') alone and in combination with cytotoxic chemotherapy on human solid tumours. BMC cancer 4:83.

209. Koyama, M., Y. Matsuzaki, S. Yogosawa, T. Hitomi, M. Kawanaka, and T. Sakai. 2007. ZD1839 induces p15INK4b and causes G1 arrest by inhibiting the mitogen-activated protein kinase/extracellular signal-regulated kinase pathway. Molecular cancer therapeutics 6:1579-1587.

210. Tracy, S., T. Mukohara, M. Hansen, M. Meyerson, B. E. Johnson, and P. A. Janne. 2004. Gefitinib induces apoptosis in the EGFRL858R non-small-cell lung cancer cell line H3255. Cancer research 64:7241-7244.

211. Chakravarti, A., M. Wang, H. I. Robins, T. Lautenschlaeger, W. J. Curran, D. G. Brachman, C. J. Schultz, A. Choucair, M. Dolled-Filhart, J. Christiansen, M. Gustavson, A. Molinaro, P. Mischel, A. P. Dicker, M. Bredel, and M. Mehta. 2013. RTOG 0211: a phase 1/2 study of radiation therapy with concurrent gefitinib for newly diagnosed glioblastoma patients. International journal of radiation oncology, biology, physics 85:1206-1211.

212. Uhm, J. H., K. V. Ballman, W. Wu, C. Giannini, J. C. Krauss, J. C. Buckner, C. D. James, B. W. Scheithauer, R. J. Behrens, P. J. Flynn, P. L. Schaefer, S. R. Dakhill, and K. A. Jaeckle. 2011. Phase II evaluation of gefitinib in patients with newly

diagnosed Grade 4 astrocytoma: Mayo/North Central Cancer Treatment Group Study N0074. International journal of radiation oncology, biology, physics 80:347-353.

213. Hegi, M. E., A. C. Diserens, P. Bady, Y. Kamoshima, M. C. Kouwenhoven, M. Delorenzi, W. L. Lambiv, M. F. Hamou, M. S. Matter, A. Koch, F. L. Heppner, Y. Yonekawa, A. Merlo, K. Frei, L. Mariani, and S. Hofer. 2011. Pathway analysis of glioblastoma tissue after preoperative treatment with the EGFR tyrosine kinase inhibitor gefitinib--a phase II trial. Molecular cancer therapeutics 10:1102-1112.

214. Li, S., K. R. Schmitz, P. D. Jeffrey, J. J. Wiltzius, P. Kussie, and K. M. Ferguson. 2005. Structural basis for inhibition of the epidermal growth factor receptor by cetuximab. Cancer cell 7:301-311.

215. Eller, J. L., S. L. Longo, M. M. Kyle, D. Bassano, D. J. Hicklin, and G. W. Canute. 2005. Anti-epidermal growth factor receptor monoclonal antibody cetuximab augments radiation effects in glioblastoma multiforme in vitro and in vivo. Neurosurgery 56:155-162; discussion 162.

216. Yang, S. H., Y. K. Hong, S. S. Jeun, I. S. Kim, J. T. Hong, J. H. Sung, B. C. Son, S. W. Lee, M. C. Kim, and K. S. Lee. 2009. Assessment of cetuximab efficacy by bioluminescence monitoring of intracranial glioblastoma xenograft in mouse. Journal of neuro-oncology 95:23-28.

217. Neyns, B., J. Sadones, E. Joosens, F. Bouttens, L. Verbeke, J. F. Baurain, L. D'Hondt, T. Strauven, C. Chaskis, P. In't Veld, A. Michotte, and J. De Greve. 2009. Stratified phase II trial of cetuximab in patients with recurrent high-grade glioma. Annals of oncology : official journal of the European Society for Medical Oncology / ESMO 20:1596-1603.

218. Lv, S., E. Teugels, J. Sadones, S. De Brakeleer, J. Duerinck, S. Du Four, A. Michotte, J. De Greve, and B. Neyns. 2012. Correlation of EGFR, IDH1 and PTEN status with the outcome of patients with recurrent glioblastoma treated in a phase II clinical trial with the EGFR-blocking monoclonal antibody cetuximab. International journal of oncology 41:1029-1035.

219. Hasselbalch, B., U. Lassen, H. S. Poulsen, and M. T. Stockhausen. 2010. Cetuximab insufficiently inhibits glioma cell growth due to persistent EGFR downstream signaling. Cancer investigation 28:775-787.

220. Clark, P. A., M. Iida, D. M. Treisman, H. Kalluri, S. Ezhilan, M. Zorniak, D. L. Wheeler, and J. S. Kuo. 2012. Activation of multiple ERBB family receptors mediates

glioblastoma cancer stem-like cell resistance to EGFR-targeted inhibition. Neoplasia 14:420-428.

221. Combs, S. E., D. Schulz-Ertner, W. Roth, C. Herold-Mende, J. Debus, and K. J. Weber. 2007. In vitro responsiveness of glioma cell lines to multimodality treatment with radiotherapy, temozolomide, and epidermal growth factor receptor inhibition with cetuximab. International journal of radiation oncology, biology, physics 68:873-882.

222. Combs, S. E., S. Heeger, R. Haselmann, L. Edler, J. Debus, and D. Schulz-Ertner. 2006. Treatment of primary glioblastoma multiforme with cetuximab, radiotherapy and temozolomide (GERT)--phase I/II trial: study protocol. BMC cancer 6:133.

223. Talavera, A., R. Friemann, S. Gomez-Puerta, C. Martinez-Fleites, G. Garrido, A. Rabasa, A. Lopez-Requena, A. Pupo, R. F. Johansen, O. Sanchez, U. Krengel, and E. Moreno. 2009. Nimotuzumab, an antitumor antibody that targets the epidermal growth factor receptor, blocks ligand binding while permitting the active receptor conformation. Cancer research 69:5851-5859.

224. Berger, C., U. Krengel, E. Stang, E. Moreno, and I. H. Madshus. 2011. Nimotuzumab and cetuximab block ligand-independent EGF receptor signaling efficiently at different concentrations. J Immunother 34:550-555.

225. Diaz Miqueli, A., J. Rolff, M. Lemm, I. Fichtner, R. Perez, and E. Montero. 2009. Radiosensitisation of U87MG brain tumours by anti-epidermal growth factor receptor monoclonal antibodies. British journal of cancer 100:950-958.

226. Bode, U., M. Massimino, F. Bach, M. Zimmermann, E. Khuhlaeva, M. Westphal, and G. Fleischhack. 2012. Nimotuzumab treatment of malignant gliomas. Expert opinion on biological therapy 12:1649-1659.

227. Solomon, M. T., J. C. Selva, J. Figueredo, J. Vaquer, C. Toledo, N. Quintanal, S. Salva, R. Domingez, J. Alert, J. J. Marinello, M. Catala, M. G. Griego, J. A. Martell, P. L. Luaces, J. Ballesteros, N. de-Castro, F. Bach, and T. Crombet. 2013. Radiotherapy plus nimotuzumab or placebo in the treatment of high grade glioma patients: results from a randomized, double blind trial. BMC cancer 13:299.

228. Allan, D. G. 2005. Nimotuzumab: evidence of clinical benefit without rash. The oncologist 10:760-761.

229. Lenz, H. J. 2006. Anti-EGFR mechanism of action: antitumor effect and underlying cause of adverse events. Oncology (Williston Park) 20:5-13.

230. Saif, M. W., and R. Kim. 2007. Incidence and management of cutaneous toxicities associated with cetuximab. Expert opinion on drug safety 6:175-182.

231. Garrido, G., I. A. Tikhomirov, A. Rabasa, E. Yang, E. Gracia, N. Iznaga, L. E. Fernandez, T. Crombet, R. S. Kerbel, and R. Perez. 2011. Bivalent binding by intermediate affinity of nimotuzumab: a contribution to explain antibody clinical profile. Cancer biology & therapy 11:373-382.

232. Diaz Miqueli, A., R. Blanco, B. Garcia, T. Badia, A. E. Batista, R. Alonso, and E. Montero. 2007. Biological activity in vitro of anti-epidermal growth factor receptor monoclonal antibodies with different affinities. Hybridoma (Larchmt) 26:423-431.

233. Del Vecchio, C. A., G. Li, and A. J. Wong. 2012. Targeting EGF receptor variant III: tumor-specific peptide vaccination for malignant gliomas. Expert review of vaccines 11:133-144.

234. Sampson, J. H., G. E. Archer, D. A. Mitchell, A. B. Heimberger, J. E. Herndon, 2nd, D. Lally-Goss, S. McGehee-Norman, A. Paolino, D. A. Reardon, A. H. Friedman, H. S. Friedman, and D. D. Bigner. 2009. An epidermal growth factor receptor variant III-targeted vaccine is safe and immunogenic in patients with glioblastoma multiforme. Molecular cancer therapeutics 8:2773-2779.

235. Sampson, J. H., A. B. Heimberger, G. E. Archer, K. D. Aldape, A. H. Friedman, H. S. Friedman, M. R. Gilbert, J. E. Herndon, 2nd, R. E. McLendon, D. A. Mitchell, D. A. Reardon, R. Sawaya, R. J. Schmittling, W. Shi, J. J. Vredenburgh, and D. D. Bigner. 2010. Immunologic escape after prolonged progression-free survival with epidermal growth factor receptor variant III peptide vaccination in patients with newly diagnosed glioblastoma. Journal of clinical oncology : official journal of the American Society of Clinical Oncology 28:4722-4729.

236. Snuderl, M., L. Fazlollahi, L. P. Le, M. Nitta, B. H. Zhelyazkova, C. J. Davidson, S. Akhavanfard, D. P. Cahill, K. D. Aldape, R. A. Betensky, D. N. Louis, and A. J. Iafrate. 2011. Mosaic amplification of multiple receptor tyrosine kinase genes in glioblastoma. Cancer cell 20:810-817.

237. Little, S. E., S. Popov, A. Jury, D. A. Bax, L. Doey, S. Al-Sarraj, J. M. Jurgensmeier, and C. Jones. 2012. Receptor tyrosine kinase genes amplified in glioblastoma exhibit a mutual exclusivity in variable proportions reflective of individual tumor heterogeneity. Cancer research 72:1614-1620.

238. Stommel, J. M., A. C. Kimmelman, H. Ying, R. Nabioullin, A. H. Ponugoti, R. Wiedemeyer, A. H. Stegh, J. E. Bradner, K. L. Ligon, C. Brennan, L. Chin, and R. A. DePinho. 2007. Coactivation of receptor tyrosine kinases affects the response of tumor cells to targeted therapies. Science 318:287-290.

239. Jun, H. J., J. Acquaviva, D. Chi, J. Lessard, H. Zhu, S. Woolfenden, R. T. Bronson, R. Pfannl, F. White, D. E. Housman, L. Iyer, C. A. Whittaker, A. Boskovitz, A. Raval, and A. Charest. 2012. Acquired MET expression confers resistance to EGFR inhibition in a mouse model of glioblastoma multiforme. Oncogene 31:3039-3050.

240. Bao, S., Q. Wu, R. E. McLendon, Y. Hao, Q. Shi, A. B. Hjelmeland, M. W. Dewhirst, D. D. Bigner, and J. N. Rich. 2006. Glioma stem cells promote radioresistance by preferential activation of the DNA damage response. Nature 444:756-760.

241. Tamura, K., M. Aoyagi, N. Ando, T. Ogishima, H. Wakimoto, M. Yamamoto, and K. Ohno. 2013. Expansion of CD133-positive glioma cells in recurrent de novo glioblastomas after radiotherapy and chemotherapy. Journal of neurosurgery 119:1145-1155.

242. Nagaraj, S., J. I. Youn, and D. I. Gabrilovich. 2013. Reciprocal relationship between myeloid-derived suppressor cells and T cells. J Immunol 191:17-23.

243. Callahan, M. K., and J. D. Wolchok. 2013. At the bedside: CTLA-4- and PD-1-blocking antibodies in cancer immunotherapy. Journal of leukocyte biology 94:41-53.

244. Rabinovich, G. A., D. Gabrilovich, and E. M. Sotomayor. 2007. Immunosuppressive strategies that are mediated by tumor cells. Annual review of immunology 25:267-296.

245. Leen, A. M., C. M. Rooney, and A. E. Foster. 2007. Improving T cell therapy for cancer. Annual review of immunology 25:243-265.

246. Gajewski, T. F., Y. Meng, C. Blank, I. Brown, A. Kacha, J. Kline, and H. Harlin. 2006. Immune resistance orchestrated by the tumor microenvironment. Immunological reviews 213:131-145.

247. Jackson, C., J. Ruzevick, J. Phallen, Z. Belcaid, and M. Lim. 2011. Challenges in immunotherapy presented by the glioblastoma multiforme microenvironment. Clinical & developmental immunology 2011:732413.

248. Wei, J., J. Barr, L. Y. Kong, Y. Wang, A. Wu, A. K. Sharma, J. Gumin, V. Henry, H. Colman, R. Sawaya, F. F. Lang, and A. B. Heimberger. 2010. Glioma-associated cancer-initiating cells induce immunosuppression. Clinical cancer research : an official journal of the American Association for Cancer Research 16:461-473.

249. Jacobs, J. F., A. J. Idema, K. F. Bol, S. Nierkens, O. M. Grauer, P. Wesseling, J. A. Grotenhuis, P. M. Hoogerbrugge, I. J. de Vries, and G. J. Adema. 2009. Regulatory T cells and the PD-L1/PD-1 pathway mediate immune suppression in malignant human brain tumors. Neuro-oncology 11:394-402.

250. Jansen, T., B. Tyler, J. L. Mankowski, V. R. Recinos, G. Pradilla, F. Legnani, J. Laterra, and A. Olivi. 2010. FasL gene knock-down therapy enhances the antiglioma immune response. Neuro-oncology 12:482-489.
251. El Andaloussi, A., and M. S. Lesniak. 2006. An increase in CD4+CD25+FOXP3+ regulatory T cells in tumor-infiltrating lymphocytes of human glioblastoma multiforme. Neuro-oncology 8:234-243.
252. Rodrigues, J. C., G. C. Gonzalez, L. Zhang, G. Ibrahim, J. J. Kelly, M. P. Gustafson, Y. Lin, A. B. Dietz, P. A. Forsyth, V. W. Yong, and I. F. Parney. 2010. Normal human monocytes exposed to glioma cells acquire myeloid-derived suppressor cell-like properties. Neuro-oncology 12:351-365.
253. Jarboe, J. S., K. R. Johnson, Y. Choi, R. R. Lonser, and J. K. Park. 2007. Expression of interleukin-13 receptor alpha2 in glioblastoma multiforme: implications for targeted therapies. Cancer research 67:7983-7986.
254. Wykosky, J., D. M. Gibo, C. Stanton, and W. Debinski. 2008. Interleukin-13 receptor alpha 2, EphA2, and Fos-related antigen 1 as molecular denominators of high-grade astrocytomas and specific targets for combinatorial therapy. Clinical cancer research : an official journal of the American Association for Cancer Research 14:199-208.
255. Brown, C. E., C. D. Warden, R. Starr, X. Deng, B. Badie, Y. C. Yuan, S. J. Forman, and M. E. Barish. 2013. Glioma IL13Ralpha2 is associated with mesenchymal signature gene expression and poor patient prognosis. PloS one 8:e77769.
256. Krebs, S., T. G. Rodriguez-Cruz, C. Derenzo, and S. Gottschalk. 2013. Genetically Modified T Cells to Target Glioblastoma. Frontiers in oncology 3:322.
257. Ahmed, N., V. S. Salsman, Y. Kew, D. Shaffer, S. Powell, Y. J. Zhang, R. G. Grossman, H. E. Heslop, and S. Gottschalk. 2010. HER2-specific T cells target primary glioblastoma stem cells and induce regression of autologous experimental tumors. Clinical cancer research : an official journal of the American Association for Cancer Research 16:474-485.
258. Mineo, J. F., A. Bordron, M. Baroncini, C. A. Maurage, C. Ramirez, R. M. Siminski, C. Berthou, and P. Dam Hieu. 2007. Low HER2-expressing glioblastomas are more often secondary to anaplastic transformation of low-grade glioma. Journal of neuro-oncology 85:281-287.
259. Hegde, M., A. Corder, K. K. Chow, M. Mukherjee, A. Ashoori, Y. Kew, Y. J. Zhang, D. S. Baskin, F. A. Merchant, V. S. Brawley, T. T. Byrd, S. Krebs, M. F. Wu, H. Liu, H. E. Heslop, S. Gottachalk, E. Yvon, and N. Ahmed. 2013. Combinational targeting

offsets antigen escape and enhances effector functions of adoptively transferred T cells in glioblastoma. Molecular therapy : the journal of the American Society of Gene Therapy 21:2087-2101.

260. Singh, H., M. J. Figliola, M. J. Dawson, H. Huls, S. Olivares, K. Switzer, T. Mi, S. Maiti, P. Kebriaei, D. A. Lee, R. E. Champlin, and L. J. Cooper. 2011. Reprogramming CD19-specific T cells with IL-21 signaling can improve adoptive immunotherapy of B-lineage malignancies. Cancer research 71:3516-3527.

261. Central Brain Tumor Registry of the United States (CBTRUS). CBTRUS Statistical Report: Primary Brain and Central Nervous System Tumors Diagnosed in the United States in 2004-2008. Available at cbtrus.org/2012-CBTRUS-SEER/CBTRUS_Report_2004-2008_3-23-2012.pdf. Accessed 02-05-2014.

262. Nicholas, M. K., R. V. Lukas, N. F. Jafri, L. Faoro, and R. Salgia. 2006. Epidermal growth factor receptor - mediated signal transduction in the development and therapy of gliomas. Clinical cancer research : an official journal of the American Association for Cancer Research 12:7261-7270.

263. Lo, H. W. 2010. EGFR-targeted therapy in malignant glioma: novel aspects and mechanisms of drug resistance. Current molecular pharmacology 3:37-52.

264. Yoon, S. H., J. M. Lee, S. J. Woo, M. J. Park, J. S. Park, H. S. Kim, M. Y. Park, H. J. Sohn, and T. G. Kim. 2009. Transfer of Her-2/neu specificity into cytokine-induced killer (CIK) cells with RNA encoding chimeric immune receptor (CIR). Journal of clinical immunology 29:806-814.

265. Zhao, Y., Z. Zheng, C. J. Cohen, L. Gattinoni, D. C. Palmer, N. P. Restifo, S. A. Rosenberg, and R. A. Morgan. 2006. High-efficiency transfection of primary human and mouse T lymphocytes using RNA electroporation. Molecular therapy : the journal of the American Society of Gene Therapy 13:151-159.

266. Beatty, G. L., A. R. Haas, M. V. Maus, D. A. Torigian, M. C. Soulen, G. Plesa, A. Chew, Y. Zhao, B. L. Levine, S. M. Albelda, M. Kalos, and C. H. June. 2014. Mesothelin-specific Chimeric Antigen Receptor mRNA-Engineered T cells Induce Anti-Tumor Activity in Solid Malignancies. Cancer immunology research 2:112-120.

267. Li, Y., and R. J. Kurlander. 2010. Comparison of anti-CD3 and anti-CD28-coated beads with soluble anti-CD3 for expanding human T cells: differing impact on CD8 T cell phenotype and responsiveness to restimulation. Journal of translational medicine 8:104.

268. Maus, M. V., A. K. Thomas, D. G. Leonard, D. Allman, K. Addya, K. Schlienger, J. L. Riley, and C. H. June. 2002. Ex vivo expansion of polyclonal and antigen-specific cytotoxic T lymphocytes by artificial APCs expressing ligands for the T-cell receptor, CD28 and 4-1BB. Nature biotechnology 20:143-148.

269. Gong, W., M. Ji, Z. Cao, L. Wang, Y. Qian, M. Hu, L. Qian, and X. Pan. 2008. Establishment and characterization of a cell based artificial antigen-presenting cell for expansion and activation of CD8+ T cells ex vivo. Cellular & molecular immunology 5:47-53.

270. Gattinoni, L., X. S. Zhong, D. C. Palmer, Y. Ji, C. S. Hinrichs, Z. Yu, C. Wrzesinski, A. Boni, L. Cassard, L. M. Garvin, C. M. Paulos, P. Muranski, and N. P. Restifo. 2009. Wnt signaling arrests effector T cell differentiation and generates CD8+ memory stem cells. Nature medicine 15:808-813.

271. Gattinoni, L., C. A. Klebanoff, and N. P. Restifo. 2012. Paths to stemness: building the ultimate antitumour T cell. Nature reviews. Cancer 12:671-684.

272. Geginat, J., A. Lanzavecchia, and F. Sallusto. 2003. Proliferation and differentiation potential of human CD8+ memory T-cell subsets in response to antigen or homeostatic cytokines. Blood 101:4260-4266.

273. Kamphorst, A. O., and R. Ahmed. 2013. CD4 T-cell immunotherapy for chronic viral infections and cancer. Immunotherapy 5:975-987.

274. Bourgeois, C., H. Veiga-Fernandes, A. M. Joret, B. Rocha, and C. Tanchot. 2002. CD8 lethargy in the absence of CD4 help. European journal of immunology 32:2199-2207.

275. Sun, J. C., and M. J. Bevan. 2003. Defective CD8 T cell memory following acute infection without CD4 T cell help. Science 300:339-342.

276. Muranski, P., and N. P. Restifo. 2009. Adoptive immunotherapy of cancer using CD4(+) T cells. Current opinion in immunology 21:200-208.

277. Robbins, P. F., M. E. Dudley, J. Wunderlich, M. El-Gamil, Y. F. Li, J. Zhou, J. Huang, D. J. Powell, Jr., and S. A. Rosenberg. 2004. Cutting edge: persistence of transferred lymphocyte clonotypes correlates with cancer regression in patients receiving cell transfer therapy. J Immunol 173:7125-7130.

278. Stephan, M. T., V. Ponomarev, R. J. Brentjens, A. H. Chang, K. V. Dobrenkov, G. Heller, and M. Sadelain. 2007. T cell-encoded CD80 and 4-1BBL induce auto- and transcostimulation, resulting in potent tumor rejection. Nature medicine 13:1440-1449.

279. Wu, F., W. Zhang, H. Shao, H. Bo, H. Shen, J. Li, Y. Liu, T. Wang, W. Ma, and S. Huang. 2013. Human effector T cells derived from central memory cells rather than CD8(+)T cells modified by tumor-specific TCR gene transfer possess superior traits for adoptive immunotherapy. Cancer letters 339:195-207.

280. Schaft, N., J. Dorrie, I. Muller, V. Beck, S. Baumann, T. Schunder, E. Kampgen, and G. Schuler. 2006. A new way to generate cytolytic tumor-specific T cells: electroporation of RNA coding for a T cell receptor into T lymphocytes. Cancer immunology, immunotherapy : CII 55:1132-1141.

281. Barker, F. G., 2nd, M. L. Simmons, S. M. Chang, M. D. Prados, D. A. Larson, P. K. Sneed, W. M. Wara, M. S. Berger, P. Chen, M. A. Israel, and K. D. Aldape. 2001. EGFR overexpression and radiation response in glioblastoma multiforme. International journal of radiation oncology, biology, physics 51:410-418.

282. Lacunza, E., M. Baudis, A. G. Colussi, A. Segal-Eiras, M. V. Croce, and M. C. Abba. 2010. MUC1 oncogene amplification correlates with protein overexpression in invasive breast carcinoma cells. Cancer genetics and cytogenetics 201:102-110.

283. Hirsch, F. R., M. Varella-Garcia, and F. Cappuzzo. 2009. Predictive value of EGFR and HER2 overexpression in advanced non-small-cell lung cancer. Oncogene 28 Suppl 1:S32-37.

284. Adams, G. P., R. Schier, A. M. McCall, H. H. Simmons, E. M. Horak, R. K. Alpaugh, J. D. Marks, and L. M. Weiner. 2001. High affinity restricts the localization and tumor penetration of single-chain fv antibody molecules. Cancer research 61:4750-4755.

285. Zuckier, L. S., E. Z. Berkowitz, R. J. Sattenberg, Q. H. Zhao, H. F. Deng, and M. D. Scharff. 2000. Influence of affinity and antigen density on antibody localization in a modifiable tumor targeting model. Cancer research 60:7008-7013.

286. Rushworth, D. J., B.; Olivares, S.; Maiti, S.; Briggs, N.; Somanchi, S.; Dai, J.; Lee, D.A.; Cooper, L.J.N. 2014. Universal artificial antigen presenting cells to selectively propagate T cells expressing chimeric antigen receptors independent of specificity. Journal of Immunotherapy.

287. Lim, D. G., P. Hollsberg, and D. A. Hafler. 2002. Strength of prior stimuli determines the magnitude of secondary responsiveness in CD8+ T cells. Cellular immunology 217:36-46.

288. Crombet, T., M. Osorio, T. Cruz, C. Roca, R. del Castillo, R. Mon, N. Iznaga-Escobar, R. Figueredo, J. Koropatnick, E. Renginfo, E. Fernandez, D. Alvarez, O. Torres, M. Ramos, I. Leonard, R. Perez, and A. Lage. 2004. Use of the humanized

anti-epidermal growth factor receptor monoclonal antibody h-R3 in combination with radiotherapy in the treatment of locally advanced head and neck cancer patients. Journal of clinical oncology : official journal of the American Society of Clinical Oncology 22:1646-1654.

289. Rodriguez, M. O., T. C. Rivero, R. del Castillo Bahi, C. R. Muchuli, M. A. Bilbao, E. N. Vinageras, J. Alert, J. J. Galainena, E. Rodriguez, E. Gracias, B. Mulen, B. Wilkinson, E. L. de Armas, K. Perez, I. Pineda, M. Frometa, I. Leonard, V. Mullens, C. Viada, P. Luaces, O. Torres, N. Iznaga, and T. Crombet. 2010. Nimotuzumab plus radiotherapy for unresectable squamous-cell carcinoma of the head and neck. Cancer biology & therapy 9:343-349.

290. Ramos, T. C., J. Figueredo, M. Catala, S. Gonzalez, J. C. Selva, T. M. Cruz, C. Toledo, S. Silva, Y. Pestano, M. Ramos, I. Leonard, O. Torres, P. Marinello, R. Perez, and A. Lage. 2006. Treatment of high-grade glioma patients with the humanized anti-epidermal growth factor receptor (EGFR) antibody h-R3: report from a phase I/II trial. Cancer biology & therapy 5:375-379.

291. Lal, S., M. Lacroix, P. Tofilon, G. N. Fuller, R. Sawaya, and F. F. Lang. 2000. An implantable guide-screw system for brain tumor studies in small animals. Journal of neurosurgery 92:326-333.

292. Szerlip, N. J., A. Pedraza, D. Chakravarty, M. Azim, J. McGuire, Y. Fang, T. Ozawa, E. C. Holland, J. T. Huse, S. Jhanwar, M. A. Leversha, T. Mikkelsen, and C. W. Brennan. 2012. Intratumoral heterogeneity of receptor tyrosine kinases EGFR and PDGFRA amplification in glioblastoma defines subpopulations with distinct growth factor response. Proceedings of the National Academy of Sciences of the United States of America 109:3041-3046.

293. Zhou, X., J. Li, Z. Wang, Z. Chen, J. Qiu, Y. Zhang, W. Wang, Y. Ma, N. Huang, K. Cui, and Y. Q. Wei. 2013. Cellular immunotherapy for carcinoma using genetically modified EGFR-specific T lymphocytes. Neoplasia 15:544-553.

294. Mutsaers, A. J., G. Francia, S. Man, C. R. Lee, J. M. Ebos, Y. Wu, L. Witte, S. Berry, M. Moore, and R. S. Kerbel. 2009. Dose-dependent increases in circulating TGF-alpha and other EGFR ligands act as pharmacodynamic markers for optimal biological dosing of cetuximab and are tumor independent. Clinical cancer research : an official journal of the American Association for Cancer Research 15:2397-2405.

295. Stone, J. D., and D. M. Kranz. 2013. Role of T cell receptor affinity in the efficacy and specificity of adoptive T cell therapies. Frontiers in immunology 4:244.

296. Sampson, J. H., B. D. Choi, L. Sanchez-Perez, C. M. Suryadevara, D. J. Snyder, C. T. Flores, S. K. Nair, R. J. Schmittling, E. A. Reap, P. K. Norberg, J. E. Herndon, 2nd, C. T. Kuan, R. A. Morgan, S. A. Rosenberg, and L. A. Johnson. 2013. EGFRvIII mCAR-modified T cell therapy cures mice with established intracerebral glioma and generates host immunity against tumor-antigen loss. Clinical cancer research : an official journal of the American Association for Cancer Research.

297. Singer, J., M. Weichselbaumer, T. Stockner, D. Mechtcheriakova, Y. Sobanov, E. Bajna, F. Wrba, R. Horvat, J. G. Thalhammer, M. Willmann, and E. Jensen-Jarolim. 2012. Comparative oncology: ErbB-1 and ErbB-2 homologues in canine cancer are susceptible to cetuximab and trastuzumab targeting. Molecular immunology 50:200-209.

298. Higgins, R. J., P. J. Dickinson, R. A. LeCouteur, A. W. Bollen, H. Wang, L. J. Corely, L. M. Moore, W. Zang, and G. N. Fuller. 2010. Spontaneous canine gliomas: overexpression of EGFR, PDGFRalpha and IGFBP2 demonstrated by tissue microarray immunophenotyping. Journal of neuro-oncology 98:49-55.

299. Perez, R., E. Moreno, G. Garrido, and T. Crombet. 2011. EGFR-Targeting as a Biological Therapy: Understanding Nimotuzumab's Clinical Effects. Cancers 3:2014-2031.

300. Chan, D. A., P. D. Sutphin, S. E. Yen, and A. J. Giaccia. 2005. Coordinate regulation of the oxygen-dependent degradation domains of hypoxia-inducible factor 1 alpha. Molecular and cellular biology 25:6415-6426.

301. Vartanian, A., S. K. Singh, S. Agnihotri, S. Jalali, K. Burrell, K. D. Aldape, and G. Zadeh. 2014. GBM's multifaceted landscape: highlighting regional and microenvironmental heterogeneity. Neuro-oncology.

302. Wilkie, S., M. C. van Schalkwyk, S. Hobbs, D. M. Davies, S. J. van der Stegen, A. C. Pereira, S. E. Burbridge, C. Box, S. A. Eccles, and J. Maher. 2012. Dual targeting of ErbB2 and MUC1 in breast cancer using chimeric antigen receptors engineered to provide complementary signaling. Journal of clinical immunology 32:1059-1070.

303. Lanitis, E., M. Poussin, A. W. Klattenhoff, D. Song, R. Sandaltzopoulos, C. H. June, and D. J. Powell, Jr. 2013. Chimeric antigen receptor T cells with dissociated signaling domains exhibit focused anti-tumor activity with reduced potential for toxicity. Cancer immunology research 1.

304. Kloss, C. C., M. Condomines, M. Cartellieri, M. Bachmann, and M. Sadelain. 2013. Combinatorial antigen recognition with balanced signaling promotes selective tumor eradication by engineered T cells. Nature biotechnology 31:71-75.

305. Fedorov, V. D., M. Themeli, and M. Sadelain. 2013. PD-1- and CTLA-4-Based Inhibitory Chimeric Antigen Receptors (iCARs) Divert Off-Target Immunotherapy Responses. Science translational medicine 5:215ra172.

306. Zeng, J., A. P. See, J. Phallen, C. M. Jackson, Z. Belcaid, J. Ruzevick, N. Durham, C. Meyer, T. J. Harris, E. Albesiano, G. Pradilla, E. Ford, J. Wong, H. J. Hammers, D. Mathios, B. Tyler, H. Brem, P. T. Tran, D. Pardoll, C. G. Drake, and M. Lim. 2013. Anti-PD-1 blockade and stereotactic radiation produce long-term survival in mice with intracranial gliomas. International journal of radiation oncology, biology, physics 86:343-349.

307. Joseph, J. V., V. Balasubramaniyan, A. Walenkamp, and F. A. Kruyt. 2013. TGF-beta as a therapeutic target in high grade gliomas - promises and challenges. Biochemical pharmacology 85:478-485.

308. Bogdahn, U., P. Hau, G. Stockhammer, N. K. Venkataramana, A. K. Mahapatra, A. Suri, A. Balasubramaniam, S. Nair, V. Oliushine, V. Parfenov, I. Poverennova, M. Zaaroor, P. Jachimczak, S. Ludwig, S. Schmaus, H. Heinrichs, and K. H. Schlingensiepen. 2011. Targeted therapy for high-grade glioma with the TGF-beta2 inhibitor trabedersen: results of a randomized and controlled phase IIb study. Neuro-oncology 13:132-142.

309. Bendle, G. M., C. Linnemann, L. Bies, J. Y. Song, and T. N. Schumacher. 2013. Blockade of TGF-beta signaling greatly enhances the efficacy of TCR gene therapy of cancer. J Immunol 191:3232-3239.

310. Chow, K. K., S. Naik, S. Kakarla, V. S. Brawley, D. R. Shaffer, Z. Yi, N. Rainusso, M. F. Wu, H. Liu, Y. Kew, R. G. Grossman, S. Powell, D. Lee, N. Ahmed, and S. Gottschalk. 2013. T cells redirected to EphA2 for the immunotherapy of glioblastoma. Molecular therapy : the journal of the American Society of Gene Therapy 21:629-637.

311. Choi, B. D., C. M. Suryadevara, P. C. Gedeon, J. E. Herndon Ii, L. Sanchez-Perez, D. D. Bigner, and J. H. Sampson. 2014. Intracerebral delivery of a third generation EGFRvIII-specific chimeric antigen receptor is efficacious against human glioma. Journal of clinical neuroscience : official journal of the Neurosurgical Society of Australasia 21:189-190.

312. Grada, Z., M. Hegde, T. Byrd, D. R. Shaffer, A. Ghazi, V. S. Brawley, A. Corder, K. Schonfeld, J. Koch, G. Dotti, H. E. Heslop, S. Gottschalk, W. S. Wels, M. L. Baker, and N. Ahmed. 2013. TanCAR: A Novel Bispecific Chimeric Antigen Receptor for Cancer Immunotherapy. Molecular therapy. Nucleic acids 2:e105.

313. Patel, D., A. Lahiji, S. Patel, M. Franklin, X. Jimenez, D. J. Hicklin, and X. Kang. 2007. Monoclonal antibody cetuximab binds to and down-regulates constitutively activated epidermal growth factor receptor vIII on the cell surface. Anticancer research 27:3355-3366.

314. Jaramillo, M. L. G., S.; Baardsnes, J.; Banville, M.; Paul-Roc, B.; Tikhomirov, I.A.; Thompson, S.E.; O'Connor, M. 2010. Nimotuzumab, a humanized anti-epidermal growth factor receptor antibody, interacts with EGFRvIII. AACR 101st annual meeting:Abstract #1778.

315. Davies, J. K., H. Singh, H. Huls, D. Yuk, D. A. Lee, P. Kebriaei, R. E. Champlin, L. M. Nadler, E. C. Guinan, and L. J. Cooper. 2010. Combining CD19 redirection and alloanergization to generate tumor-specific human T cells for allogeneic cell therapy of B-cell malignancies. Cancer research 70:3915-3924.

316. Boczkowski, D., S. K. Nair, J. H. Nam, H. K. Lyerly, and E. Gilboa. 2000. Induction of tumor immunity and cytotoxic T lymphocyte responses using dendritic cells transfected with messenger RNA amplified from tumor cells. Cancer research 60:1028-1034.

317. Hurton, L. V. 2014. Tethered IL-15 to augment the therapeutic potential of T cells expressing chimeric antigen receptor: Maintaining memory potential, persistence, and antitumor activity. (Doctoral Dissertation) The University of Texas Health Science Center at Houston.

318. Turkman, N., A. Shavrin, R. A. Ivanov, B. Rabinovich, A. Volgin, J. G. Gelovani, and M. M. Alauddin. 2011. Fluorinated cannabinoid CB2 receptor ligands: synthesis and in vitro binding characteristics of 2-oxoquinoline derivatives. Bioorganic & medicinal chemistry 19:5698-5707.

319. Zhang, M., S. Maiti, C. Bernatchez, H. Huls, B. Rabinovich, R. E. Champlin, L. M. Vence, P. Hwu, L. Radvanyi, and L. J. Cooper. 2012. A new approach to simultaneously quantify both TCR alpha- and beta-chain diversity after adoptive immunotherapy. Clinical cancer research : an official journal of the American Association for Cancer Research 18:4733-4742.

320. Deniger, D. C., K. Switzer, T. Mi, S. Maiti, L. Hurton, H. Singh, H. Huls, S. Olivares, D. A. Lee, R. E. Champlin, and L. J. Cooper. 2013. Bispecific T-cells expressing polyclonal repertoire of endogenous gammadelta T-cell receptors and introduced CD19-specific chimeric antigen receptor. Molecular therapy : the journal of the American Society of Gene Therapy 21:638-647.

321. Geiss, G. K., R. E. Bumgarner, B. Birditt, T. Dahl, N. Dowidar, D. L. Dunaway, H. P. Fell, S. Ferree, R. D. George, T. Grogan, J. J. James, M. Maysuria, J. D. Mitton, P. Oliveri, J. L. Osborn, T. Peng, A. L. Ratcliffe, P. J. Webster, E. H. Davidson, L. Hood, and K. Dimitrov. 2008. Direct multiplexed measurement of gene expression with color-coded probe pairs. Nature biotechnology 26:317-325.

322. O'Connor, C. M., S. Sheppard, C. A. Hartline, H. Huls, M. Johnson, S. L. Palla, S. Maiti, W. Ma, R. E. Davis, S. Craig, D. A. Lee, R. Champlin, H. Wilson, and L. J. Cooper. 2012. Adoptive T-cell therapy improves treatment of canine non-Hodgkin lymphoma post chemotherapy. Scientific reports 2:249.

323. Audic, S., and J. M. Claverie. 1997. The significance of digital gene expression profiles. Genome research 7:986-995.

324. Eisen, M. B., P. T. Spellman, P. O. Brown, and D. Botstein. 1998. Cluster analysis and display of genome-wide expression patterns. Proceedings of the National Academy of Sciences of the United States of America 95:14863-14868.

325. Robins, H. S., P. V. Campregher, S. K. Srivastava, A. Wacher, C. J. Turtle, O. Kahsai, S. R. Riddell, E. H. Warren, and C. S. Carlson. 2009. Comprehensive assessment of T-cell receptor beta-chain diversity in alphabeta T cells. Blood 114:4099-4107.

VITA

Hillary Gibbons Caruso was born June 23, 1986 in Fort Worth, Texas to Tom and Lorie Gibbons. She graduated from Burleson High School as class salutatorian in 2004, where she played the flute in the high school symphonic band. She attended Texas Christian University in Fort Worth, Texas, with an academic scholarship, and worked on two research projects involving body temperature regulation of Jamaican *Anolis* lizards under Dr. Gary Ferguson and mechanisms of control of septic shock under Dr. Dennis Cheek. She graduated *summa cum laude* with a Bachelor's Degree of Science in Biology with a minor in Chemistry in 2007. In the fall of 2007, Hillary entered the Ph.D. program at the University of Texas Health Science Center's Graduate School of Biomedical Sciences in Houston, TX. In May 2008, she joined the Immunology Ph.D. program and began her dissertation work studying genetic modification of T cells for immunotherapy under Dr. Laurence Cooper.